New regulators of oligodendrocyte development and CNS myelin organization

Omar de Faria Jr.

Integrated Program in Neuroscience
Department of Neurology and Neurosurgery
Montreal Neurological Institute
McGill University
Montreal, Quebec, Canada

November 2015

A thesis submitted to McGill University
in partial fulfillment of the requirements for
the degree of Doctor of Philosophy

TABLE OF CONTENTS

ACKNOWLEDGEMENTS

I would like to first thank Dr. Tim Kennedy for accepting me as a graduate student in his lab and for his supervision over the last few years. Thank you for the opportunity to carry on with my PhD studies and for always being open to listen and ready to advise. I also thank you for allowing me to conduct my project with a great deal of freedom. I would like to thank Dr. David Colman, whose lab I first joined more than six years ago. Thank you for the opportunity to come to the Neuro and for your guidance on subjects well beyond my project. You are deeply missed and I will carry your lessons for my entire career. I also thank Dr. Ajit Dhaunchak for being such an incredible role model and dear friend. Thank you for every bit of enthusiasm and passion that you have shared with me during my initial student years. You too are deeply missed and your example will always have a tremendous impact on my attitude as researcher. I would also like to thank Dr. Margaret Magdesian, who first brought me to Montreal and the Neuro and who has always been a great source of inspiration in my studies. I thank the members of my Advisory Committee, Dr. Amit Bar-Or and Dr. Jack Antel for their guidance throughout my studies and Dr. Alyson Fournier and Dr. Rashmi Kothary for examining this thesis.

I am also in debt with many colleagues and friends at the Neuro, who have made graduate school a much more enjoyable experience. In special, I thank Kennedy lab members Karen, Ian, Dong, Nathalie, Stephen, Jenea, Diane, Steph, Xin, Greta, James, Sebastien, Jennifer, Maran and Yasmine and Colman lab members Wiam, Anshul, Gopan, Caroline, Patricia, Dalinda, Ziwei and Liliana. I also thank friends in the Founier lab, Ricardo, Camille, Marie-Pierre, Isabel and Gino.

I have been blessed with wonderful friends here in Montreal and back in Brasil. Thank you Ronan, Ricardo, Lucas, Kika, João, Ciça, Igor, Cris, Marcos, Ana, Luísa, Shawn, Alex,

Bernardo, Roberta, Ney, Mariana, Luzia, Rodrigo, Paulo and Isabella. Your support and friendship were very important throughout these years. I also thank my family back at home, whom I will always be in debt with: my mother Elizete and my father Omar, who taught me so much and have always pushed me to learn more, my sister Carine, and grandparents Aparecida, Valdo, Orlanda and Esperidião.

I'm extremely fortunate to have found Luciana. I thank you for your support in every aspect of my studies. You are the love of my life and none of this would have made sense without you. I would also like to thank God, the Father, Jesus and the Holy Spirit. Thank You for making this PhD possible and for making me capable of writing/defending this thesis. You give me hope every day and I wish to keep knowing and loving You for all my life.

ABSTRACT

During development, oligodendrocyte lineage cells are generated at the ventricular zone of the developing neural tube and subsequently migrate to white matter forming regions of the embryonic Central Nervous System (CNS). In these areas, cell cycle-exited oligodendrocyte precursor cells (OPCs) differentiate into myelinating oligodendrocytes that spirally wrap axon segments with extensions of their own plasma membrane. As myelination proceeds, distinct axoglial domains are assembled along the axon, establishing the structural basis for the saltatory conduction of the action potential. Complex regulatory mechanisms orchestrate these various steps in oligodendrocyte development and myelin organization. Here, we use different *in vitro* and *in vivo* experimental approaches to investigate novel aspects of this regulation.

In rodents, OPC proliferation and differentiation are regulated by short non-coding RNAs, known as microRNAs (miRNAs). miRNA function is not always conserved and the role miRNAs play during human OPC development is poorly understood. Using endpoint RT-PCR assays and quantitative real-time PCR, we demonstrate that rodent relevant miRNAs are enriched in human white matter and expressed in OPC/oligodendrocytes acutely isolated from the adult human brain. Our findings suggest that miRNA regulation of OPC proliferation and differentiation is conserved between rodents and humans.

During OPC differentiation, levels of Transmembrane Protein 10 (TMEM10) are highly upregulated. We demonstrate that TMEM10 overexpression in the OPC cell line oli-neu results in process extension and branching, in addition to upregulated myelin gene expression. Knockdown experiments in oli-neu and primary OPC cultures indicate that differentiation is

limited in the absence of TMEM10. We conclude that TMEM10 contributes to OPC differentiation *in vitro*.

After oligodendrocyte development, maintenance of paranode domains in myelinated axons requires netrin-1. Our results indicate that the netrin-1 receptor UNC5B is enriched at the paranodes and that following UNC5B deletion *in vivo*, paranodes become severely disorganized and axonal domain segregation is lost. Paranodal disruption is less severe in younger animals, suggesting that the phenotype is progressive and UNC5B function is required for paranode maintenance.

These findings provide new insights into the regulation of OPC development and myelin organization. Identification of new regulators of myelin biology will further our understanding of CNS function and pave the way to the cure of demyelinating neurological disorders.

RÉSUMÉ

Les cellules de la lignée des oligodendrocytes se développent dans un domaine spécifique de la zone ventriculaire du tube neural et migrent ensuite vers les régions qui formeront la substance blanche du système nerveux central (SNC). Dans ces zones, les cellules précurseurs d'oligodendrocytes (CPOs) qui ont quittées le cycle cellulaires se différencient en oligodendrocytes myélinisantes. Les oligodendrocytes myélinisantes entourent les segments axonales par les extensions de leur propre membrane plasmique. Tandis que la myélinisation continue, les domaines axogliaux sont assemblés au long de l'axone établissant la base structurelle de la conduction saltatoire du potentiel d'action. Des mécanismes complexes de régulation orchestrent ces différentes étapes dans le développement des oligodendrocytes et de l'organisation de la myéline. Ici, nous utilisons différentes approches expérimentales *in vitro* et *in vivo* pour étudier des nouveaux aspects de cette régulation.

Chez les rongeurs, la prolifération et la différenciation des CPO sont régulées par de ARN non-codants courts appelés microARN (miRNAs). La fonction de ces miRNA n'est pas toujours conservée et le rôle que les miRNAs jouent au cours du développement des CPO chez les humain est encore mal compris. En utilisant la RT-PCR et la PCR quantitative en temps réel, nous démontrons que les miRNAs pertinents pour les rongeurs sont enrichis dans la substance blanche humaine et exprimés chez les CPO isolés de manière aiguë du cerveau humain adulte. Nos résultats suggèrent que la régulation de la prolifération et la différenciation des CPO par le miRNA est conservée entre les rongeurs et les humains.

Au cours de la différenciation, les taux de la protéine transmembranaire 10 (TMEM10) sont fortement augmentés. Nous démontrons que la surexpression de TMEM10 dans la lignée

cellulaire CPO oli-neu résulte, de l'extension et la ramification de processus, en plus de l'augmentation de l'expression du gène de la myéline. L'induction de la sous-expression de la protéine TMEM10 dans des cellules oli-neu et des cultures primaires des CPO indiquent que la différenciation est limitée en l'absence de TMEM10. Nous concluons donc que la protéine TMEM10 contribue à la différenciation *in vitro* des CPO.

Après le développement, la maintenance de la région paranodal dans les axones myélinisés est dépendante la protéine nétrine-1. Nos résultats indiquent que le récepteur de nétrine-1 UNC5B est enrichi aux paranodes et qu'après la délétion *in vivo* de UNC5B, les paranodes deviennent fortement désorganisés et la ségrégation de domaine axonale est perdue. La perturbation de la région paranodal est moins grave chez les jeunes animaux, ce qui suggère que le phénotype est progressif et que la fonction de UNC5B est principalement de maintenir la région paranodal.

Nos données apportent un éclairage nouveau sur la biologie de la myéline. L'identification de nouveaux régulateurs du développement de lignée cellulaire CPO et de l'organisation de la myéline nous aide à approfondir notre compréhension de la fonction du SNC et est une étape de plus vers la guérison des troubles neurologiques.

LIST OF FIGURES AND TABLES

LIST OF ABBREVIATIONS

BSA	Bovine Serum Albumin
cAMP	Cyclic Adenosine Monophosphate
CGT	Ceramyl Galactosyl Transferase
CNP	2′,3′-Cyclic Nucleotide 3′-Phosphodiesterase
CNS	Central Nervous System
CREB	cAMP Responsive Element Binding protein
CST	Ceramyl Sulfatyl Transferase
DCC	Deleted in Colorectal Cancer
DAPK	Death Associated Protein Kinase
DIV	Days *in vitro*
DMEM	Dulbecco's Modified Eagle Medium
DSCAM	Down's syndrome Cell Adhesion Molecule
ECM	Extracellular Matrix
EGF	Epidermal Growth Factor
ERK	Extracellular signal Regulated Kinase
FAK	Focal Adhesion Kinase
FBS	Fetal Bovine Serum
FGF	Fibroblast Growth Factor
FNIII	Fibronectin type III
GalC	Galactocerebroside
GAPDH	Glyceraldehyde 3-Phosphate Dehydrogenase
GEF	Guanine Exchange Factor
GFAP	Glial Fibrillary Acidic Protein
GPI	Glycophosphatidylinositol
HSPG	Heparin Sulfate Proteoglycan
Ig	Immunoglobulin
IGF-1	Insulin-like Growth Factor-1

IGF1R	Insulin-like Growth Factor Receptor-1
MAG	Myelin Associated Glycoprotein
MAL	Myelin and Lymphocyte protein
MAPK	Mitogen-Activated Protein Kinase
MBP	Myelin Basic Protein
MiRNA	MicroRNA
MS	Multiple Sclerosis
mTor	Mammalian Target Of Rapamycin
NCAM	Neural Cell Adhesion Molecule
NF155	Neurofascin 155
NF186	Neurofascin 186
NrCAM	Neural-glial-Related Cell Adhesion Molecule
NRG	Neuregulin
OPC	Oligodendrocyte Precursor Cell
OL	Oligodendrocyte
OMgp	Oligodendrocyte-Myelin Glycoprotein
PBS	Phosphate buffered saline
PDGF-A	Platelet Derived Growth Factor-Alpha
PDGFαR	Platelet Derived Growth Factor-Alpha Receptor
PDL	Poly-D-Lysine
PLL	Poly-L-Lysine
PFA	Paraformaldehyde
PI3K	Phosphoinositide 3-Kinase
PKA	Protein Kinase A
PLP	Proteolipid Protein
pMN	Motor Neuron progenitor domain
PNS	Peripheral nervous system
PSA	Polysialylated
PTEN	Phosphatase and Tensin homolog

RGC	Retinal Ganglion Cell
ROCK	Rho Kinase
RT	Room Temperature
Shh	Sonic hedgehog
TB	Transverse band
TMEM10	Transmembrane protein 10

CONTRIBUTION OF AUTHORS

Chapter 1:

Omar de Faria Jr.: wrote the manuscript and prepared the figures.

Timothy E. Kennedy: edited the manuscript.

Chapter 2:

Omar de Faria Jr.: Developed rationale, performed all experiments, analyzed data and wrote the manuscript.

Qiao-Ling Cui: Isolated oligodendrocyte lineage cells from human adult brain and performed RNA extraction from these cells.

Jenea M. Bin: Prepared OPC cultures.

Sarah-Jane Bull: Prepared OPC cultures.

Timothy E. Kennedy: Provided equipment and reagents.

Amit Bar-Or: Developed rationale and provided equipment and reagents.

Jack P Antel: Developed rationale and provided equipment and reagents.

David R Colman: Developed rationale and provided equipment and reagents.

Ajit S Dhaunchak: Developed rationale, analyzed data and wrote the manuscript.

Chapter 3:

Omar de Faria Jr.: Developed rationale, performed all experiments except immunohistochemistry in figures 1A, 1C and 2A, analyzed data and wrote the manuscript.

Ajit S. Dhaunchack: Developed rationale, performed immunohistochemistry in figures 1A, 1C and 2A, generate TMEM10-Oli-neu cell line and analyzed data.

Alejandro D. Roth: Generated TMEM10 antibody.

David R Colman: Developed rationale and analyzed data.

Timothy E Kennedy: Developed rationale and edited the manuscript.

Chapter 4:

Omar de Faria Jr.: Developed rationale, performed all experiments, except Beta-Gal activity assay on Figure 2C, analyzed data and wrote the manuscript.

Jenea M. Bin: Performed Beta-Gal activity assay on Figure 2C.

Abbas Sadikot: Provided equipment.

Timothy E. Kennedy: Developed rationale and edited the manuscript.

Chapter 5:

Omar de Faria Jr.: Wrote the manuscript and prepared the figures.

Timothy E. Kennedy: Edited the manuscript.

Preface to chapter 1

During development, OPCs are specified in germinative zones of the neural tube and then migrate, proliferate and differentiate into mature oligodendrocytes that contact and myelinate axons of the CNS. OPC development and myelin organization are regulated by multiple mechanisms, which function has been studied over the last thirty years. In the first section of Chapter 1, we review the literature available on these regulatory mechanisms. In the sections that follow, we provide background information on molecules that were studied in Chapters 2, 3 and 4. These molecules, namely miRNAs, TMEM10 and Netrins, are novel regulators of OPC development and myelin organization in the CNS.

CHAPTER 1: LITERATURE REVIEW

1 Regulation of oligodendrocyte development and myelin organization

Early descriptions of brain structure by Virchow, in the late XIX century, and Ramon Y Cajal, in the 1910s, recognized the existence of a third cell type, beyond neurons and astrocytes, enriched in the white matter of the Central Nervous System (CNS). Limitations of the staining methods available prevented further characterization of this cell type, referred to then as the "third element" (Cajal, 1913). It was Cajal's student Pío del-Rio-Hortega who developed an improved silver carbonate staining method that identified two distinct cell types contained within the "third element". Because these were small cells, bearing multiple short processes, they were named microglia and oligodendroglia (Río-Hortega, 1922). Wilder Penfield, working with del-Río-Hortega, confirmed these earlier results and additionally suggested that myelin was generated by oligodendrocytes (Penfield, 1924). At that time, observations indicating that oligodendrocytes were responsible for myelin formation included their substantial numbers in white matter tracts, localization close to the myelin sheath and appearance coincident with myelination. However, it was not before the seminal article of Beth Ben Geren on myelin ultrastructure that definitive evidence established that myelin is not generated by axons, but rather derives from plasma membrane extensions of glial cells (Geren, 1954).

We now know that myelin is generated by oligodendrocytes in the CNS and Schwann cells in the Peripheral Nervous System (PNS). It consists of a multilayered, lipid-rich membrane that electrically insulates axons. In myelinated fibers, membrane depolarization is confined to unmyelinated nodal regions and as a result action potentials rapidly propagate from node to

node. The emergence of myelin and the saltatory conduction of action potential represented a critical step in the evolution of the vertebrate nervous system and constitute one of the bases for fast and efficient neural activity in higher order animals. In this section of Chapter 1, the mechanisms that regulate oligodendrocyte development and myelin organization will be reviewed in detail (Figure 1.1).

1.1 Oligodendrocyte lineage specification

Dorsal-ventral gradients of secreted morphogens coordinate cell lineage specification in the developing neural tube. Because fate determinant transcription factors exhibit differential threshold response to these gradients, downstream regulators are selectively expressed in spatially restricted areas along the dorsal-ventral axis. As a result, CNS cell lineages are generated in well-defined domains of the embryonic neural tube; later in development, precursors migrate away from these germinative foci and populate target regions in the CNS, where they differentiate and exert specialized functions in the adulthood.

OPC specification was first suggested to be spatially restricted when dorsal and ventral halves of embryonic rat spinal cord were cultured *in vitro*, but only the ventral part showed the capacity for oligodendrogenesis (Warf et al., 1991). Identification of PDGFαR as a marker for OPCs made possible the identification of a focal site for OPC production in the ventral ventricular zone of the developing spinal cord just dorsal to the floor plate (Pringle and Richardson, 1993). At this site, the notochord and floor plate-derived morphogen Sonic Hedgehog (Shh) influences cell specification and is necessary for OPC production (Cai et al., 2005; Lu et al., 2000; Orentas et al., 1999). Shh induces the expression of the basic Helix-Loop-Helix (bHLH) transcription factor

Olig2, which defines the domain that gives rise to OPCs in the ventral embryonic spinal cord (Lu et al., 2000; Orentas et al., 1999). Olig2 expression induces oligodendrogenesis and loss of Olig2 prevents OPC generation, indicating that Olig2 is sufficient and necessary for oligodendroglial lineage specification (Takebayashi et al., 2002; Zhou et al., 2001). Interestingly, the area defined by Olig2 expression in the embryonic neural tube, the pMN domain, produces both OPCs and motor neurons in temporally distinct phases, with OPCs being generated once motor neuron specification is complete (Orentas et al., 1999; Zhou et al., 2001). This is consistent with early observations indicating that oligodendrocytes are the last cell type specified during development (Altman and Bayer, 1984). Changes in the complimentary set of transcription factors that interact with Olig2 underlie this switch in lineage specification that occurs at the pMN. Shortly before OPCs are generated, the pattern of Olig2 and NKx2.2 expression changes from mutually exclusive to coincident, whereas Neurogenin expression is globally downregulated. Ectopic Olig2 / Nkx2.2 coexpression induces oligodendrogenesis, whereas Olig2 expressed alone in Neurogenin positive regions promotes motor neuron specification (Zhou et al., 2001). This suggested a model where oligodendrocyte identity is acquired following Olig2 / Nkx2.2 transcriptional activation, in the absence of Neurogenin (Fu et al., 2002; Li et al., 2011; Mizuguchi et al., 2001; Novitch et al., 2001; Soula et al., 2001; Zhou et al., 2001) Additionally, the motor neuron-OPC fate switch correlates with changes in Olig2 post-translational modifications. Before E11.5, when motor neurons are produced at the pMN domain, Olig2 serine residue 147 (ser147) is phosphorylated, which favors Olig2 homodimerization. After E11.5, ser147 becomes dephosphorylated and Olig2 tends to dimerize with other bHLH transcription factors (Li et al., 2011). Additional transcription factors that are important for oligodendroglial

lineage specification include Olig1, Sox 9, Sox 10 and Mash. In the absence of these regulators, OPC populations are lost or drastically reduced (Lu et al., 2002; Parras et al., 2007; Stolt et al., 2003; Sugimori et al., 2008; Takebayashi et al., 2002).

The pMN domain is not the sole OPC source in the developing spinal cord. In Shh-deficient mice, Olig2 expression is abolished at the pMN and ventrally derived OPCs are not produced. However, a population of Olig2 / PDGFαR double-positive OPCs, which also expresses the dorsal spinal cord markers dbx1 and pax7, arises from the dorsal ventricular zone (Cai et al., 2005). There, Olig2 expression and OPC lineage specification does not depend on Shh signaling. Dorsally derived OPCs appear late in mouse embryonic development (E14.5) generating a second wave of OPCs in the spinal cord. Fate-mapping studies revealed that this population accounts for ~20% of total OPCs in the spinal cord of adult mice (Tripathi et al., 2011).

Other OPC sources also exist in more anterior regions of the developing neural tube. Using Cre-lox technology to fate map neural stem cells from different germinative areas of the developing forebrain, Kessaris et al. (2006) showed that three waves of OPCs are sequentially generated in this part of the CNS (Kessaris et al., 2006). PDGFαR positive OPCs are first generated around E14.5 from Nkx2.1-expressing cells in the Medial Ganglionic Eminence (MGE) in the ventral mouse forebrain. A second OPC population arises a day later from Gsx2 positive cells of the Lateral Ganglionic Eminence (LGE). Finally, a third OPC wave is generated within the cortex, close to the dorsal ventricular zone, from Emx1-expressing cells. Like dorsally derived OPCs in the spinal cord, OPCs generated in dorsal regions of the forebrain arise late in development (Cai et al., 2005; Kessaris et al., 2006). Although early MGE-derived OPCs migrate throughout the

mouse forebrain, they are eliminated during postnatal development, being replaced by late-generated OPC populations (Kessaris et al., 2006).

1.2 OPC migration

OPCs emerge in isolated foci along the neural tube but migrate and proliferate extensively throughout the CNS. During telencephalon development, early generated OPCs disperse away from their origin in the MGE and colonize the forebrain (Kessaris et al., 2006). In the developing spinal cord, pMN domain-derived OPCs migrate dorsally and peripherally to populate areas of future spine white matter (Miller et al., 1997; Ono et al., 1995). During optic nerve formation, OPCs generated in the subventricular zone of the third ventricle, enter the nerve through the chiasm and migrate towards the retina (Ono et al., 1997; Small et al., 1987).

Observation that labeled OPCs accumulate in the retina-proximal portion of the optic nerve following third ventricle injection with DiI suggested that OPCs migrate onto existing axon tracts of the developing CNS (Ono et al., 1997). Axophilic migration is at least in part regulated by substrate and cell-bound ligands acting as short-range cues for migrating OPCs. However, the finding that OPCs migrate normally after optic nerve transection suggested that migration does not require viable retina ganglion cells and that secreted factors, acting at a distance, might also direct OPC migration during CNS development (Ueda et al., 1999). In fact, both short and long-range mechanisms exist that guide OPCs as they disperse throughout the CNS.

In vitro experiments, using different microchemotaxis assays, have contributed to identify some of these factors. The extracellular matrix (ECM) components, fibronectin and laminin, when

immobilized on the surface of a filter that separates two cell culture compartments, promoted migration of chick OPCs from one compartment to the other. Soluble forms of these proteins failed to induce OPC migration, indicating that incorporation onto the substrate is critical for the fibronectin and laminin function (Armstrong et al., 1990). Fibronectin but not laminin-induced OPC migration was negatively modulated by the ECM protein Tenascin-C (Frost et al., 1996; Kiernan et al., 1996). In Tenascin-C null mice, enhanced rates of OPC migration are observed, suggesting that Tenascin-C also limits OPC migration *in vivo*, possibly regulating individual cell-ECM interactions (Frost et al., 1996; Garcion et al., 2001). ECM signaling regulating OPC migration depends in part on the activity of specific integrins, as function-blocking antibodies directed against αVβ1 integrin impairs OPC migration out of an agarose drop containing high density cells (Milner et al., 1996).

Platelet-derived Growth Factor Alpha (PDGF-A) is a potent OPC mitogen and also a diffusible chemoattractant that regulates OPC migration *in vitro* (Armstrong et al., 1990). PDGF-A induced chemoattraction was not impaired by inhibitors of DNA replication, suggesting that effects on OPC migration are independent of PDGF-A influence on OPC proliferation (Armstrong et al., 1990). Another mitogen, Basic Fibroblast Growth Factor (bFGF), signals through FGFR1 to direct OPC migration (Simpson and Armstrong, 1999). bFGF chemoattraction is blocked by the ECM protein Anosmin-1, which competes with bFGF for its binding site on FGFR1 (Bribian et al., 2006).

Traditional axon guidance cues also regulate OPC migration. Netrin-1 is a chemoattractant for migrating OPCs that express DCC in the developing optic nerve, but a repellent for OPCs migrating away from the spinal cord ventral midline (Jarjour et al., 2003; Spassky et al., 2002;

Tsai et al., 2003). In the developing spinal cord, migrating OPCs express the netrin receptor Unc5A, in addition to DCC (Jarjour et al., 2003; Tsai et al., 2003). Experiments using optic nerve explants cultured in a collagen matrix revealed that members of the semaphorin family of guidance cues also direct OPC migration. *In vitro*, Sema 3A, expressed by mesenchymal cells surrounding the optic nerve, is a chemorepellent that prevents OPCs from dispersing away from the nerve while migrating along RGC axons (Spassky et al., 2002). On the other hand, Sema 3F, expressed at the retina, attract OPCs towards the anterior parts of the nerve (Spassky et al., 2002).

Surprisingly, chemokines CXCL1 and CXCL12 are involved in the control of OPC migration. CXCL1 decreases OPC motility *in vitro* and, in the absence of CXCL1 signaling *in vivo*, oligodendrocytes are abnormally concentrated at the spinal cord periphery. These results suggested that CXCL1, acting through its receptor CXCR2, function as a stop sign for migrating OPCs (Tsai et al., 2002). CXCL12 induces OPC motility *in vitro* and, in the absence of CXCL12 signaling *in vivo*, the number of OPCs migrating to dorsal regions of developing spinal cord is decreased (Dziembowska et al., 2005). Collectively, these findings demonstrate that multiple substrate-bound and diffusible molecules regulate OPC migration in the developing CNS.

1.3 Regulation of Oligodendrocyte cell number

OPC Proliferation

Oligodendroglia cell number is tightly regulated by mechanisms that control OPC proliferation and oligodendrocyte survival. Experimental manipulation of oligodendrocyte numbers revealed a

remarkable degree of plasticity and interplay between mechanisms that enhance and limit the final count of myelinating oligodendrocytes. Optimum oligodendrocyte cell number is critical to ensure that CNS myelinating capacity matches the axonal demand for myelination.

A relatively low number of highly proliferative OPCs migrate from germinative zones in the developing neural tube and subsequently undergo extensive local proliferation to colonize regions of future white matter (Miller et al., 1997). Many regulators of OPC proliferation also control OPC migration and the onset of differentiation. Coupling these different steps is important to provide temporal coordination to overall OPC development and myelin formation.

In addition to playing an important role during OPC migration, PDGF-A is the major regulator of OPC proliferation. PDGF-A is ubiquitously expressed in the developing CNS and its receptor PDGFαR is a marker of proliferative OPCs (Noble et al., 1988; Raff et al., 1984; Yeh et al., 1991). In PDGF-A null mice, very few OPCs and oligodendrocytes develop, whereas transgenic PDGF-A overexpression increases the abundance of these cells *in vivo* (Calver et al., 1998; Fruttiger et al., 2000; Fruttiger et al., 1999). These findings indicated that rates of OPC proliferation are directly related to the levels of PDGF-A in the developing CNS. Interestingly, *in vivo* levels of PDGF-A are not sufficient to induce OPC proliferation *in vitro*, unless OPCs are cultured on a substrate containing ECM ligands (Baron et al., 2002). In this case, PDGFαR and αVβ3 integrin interact at the OPC plasma membrane and signal through the PI3K/PKC pathway to promote proliferation (Baron et al., 2002). Tenascin-C is an ECM ligand that binds to αVβ3 integrin and Tenascin-C-deficient mice display reduced rates of proliferation in different regions of developing white matter (Garcion et al., 2001). Moreover, the migration-relevant β1 integrin chain is downregulated whereas β3 integrin expression is upregulated during the time OPCs stop

to migrate and begin to proliferate in response to PDGF-A (Blaschuk et al., 2000; Milner et al., 1996). This suggests that changes in the composition in the integrin complex might underlie the switch in response that OPCs make to PDGF-A.

CXCL1 signaling is another regulatory mechanism contributing to the migration-proliferation transition during OPC development. This chemokine provides a stop signal for migrating OPCs while acting synergistically with PDGF-A to promote proliferation *in vitro* (Robinson et al., 1998). Deletion of the CXCL1 receptor CXCR2 reduces OPC numbers in the developing spinal cord, indicating that CXCL1 regulation of OPC proliferation is also relevant *in vivo* (Tsai et al., 2002).

Like PDGF-A, bFGF is expressed throughout the developing CNS (Ernfors et al., 1990). It promotes proliferation and prevents OPC differentiation *in vitro* (Fok-Seang and Miller, 1994; Gard and Pfeiffer, 1993; McKinnon et al., 1990). No changes in proliferation were observed in bFGF null mouse, although, in this mouse model, oligodendrocytes do differentiate prematurely (Murtie et al., 2005).

Oligodendrocyte survival

Early studies revealed a surprising discrepancy between the numbers of OPCs formed during initial stages of development and the numbers of mature oligodendrocytes myelinating axons postnatally. This analysis estimated that as much as 50% of OPCs generated in the developing chick neural tube undergo apoptosis during differentiation (Barres et al., 1992). Fate-mapping studies showing that entire OPC lineages are eliminated in the postnatal nervous system reinforced the notion that survival mechanisms regulate oligodendroglia cell number during

development (Kessari et al., 2006). Oligodendrocyte survival is clearly coupled to OPC proliferation since increased rates of proliferation in PDGF-A overexpressor mice were subsequently compensated by increased levels of apoptosis. Conversely, reduced apoptotic levels were coincident with the diminished proliferation rate observed in Tenascin-C knockout mice (Calver et al., 1998; Garcion et al., 2001). As a result, final numbers of myelinating oligodendrocytes were normal in the two mouse lines and myelination proceeded without further abnormalities.

Regulation of oligodendrocyte survival was proposed to result from oligodendrocyte competition for factors that are limited in the developing CNS. These include PDGF-A, neuregulin-1, laminin-2α and IGF-1 (Barres et al., 1992; Barres and Raff, 1999). Pro-survival signaling initiated by PDGF-A can be dissociated from that promoting OPC migration and proliferation, as it requires the function of a different integrin, α6β1, which interacts with PDGFαR at the plasma membrane. Consistently, block of α6β1 impairs OPC survival *in vitro* (Frost et al., 1999). Neuregulin-1 binds to oligodendrocyte receptor ErbB and signals through PI3K/Akt pathway to induce survival (Canoll et al., 1999; Fernandez et al., 2000; Flores et al., 2000). Neutralization of endogenous Neuregulin-1 increases OPC cell death, whereas additional neuregulin-1 reduces apoptotic levels in developing optic nerve (Fernadez et al., 2000). ECM ligand Laminin-2α binds to α6β1 integrin, which associates with ErbB to activate MAPK signaling and reinforce Neuregulin-1 pro-survival signaling (Colognato et al., 2004). Consistently, laminin-2α knockout mice develop fewer oligodendrocytes in spinal cord white matter (Chun et al., 2003). Finally, Insulin-like Growth Factor 1 (IGF-1) binds to its receptor IGF-1R and also activates PI3K/Akt pro-survival signaling (Pang et al., 2007). Alternatively, it acts synergistically with bFGF to

activate ERK1/2 pathway and promote proliferation (Frederick et al., 2007; Frederick and Wood, 2004; Mi et al., 2004).

1.4 OPC Differentiation

Cell cycle-exited OPCs undergo dramatic changes in morphology and gene expression as they differentiate into myelinating oligodendrocytes. Intracellular signaling regulating actin polymerization drives the extension of numerous cellular processes that further develop into axon-ensheathing myelin membranes. The myelin program of gene expression is activated and proteins such as 2', 3'-Cyclic-Nucleotide 3'-Phosphodiesterase (CNP), Myelin Associated Glycoprotein (MAG), Proteolipid Protein 1 (PLP) and Myelin Basic Protein (MBP) are expressed.

OPC differentiation is a major checkpoint during oligodendrocyte development. Inhibitory signaling initiated by mitogens and axon-derived factors prevents precocious OPC differentiation when OPC numbers are too small or axons are not ready for myelination. As a result, OPCs maintain their precursor properties for days-weeks and some of them will only differentiate during adulthood. Contrary to OPCs, the immature/pre-myelinating oligodendrocyte is a transient cell, which rapidly differentiates into a myelinating oligodendrocyte or undergoes apoptosis. This results from feed-forward regulatory mechanisms that accelerate differentiation and allow for the appearance of mature oligodendrocytes shortly after differentiation has started. Because OPC differentiation and myelination are coupled to each other, mechanisms that regulate differentiation often regulate myelination. Some of these mechanisms are discussed below, others are discussed in the next topic of this section.

Leucine-rich repeat and immunoglobulin domain containing 1 (LINGO-1) is a transmembrane protein originally identified as a myelin associated inhibitor of neurite outgrowth (Mi et al., 2004). Later, it was found that LINGO-1 protein expressed at the axonal membrane binds *in trans* with LINGO-1 expressed by OPCs to inhibit oligodendrocyte differentiation. LINGO-1 inhibitory signaling in OPCs involves Fyn kinase inhibition and activation of RhoA GTPase (Jepson et al., 2012; Mi et al., 2005).

G-protein-coupled receptor 17 (GPR17) is an oligodendrocyte-specific receptor, transiently expressed in OPCs, which inhibits oligodendrocyte differentiation. *In vitro,* GPR17 activation increases the expression and induces the translocation to the nucleus of inhibitory transcriptional factors ID2 and ID4 (Chen et al., 2009). These bHLH transcription factors interact with Olig1, preventing Olig1-induced transcription of pro-differentiation factors (Samantha and Kessler, 2004). In GPR17 knockout mice, the onset of myelination is premature, indicating that GPR17 inhibits OPC differentiation *in vivo* (Chen et al., 2009).

Jagged-1 and Delta-1 are neuronal proteins presented at the axonal surface. Binding to Notch-1 at the OPC plasma membrane promotes cleavage of the Notch intracellular domain. This fragment translocates to the nucleus and activates inhibitory transcriptional factors Hes1 and Hes5 (Wang et al., 1998). Part of the function of Hes transcription factors involves inhibition of the pro-differentiation factor Sox10 (Liu et al., 2007).

The Wnt signaling is another neuron-derived mechanism controlling OPC differentiation. Wnt binds to its receptor Frizzled, expressed by OPCs. Frizzled activation induces β-catenin to

translocate to the nucleus, where it interacts with the inhibitory transcriptional factor Tcf4 and blocks OPC differentiation (Huang et al., 2012; Shimizu et al., 2005).

Extracellular signals that promote OPC differentiation include Thyroid hormone (T3) and IGF-1. *In vitro*, T3 inhibits proliferation and promotes differentiation of rodent OPCs (Barres and Raff, 1994; Gao et al., 1997), whereas, *in vivo,* hypo and hyperthyroidism induce deficient and precocious myelination, respectively (Marta et al., 1998; Rodriguez-Pena et al., 1993). Consistently, myelination defects are observed in patients with congenital human hypothyroidism (Gupta et al., 1995; Jagannathan et al., 1998). In addition to a role on OPC survival, IGF-1 might also be involved in OPC differentiation, as IGF-1 or IGF-1R knockouts have reduced number of mature oligodendrocytes and decreased myelin gene expression (Ye et al., 2002; Zeger et al., 2007). Conversely, *in vivo* IGF-1 overexpression leads to increased oligodendrocyte number, expression of myelin genes and myelin thickness (Carson et al., 1993; Ye et al., 1995). IGF-1 induces a sustained increase in Akt signaling, a pathway involved in OPC survival and differentiation. Transgenic overexpression of a constitutively active form of Akt enhanced myelination in the murine CNS, but not PNS (Flores et al., 2010). In addition, downregulation of PTEN, an Akt pathway repressor, results in hypermyelinated brain and spinal cord (Goebbels et al., 2010).

The majority of inhibitory pathways preventing OPC differentiation converge on the activation of inhibitory transcription factors such as ID2, ID4, Hes1, Hes5, Tcf4 and Sox6. The pro-differentiation signaling initiated by T3 and IGF-1 is reinforced by additional regulatory mechanisms that release OPCs from this inhibitory influence. *In vitro*, miRNAs miR-219 and miR-338 directly target and down regulate the levels of ID2, ID4, Hes5 and Sox6, in addition to

down regulating PDGFαR (Dugas et al., 2010; Zhao et al., 2010). Knockout mice null for Dicer, a key enzyme in miRNA biogenesis, are hypomyelinated, suggesting that miR-219 and miR-338 are also necessary for OPC differentiation *in vivo* (Dugas et al., 2010). Activation of Histone Deacetylases (HDAC) also contributes to remove this "brake" on oligodendrocyte differentiation. *In vivo* administration of valproic acid (VPA), a specific inhibitor of HDACs, resulted in hypomyelination and delayed expression of mature oligodendrocyte markers, in addition to retained expression of inhibitory transcription factors (Shen et al., 2005a). During remyelination, down regulation of inhibitory transcription factors was associated with HDAC recruitment to promoter regions, suggesting that HDAC-mediated down regulation of inhibitory transcription factors might also be involved in myelin repair (Shen et al., 2008).

1.5 Myelination

As OPCs differentiate, they extend an elaborate network of cell processes. The highly dynamic edges of these processes are able to sort out, contact and wrap axons. As membrane extension continues, the nascent myelin segment grows both radially and longitudinally along the axon to form the myelin internode. Time-lapse imaging studies indicate that this is a very rapid process, which is complete in only 5 hours in zebrafish (Watkins et al., 2008).

Early observations on the ultrastructure of developing myelin suggested that myelin forms by the continuous homogeneous growth of the inner mesaxon around the axon along the entire internode length. In this model, known as the "carpet crawler", the myelinating oligodendrocyte process first extends along the axon segment and then around it, with new myelin layers added underneath the previously deposited, innermost membrane (Bunge et al., 1989). Although a

widely accepted model, uniform thickening of the myelin sheath is not consistent with the observation that the number of myelin layers varies along the internode length during myelin formation (Knobler et al., 1976). This has been revised in recent models where the leading edges of myelin grow along the length and circumference of the axon simultaneously (Snaidero et al., 2014; Sobottka et al., 2011). Alternatively, a model for myelination has been proposed, in which the oligodendrocyte process coils in a spiral around the axons, followed by lateral growth of the individual layers (D. Colman, unpublished). This "Yo-yo" model builds on the observation of a Caspr immunopositive coil around the axon that mirrors the coiling of the oligodendrocyte process during myelin formation (Pedraza et al., 2009). This observation implies that stable axoglial interactions form very early during myelination, which challenges the idea that myelin can grow by the addition of new membranes underneath the innermost layer.

Not every axon is myelinated in the nervous system. In the PNS, 1 μm or larger caliber axons are myelinated while smaller diameter axons are not. In the CNS, the axon caliber cut off is lower and axons as small as 300 nm in diameter are myelinated. Axon caliber is not only important for axon target selection; it is also a direct determinant of myelin thickness: larger caliber axons have thicker myelin. These observations indicate that, in addition to neuron-glia signaling, the biophysical properties of axons are important for target selection. In fact, rat OPCs co-cultured with DRG neurons *in vitro* retained the capacity to wrap axons even when neurons were para-formaldehyde fixed before the addition of OPCs (Rosenberg et al., 2008). Moreover, OPCs were able to concentrically wrap inert glass nanofibers, as visualized by immunostaining for MBP and electron microscopy (Lee et al., 2012). Interestingly, OPCs "myelinated" glass fibers as small as 400 nm in diameter, a caliber that approaches the minimum diameter of axons that are

myelinated *in vivo*. While oligodendrocyte wrapping of fixed axons and glass nanofibers does not recapitulate all the features that myelination exhibits *in vivo*, it does indicate that target selection and initial axon wrapping can occur in absence of neuron-glia signaling and that biophysical properties can instruct these processes.

Neuron-derived signals, on the other hand, have been demonstrated to play an important role on myelination *in vivo*. These regulatory mechanisms control OPC differentiation, membrane extension, axon target selection and myelin thickening. Often, one mechanism regulates more than one process and the same process is regulated by multiple compensatory mechanisms functioning in parallel. In fact, thus far, no single molecule has been shown to be absolutely essential for myelin formation in the CNS.

Poly-Sialylated Neural Cell Adhesion Molecule (PSA-NCAM) down regulation at the axonal surface coincides with the onset of myelination and myelination proceeds exclusively along axons that do not express PSA-NCAM (Charles et al., 2000). Removal of PSA moieties induces a transient increase in the number of myelinated axons in the optic nerve, suggesting that PSA-molecules negatively regulate CNS myelination and that PSA-NCAM down regulation may constitute a signal for myelination onset *in vivo* (Charles et al., 2000). In the PNS, Neuregulin-1 type III (NRG-1) expression at the axon surface underlies axon sorting. Sensory neurons from NRG-1 deficient mice fail to myelinate, whereas ectopic NRG-1 expression results in myelination of small caliber axons that otherwise would not be myelinated (Taveggia et al., 2005). Although initial analysis revealed little effect following NRG-1 downregulation on CNS myelination (Brinkmann et al., 2002), recent studies indicated that hypomyelination and thinner myelin sheaths develop in the prefrontal cortex in the absence of NRG-1, suggesting that

myelination in specific CNS regions might be regulated by NRG-1 signaling (Makinodan et al., 2012).

Laminin-α2 binds to β1chain-containing integrins to signal oligodendrocyte process extension (Colognato et al., 2004). Activation of β1 integrin induces Fyn dephosphorylation at tyrosine residue Tyr531, followed by activation of Integrin-linked Kinase (IKL) and signaling to promote actin polymerization (Bauer et al., 2009; Liang et al., 2004; O'Meara et al., 2013). The Src Family Kinase Fyn is also downstream of other molecules that regulate oligodendrocyte membrane extension, such as the ligand/receptor pairs L1/Contactin and netrin-1/DCC. Signaling initiated by these molecules down regulates the activity of the RhoGTPase RhoA, resulting in process branching and membrane extension (Laursen et al., 2009; Rajasekharan et al., 2009). Consistently, Fyn knockouts display fewer myelinated axons and thinner myelin sheaths (Goto et al., 2008; Umemori et al., 1994). MAPK and PI3K/Akt signaling are also involved in the regulation of myelin growth since constitutive activation of these pathways results in increased myelin thickness *in vivo* (Ishii et al., 2013) (Flores et al., 2010).

1.6 Myelin domain formation

Discrete axoglial domains are assembled along the length of an axon as oligodendrocytes form myelin (Figure 1.2). Organization of node, paranode, juxtaparanode and internode are essential for the saltatory conduction of action potentials. For technical reasons, a large number of the studies investigating myelin domain formation have focused on the PNS. Some of these studies are mentioned below, and when possible, differences between CNS and PNS are highlighted.

Node of Ranvier

Expression of voltage-dependent Na^+ channels in the nodes of Ranvier is critical for saltatory conduction of the action potential. During development, $Na_v1.2$ is recruited to immature nodes, but $Na_v1.6$ is the predominant Na^+ channel isoform in the adult CNS (Boiko et al., 2001). In the node, Na^+ channels form highly ordered complexes, physically interacting with adhesion molecules and cytoskeletal adaptor proteins. Cell adhesion molecules include Neurofascin-186 (NF186, the 186 KDa isoform of Neurofascin) and Contactin-1 in the CNS and NF-186 and Neural-Glial-related cell adhesion molecule (NrCAM) in the PNS. Ankyrin-G and βIV-spectrin link this transmembrane complex to the underlying axonal cytoskeleton.

During early postnatal development, Na^+ channels are diffusely expressed along the axon, but become concentrated at the node as myelination proceeds (Peles and Salzer, 2000). Na^+ channel clustering could in principle be directed by mechanisms that are intrinsic to the axon, mediated by interactions with the axonal cytoskeleton. Alternatively, clustering could be instructed by a glial-derived signal, delivered to the axon at the onset of myelination. In cultures of Retinal Ganglion Cells (RGCs), maintained alone for 2.5 weeks, Na^+ channel expression remained diffuse and clustering was not observed. However, co-culture of RGC neurons with myelinating oligodendrocytes, induced extensive Na+ channel clustering at regularly spaced focal regions of axons. Na^+ channel clustering was also observed following incubation of RGC cultures with oligodendrocyte-conditioned medium, in the absence of glial contact, suggesting that a soluble signal, secreted by oligodendrocytes is sufficient to cluster Na^+ channels in the CNS (Kaplan et al., 1997). In contrast, Na^+ channel clustering was observed in peripheral sensory neurons co-cultured with Schwann cells, but not in cultures of PNS neurons alone or in the presence of

Schwann cell-conditioned medium. These findings imply that Schwann cell contact is required for Na^+ channel clustering in the PNS (Ching et al., 1999; Joe and Angelides, 1992). Additionally, clustering of Na^+ channels in sensory neurons preceded clustering of Ankyrin-G and spectrin, indicating that recruitment of Na^+ channels to future nodes does not depend on the interaction with the underlying axonal cytoskeleton (Joe and Angelides, 1992). These experiments suggested that node formation is directed by a glial-derived signal that is diffusible in the CNS and contact-mediated in the periphery.

Screening of a Schwann cell cDNA library for ligands of nodal components has identified the collagen-related protein gliomedin as a ligand for NF186 and NrCAM (Eshed et al., 2005). Gliomedin is enriched in the Schwann cell microvilli that contact the nodal axolemma and, following gliomedin knockdown, Na^+ channel, NF186 and Ankyrin-G fail to cluster in co-cultures of DRG neurons and Schwann cells. Ectopic treatment of DRG cultures with soluble gliomedin induced Na^+ channel clustering in absence of Schwann cells, indicating that gliomedin is sufficient to induce node formation *in vitro* (Eshed et al., 2005). Transgenic ablation of gliomedin impaired Na^+ clustering in axons of mouse sciatic nerve, suggesting that gliomedin is also required for PNS node formation *in vivo* (Feinberg et al., 2010). These results indicated that gliomedin is a Schwann cell-derived signal that binds NF186 and instructs node formation in the PNS. Gliomedin is not expressed in the CNS and a similar oligodendrocyte signal has not been identified thus far.

In both CNS and PNS, Na^+ channel clustering relies on NF186 expression (Sherman et al., 2005; Zonta et al., 2008). NF186 is the first axonal protein to cluster in the node of Ranvier and in neurofascin null mice, in which both NF155 and NF186 isoforms are absent, none of the

remaining nodal components are clustered. Transgenic expression of NF186 in a neurofascin null background was sufficient to rescue node formation, confirming that NF186 is the specific Neurofascin isoform necessary for node formation (Sherman et al., 2005; Zonta et al., 2008).

During development, Na^+ channel clusters are first observed as heminodes, located adjacent to individual extending internodes (Ching et al., 1999; Schafer et al., 2006; Vabnick et al., 1996). As internodes grow along the axon, heminodes of two adjacent myelin segments fuse to form a mature node, flanked by two paranodes (Dugandzija-Novakovic et al., 1995; Vabnick et al., 1996). Observation of this developmental pattern suggested that opposing paranodes, moving along the axon, function as a diffusion barrier to restrict Na^+ channel expression to the node (Pedraza et al., 2001). Consistent with this model, reintroduction of NF155 in a neurofascin null background was sufficient to rescue CNS node formation in absence of NF186. Moreover CGT-deficient mice in which paranodes are not properly formed, exhibit a diffuse distribution of Na^+ channels and increased frequency of hemi-nodes. Therefore, two independent and largely compensatory mechanisms provided by myelinating glia collaborate to direct node formation during postnatal development.

Paranode

A series of cytoplasmic glial loops that form specialized junctions with the axonal plasma membrane flanks the nodes of Ranvier on both sides (Figure 1.2). These specialized junctions resemble the septate junctions found in invertebrates and appear as electron-dense transverse bands (TBs) in EM micrographs of longitudinal sections of myelinated axons. In addition to the septate-like junctions on the axoglial interface, specialized junctions, similar to adherens and

tight junctions, provide adhesion between the glial loops. The paranode, as this myelin domain is referred to, functions as an ion diffusion barrier that prevents current loss and as a molecular sieve that segregates K+ channels to the juxtaparanode and Na+ channels to the node of Ranvier (Pedraza et al., 2001; Rosenbluth et al., 1995).

Contactin-associated protein (Caspr) was the first protein to be associated with the axoglial paranode junctions (Einheber et al., 1997). Caspr expression is initially diffuse along the axon, but becomes enriched at paranodes at the onset of myelination. Immuno-EM analysis of the distribution of Caspr protein in longitudinal sections of rat corpus callosum revealed that Caspr localizes to the axoglial paranode junctions (Einheber et al., 1997). Contactin is a GPI-anchored protein, member of the immunoglobulin superfamily, with a function in axon guidance during embryonic development (Faivre-Sarrailh and Rougon, 1997; Ranscht, 1988). Contactin clusters in the paranode during postnatal development and interact *in cis* with Caspr (Boyle et al., 2001; Rios et al., 2000). This interaction is necessary for Caspr localization at the paranode, as Caspr disperses along the axon in the absence of Contactin (Boyle et al., 2001). The glial-specific isoform of Neurofascin, NF155 (155 KDa isoform) also clusters at the paranodes around the onset of myelination. Immuno-EM analysis of NF155 indicated that it localizes to the axoglial junctions of the paranode (Tait et al., 2000). The extracellular domain of NF155 binds to cells that express Caspr and Contactin, but not to cells expressing only Contactin. In addition, both Caspr and Contactin are eluted from a column containing immobilized NF155 extracellular domain (Charles et al., 2002). In the absence of Caspr, Contactin or NF155, transverse bands are lost, the gap between the axon and glia membranes is wider, and the organization of glial loops is disrupted (Bhat et al., 2001; Boyle et al., 2001; Pillai et al., 2009; Sherman et al., 2005).

Together, these results provided evidence that Caspr and Contactin on the axonal surface and NF155 on the glial loop membrane form an adhesive complex across the axoglial interface and that this complex represents a major component of the septate-like axoglial paranode junctions. Interestingly, NF155 clusters at the paranode even in the absence of Contactin, but neither Contactin nor Caspr are enriched at the paranodes following NF155 ablation, suggesting that NF155 is an instructive signal necessary for paranode junction formation (Boyle et al., 2001; Sherman et al., 2005).

In vivo ablation of *UDP*:galactose Ceramide Galactosyl-Transferase (CGT), 3'-phosphoadenosine-5'phosphosulfate:cerebroside sulfotransferase (CST), Myelin and Lymphocyte protein (MAL) and Deleted in Colorectal Cancer (DCC) also results in defective axoglial paranode junction formation or maintenance (Bull et al., 2014; Dupree et al., 1998; Marcus et al., 2006; Schaeren-Wiemers et al., 2004). CGT is a key enzyme in the biochemical pathway that synthesizes Galactocerebroside and Sulfatide, whereas CST is necessary exclusively for Sulfatide synthesis; these major oligodendrocyte galactolipids are required for the correct partitioning of NF155 on lipid rafts (Schafer et al., 2004). MAL is a raft-associated protein with a function in protein trafficking and sorting and may be involved in NF155 distribution as well (Frank, 2000). DCC is a netrin receptor required for axon guidance and is involved in the regulation of cell-cell adhesion (Keinu-Masu et al., 1996; Srinivasan et al., 2003). DCC/netrin-1 may form an instructive signal that regulates adhesion at the paranodes.

Axoglial paranode junction disruption results in loss of axonal domain segregation, with K^+ channels generally invading the paranode and partially overlapping with Na^+ channels at the node. As a consequence, conduction velocity is substantially reduced in axons of paranode

mutants and these animals typically exhibit behavioural impairments (Boyle et al., 2001; Bhat et al., 2001; Sherman et al., 2005; Dupree et al., 1998; Marcus et al., 2006; Schaeren-Wiemers et al., 2004; Bull et al., 2014).

Juxtaparanode

The juxtaparanode is the myelin domain located under the compact myelin, adjacent to the paranode. Delayed rectifier K^+ channels cluster at the juxtaparanode, where they prevent hyperexcitation and backfiring following the generation of an action potential and contribute to maintaining the internodal resting potential (Poliak et al., 2003; Vabnick et al., 1999). K^+ channels form a complex with Transient Axonal Glycoprotein-1 (TAG-1) and Caspr-2 (Traka et al., 2002). Both TAG-1 and Caspr-2 are required for K^+ channel clustering at the juxtaparanode (Traka et al., 2002). This complex interacts with the apposing oligodendrocyte membrane through homophilic biding of axonal and myelin TAG-1 and with the underlying cytoskeleton via interaction of Caspr-2 and protein 4.1B (Traka et al., 2002; Horresh et al., 2010). In addition, juxtaparanode formation and maintenance requires intact axoglial paranode junctions, since disruption of these junctions results in loss of segregation of K^+ channels in the juxtaparanode (Boyle et al., 2001; Bhat et al., 2001; Sherman et al., 2005; Dupree et al., 1998; Marcus et al., 2006; Schaeren-Wiemers et al., 2004; Bull et al., 2014).

Internode

Multiple layers of compact oligodendrocyte plasma membrane form the myelin internode. A characteristic periodic pattern emerges in EM micrographs of transverse sections of myelin internodes, in which electron-dense Major Dense Lines (MDL) alternate with electron-light

Intraperiod Lines (IPL). The former corresponds to closely apposed cytoplasmic leaflets of the oligodendrocyte membrane, whereas the later results from the interaction between the outer leaflets of two adjacent myelin layers. MDL and IPL formation results from myelin compaction, which is largely attributed to the function of Myelin Basic Proteins (MBPs) (Aggarwal et al., 2013; Fitzner et al., 2006).

MBP is the second most abundant protein in the CNS myelin, comprising ~40% of the central myelin protein content. Four MBP isoforms, derived from alternative splicing, are developmentally regulated (Boggs, 2006). MBP is locally translated at the distal tips of oligodendrocyte processes and localizes to the cytoplasmic leaflet of oligodendrocyte plasma membrane (Colman et al., 1982; Dupouey et al., 1979). Initial evidence suggesting that MBP contributes to CNS myelin compaction derived from characterization of the naturally occurring myelin mutant Shiverer mice (Dupouey et al., 1979). A large portion of the *mbp* gene is deleted in these mice and as a result, Shiverer mice are hypomyelinated and any myelin that is formed is not compacted (Readhead et al., 1987; Roach et al., 1985). Recent investigation of MBP properties revealed that MBP binding to the cytoplasmic leaflets of oligodendrocyte membranes causes conformational changes that results in amyloid-like aggregation. Self-assembly organization of MBP into an intracellular meshwork drives protein exclusion and membrane fusion, ultimately leading to myelin compaction (Aggarwal et al., 2013; Fitzner et al., 2006).

Proteolipid protein (PLP), the most abundant CNS myelin protein, is a transmembrane protein whose recruitment to the plasma membrane is controlled by neuron-derived signals (Trajkovic et al., 2006; Wight and Dobretsova, 2004). Initial analyses of CNS myelin in PLP knockout animals did not show any abnormalities; however, in older animals, myelin becomes

disorganized and axons degenerate in the absence of PLP (Griffiths et al., 1998; Klugmann et al., 1997). These results indicate that PLP is required for myelin internode maintenance.

2 MiRNAS

2.1 RNA interference

Ectopic expression of antisense RNAs has long been used as a tool for interfering with gene expression, although early studies have generally failed to produce a robust down regulation effect on the protein output. Efficiency continued to be a limiting factor in RNA interference (RNAi) until Fire and colleagues discovered that long double-stranded RNAs (dsRNAs) are at least 2 orders of magnitude more potent in mediating gene silencing than sense or antisense strands delivered individually to cells (Fire et al., 1998). DsRNA-induced interference was in fact so effective that a few copies of dsRNA per cell were sufficient to degrade endogenous mRNAs, which in abundance surpassed by far the amount of injected dsRNA. Such surprising stoichiometry suggested that RNAi wasn't simply the result of antisense-sense RNA hybridization but that, instead, a catalytic activity was also involved. That was an important suggestion, as it implicated dsRNA-mediated regulation of gene expression as a cell endogenous mechanism.

In fact, an RNAi-resembling mechanism, known as post-transcriptional gene silencing (PTGS), had earlier been described in plants as a natural defense against viral infection and mobile genetic elements. During PTGS, mRNAs are degraded in a process proposed to be dependent on antisense RNA-target mRNA duplex formation; however, the existence of such antisense RNA

was never detected during PTGS. Hamilton and colleagues speculated that this was in part because RNAs mediating PTGS were too small to be consistently detected with traditional molecular biology tools. Indeed, using a modified protocol, they were able to detect 25 nucleotide (nt)- long sense and antisense RNAs that were homologous to the exogenous transgene used to induce PTGS (Hamilton and Baulcombe, 1999). Later, while purifying the RNAi activity-containing fraction from induced Drosophila cell extracts, Hammond and colleagues showed that the isolated fraction also contained a 25 nt RNA that was homologous to the long dsRNA used to induce interference (Hammond et al., 2000). These findings were therefore very influential in suggesting that long dsRNA-induced RNAi is actually mediated by small RNAs.

Definitive proof of the importance of small RNAs in the mechanism of RNAi came from studies by Zamore and colleagues in 2000 and Elbashir and colleagues in 2001. In addition to confirming that long dsRNAs are processed into small 21-23 nt RNAs (named siRNA by Elbashir et al.), they showed that the target mRNA is cleaved into different fragments that are between 21-23 nt in size. This pattern of cleavage product indicated that the target mRNA is cleaved at regular intervals and strongly suggested that this cleavage is directed by the 21-23 nt siRNAs generated from the long dsRNA (Elbashir et al., 2001b; Zamore et al., 2000). Additional data supporting this mechanism came from the demonstration that transfection of RNA duplexes of 21 nt, instead of the long dsRNA, are sufficient to induce RNAi (Elbashir et al., 2001a). Together, these findings established that during RNAi, long dsRNAs are processed into 21-23 nt siRNAs that guide sequence-specific degradation of target mRNAs.

2.2 MiRNAs: a new class of endogenous small non-coding RNAs

While characterizing the mechanism underlying RNAi *in vitro*, Elbashir and colleagues sought to clone the small RNAs generated after processing of long dsRNAs. Surprisingly, many of the RNAs cloned were endogenously expressed, indicating that small endogenous RNAs may regulate gene expression physiologically (Elbashir et al., 2001b). In fact, shortly after these initial findings, three groups independently reported the cloning of tens of small RNAs endogenously expressed in *C. elegans*, *D. melanogaster* and humans (Lagos-Quintana et al., 2001; Lau et al., 2001; Lee and Ambros, 2001). Given their small size, this new class of endogenous RNAs was named microRNAs (miRNAs).

Sequencing of cloned miRNAs confirmed that they are encoded in the genome and do not represent breakdown products of any known mRNA. In addition, analysis of the genomic location of miRNA sequences established that miRNAs are not endogenous siRNAs. While endogenous siRNAs would be expected to match to coding regions of proteins, none of the ~100 miRNAs were encoded into exons; instead miRNAs were located into intergenic or intronic regions. Further analysis revealed that the 21-23 nt sequences were flanked in the genome by regions with the potential to form stem-loop structures, suggesting that similar to siRNAs, miRNAs are processed from longer dsRNA precursors. Indeed, northern blot analysis using probes specific for the 21-23 nt sequences also detected ~70 nt-long species corresponding to the putative miRNA precursor (pre-miRNA). Finally, miRNA genes were occasionally found to be tightly clustered in regions of the genome, forming presumably single transcriptional units. Further northern blot analysis indicated that some miRNAs are regulated during development and confirmed that miRNAs also exist in fish, frog and mouse. Evidence of regulated expression

and conservation across species suggested that this new class of small RNAs is functionally relevant (Lagos-Quintana et al., 2001; Lau et al., 2001; Lee and Ambros, 2001).

Although miRNAs as a large class of small RNAs were described only in 2001, the first discovered miRNA was reported almost ten years before (Lee et al., 1993; Wightman et al., 1993). Lin-4 is a *C. elegans* gene shown to transcribe a small (22 nt) non-coding RNA. A second RNA product transcribed from the lin-4 gene is ~70 nt in length and was predicted to form a stem-loop like secondary structure (Lee et al., 1993). Interestingly, lin-4 small RNAs were found to be partially complementary to a motif in the 3' untranslated region (UTR) of another heterochronic gene, lin-14. Lin-14 is developmentally down regulated at the protein level through a mechanism that is dependent on its 3'UTR and lin-4 expression (Wightman et al., 1993). Failure to down regulate lin-14 protein levels results in the expression of inappropriate developmental programs at late stages of development. At the time, the authors concluded that lin-4 controls developmental timing through the regulation of lin-14 gene expression and that lin-14 is down regulated at the protein level through the binding of lin-4 to lin-14 3'UTR. A second small RNA gene also controlling developmental timing in *C. elegans* was later described. Let-7 gene was shown to code for a 21 nt-long RNA that post-transcriptionally regulates lin-41 gene expression through binding to its 3'UTR (Reinhart et al., 2000). Since lin-4 and let-7 RNAs are critical regulators of developmental timing they were originally named "short temporal RNAs" (stRNAs), but were later recognized as the "founding" members of the large miRNA class of small RNAs. Functional insights provided by the early description of lin-4 and let-7 combined with the new findings on miRNA expression, abundance and biogenesis helped to establish that: 1) miRNAs are an evolutionary conserved and abundant class of endogenous small (21-23 nt)

non-coding RNAs derived from the processing of longer dsRNA precursors and 2) they regulate gene expression at the post-transcriptional level through direct binding to complementary motifs located in the 3'UTR of target mRNAs.

2.3 MiRNA biogenesis

In 2001, Bernstein and colleagues, while studying RNAi in Drosophila, were able to physically separate RNAi effector and initiator activities through extensive centrifugation. While the effector activity was previously associated with an enzymatic complex loaded with a guiding siRNA (the RNA-induced silencing complex, RISC) (Hammond et al., 2000), the initiator activity was assumed to be mediated by a putative ribonuclease (RNase) that is able to process long dsRNAs into siRNAs. Many members of the dsRNA-specific RNase III family were tested in an RNAi *in vitro* system and the previously uncharacterized RNase III CG4792 was found to produce 22 nt RNA fragments when incubated with extracts of cells transformed with dsRNA (Bernstein et al., 2001). Dicer, as it was named after its ability to cleave dsRNAs, was further validated as the RNAi initiator activity after specific knockdown of this enzyme disrupted siRNA generation and RNAi *in vitro* (Bernstein et al., 2001). Since initial findings predicted that miRNAs were also processed from longer dsRNA precursors (pre-miRNAs), Dicer was tested for its ability to generate mature miRNA sequences from pre-miRNAs. Indeed, dicer knockdown dramatically decreased the amount of mature let-7 miRNA formed and induced the accumulation of the pre-let-7, indicating that the same enzyme processes siRNA and miRNAs from longer dsRNAs.

MiRNAs found to be tightly clustered in the genome were predicted to transcribe together into long polycistronic transcripts. RT-PCR studies showed that, in fact, large amplification products, longer then the ~70 bp product that would be expected for pre-miRNAs are detected when primers are designed to amplify the entire region spanning miRNA clusters. Surprisingly, large products were also detected for non-clustered miRNAs, indicating that pre-miRNAs may be derived from longer primary transcripts (pri-miRNAs) in general (Lee et al., 2002). Interestingly, these large pri-miRNAs can be processed *in vitro* by cellular extracts into pre-miRNAs, which in turn can also generate mature 22 nt-long miRNAs (Lee et al., 2002). As pri-miRNAs accumulate in the nucleus, but not in the cytoplasm (Lee et al., 2002) the nuclear-specific RNAse III Drosha seemed to be an interesting candidate for the catalytic activity that processes these long transcripts. As expected, Drosha immunoprecipitates are able to process pri-miRNAs into pre-miRNAs *in vitro*. Furthermore, Drosha knockdown leads to the accumulation of pri-miRNAs and depletion of detectable pre-miRNA (Lee et al., 2003).

As pre-miRNAs are produced in the nucleus but processed into mature miRNAs in the cytoplasm, a mechanism must exist to transport pre-miRNAs across the nuclear envelope. In fact, nuclear export of pre-miRNAs injected in the nucleus of Xenopus oocytes can be saturated by competing pre-miRNAs, indicating that pre-miRNA export is carrier-mediated (Lund et al., 2004). Exportin-5 was an interesting candidate to export pre-miRNAs because it is known to mediate the transport of small mini-helix containing RNAs. As expected, saturation of pre-miRNA export by competing pre-miRNAs is alleviated by exportin-5 overexpression. In addition, knockdown of exportin-5 decreases the levels of mature miRNAs in the cytoplasm

indicating that this nuclear carrier mediates pre-miRNA export to the cytoplasm (Lund et al., 2004).

Together, these findings suggested a step-wise model for miRNA biogenesis in which: 1) miRNA genes are transcribed as long primary transcripts, named pri-miRNAs, which are processed in the nucleus by Drosha (alternatively, intronic pri-miRNAs can be processed by the splicing machinery), generating the ~70 nt-long pre-miRNAs. 2) Pre-miRNAs are then exported from the nucleus through the carrier exportin-5 and, once in the cytoplasm, 3) they are further processed by Dicer to generate 21-23 nt mature miRNAs (Figure 1.3A).

2.4 miRNAs regulate gene expression

Functional insights provided by the study of RNAi and the early characterization of lin-4/let-7 suggested that small RNAs are negative regulators of gene expression. These early studies also indicated that miRNAs bind specifically to 3' UTR motifs located in the target mRNAs and that translational repression, rather than mRNA destabilization, is the preferential mechanism underlying miRNA control of gene expression (Reinhart et al., 2000; Wightman et al., 1993). As predicted, computational analysis found that several miRNAs are partially complementary to regions in the 3'UTR of many mRNAs, including UTR motifs known to mediate negative post-transcriptional regulation (Lai, 2002). Surprisingly, complementarity between miRNAs and putative targets was limited to ~ 8 nt and complementary sites were exclusively located at the 5' end of miRNAs. This partial complementarity rather than the perfect base-pairing featured in RNAi led to the prediction that not one, but multiple targets are regulated by each miRNA (Lai, 2002). In fact, ectopic overexpression of miR-1 followed by microarray analysis of gene

expression detected 84 non-redundant mRNAs that were down regulated and contained miR-1 binding sites at their 3'UTRs (Lim et al., 2005). Similar experiments carried out in a miRNA knockout system confirmed that endogenous miRNAs directly regulate the expression of dozens of genes (Baek et al., 2008; Selbach et al., 2008). In addition, the identification of target genes that are down regulated after manipulation of miRNA levels helped to better characterize the base-pairing requirements for functional miRNA targeting. It was determined that predicted mRNA targets have in their 3' UTRs at least one motif that is complementary to nucleotides 2-7 in the miRNA sequence (the seed region) in addition to an Adenosine pairing with the first miRNA nucleotide and/or an extra complementary nucleotide at miRNA position 8 (Baek et al., 2008) (Figure 1.3B). Consistent with these requirements, mutations in the seed region of miR-1 and miR-124 drastically changed the set of genes down regulated in response to ectopic miRNA expression (Lim et al., 2005). Currently, many software applications exist that use experimentally-derived rules to predict miRNA targets with good rates of confidence (for a review describing miRNA target prediction see (Rajewsky, 2006)).

Although lin-4 and let-7 regulation had been originally described as a form of translational repression, rather than mRNA destabilization, it was clear from the findings described above that mRNA degradation is an important component of miRNA control of gene expression (Baek et al., 2008; Lim et al., 2005). Interestingly, these studies also indicated that, while targeting many different genes, the impact of an individual miRNA on protein expression is often modest, suggesting that combinatorial regulation of miRNAs might be important and that miRNAs are relatively fine regulators of the protein output (Baek et al., 2008). In summary, studies of miRNA function led to the conclusion that miRNAs are negative post-transcriptional regulators

of gene expression that target dozens of different mRNAs containing seed-matched motifs at their 3' UTR. These studies additionally indicated that miRNAs regulate gene expression by inducing mRNA destabilization and/or translational repression.

2.5 miRNAs are critical for normal development and physiology of adult animals

miRNA effects on gene expression suggested that this class of small RNAs is a key element in the coordination of developmental programs of gene expression. Definitive evidence establishing that miRNAs are important during development was provided by zebrafish and mice dicer mutants. Dicer activity is disrupted or non-existent in these animal models and, as a consequence, mature miRNA levels are negligible. In the absence of miRNAs and miRNA regulation of gene expression, developmental growth is arrested and embryos die early in the development, indicating that miRNA-deficient animals are not viable (Bernstein et al., 2003; Wienholds et al., 2003). For that reason, several conditional dicer knockouts were generated to test miRNA function in specific contexts. Developmental deficiencies were reported for every dicer mutant examined, indicating that miRNAs are critical to the development of several tissues and organs. The extensive list of tissues and cell-types in which dicer deletion has revealed a developmental function for miRNAs includes brain cortex and hippocampus (Davis et al., 2008), neural crest cells (Zehir et al.), lens and corneal epithelium (Li and Piatigorsky, 2009), heart (Huang et al.), vascular smooth muscle (Pan et al.), T lymphocytes (Muljo et al., 2005), B lymphocytes (Koralov et al., 2008), lung epithelium (Harris et al., 2006), liver (Sekine et al., 2009), kidney (Nagalakshmi et al.), pancreatic islets (Lynn et al., 2007), adipose tissue (Mudhasani et al.), chondrocytes (Kobayashi et al., 2008), osteoclasts (Sugatani and Hruska,

2009), thyroid gland (Frezzetti et al.), among others. Specific miR-deficient mutants also supported the importance of miRNAs during development. Naturally occurring lin-4 loss-of-function and lin-14 gain-of-function (a lin-14 variant that is not sensitive to lin-4 regulation) mutations lead to inappropriate activation of early developmental programs in late stages of *C. elegans* development (Ambros and Horvitz, 1987).

In addition to reveal a key function for miRNAs during development, miR-specific knockout models have suggested that these small non-coding RNAs participate in the normal physiology of adult animals. MiR-155-null mice exhibit clear signs of defective adaptive immunity, although no gross developmental defects are observed in myeloid and lymphoid organs. C-maf, a potent transcriptional activator of interleukin-4, is a target of miR-155 that is upregulated in the mutant mice and is thought to be downstream of miR-155 in normal immune activity (Rodriguez et al., 2007). In addition, as expected for a broad class of regulators, miRNA dysregulation is associated with human diseases, especially cancer. Analysis of miRNA expression in tumors has revealed altered miRNA profiles, probably because pri-miRNA transcription and pre-miRNA processing are altered in cancer cells. MiR-124a has been shown to induce CDK6 overexpression and miRNAs miR-34, miR-9, miR-151 and miR-148 promote metastasis in many different tumor types. In addition to a role in cancer, further examples of the involvement of miRNAs in human diseases include miR-208 control of stress-dependent cardiac growth (van Rooij et al., 2007), miR-206 role in delaying the progression of amyotrophic lateral sclerosis (Williams et al., 2009), miR-326 elevation in multiple sclerosis patient's active lesions and miRNAs miR-29, miR-146 and miR-107 involvement in Alzheimer's disease (for a review, see (Esteller, 2011). The fact that miRNA dysregulation is associated with several human diseases confirms that miRNA

control of gene expression is critical for the normal development and function of cells and organisms.

2.6 MiRNAs control oligodendrocyte proliferation and differentiation

Oligodendrocyte gene expression is also regulated by miRNAs. Lau and colleagues have defined a set of miRNAs that are expressed in two distinct populations of oligodendrocyte lineage cells: $A2B5^+$ $Galc^-$ OPCs and $A2B5^-$ $Galc^+$ mature oligodendrocyte. 98 miRNAs are expressed in at least one of these two populations, with 43 of these miRNAs dynamically regulated between OPCs and mature oligodendrocytes (Lau et al., 2008). Highly upregulated miRNAs include miR-223, miR-338, miR-219, miR-146 and miR-145 whereas miR-7, miR-124a, miR-449, miR-335 and miR-9 are among the most downregulated. Target bias analysis indicated that among these regulated miRNAs some might be functionally relevant during OPC differentiation. Lau and colleagues showed that miR-9 represses the translation of PMP22 mRNA. As a result, this PNS-specific protein is not expressed by oligodendrocytes even though PMP22 mRNA is found in the cytoplasm of these cells. The authors conclude that miR-9 acts as "guardian" of the oligodendrocyte transcriptome (Lau et al., 2008).

MiR-23 is another miRNA with functional properties in oligodendrocytes. MiR-23 ranks among the top 15 miRNAs that are upregulated during OPC differentiation (Lau et al., 2008). Ectopic overexpression of miR-23 in OPC cultures increases the number of MBP expressing cells and the expression of myelin genes in general (Lin and Fu, 2009). At least part of this pro-differentiation effect is mediated through the repression of LaminB1, a nuclear envelope protein that inhibits OPC differentiation and myelination *in vitro* (Lin and Fu, 2009). MiR-23 is the first of a group of

oligodendrocyte miRNAs that promote OPC differentiation by inhibiting OPC differentiation inhibitors.

In 2009, the first oligodendrocyte-specific dicer mutant was generated by Shin and colleagues. In this conditional knockout, an inducible Cre recombinase is under the transcriptional control of the PLP promoter. Recombinase activation at P14-18 promoted oligodendrocyte-specific dicer deletion and led to the appearance of hind limb ataxia, kyphosis and tremor followed by death within a year. The brains of these mutant mice are severely demyelinated and present signs of inflammation, oxidative stress and neurodegeneration. miRNA microarray and biochemical analysis indicated that miRNAs miR-219, miR-32 and miR-144 are drastically reduced in the dicer knockout mice while ELOVL7, a putative target of miR-219, is elevated. ELOVL7 is a key enzyme in the synthesis of very long chain fatty acids and as expected, increased levels of lipid inclusions were found in the brains of knockout mice (Shin et al., 2009). These findings indicated that normal oligodendrocyte physiology relies on miRNA regulation of gene expression, and that miR-219, in particular, is crucial to oligodendrocyte function.

If dicer ablation in mature oligodendrocytes revealed a critical role for miRNAs in adult brain function, OPC-specific dicer deficient mice showed that miRNAs are also required for normal oligodendrocyte differentiation and myelination (Dugas et al., 2010; Zhao et al., 2010). Dicer flox animals were crossed with lines expressing Cre recombinase under the control of Olig1 and Olig2 promoters to generate transgenic mice lacking dicer in OPCs. These animals display a shivering phenotype starting at postnatal day 9-10 and an acute loss of myelin. Interestingly, PLP^+ mature oligodendrocytes are reduced in the white matter of P24 and P60 knockout mice and OPCs purified from the mutant animals fail to differentiate *in vitro*, suggesting that an arrest

of oligodendrocyte differentiation is the probable cause of myelin deficits and behavioral defects. Microarray analysis of miRNA expression revealed that miR-219, miR-338-5p, miR-338-3p and miR-138 are the most deficient miRNAs in the spinal cord of mutant mice (Zhao et al., 2010) and also the most upregulated miRNAs during oligodendrocyte differentiation *in vivo* (Dugas et al., 2010; Lau et al., 2008). As expected, ectopic expression of these miRNAs can induce OPC differentiation *in vitro* and *in vivo*, whereas block of miRNA function prevents differentiation. In addition, miR-219, miR-338-5p, miR-338-3p and miR-138 directly regulate the expression of OPC differentiation inhibitors such as Sox6, HES5, PDGFRα, ZFP238 and FoxJ3. Therefore, similar to miR-23, these oligodendrocyte-enriched miRNAs promote oligodendrocyte differentiation and myelination by negatively regulating the expression of differentiation inhibitors (Dugas et al., 2010; Zhao et al., 2010).

Another oligodendrocyte-enriched miRNA appears to have a function during development; however, instead of regulating OPC differentiation, miR-17-92 controls oligodendrocyte cell number. MiR-17-92 knockout mice have decreased counts of Olig 2^{+} cells in the brain and overexpression of this miRNA promotes OPC proliferation *in vitro* (Budde et al., 2010). PTEN was shown to be a miR-17-92 target and at least part of the effect of miR-17-92 on cell proliferation is mediated through the down regulation of PTEN and increased Akt signaling.

The findings summarized above illustrate how critical miRNAs are in the context of myelin biology. In fact, efficient control of gene expression is a major aspect of oligodendrocyte physiology, largely because of the requirement for massive protein synthesis during myelination. Moreover, gene expression must be tightly regulated in oligodendrocytes as altered myelin

protein dosage leads to disease. Myelinating oligodendrocytes are therefore a good model to study gene expression regulation, including regulation provided by miRNAs.

3 TMEM10

Transmembrane protein 10 (TMEM10), also known as Oligodendrocytic Myelin Paranodal and Inner Loop protein (Opalin), was identified in the search for gene products that are highly expressed in the mammalian brain (Bangsow et al., 1998; Nobile et al., 2002; Yoshikawa et al., 2008). The original TMEM10 sequence was cloned from a cDNA library from porcine brain (Bangsow et al., 1998), but conserved TMEM10 orthologues were also isolated from murine and human libraries (Yoshikawa et al., 2008; Nobile et al., 2002). Despite being largely conserved among mammalian species, no TMEM10 orthologues were found in BLAST searches against the genome of other vertebrate groups, including those from chick, zebrafish and pufferfish, suggesting that TMEM10 might be a mammalian-specific gene (Aruga et al., 2007). The mouse TMEM10 gene is composed of 6 exons and 5 large introns, spanning through 13.7 Kb of the genome. Tolloid-like 2 (Tll2) is located upstream of TMEM10, whereas Deoxinucleotydil transferase (Dntt) is located downstream of it. Interestingly, these and other neighboring genes were identified in non-mammalian vertebrate groups, although arranged in a different order (Aruga et al., 2007). This suggests that mechanisms of local genomic rearrangement may have led to the appearance of TMEM10 in a mammalian ancestor.

Analysis of the predicted protein sequence and structure indicated that TMEM10 encodes a protein of 143 amino acids (mouse orthologue, predicted molecular weight of 15.8 KDa) with a single transmembrane domain (amino acids 31-53 of the mouse orthologue; Bangsow et al.,

1998; Nobile et al., 2002; Yoshikawa et al., 2008). Western blot analysis of avidin-precipitated biotinylated cell lysates and live staining of non-permeabilized cells confirmed that TMEM10 is located at the plasma membrane (Golan et al., 2008; Kippert et al., 2008). Multiple putative N- and O- glycosylation sites were identified in the N-terminal extracellular domain of TMEM10 (amino acids 1-30 of the mouse orthologue). Post-translational modifications were expected because TMEM10 protein runs as a broad band, centered at approximately 37 KDa, in SDS-PAGE gels (Yoshikawa et al., 2008). Enzymatic deglycosylation of cell extracts using N-glycosidase F, O-glycosidase and neuraminidase confirmed that TMEM10 is heavily glycosylated and that a fraction of TMEM10 carbohydrates is additionally sialylated. Mutational experiments mapped glycosylation sites to Asn-6, Asn-12 and Thr-14, and indicated that glycosylation at these residues is necessary for correct localization of TMEM10 at the plasma membrane (Yoshikawa et al., 2008; Golan et al., 2008). The intracellular domain (amino acids 54-143 in the mouse orthologue) lacks any obvious homology with known protein domains; however, several consensus sites for phosphorylation were described within the TMEM10 C-terminal region (Golan et al., 2008; Yoshikawa et al., 2008) (Figure 1.4).

Initially, TMEM10 was isolated as a brain-enriched gene (Bangsow et al., 1998; Nobile et al., 2002). Additional evidence confirming preferential expression in the nervous system was provided by RT-PCR and Western blot analyses of tissue lysates derived from several body organs, including thymus, lung, heart, liver, spleen, kidney and testis. In addition to brain, only liver showed some level of TMEM10 expression (Golan et al., 2008; Yoshikawa et al., 2008). Sequence analysis of the TMEM10 locus in twelve mammalian species revealed a phylogenetically conserved region in the first TMEM10 intron. When this 490 bp-long sequence

was cloned upstream of a reporter cassette and expressed *in vivo* in transgenic mice, a strong and specific signal was detected in CNS white matter (Aruga et al., 2007). Further immunohistochemical analysis showed that this Opalin Oligodendrocyte Enhancer (OOE) directs reporter expression to MBP-TMEM10 double positive cells of the white matter, indicating that TMEM10 is expressed by oligodendrocytes and that OOE exerts a crucial role in restricting the spatial pattern of TMEM10 gene expression (Aruga et al., 2007). *In situ* hybridization and immunolabelling of brain sections confirmed that TMEM10 is highly expressed in white matter-enriched regions (Yoshikawa et al., 2008; Golan et al., 2008) while double immunocytochemistry for TMEM10 and different cell lineage markers showed that TMEM10 is expressed by oligodendrocytes but not neurons, astrocytes or microglia (Kippert et al., 2008). Consistent with oligodendrocytes being the primary source of TMEM10 in the brain, a 23-fold downregulation of TMEM10 transcript levels was observed following genetic ablation of oligodendrocytes in transgenic mice (Golan et al., 2008). Both *in vitro* and *in vivo*, TMEM10 staining localizes to the oligodendrocyte cell body and processes. In addition, a spiral of TMEM10 protein is detected along myelin internodes, where it colocalizes with MAG, and at the paranodes, where it colocalizes with Caspr. Immuno-electron microscopy of myelinated fibers confirmed that TMEM10 is enriched at the inner and outer membranes of internodes and at the glial loops of myelin paranodes (Yoshikawa et a., 2008; Golan et al., 2008). Interestingly, TMEM10 expression was absent from PNS (Golan et al., 2008). Taken together, these studies indicate that TMEM10 is a CNS-specific myelin glycoprotein, associated with the plasma membrane of oligodendrocyte soma, processes and non-compact membranes of myelinated fibers.

The developmental timing of TMEM10 expression has also been studied. RT-PCR analysis of brain tissue extracts has shown that TMEM10 transcripts are initially detected at P9. Western blot and immunohistochemical studies indicated that TMEM10 protein begins to be expressed around the same time, depending on the CNS region. Thereafter, TMEM10 continues to be expressed and is found at high levels in the adult brain (Golan et al., 2008; Yoshikawa et al., 2008). *In vitro*, TMEM10 is first detected in 2 DIV OPC cultures, associated with cells that are double positive for NG2 and O4, but not in O4 negative OPCs. Differentiating and mature cells that express the mature marker MBP also express TMEM10 (Kippert et al., 2008). The OOE enhancer contains binding sites for CREB and Myt1, two transcription factors involved in the regulation of oligodendrocyte differentiation. DNA gel shift assays showed that these transcription factors physically interact with OOE, suggesting that TMEM10 expression is up regulated during OPC differentiation by these regulatory proteins. Indeed, TMEM10 was the most up regulated transcript during neuron-conditioned medium-induced differentiation of the oligodendroglial-like oli-neu cell line, an *in vitro* model for OPC differentiation (Kippert et al., 2008). In addition, TMEM10 was among the top 50 up regulated genes during primary OPC differentiation *in vitro* (Dugas et al., 2006). These observations indicated that TMEM10 is up regulated during OPC differentiation and myelination and that TMEM10 expression is maintained in the adult brain.

The functional significance of TMEM10 is yet to be established. A role in differentiation and myelination has been suggested because TMEM10 is highly up regulated in the brain as OPCs differentiate and myelinate axons *in vivo* (Golan et al. 2008, Kippert et al., 2008). Because expression continues in the adult brain, TMEM10 might also have a function in the mature CNS.

The localization of TMEM10 at the plasma membrane and distribution to the cell body, processes and non-compact membranes is consistent with a function that depends on an interaction with cytoplasmic components, possibly in transmembrane signal transduction. Putative phosphorylation sites on the intracellular region are consistent with a signaling role. Interestingly, TMEM10 colocalizes with actin filaments in thin cellular processes, and in the absence of an intact actin cytoskeleton a fraction of TMEM10 is relocated from the plasma membrane to the cytoplasm (Kippert et al., 2008). Expression at the paranode loops and myelin inner membrane suggests that TMEM10 may alternatively participate in an intermembranous function, regulating adhesive mechanisms between glial loops or axon-glia membranes (Yoshikawa et al., 2008). Sialic acids located on the extracellular domain of TMEM10 may provide hydrophilicity to the cell surface and may be relevant for cell-cell interaction in non-compact myelin membranes (Rutishauser and Landmesser, 1996). Interestingly, MAG, which is also localized to inner membranes of myelinated axons, binds sialic acid residues and contributes to myelin maintenance (Crocker, 2002). Further studies will be necessary to test these hypotheses and define a function for TMEM10.

4 Netrins

4.1 The netrin family

During development, axons extend considerable distances along stereotyped pathways before reaching their final targets. Guidance to this process can be provided by short-range cues that are bound to the substrate or expressed on the surface of encountering cells. In addition, axon guidance can be mediated by diffusible cues that are secreted by the target and act at a distance.

Ramón Y Cajal had hypothesized the existence of such long-range guidance mechanism on the light of his observations on the anatomy of embryonic spinal cord (Cajal, 1909). There, dorsally located commissural neurons project axons towards the ventrally located floor plate, suggesting that a diffusible signal, secreted by the floor plate, and distributed as a gradient along the dorsal-ventral axis, directs commissural axon extension. Initial evidence supporting this hypothesis was provided by experiments in which dorsal embryonic spinal cord explants were cultured in a collagen matrix gel alone or in the presence of dissected floor plates. In these co-cultures, floor plates were positioned a few hundred micrometers away from dorsal spinal cord explants and orientated perpendicularly or parallel to the original dorsal-ventral axis. Only when cultured in the presence of floor plates, commissural axons extended beyond the spinal cord explant, into the matrix gel. In addition, outgrowing axons were invariably attracted to the floor plate, even when axons had to deviate from their original trajectory to reach floor plates that were positioned parallel to the dorsal-ventral axis. These experiments showed that floor plate cells are able to direct commissural axon extension at a distance and suggested, as predicted by Ramon Y Cajal, that a diffusible chemotropic factor (s), secreted by these cells, must exist (Tessier-Lavigne et al., 1988).

Two factors, containing a similar commissural axon outgrowth-promoting activity, were isolated from the embryonic chick brain (Serafini et al., 1994). They were named netrin 1 and 2, after the Sanskrit word “netr”, which means “one who guides”. Cloning of the genes encoding these proteins revealed that netrins shared homology with the *Caenorhabditis elegans* UNC-6, a laminin-related protein necessary for circumferential axon extension (Ishii et al., 1992). *In situ* hybridization and immunohistochemistry analysis showed that netrin-1 is secreted by the

embryonic floor plate and forms a gradient along the dorsal-ventral axis of embryonic spinal cord (Kennedy et al., 1994; Kennedy et al., 2006). Importantly, aggregates of netrin-1 or netrin-2-expressing COS7 cells were able to mimic the chemotropic effect of floor plate explants, indicating that netrins are chemoattractant factors secreted by the floor plate during commissural axon extension (Kennedy et al., 1994). Parallel experiments using ventrally located trochlear motor neurons, which normally extend away from the floor plate, showed that netrin-1 can act as a chemorepellent for certain types of neurons (Colamarino and Tessier-Lavigne, 1995). Taken together, these results suggested that netrins are bifunctional guidance cues that mediate floor plate regulation of axon extension in the embryonic neural tube. Netrin orthologues were identified in additional invertebrate species, such as the fruit fly *Drosophyla melanogaster*, in non-mammalian vertebrates, such as the frog *Xenopus laevis*, and in mammalian species such as mouse, rat and humans (Harris et al., 1996; Manitt et al., 2001; Mitchell et al., 1996; Serafini et al., 1996). Notably, a netrin orthologue was also identified in the sea anemone *Nematostella vectensis*, suggesting that netrins have appeared very early in animal evolution, along with bilateral symmetry (Matus et al., 2006). In every animal group studied thus far, a conserved function in directing axon extension towards the ventral midline has been described for netrins. Sequence and function conservation throughout animal evolution highlights the relevance of netrins for nervous system development in animals.

In mammals, 3 secreted netrin homologues were identified: netrin-1, netrin-3 and netrin-4 (Koch et al., 2000; Wang et al., 1999; Yin et al., 2000). An orthologue for netrin-2, originally cloned from chicken, has not been identified in mammalian species. Additionally, 2 other netrin homologues, which are not secreted, were cloned in mammals and are predicted to exist in other

vertebrate groups. Netrin-G1 and netrin-G2 are glycophosphatidylinositol (GPI)-anchored netrins that have evolved independently of classic secreted netrins (Nakashiba et al., 2000).

All netrins have ~ 600 amino acids (~70 KDa) and are homologues to laminin: N-terminal region of netrins 1, 2 and 3 are related to N-terminal laminin γ1 chain, whereas netrins 4, G1 and G2 relate at the same region to laminin ß1 chain (Serafini et al., 1996; Wang et al., 1999; Koch et al., 2000; Nakashiba et al., 2000) (Figure 1.5A). Netrin N-terminal domains VI and V were named after homologue domains in laminin. Domain VI is a globular polypeptide required for netrin chemoattraction and repellence (Lim and Wadsworth, 2002). Domain V contains three epidermal growth factor (EGF) repeats and is also necessary for netrin function (Lim et al., 2002). The C-terminal region of secreted netrins, known as domain C or NTR (netrin)-like module, is rich in basic amino acids and binds to heparin and other negatively charged proteoglycans located at the extracellular matrix (ECM) and cell surfaces (Kappler et al., 2000). GPI-anchored netrin-Gs lack domain C in their structure (Nakashiba et al., 2000).

Netrins are found throughout the nervous system and in other organs and tissues during embryonic and postnatal development. Netrin-1 is expressed at the floor plate of the embryonic neural tube (Kennedy et al., 1994), cerebellum (Livesey and Hunt, 1997), visual system (Deiner et al., 1997; Livesey and Hunt, 1997; Spassky et al., 2002), olfactory system (Astic et al., 2002), forebrain (Shatzmiller et al., 2008) and in periaxonal membranes of myelinated fibers in the adult white matter (Manitt et al., 2001). Netrin-3 is found in sensory ganglia, mesenchymal cells and muscle (Wang et al., 1999), whereas netrin-4 is expressed at the lateral margins of embryonic floor plate, olfactory bulb, cerebellar granule cells, hippocampal pyramidal cells and dorsal root ganglia (Koch et al., 2000; Yin et al., 2000). Netrin-Gs have complimentary expression across

the CNS, with netrin-G1 preferentially located at dorsal thalamus, olfactory bulb and inferior colliculus and netrin-G2 at cerebral cortex, habenular nucleus and superior colliculus (Nakashiba et al., 2002). Outside the nervous system, netrins are expressed in lung, pancreas, mammary gland, vasculature, muscle, heart and kidney (Liu et al., 2004; Shin et al., 2007; Srinivasan et al., 2003; Yebra et al., 2003; Yin et al., 2000; Zhang and Cai, 2010). In addition, once development is completed, netrins continue to be expressed in the adult CNS, and are upregulated in certain pathological conditions (Bin et al., 2013; Manitt et al., 2001; Manitt et al., 2004).

4.2 Netrin receptors

Four families of receptors mediate netrin signaling during development of nervous system (Figure 1.5B). Three of them, Deleted in Colorectal Cancer (DCC), UNC5 homologues and Down Syndrome Cell Adhesion Molecule (DSCAM) are receptors for secreted netrins, whereas Netrin-G ligands are receptors for Netrin-Gs. All netrin receptors are type 1 transmembrane proteins and members of the Immunoglobulin superfamily. *In vivo* deletion of netrin receptors recapitulates the defects observed in Netrin-1 knockout mice, highlighting the importance of these receptors in mediating Netrin function during development (Ackerman et al., 1997; Fazeli et al., 1997; Lu et al., 2004; Williams et al., 2006).

Originally isolated as a candidate tumor suppressor (Fearon et al., 1990), DCC was the first netrin receptor identified (Keino-Masu et al., 1996). Its paralogue, Neogenin, shares 50% of amino acid identity and is found exclusively in vertebrates. Orthologues of DCC in invertebrate species include Frazzled in *D. melanogaster* and UNC-40 in *C. elegans* (Chan et al., 1996; Kolodziej et al., 1996). The DCC family of receptors mediates netrin-induced chemoattraction

when expressed alone and repulsion when co-expressed with UNC5 homologues. Their extracellular region comprises four Immunoglobulin-like (Ig) domains and six Fibronectin type III (FNIII) domains, with netrin proposed to bind between the fourth and fifth FNIII modules (Geisbrecht et al., 2003). The intracellular region lacks catalytic activity, but three regions, named domains P1, P2 and P3, are highly conserved across the family. Domain P1 is necessary for DCC dimerization, whereas P2 is enriched in proline residues and contains four consensus motifs for biding of SH3 domain-containing proteins. Domain P3 comprises several putative phosphorylation sites and is required for Focal Adhesion Kinase (FAK) binding and dimerization with UNC5 homologues (Hong et al., 1999; Keino-Masu et al., 1996; Ren et al., 2004; Stein et al., 2001).

The UNC5 family of netrin receptors comprises four homologues in vertebrates (UNC5A-D) (Ackerman et al., 1997; Engelkamp, 2002; Leonardo et al., 1997) and one orthologue in *D. melanogaster* and *C. elegans* (Dickson and Keleman, 2002; Keleman and Dickson, 2001; Leung-Hagesteijn et al., 1992). These receptors mediate netrin-induced chemorepulsion. Their extracellular region comprises two Ig domains, where netrins bind to, follow by two Thrombospondin type 1 domains (Leonardo et al., 1997; Geisbrecht et al., 2003). UNC5 receptor intracellular region contains a ZU5 domain, a DCC binding motif (DB motif) and a Death domain (DD). The ZU-5 domain is also present in the tight junction adaptor Zona Occludens-1 (ZO-1) and the septate-like junction adaptor Ankyrin B, and is involved in the interaction between transmembrane proteins and the actin cytoskeleton (Schultz et al., 1998). The DD domain is homologous to the death domain in dependence receptors and can induce apoptosis following cleavage by caspase-3 (Llambi et al., 2001).

DSCAM was originally identified as a gene that is duplicated in Down syndrome (Yamakawa et al., 1998). More recently, it was demonstrated that commissural axons in the developing spinal cord express DSCAM and that this receptor is required for chemoattractant responses to netrin-1 (Andrews et al., 2008; Liu et al., 2009; Ly et al., 2008). DSCAM extracellular region comprises ten Ig domains, where netrin binds to, and six FNIII domains (Ly et al., 2008).

The Netrin-G ligands are transmembrane proteins that function as receptors for Netrin-Gs, but not secreted netrins. Netrin-G ligands 1 and 2 contain one Leucine-rich Repeat domain follow by one Ig domain (Kim et al., 2006; Lin et al., 2003). They are enriched at glutamatergic synapses, where they regulate synapse formation (Woo et al., 2009).

4.3 Netrin Signaling

Initial studies on netrin function revealed that some axons are attracted to netrin gradients, while others are repelled (Kennedy et al., 1994; Colamarino et al., 1995). Observations that DCC and orthologues are required for axon extension towards the ventral midline whereas UNC5 homologues are necessary for extension away from the floor plate suggested that bifunctional responses to netrin gradients are elicited by the activation of distinct receptors (Chan et al., 1996; Colavita and Culotti, 1998; Fazeli et al., 1997; Hedgecock et al., 1990; Keleman and Dickson, 2001; Kolodziej et al., 1996; McIntire et al., 1992). The demonstration that ectopic UNC5 expression in *Xenopus* spinal axons is sufficient to convert attraction to repulsion further supported this initial conclusion. However, it also suggested that UNC5 and DCC might function together to mediate netrin repulsion because UNC5-induced switch on netrin response relied on the formation of a complex with DCC at the spinal axon plasma membrane (Hong et al., 1999).

Consistent with UNC5s functionally interacting with DCC, UNC-40 loss of function, in addition to UNC5, impairs migration away from the UNC-6 source in *C. elegans* (Hedgecock et al., 1990; McIntire et al., 1992); the same phenotype was observed with precursor cells migrating away from the floor plate at the developing mouse spinal cord (Jarjour et al., 2003). In contrast, short-range repulsion appears to be DCC independent (Keleman and Dickson, 2001; Macabenta et al., 2013; Merz et al., 2001), even in the case where DCC and UNC5 are expressed in the same cell: during *Drosophila* blood vessel formation, Frazzled and UNC5 are expressed at different plasma membrane domains of cardioblasts, with one receptor mediating adhesion and the other repulsion (Macabenta et al., 2013). These findings suggested a model where DCC and orthologues mediate chemoatraction responses to netrin whereas chemorepulsion requires UNC5 and, in some cases, the two receptors.

Alternatively, netrin bifunctionality may depend on the recruitment of different downstream effectors following activation of the same netrin receptor. This possibility is supported by *in vitro* experiments in which reduction of cAMP intracellular levels or pharmacological inhibition of Protein Kinase A (PKA) was sufficient to convert DCC-mediated spinal axon attraction into repulsion (Ming et al., 1997). Interestingly, PKA activation recruits vesicular DCC into the plasma membrane, whereas PKC activation induces UNC5 endocytosis. This regulation suggests that mechanisms modulating cAMP levels and PKA/PKC activation may in fact regulate growth cone responses by changing the levels of netrin receptors on the plasma membrane (Bartoe et al., 2006; Bouchard et al., 2004).

Chemoattractant and chemorepellent responses initiated by the activation of netrin receptors are ultimately driven by rearrangements of the actin cytoskeleton. A complex signaling cascade, in

which several players are involved, transduces netrin receptor activation into changes of actin dynamics. In recent years, we have begun to understand the sequence of biochemical events underlying netrin responses, with DCC-dependent mechanisms being the major focus of netrin signaling research.

Initial experiments have shown that, following netrin-1 binding, DCC homodimerizes through its P3 domain and becomes phosphorylated at a tyrosine residue (Ren et al., 2004; Stein et al., 2001). DCC phosphorylation was blocked by a Src Family of Kinases (SFKs) inhibitor, suggesting that the recruitment and activation of SFKs is an early event necessary for DCC signaling. Focal Adhesion Kinase (FAK), which is constitutively bound to DCC P3 domain, is also phosphorylated and this phosphorylation is critical because inhibition of FAK signaling block *Xenopus* spinal axon attractance to netrin-1 (Ren et al., 2004).

The formation of this signaling complex is required for the activation of Rho family of small GTPases. Rho GTPases are G-proteins that regulate actin cytoskeleton dynamics. They are implicated in netrin signaling as Toxin B, a general inhibitor of Rho GTPases, blocks spinal axon extension in response to netrin-1 (Li et al., 2002). CDC42 and RAC1 are the primary Rho GTPases contributing to DCC signaling, as transfection of commissural axons with dominant negative forms of these Rho GTPases impairs netrin-induced increases in growth cone filopodia and surface area (Shekarabi et al., 2005). Furthermore, RAC1 activity is upregulated following netrin-1 biding to DCC (Li et al., 2004; Shekarabi and Kennedy, 2002; Shekarabi et al., 2005). In contrast, RhoA GTPase is inhibited during commissural axon response to netrin-1 (Moore et al., 2008). Additional experiments have shown that RAC1 activation depends on Guanine Exchange Factors (GEFs) TRIO and DOCK180, as downregulation of these GEFs impairs netrin-1-induced

axon extension (Li et al., 2008). Rho GTPase effectors Enabled/vasodilator-stimulated phosphoprotein (ENA/VASP) and Wiskott-Aldrich syndrome protein (N-WASP) are also recruited to the DCC signaling complex; these proteins act downstream of Rho GTPases and directly regulate actin polymerization (Lebrand et al., 2004; Shekarabi et al., 2005).

In addition to control actin dynamics, netrin-1 signaling seems to regulate another critical aspect of axon extension: local membrane insertion. Following netrin-1 binding, DCC recruits syntaxin-1, a plasma membrane target Soluble NSF Attachment Protein Receptor (SNARE) and VAMP7, a vesicle SNARE. SNAREs have a well-established function in vesicle exocytosis and disruption of syntaxin-1 or VAMP7 function blocks netrin-1-induced cell migration and axon extension (Cotrufo et al., 2012; Cotrufo et al., 2011). Interestingly, DCC activation also induces Phosphatidylinositol (4,5) biphosphate (PIP2) hydrolysis, Protein Kinase C (PKC) activation and calcium release from internal storages (Ming et al., 1999; Xie et al., 2006). Such increase in intracellular calcium levels might also contribute to vesicle exocytosis and local membrane insertion following DCC activation.

4.4 Additional netrin functions

Netrins were originally identified as guidance cues secreted by the floor plate in the embryonic neural tube (Serafini et al., 1994; Kennedy et al., 1994). In addition to serve as guidance cues for extending axons in different contexts, netrins regulate cell migration, synaptogenesis and cell survival (Colon-Ramos et al., 2007; Goldman et al., 2013; Kolodziej et al., 1996; Mehlen et al., 1998). Beyond a function in the nervous system, evidence for netrin participation in organogenesis of tissues and organs suggests that these proteins are broader regulators of animal

development (Srinivasan et al., 2003; Liu et al., 2004; Yebra et al., 2003; Han, unpublished data). Moreover, netrins continue to be expressed after development, in the mature nervous system, where they are required for tissue maintenance and proper function of the adult CNS (Bull et al., 2014; Horn et al., 2013). Aspects of netrin functions, beyond axon guidance in the embryonic nervous system, are discussed next in this chapter.

Cell migration and synaptogenesis

Precursor cells are required to migrate long distances in the developing nervous system. Early experiments in *C. elegans* suggested that netrins function as guidance cues for migrating cells, as dorsal and ventral migration along the worm body wall was disrupted by loss of function UNC-6 mutations (Ishii et al., 1992). In mammals, netrin-regulated cell migration has been particularly studied in the developing cerebellum. Examples of this regulation include lower rhombic lip precursor cells that are attracted by netrin-1 towards the ventral midline and cerebellar granule precursors repelled by netrin-1 as they migrate away from the external granule layer (Alcantara et al., 2000).

A function on synaptogenesis has also been demonstrated in various animal models. In *C. elegans*, UNC-6 released by postsynaptic cells induces the formation of presynaptic specializations on dendrites of neurons that express UNC-40 (Colon-Ramos et al., 2007; Park et al., 2011). During *Drosophila* Neuro-Muscular Junction (NMJ) formation, loss-of-function Frazzled mutations result in the formation of abnormally few synapses (Kolodziej et al., 1996; Winberg et al., 1998). In *Xenopus*, netrin-1 application in the optic tectum increases the number of Retinal Ganglion Cell (RGC) presynaptic specializations (Manitt et al., 2009). In cultures or

mouse cortical neurons, netrin-1 drives neurite arborization, increasing the probability of contact between axon and dendrites. In addition, pre- and postsynaptic specializations are rapidly assembled following contact of neurites with a local source of netrin (Goldman et al., 2013). Together, these observations suggest that netrins have a conserved role on synapse formation.

Survival

Netrin receptors are considered dependence receptors because they create "cellular states of dependence on their ligand" and, in the absence of netrin, can initiate apoptosis (Llambi et al., 2001; Mehlen et al., 1998; Thiebault et al., 2003). Consistent with this finding, multiplex analysis of p53-induced gene expression revealed that UNC5B is a p53 transcriptional target and that p53-initiated apoptosis requires UNC5B expression (Tanikawa et al., 2003). Observation that apoptosis levels are elevated in the developing spinal cord of netrin-null mice further indicated that netrins regulate cell survival during development (Llambi et al., 2001). In addition, absence/downregulation of DCC and UNC5 homologues in multiple cancers suggests that netrin receptors are potential tumor suppressors (Thiébault et al., 2003).

In vitro experiments showed that DCC and UNC5 homologues are cleaved by caspase-3 and that this cleavage leads to the release of an intracellular fragment that is required for apoptosis (Mehlen et al., 1998; Llambi et al., 2001). In the case of UNC5, this fragment contains a Death Domain (DD) with homology to domains in the dependence receptor $p75^{NTR}$ and the death receptors Fas and Tumor Necrosis Factor Receptor (TNFR) (Ashkenazi and Dixit, 1998; Bredesen et al., 1998; Hofmann and Tschopp, 1995). During Fas-initiated apoptosis, DD mediates the formation of a complex with the adaptor protein FADD that subsequently drives the

activation of downstream caspases (Ashkenazi and Dixit, 1998). UNC5B DD interacts with Death-Associated Protein kinase (DAP-kinase) and this interaction is required for UNC5B-initiated apoptosis (Llambi et al., 2005). The mechanism by which netrin binding prevents DCC and UNC5-induced apoptosis is poorly understood. It might involve the recruitment of the brain-specific GTPase PIKE-L, which interacts with UNC5B following netrin binding and blocks UNC5B apoptosis. This interaction is dependent on FYN, as knockouts for this kinase do not display netrin-induced interaction between UNC5B and PIKE-L (Tang et al., 2008).

Netrins and oligodendrocytes

Netrins and netrin receptors are important in multiple aspects of oligodendrocyte biology during development and in the mature CNS. In the embryonic spinal cord, oligodendrocyte precursor cells (OPCs) are generated in a restricted area of the ventral ventricular zone but subsequently migrate away from the ventral midline and disperse across the spinal cord (Pringle and Richardson, 1993; Calver et al., 1998). Netrin-1 expressed by floor plate cells at the ventral midline plays a critical role in this process, as a fraction of migrating OPCs fail to reach the dorsal third of developing spinal cord in netrin-1 or DCC deficient mice (Jarjour et al., 2003). *In vitro* chemotaxis experiments confirmed that netrin-1 acts as chemorepellent cue for migrating OPCs and, consistently, that OPC processes retract in response to netrin-1 treatment (Jarjour et al., 2003; Tsai et al., 2003). In OPCs, netrin-1 binding to DCC/UNC5 elevates RhoA activity and induces RhoA kinase (ROCK) phosphorylation; inhibition of either RhoA or ROCK blocks netrin-1-induced repulsion and OPC process retraction (Rajasekharan et al., 2009). In contrast, postmigratory premyelinating oligodendrocytes extend more processes and larger myelin-like membranes in response to netrin-1 *in vitro*. *In vivo*, oligodendrocyte process extension appears

limited in the absence of netrin-1 or DCC. In post-migratory premyelinating oligodendrocytes, netrin-1 binding to DCC induces RhoA inhibition, rather than activation (Rajasekharan et al., 2010). This switch in the downstream signaling underlies the different responses OPCs and premyelinating oligodendrocytes exhibit to netrin-1.

Once development is complete, netrin and netrin receptors continue to be expressed in the nervous system (Manitt et al., 2004). In the mature CNS, netrin-1 accumulates in periaxonal membranes of myelinated axons, where it is enriched at the paranodes (Jarjour et al., 2008; Manitt et al., 2004). The paranode is essential for the segregation of myelinated axons into distinct domains and, therefore, for the rapid conduction of action potentials. In cerebellar slice cultures derived from netrin-1 or DCC deficient mice, paranodes form normally, but fail to maintain and become disorganized over time. As a result, ion channels that normally segregate into distinct domains disperse along the axon (Jarjour et al., 2008). Bull et al. (2014) demonstrated that netrin-1 and DCC have a function on paranode maintenance *in vivo* by deleting DCC from mature oligodendrocytes in the adult mouse CNS. Following DCC deletion, mature paranodes that had formed properly during development become disorganized and axonal domain segregation is compromised (Bull et al., 2014). Therefore, DCC-mediated netrin-1 signaling is required for maintenance of paranode organization.

Netrin functions outside the nervous system

The following are examples of netrin function in the morphogenesis of tissues and organs outside the nervous system: (1) During mammary gland formation, netrin-1, expressed by the luminal cell layer of terminal end buds, and Neogenin, expressed by the cap cell layer, provide adhesion

between the two layers (Srinivasan et al., 2003) (2) In lung morphogenesis, netrins 1 and 4 are secreted in the surrounding basal lamina and inhibit exacerbated branching of distal tip cells (Liu et al., 2004) (3) During vascular system development, UNC5B-mediated netrin-1 signaling prevents excessive vessel branching and abnormal extension of endothelial tip cell filopodia (Lu et al., 2004).

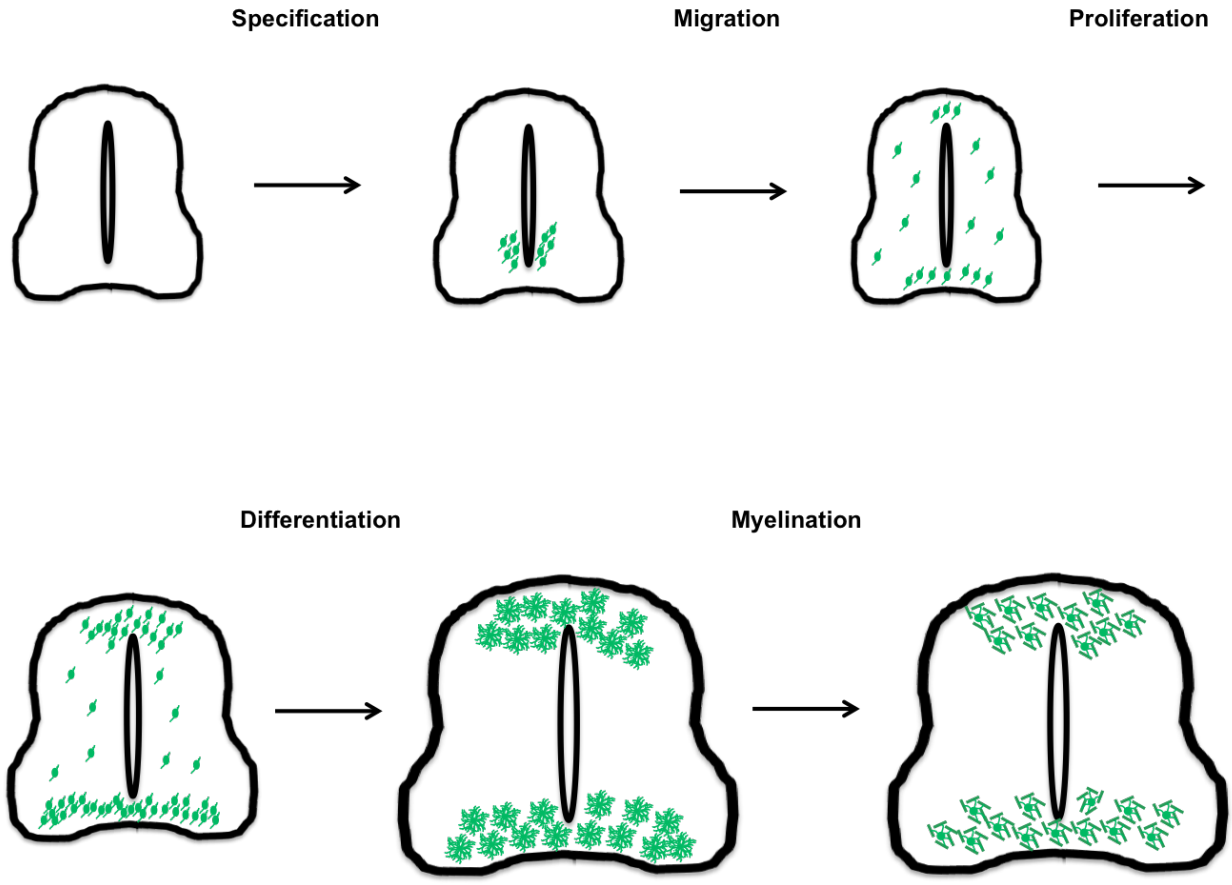

Figure 1.1: OPC development - During spinal cord (and other CNS regions) development, OPCs are specified in the ventral ventricular zone and migrate to putative white matter regions. Post-migratory OPCs proliferate and differentiate into myelinating oligodendrocytes. As OPCs differentiate, OPC number is adjusted to match axon demand for myelination.

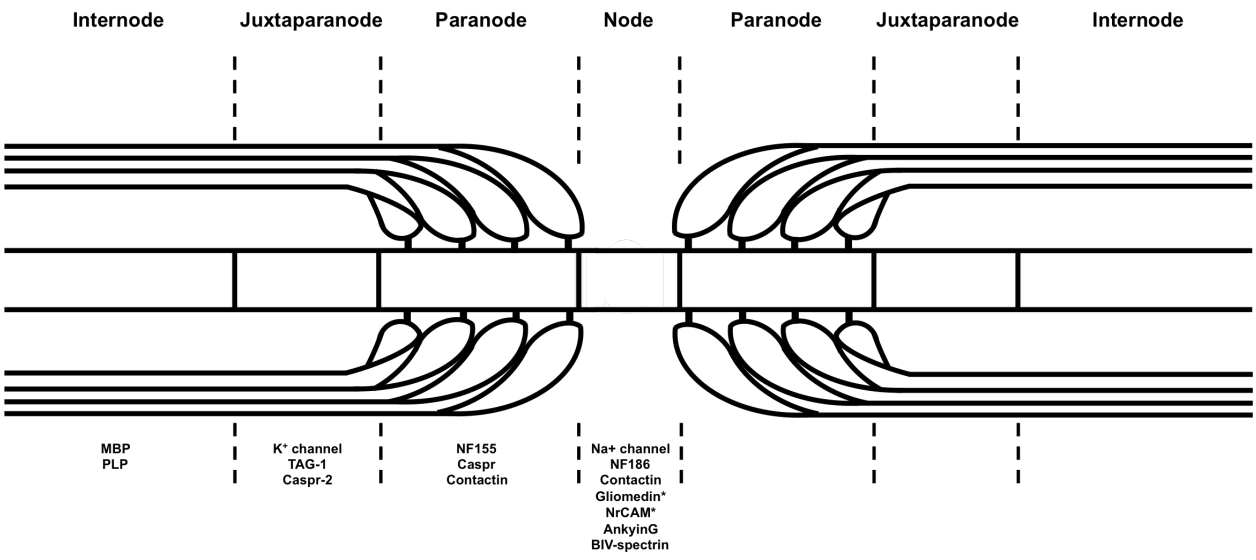

Figure 1.2: Axoglial domains of myelinated axons – Distinct axoglial domains are assembled along the axon as oligodendrocytes myelinate. (*) Gliomedin and NrCAM are expressed in the PNS, but not in the CNS.

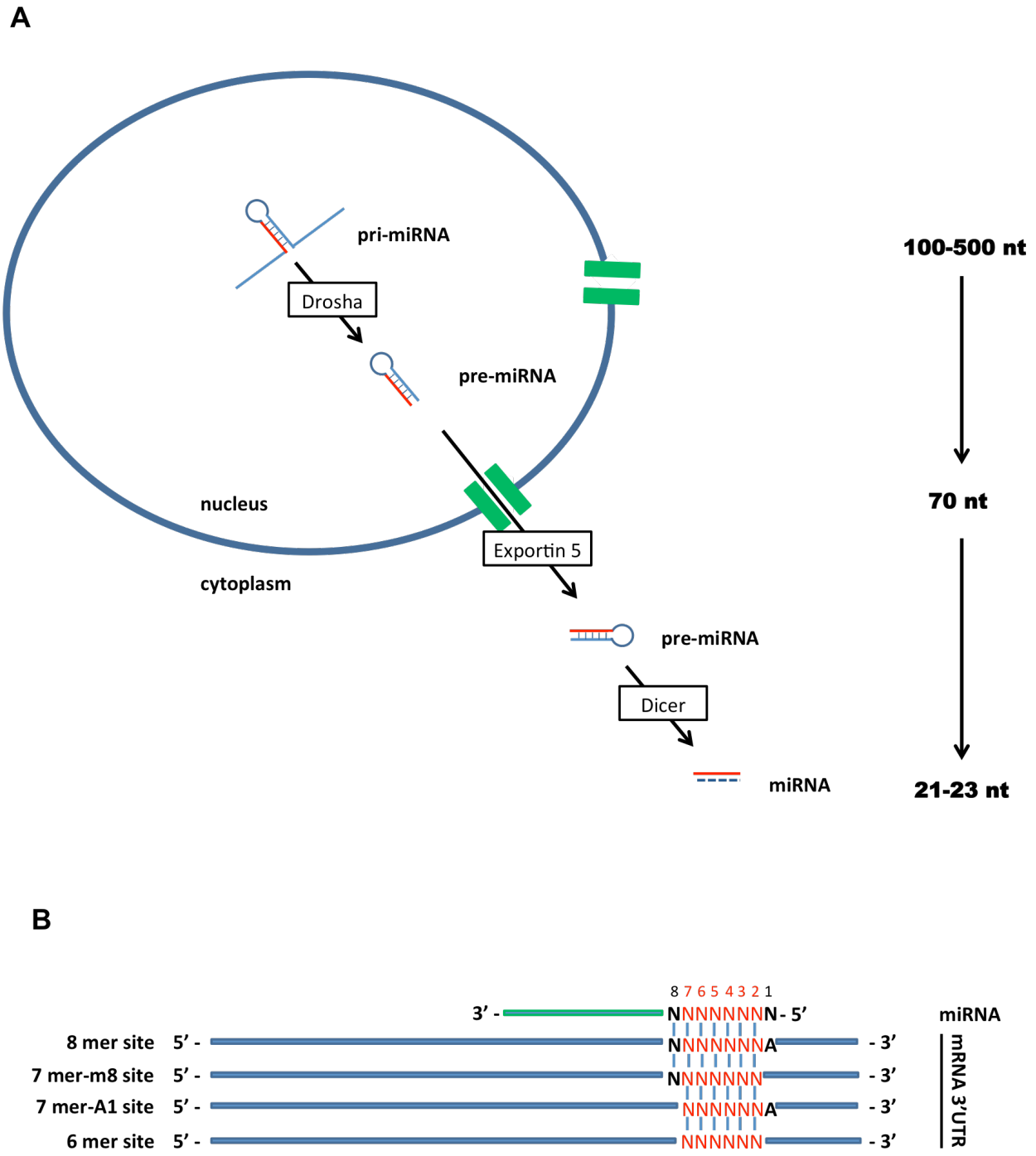

Figure 1.3: miRNA biogenesis and target binding requirements – (A) miRNAs are transcribed as long primary transcripts (pri-miRNAs, 100-500 nt) containing a stem-loop-like

portion. In the nucleus, pri-miRNAs are processed by the RNAse III Drosha to release the stem-loop precursor called pre-miRNA (70 nt). Pre-miRNAs are exported to the cytoplasm through the nuclear membrane carrier Exportin 5 and rapidly processed by Dicer. Dicer cleavage generates a 21-23 nt-long dsRNA; one strand is degraded (blue) while the complementary one (red) is incorporated in the RISC enzymatic complex to function as a guide during RNA interference. **(B)** miRNA targets contain at least one 3'UTR motif comprising of six nucleotides that are complementary to the nucleotides 2-7 (the seed region) of miRNAs. This class of binding sites (6 mer site) underlies relatively weak interactions between miRNAs and 3'UTRs; additional features such as an adenosine matching the first miRNA nucleotide (7 mer-A1 site), an extra complementary nucleotide at position 8 (7 mer-m8 site) or both (8 mer site) increase the probability of a 3'UTR to be targeted by a miRNA.

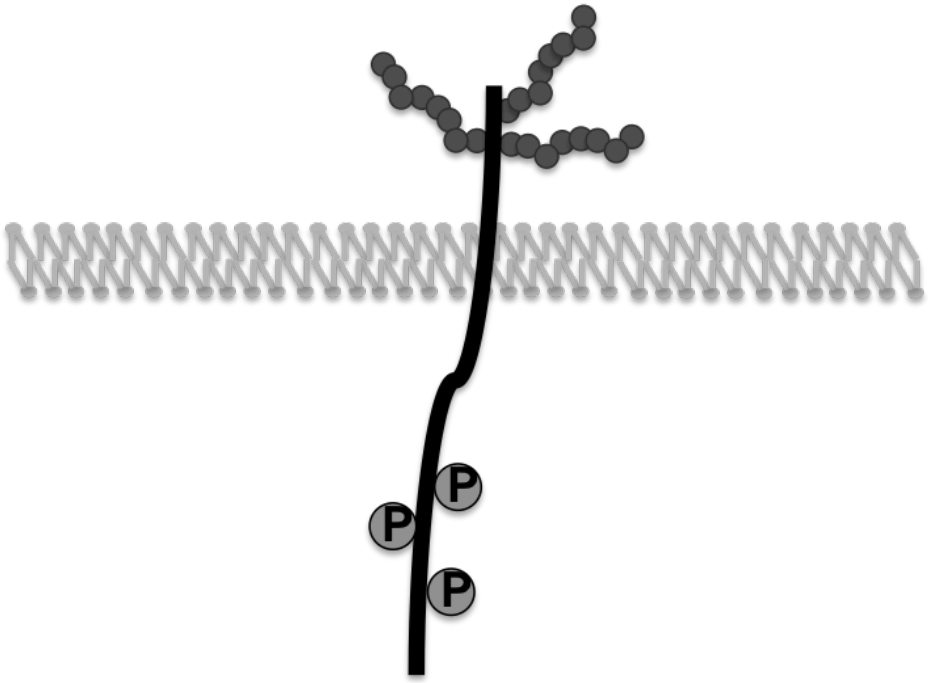

Figure 1.4: Transmembrane protein 10 (TMEM10) - *tmem10* encodes a protein of 143 amino acids with a short extracellular region, a single transmembrane domain and a long intracellular region. Asn-6, Asn-12 and Thr-14 in the extracellular region are glycosylated. The intracellular domain lacks any obvious homology with known protein domains but contains several consensus sites for phosphorylation.

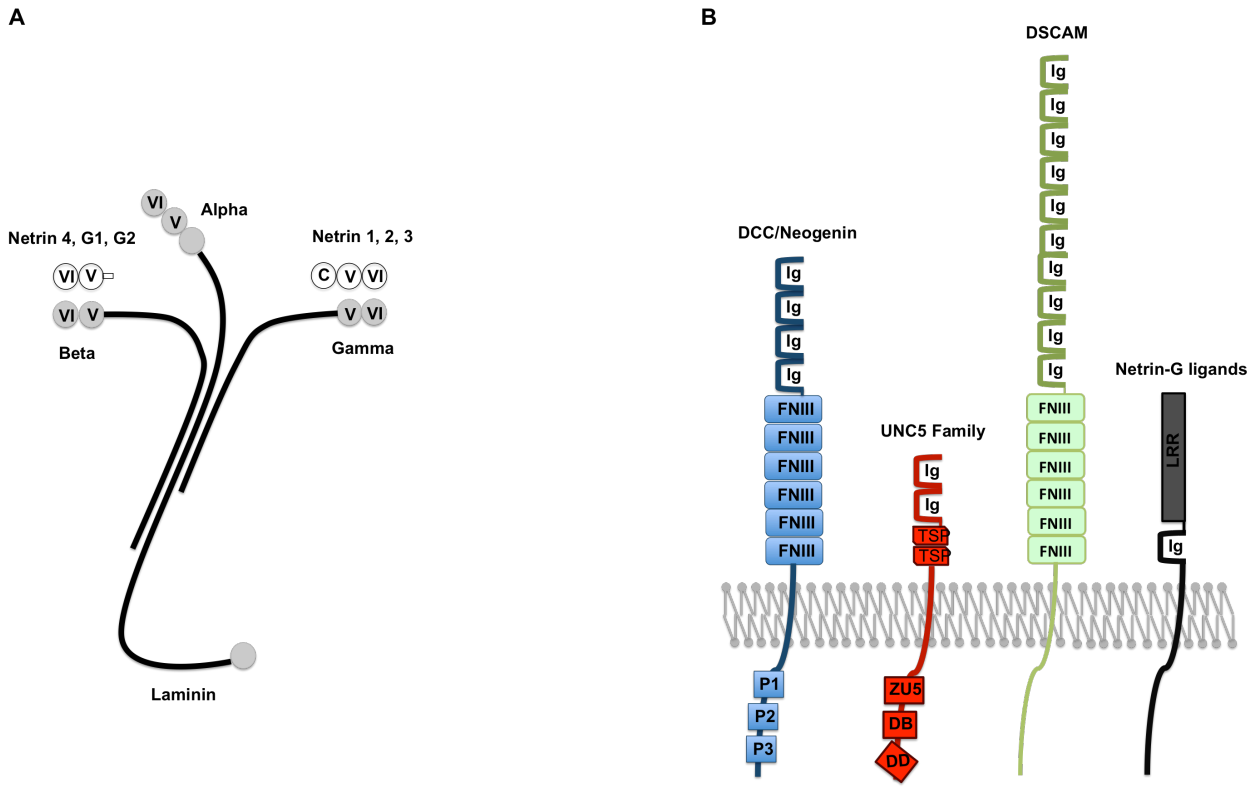

Figure 1.5: Netrins and Netrin receptors – (A) Domains V and VI of Netrins 1, 2 and 3 are homologous to Gamma chain of Laminin, whereas same domains of Netrin-4 and Netrins-G are homologous to Laminin Beta chain. **(B)** Netrin receptors DCC/Neogenin, UNC5 family, DSCAM and Netrin-G ligands. Ig, Immunoglobulin-like domain; FNIII, Fibronectin type III domain; TSP, Thrombospondin type 1 domain; LRR, Leucine-rich repeat; P1, P2 and P3, conserved domains in the intracellular region of DCC; ZU5, Zonna occludens-1/UNC5 domain; DB; DCC binding domain; DD, death domain.

RESEARCH RATIONALE AND OBJECTIVES

Myelin and saltatory conduction of the action potential are critical components of fast and efficient neural activity in vertebrates. It is not possible to comprehensively approach the mysteries of nervous system function without profound consideration on the mechanisms that regulate the development of myelinating glia and the myelin they generate. Better understanding of these regulatory mechanisms will also affect the way we perceive nervous system dysfunction, as myelin is perturbed in many neurological diseases, such as Multiple Sclerosis, Leukodystrophies, Autism and Schizophrenia. We are therefore interested in the identification of new regulators of glia development and myelin organization.

Oligodendrocyte precursor cells (OPCs) are the glial cells that generate myelin in the Central Nervous System (CNS). Different aspects of their development in rodents are regulated by short non-coding miRNAs (Budde et al., 2010; Dugas et al., 2010; Zhao et al., 2010). However, miRNA function may not be conserved between species and the role miRNAs play on human OPC development is not studied. In the second chapter of this thesis, we aimed to address this issue by studying the expression of different rodent relevant miRNAs in oligodendroglia lineage cells acutely isolated from the adult human brain.

Recently, numerous proteomic studies have contributed to extend the list of proteins that are expressed in CNS myelin (Roth et al., 2006; Ishii et al., 2009; Dhaunchak et al., 2010). Among these proteins, the oligodendrocyte-specific Transmembrane Protein 10 (TMEM10) is highly upregulated early during OPC differentiation. We hypothesized that TMEM10 plays a role on OPC differentiation and have investigated this possibility in chapter 3.

After development, myelin paranode maintenance requires the guidance cue netrin-1 (Jarjour et al., 2008; Bull et al., 2014). UNC5B is the major netrin receptor in the white matter of adult spinal cord (Manitt et al., 2004), suggesting that it mediates the netrin-1 signaling necessary for paranode maintenance in the mature CNS. We aimed to test this hypothesis in chapter 4 of this thesis.

Our hope is that the results we report in chapters 2-4 will specifically contribute to the understanding of oligodendrocyte development and CNS myelin organization and, more generally, to advance our current knowledge on CNS function.

Preface to Chapter 2

miRNAs are short non-coding RNAs that regulate gene expression. Different aspects of rodent OPC development, including migration, proliferation and differentiation, are regulated by miRNAs. miRNA sequences are well conserved; however, their predicted targets vary considerably across species. This raises the possibility that different miRNAs regulate OPC development in rodents and humans.

As an initial step to address this issue, we have studied the expression of rodent-relevant miRNAs in human OPC/oligodendrocytes. The results obtained in this study were published in the March 28th, 2012 issue of Frontiers in Genetics (de Faria et al., 2012).

CHAPTER 2

Regulation of miRNA 219 and miRNA clusters 338 and 17-92 in oligodendrocytes

Omar de Faria Jr., Qiao-Ling Cui, Jenea M Bin, Sarah-Jane Bull, Timothy E Kennedy, Amit Bar-Or, Jack P Antel, David R Colman, Ajit S Dhaunchak

1 Abstract

MicroRNAs (miRNAs) regulate diverse molecular and cellular processes including oligodendrocyte (OL) precursor cell (OPC) proliferation and differentiation in rodents. However, the role of miRNAs in human OPCs is poorly understood. To identify miRNAs that may regulate these processes in humans, we isolated OL-lineage cells from human white matter and analyzed their miRNA profile. Using endpoint RT-PCR assays and quantitative real-time PCR, we demonstrate that miR-219, miR-338 and miR-17-92 are enriched in human white matter and expressed in acutely isolated human OLs. In addition, we report the expression of closely related miRNAs (miR-219-1-3p, miR-219-2-3p, miR-1250, miR-657, miR-3065-5p, miR-3065-3p) in both rodent and human OLs. Our findings demonstrate that miRNAs implicated in rodent OPC proliferation and differentiation are regulated in human OLs and may regulate myelination program in humans. Thus, these miRNAs should be recognized as potential therapeutic targets in demyelinating disorders.

2 Introduction

In the central nervous system (CNS), the myelination program that includes OPC proliferation and differentiation is regulated by factors intrinsic and extrinsic to oligodendrocytes (OLs) (Sherman and Brophy, 2005). In addition to growth factors, neurotrophins, neuronal factors, and transcription factors, members of a recently recognized class of cell intrinsic regulators known as miRNAs (miRNAs) have emerged as key regulators of these processes (Emery, 2010). MiRNAs are small (20-22 nt), non-coding RNAs that negatively regulate gene expression by direct binding to a target mRNA. This results in either mRNA degradation or translation blockade, lowering the level of the translated protein. It is estimated that around 30% of all mammalian protein-coding genes are controlled by miRNAs (Friedman et al., 2009).

Dozens of miRNAs are expressed in OLs (Lau et al., 2008); some of them, namely miR-219-5p, miR-338-5p, miR-338 -3p, miR-17-92, miR-138 and miR-23 are implicated in the regulation of OPC proliferation or differentiation (Budde et al., 2010; Dugas et al., 2010; Lin and Fu, 2009; Zhao et al., 2010). MiRNAs 219-5p, 338-5p and 338-3p are among the most highly expressed miRNAs in $GalC^+$ OLs when compared to $A2B5^+$ precursors (Lau et al., 2008). Interestingly, transfection of these miRNAs into primary OPCs promotes differentiation and myelin gene expression (Dugas et al., 2010; Zhao et al., 2010). MiR-219-5p, miR-338-5p and miR-338-3p positively regulate OL differentiation by inhibiting the expression of differentiation inhibitors such as Sox6 and HES5 (Nave, 2010).

The miR-17-92 cluster is a polycistronic gene that is amplified in B-cell type lymphomas and lung carcinomas (Hayashita et al., 2005; Ota et al., 2004). This gene encodes six principal mature

miRNAs: miR-17, miR-18a, miR-19a, miR-20a, miR-19b-1 and miR-92a-1. In addition to a role in accelerating lymphoma tumorigenesis (He et al., 2005), the miR-17-92 cluster regulates survival and proliferation of B-cells and lung epithelia (Hayashita et al., 2005; Matsubara et al., 2007; Ventura et al., 2008). Conditional null mice lacking miR-17-92 cluster expression in OLs display a reduced number of oligodendroglial cells and therefore a function regulating OPC number has been suggested for this miRNA cluster (Budde et al., 2010).

Though a role for miR-mediated control of rodent OL differentiation is beginning to be elucidated, miRNA expression and regulation in primary human OPCs and OLs is currently uncharacterized. It is critical to address the specific role of various miRNAs in human OPC proliferation and differentiation because the majority of predicted miRNA targets are not conserved between rodents and humans (Supplementary Table 2.1). Furthermore, miR-219-5p regulates OPC differentiation in rodents, but not in chicken, and while miR-338-5p and miR-338-3p regulate differentiation in mice, they do not appear to play a similar role in rats or zebrafish (Dugas et al., 2010; Zhao et al., 2010). Moreover, the only study so far addressing miRNA expression in humans failed to detect miRNAs relevant for rodent OPCs in OLs differentiated from human embryonic stem cells (Letzen et al., 2010).

A more direct approach to obtain OL lineage cells of human origin is to directly isolate these cells from the adult human white matter (Cui et al., 2010; Ruffini et al., 2004). We have previously isolated human OLs based on the cell surface expression of the ganglioside recognized by the A2B5 antibody. Adult brain-derived A2B5-positive ($A2B5^{+}$) cells are able to ensheathe axons *in vitro* (Cui et al., 2010) and engage in extensive myelination upon transplantation into the myelin-deficient shiverer mice (Windrem et al., 2004). These cells are

extensively committed with the OL lineage although expression of NG2 and incorporation of BrdU *in vitro* indicate that they have retained some progenitor properties. Adult brain-derived A2B5-negative (A2B5$^-$) cells express MBP, PLP and MAG, but not NG2; they are post-mitotic and consistent with this, PDGFRα is highly downregulated in this fraction (Ruffini et al., 2004 and data not shown). We have therefore isolated primary human OL lineage cells from the human adult brain to analyze the expression of miRNAs that regulate OPC differentiation and proliferation in rodents. Using RT-PCR and real-time quantitative real-time RT-PCR we demonstrate that some of rodent OPC relevant miRNAs are enriched in the human white matter and regulated in acutely isolated human A2B5$^+$ and A2B5$^-$ cells. We also report the expression in human OLs of miR-219-1-3p, miR-219-2-3p, miR-1250, miR-657, miR-3065-5p and miR-3065-3p. In addition, we provide estimates of relative abundance of each miRNA in human and rodent OLs. Our data represent the first evidence that rodent-relevant miRNAs may also regulate OL proliferation and differentiation in humans.

3 Material and Methods

Rodent oligodendrocyte culture

Sprague-Dawley rat pups were obtained from Charles River Canada (Quebec, Canada). All procedures were performed in accordance with the Canadian Council on Animal Care guidelines. Mixed glial cultures were generated from postnatal day 0 Sprague-Dawley rat cortices and OPCs isolated as previously described (Armstrong, 1998). Mixed cultures were maintained for 8-10 DIV in OPC medium (DMEM, 10% FBS, 1% penicillin-streptomycin, 1% GlutaMAXprior to OPC isolation. OPCs were plated at a density of 150,000 cells per well in 12-well plates in

OLDEM (DMEM, 5 µg/ml insulin, 100 µg/ml transferrin, 30 nM sodium selenite, 30 nM triiodothyronine, 100 µg/ml penicillin-streptomycin, 2mM GlutaMAX) and allowed to mature for 8h (DIV1), 4 days (DIV5), or 7 days (DIV8) *in vitro* prior to RNA and protein isolation.

Human adult brain tissue and primary OL isolation

We obtained white matter tissue excised from surgical resections carried out to ameliorate non-tumor-related intractable epilepsy as previously described (Dhaunchak et al., 2010; Ruffini et al., 2004). The protocol was approved by an institutional review board according to the guidelines provided by the Canadian Institutes for Health Research. Informed consent was obtained from all subjects. After surgery, white and grey-matter were dissected and frozen for subsequent RNA isolation or directly processed for OL isolation. Briefly, tissue was subjected to enzymatic/mechanical dissociation and cells separated on a linear 30% percoll density gradient. The resulting suspension was plated in minimal essential medium containing 5% fetal calf serum for 24 hours. The next day, the poorly-adherent cells enriched in human OPCs/OLs were removed and incubated on ice with microbead-conjugated A2B5 IgM antibody. After washing with magnetic cell sorting (MACS) buffer (phosphate-buffered saline, 2 mM EDTA, 5% FCS), cells were sorted using a positive selection column (Miltenyi Biotech). The A2B5 positive ($A2B5^+$) and negative ($A2B5^-$) fractions were lysed, homogenized and frozen for subsequent RNA isolation.

MO3.13 cell line

MO3.13 cells (McLaurin et al., 1995) (a gift from Dr. P Talbot) were cultured and passaged as previously described (Dhaunchak et al., 2011; McLaurin et al., 1995).

Reverse transcription reaction

miRNA cDNA synthesis required miR-specific stem-loop primers designed as previously described (Chen et al., 2005; Schmittgen et al., 2008; Tang et al., 2006). 50-200 ng of total RNA was combined with 5 nM miR-specific stem-loop primers, 1X RT reaction buffer, 1mM dNTP, 0.26 U/µl ribonuclease inhibitor (Invitrogen, cat. No 10777-019) and 3.3 U/µl reverse transcriptase (Invitrogen, cat. No 18064-014) in a 15 µl total volume reaction. Reverse transcription was performed in a pulsed reaction with the following cycling parameters: 16°C for 30 minutes, followed by 60 cycles of 20°C for 30 seconds, 42°C for 30 seconds and 50°C for 1 second. Finally, reverse transcriptase was inactivated at 85°C for 5 minutes. A separate RT reaction was performed in order to synthesize 18S RNA and mRNA cDNA. Equal amounts of RNA (50-200 ng) were combined with 300 ng of random hexamer primers and heated to 65°C for 10 minutes. Samples were allowed to stand on ice for 2 minutes and a mixture containing 1X RT buffer, 1 mM dNTP, 2 U/µl ribonuclease inhibitor (Invitrogen, cat. No 10777-019) and 10 U/µl reverse transcriptase (Invitrogen, cat. No 18064-014) was added to the sample (total volume = 20 µl). The reverse transcription reaction was performed at 25°C for 5 minutes, followed by 50°C for 30 minutes and 55°C for 30 minutes. At the end of the reaction, reverse transcriptase was inactivated at 70°C for 15 minutes.

Pre-PCR

A multiplex pre-PCR step was included before PCR analysis in order to detect low expression miRNAs (Tang et al., 2006). miR-specific sense-primers and a universal anti-sense primer pairing to the cDNA stem-loop region were designed as described by Chen et al (Chen et al., 2005; Schmittgen et al., 2008; Tang et al., 2006). 5 µl of the RT product was combined with 50 nM sense primer, 2 µM universal anti-sense primer, 1X PCR buffer, 0.5 mM dNTP, and 0.25 U/µl Taq polymerase (NEB, cat. No M0324S) in a 25 µl total volume reaction. PCR cycling parameters were: 95°C for 10 minutes, 55°C for 2 minutes followed by 18 cycles of 95°C for 1 second and 65°C for 1 minute. The product was 400-fold diluted for real-time analysis.

Quantitative Real-time PCR

Diluted pre-PCR product was combined with 1 µM sense primer, 1 µM universal anti-sense primer and 2X SYBR Green PCR master mix (Invitrogen, cat. No 4364344) in a 15 µl total volume reaction. Real-time qPCR was performed in the Applied Biosystems 7000 thermocycler with the following cycling conditions: 95°C for 10 minutes, followed by 40 cycles of 95°C for 25 seconds, 59°C for 30 seconds and 72°C for 40 seconds (Schmittgen et al., 2008; Tang et al., 2006). Data analysis used the $2^{-[delta][delta]Ct}$ method (Schmittgen et al., 2000; Winer et al., 1999) and qBase software (Hellemans et al., 2007) to generate expression values. Values were normalized to 18S RNA levels.

Semi-quantitative RT-PCR

Equal volumes of diluted pre-PCR product were combined with 1 µM each sense and anti-sense primers, 5X PCR buffer, 0.5 mM dNTP, and 1 U of Taq polymerase (NEB, cat. No M0324S) in a 15 µl total volume reaction. The PCR amplification was performed in the Biometra T1 plus

thermocycler with the following cycling conditions: 95°C for 3 minutes, followed by 40 cycles of 94°C for 30 seconds, 55°C for 30 seconds and 72°C for 30 seconds. Final extension was carried out at 72°C for 10 minutes. PCR product was resolved by 20% polyacrylamide gel electrophoresis and stained with ethidium bromide for 45 minutes prior to image acquisition.

Primers

A list containing all the primers used in this study can be found in the supplemental material section (Supplementary Table 2.2).

Western Blot

Equal amounts of protein resolved by SDS-PAGE were transferred to a PVDF membrane (BioRad, cat. No 1620184). The membrane was blocked with 5% milk in TBST (25 mM Tris pH 7.4, 27 mM KCl, 137 mM NaCl, 0.1% Tween 20) for 1 hour and incubated with primary antibodies overnight at 4°C. The membrane was washed 3 times with TBST and incubated with horseradish peroxidase-conjugated secondary antibodies for 1 hour at room temperature (1:10,000 in 0.1% milk-TBST). The membrane was washed 3 times with TBST and developed with an Enhanced Chemoluminescence Detection kit (Pierce, cat. No 32106). Primary antibodies used: monoclonal mouse 3F4 anti-PLP (hybridoma supernatant) (Dhaunchak and Nave, 2007); polyclonal rabbit anti-GAPDH (Santa Cruz, SC-25778); monoclonal mouse anti-β-actin (Sigma, A5441).

Statistical Analysis

Expression analysis in murine brain developmental series was performed in pooled triplicates (n

equals minimum of 3 animals per age group). Expression analysis from cultured rat OPCs was quantified from a representative experiment, of n equals 3 independent experiments, performed in triplicates. For comparison of these developmental stages, one-way ANOVA test followed by Tukey's post-test was performed. MiRNA enrichment in human white matter was performed from two independent samples in triplicates. For miRNA expression in acutely isolated primary human cells, $A2B5^{+}$ and $A2B5^{-}$cells were obtained from four independent surgical resections from different subjects, each analyzed in triplicates. The comparison of human samples was performed by unpaired student's t-test.

4 Results

In order to profile miRNA expression in oligodendrocytes, we first validated the RT-PCR primers by conventional PCR followed by polyacrylamide gel electrophoresis and found unique amplicons (~70 nts) for every primer pair (Figure 2.1 and Supplementary Table 2.2). In addition, the dissociation curves obtained after real-time RT-PCR amplification of a representative human cDNA sample confirmed that only one major product is generated during real-time quantification. Thus the primer pairs listed in Supplementary Table 2.2 can be reliably used to profile miRNAs in human samples.

Regulation of miR-219 expression during OPC differentiation

In humans and mice, two loci encode miR-219 precursor transcripts, *miR-219-1* and *miR-219-2* (Figure 2.2A). Processing of the precursor transcripts by dicer generates three miRNAs: miR-219-5p from the 5' ends of both precursors and the miRNAs miRNA219-1-3p and miRNA219-

2-3p from the 3' end of precursors miR-219-1 and miR-219-2, respectively. Since the seed region in the three resulting mature products is unique, each miRNA is predicted to regulate the expression of unique targets. Though miR-219-5p is known to be upregulated during rodent OPC differentiation, expression of miR-219-1-3p and miR-219-2-3p has not been studied. We therefore analyzed the expression of all three miRNAs in rodent brain and cultured OPCs by quantitative real-time PCR.

MiR-219-5p levels show elevation trend after the first postnatal week in mouse brain (Figure 2B; 1.85-fold at P7, 1.76-fold at P21, p= 0.051), coinciding with the period of OPC differentiation in rodents (Kessaris et al. 2006). In contrast, both miR-219-1-3p and miR-219-2-3p show late (P21), but robust upregulation that continued into adulthood (Figure 2.2B). Since the expression changes detected in total brain could result from non-OL lineage cells, we next profiled miRNA expression in cultures enriched with rat OPCs. Prior to the miRNA expression analysis, we confirmed by endpoint RT-PCR and western blot that when cultured in the absence of mitogens, OPCs downregulate precursor genes (NG2) and upregulate myelin genes (PLP, MAG, CGT) (Figure 2.2C). Quantitative real-time RT-PCR shows that miR-219-5p is dramatically upregulated, peaking at DIV5 (>6-fold higher than at DIV1) and dropping by DIV8, but remaining higher than at DIV1 (Figure 2.2D). Interestingly, miR-219-5p levels correlate very well with PLP expression at all time points (Pearson coefficient = 0.999, p=0.01; Figure 2.2E). Additionally, we found that miRNA 219-1-3p and 219-2-3p are regulated during rodent OPC differentiation: miRNA219-1-3p peaks at DIV5, but returns to DIV1 levels by DIV8 whereas miR-219-2-3p levels remain high through DIV5 to DIV8. We also compared the relative miRNA level at each DIV and found that despite the upregulation of miR-219

products during OPC differentiation, their levels are still lower than miRNA17-92 cluster (Table 2.1). In addition, the higher levels of miR-219-5p when compared to miR-219-1/2-3p suggests that miR-219-5p may be preferentially excised from the stem-loop precursor during OPC differentiation (Table 2.1). Overall, our data establish that the levels of miR-219-5p and two related miRNAs, miR-219-1-3p and miR-219-2-3p, increase in the rodent brain as it matures *in vivo* and in rodent OPCs as they differentiate *in vitro*.

We next asked if miR-219 mature products are expressed in the human adult brain. Endpoint RT-PCRs followed by polyacrylamide gel electrophoresis shows that transcripts of all three mature miRNAs (miR-219-5p, miR-219-1-3p and miR-219-2-3p) are detectable in the human brain (Figure 2.2F). To determine if these miRNAs are enriched in human cortical white matter tracts, we compared the levels of miRNAs 219-5p, 219-1-3p and 219-2-3p in white and grey matter by quantitative real-time RT-PCR and found that these miRNAs are at least 5 times enriched in the white matter (Figure 2.2G). As this result suggests that miR-219 family members are expressed by glial cells, we profiled miRNA expression in human OLs. For this purpose, we isolated OL lineage cells from the human adult brain and used cell sorting to separate stage-specific populations of OLs based on the cell surface expression of the ganglioside recognized by the antibody A2B5; in addition, we also investigated miRNA expression in the human OPC cell line MO3.13 (McLaurin et al., 1995). Using endpoint RT-PCR followed by polyacrylamide gel electrophoresis we did not detect expression of any miR-219 mature products in MO3.13 cells. However, miR-219-5p and miR-219-2-3p were readily detected in acutely isolated human $A2B5^+$ cells, in contrast to the previously reported in Ols derived from embryonic stem cells (Letzen et al., 2010) (Figure 2.2H). Quantitative real-time RT-PCR analysis indicates that both $A2B5^+$ and

A2B5$^-$ OLs express the three miRNAs and that expression is downregulated as cells mature from A2B5$^+$ to A2B5$^-$ OLs (Figure 2.2I). In summary, our findings provide the first evidence that human OL lineage cells express mature products of the miR-219 locus, indicating a conserved role for these miRNAs during human OL differentiation.

Regulation of the miR-338 cluster during OPC differentiation

In humans, the miR-338 cluster encodes six different mature miRNAs (miR-338-5p, miR-338-3p, miR-3065-5p, miR-3065-3p, miR-657 and miR-1250) that are encoded by four independent loci (Figure 2.3A). MiR-657 and miR-1250 each encode only a single mature form (from the 3'-end of miR-657 and the 5'-end of miR-1250). Interestingly, these two miRNAs are specific to humans and have not been detected in rodents. MiRNAs 338-5p and 338-3p were previously detected in mature rodent OLs but miR-3065 expression has not been demonstrated before. We therefore used quantitative real-time RT-PCR to study the expression of all miR-338 cluster members during mouse brain development and OPC differentiation *in vitro* (Figure 2.3B, C).

During maturation of the mouse brain, miR-338-3p undergoes a robust upregulation similar to that of the 219-3p miRNAs. Specifically, there is a delayed 10-fold elevation in miR-338-3p expression at P21 and a 30-fold elevation at P60 (compared to the levels at P1). In contrast, miR-338-5p appears to be expressed throughout postnatal development. MiR-3065 shows a unique profile with significant downregulation during the first two postnatal weeks and upregulation by the third week (Figure 2.3B). Quantitative real-time RT-PCR shows that *in vitro* OPC differentiation is marked by a robust upregulation (5-fold increase) of both miR-338-5p and miR-338-3p (Figure 2.3C). Interestingly, we found miR-338-5p to be more abundant then miR-338-

3p from day 1 to day 8, indicating preferential maturation of the miRNA located at 5' arm of the pre-miR-338 (Table 2.1). MiR-3065-5p is highly expressed at DIV1 but markedly downregulated at DIV5. These data suggest that the positive and negative strands of the miR-338 locus, producing miR-338 and miR-3065, respectively, are preferentially transcribed during different stages of rodent OPC differentiation.

Since the miR-338 cluster in humans encodes two additional miRNAs not found in rodents (miR-1250 and miR-657), we investigated the expression of these miRNAs in human samples. We first studied the expression profile of all six mature miRNAs transcribed from the miR-338 cluster locus in human brain. By endpoint RT-PCR followed by polyacrylamide gel electrophoresis, we were able to detect the expression of miRNAs 338-5p, 1250, 3065-3p and 657 (Figure 2.3D). Although miR-338-3p and miR-3065-5p were not detected by RT-PCR, both miRNAs were readily amplified using more sensitive real-time RT-PCR. To our knowledge, this is the first report of the expression of miRNAs 1250, 3065-5p, 3065-3p and 657 in the human brain. We next used quantitative real-time RT-PCR to compare expression levels in white and grey matter and found that miR-338-5p and miR-338-3p are highly enriched (>15-fold) in white matter tracts (Figure 2.3E). MiR-3065-5p and miR-3065-3p do not show any clear enrichment in either white or grey matter while miR-1250 and miR-657 are slightly concentrated in the white matter (2 and 3.5-fold enrichment respectively). Interestingly, relative expression analysis grouped miR-338 cluster members together as low copy number miRNAs, indicating that they also behave as a cluster at the expression level (Table 2.1).

The enrichment of miR-338-5p and miR-338-3p in the white matter suggests that human glial cells express these miRNAs. To determine whether this is the case, we performed endpoint RT-

PCR in the MO3.13 cell line and acutely isolated OLs. Using this method, we found that miR-338-5p, miR-1250 and miR-3065-5p are expressed in the MO3.13 cell line whereas miR-338-5p, miR-3065-5p and miR-657 are expressed in $A2B5^{+}$ cells (Figure 2.3F). Quantitative real-time RT-PCR analysis shows that all miR-338 cluster members are detectable in acutely isolate OLs and that miR-338-5p, miR-1250, miR-3065-5p and miR-657 are significantly downregulated in the $A2B5^{-}$ fraction (Figure 2.3G). Interestingly, relative expression analysis grouped miR-338 cluster members together, suggesting that these miRNAs may be co-transcribed in human OLs (Table 2.1). In summary, we provide the first evidence that miR-338 cluster is expressed in human OLs, as previously demonstrated in rodents (Dugas et al. 2010; Lau et al. 2008; Zhao et al. 2010). These findings suggest a conserved role for the miR-338 cluster in regulating OPC differentiation in humans.

Regulation of the miR-17-92 cluster during OPC differentiation

The miR-17-92 cluster encodes 12 different miRNAs in both humans and rodents. Some of them (miR-17-5p, 18a-5p, 19a-3p, 20a-5p, 19b-3p and 92a-3p, highlighted in red in Figure 2.4A) have been implicated in the regulation of OPC proliferation in rodents, but their expression during postnatal brain development and cultured OPC differentiation has not been addressed (Budde et al., 2010). We used quantitative real-time RT-PCR to study the expression of these miRNAs during mouse brain development and found a dramatic downregulation within the first postnatal week, in agreement with their role in controlling OPC number (Budde et al., 2010). When compared to P1, levels at P7 are about 90% reduced and maintained at a similarly low level into adulthood (Figure 2.4B). Intriguingly, at P21, a significant upregulation from levels at P7 is seen

for all miRNAs except miR-92a-3p, suggesting that these miRNAs also play some specialized role in postnatal brain. Quantitative real-time RT-PCR shows that miRNAs 19a-3p, 20a-5p, 19b-3p and 92a-3p are also clearly downregulated in cultured OPCs during differentiation (Figure 2.4C). No significant changes are seen for miRNAs 17-5p and 18a-5p. Though most miR-17-92 cluster members are downregulated during OPC differentiation, relative expression analysis reveals that these miRNAs are the most highly expressed miRNAs in both $A2B5^+$ and $A2B5^-$ OLs (Table 2.1), suggesting that these miRNAs might play a role in regulating levels of housekeeping transcripts in OLs.

All six miR-17-92 cluster members are readily detected in the adult human brain by endpoint RT-PCR (Figure 2.4D). In addition, quantitative real-time RT-PCR shows that they are enriched in white matter tracts when compared to grey matter (>4-fold; Figure 4E). We also used endpoint RT-PCR to study their expression in human OL lineage cells and found that all miRNAs are expressed in the human OPC cell line (MO3.13) and in acutely isolated $A2B5^+$ OLs (Figure 2.4F). Quantitative real-time RT-PCR analysis revealed that expression of the miR-17-92 cluster is highly upregulated in MO3.13 cells when compared with adult primary OLs (data not shown). All miR-17-92 miRNAs were readily detectable by quantitative real-time RT-PCR in both A2B5+ and A2B5- OLs with no significant differences in expression levels between the two populations (Figure 2.4G). This data is in agreement with the relative expression analysis revealing that this cluster represents one of the most highly expressed miRNAs in both $A2B5^+$ and $A2B5^-$ OLs (Table 2.1).

5 Discussion

We have applied endpoint RT-PCR followed by polyacrylamide gel electrophoresis and quantitative real-time RT-PCR to profile miRNA expression in human OLs. Our focused approach prioritized miRNAs that have been previously shown to regulate OPC number and differentiation in rodents. The current data provides evidence for the expression of miR-219, miR-338 and miR-17-92 clusters in acutely isolated-adult brain OLs in marked contrast to what was observed with human OLs derived from embryonic stem cells (Letzen et al., 2010). In addition, we show that some of these glial enriched miRNAs are differentially expressed by human $A2B5^+$ and $A2B5^-$ OLs.

Expression profiling studies with rodent OLs have reported that several miRNA species are dramatically regulated during OPC differentiation (Budde et al., 2010; Dugas et al., 2010; Lau et al., 2008). In these studies, over-expression of miR-219-5p, miR-338-5p and miR-338-3p was shown to promote rodent OPC differentiation, indicating that these miRNAs play important roles during myelination (Budde et al., 2010; Dugas et al., 2010; Lau et al., 2008). Our results are in agreement with previous findings and we for the first time demonstrate that closely related miRNAs (miR-219-1-3p, miR-219-2-3p, miR-338-3p and miR-3065-5p) are also regulated during rodent OPC differentiation. Notably, miR-3065-5p shows a dramatic drop in expression during the first five days *in vitro*, suggesting that 3065-5p might play a role in regulating OPC proliferation and/or differentiation.

In previous microarray studies, regulation of miR-17-92 cluster expression during the OPC/OL transition was not reported (Lau et al., 2008). The high sensitivity of our real-time approach

demonstrates that miR-19a-3p, miR-19b-3p, miR-20a-5p and miR-92a-3p are downregulated during rodent OPC differentiation. This data is consistent with the proposed role of the miR-17-92 cluster in the control of cell number (Budde et al., 2010). The relative expression analysis, however, reveals that members of the miR-17-92 cluster are among the most-highly expressed miRNAs in both rodent OPCs and mature OLs (Table 2.1). In addition, the expression profile of miR-17-92 cluster members during OPC differentiation *in vitro* is very similar to the profile seen in the developing mouse brain (Figure 2.4B), suggesting that this cluster is OPC/OL enriched. This data is consistent with the finding that the miR-17-92 cluster is enriched in OPCs rather than in astrocytes (Budde et al., 2010). Thus the miR-17-92 cluster may be designated as an OL-enriched miRNA in rodents.

The human brain has also been examined for miRNA expression and miR-219-5p, miR-338-5p, miR-338-3p and members of the miR-17-92 cluster were reported to be expressed (Barad et al., 2004; Sempere et al., 2004). In addition to the above-mentioned miRNAs, we report that four other miRNAs, miRNA219-1-3p, miRNA219-2-3p, miRNA1250, and miRNA657, are enriched in white matter tracts of the human brain (Figures 2.2G and 2.3E). Our data is consistent with previous findings showing dramatic downregulation of miR-219-5p and miR-338-5p in inactive white matter lesions in multiple sclerosis patients (Junker et al., 2009). Importantly, our study is the first to report that miR-219-5p and miR-338-5p and -3p are expressed by human OLs (Figures 2.2H and 2.3F). These findings open the possibility that the same miRNAs controlling OPC differentiation in rodents (miRNA219-5p and miRNA338-5p and -3p) may also control OPC differentiation in humans. Discrepancies between our focused expression study and the microarray approach previously employed (Letzen et al., 2010) could be due to differences in the

origin of the samples and detection sensitivity. In the current study, human OLs were acutely isolated whereas in the previous report, OLs had been differentiated from human embryonic stem cells. In addition, we used very sensitive real-time qRT-PCR to profile miRNAs whereas in the previous report less sensitive miRNA microarray was used. Despite the use of different techniques, both studies show that the miR-17-92 cluster is abundantly expressed by human OLs (Figure 2.4 and Table 2.1). Taken together, our data, along with the data obtained from inactive white matter lesions in multiple sclerosis (Junker et al., 2009) strongly suggests that miR-219, miR-338 and miRNA17-92 clusters may also regulate OPC differentiation in humans.

In summary, our study establishes that rodent relevant miRNAs are also expressed by human OLs. We propose that miRNAs demonstrated to be functionally relevant in rodents perform a conserved function and regulate the proliferation and differentiation of human OPCs. Further investigation into the functional contribution of these miRNAs to human myelination may provide insights into their potential as targets to promote remyelination in demyelinating diseases.

6 Figures and figure legends

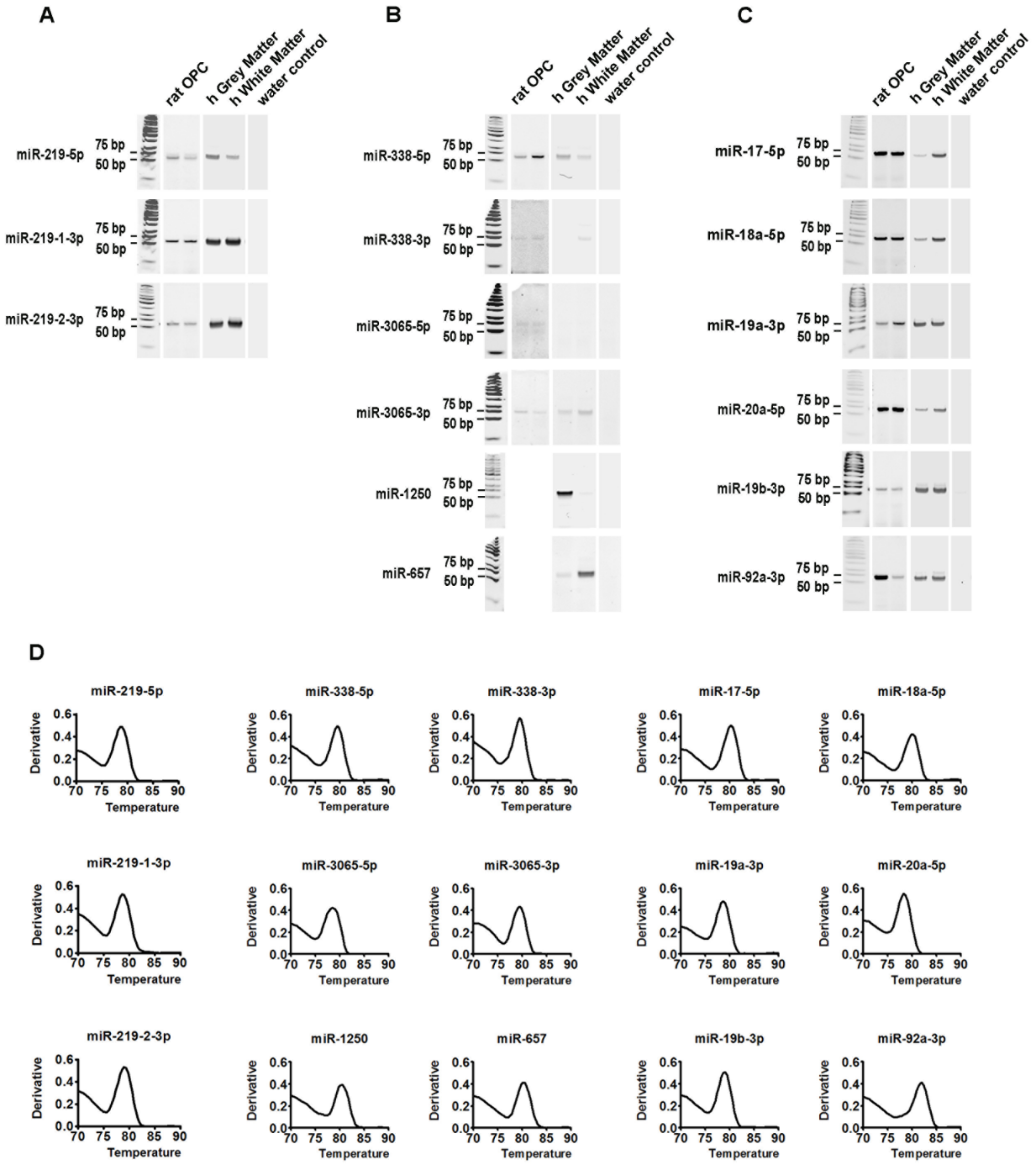

Figure 2.1: Validation of miR-specific primers - Endpoint RT-PCR followed by polyacrylamide gel electrophoresis showing that all miRNA primers yield a unique RT-PCR product with an expected amplicon of ~70nts. The entire gels are shown. Rat OPC (lane 1; 1 DIV and lane 2; 5 DIV), human brain (lane 3; h grey matter and lane 4; h white matter) and water control (lane 5). (A) Amplification of miRNAs 219 locii products yield a single amplicon in both human and rodent samples. (B) Amplification of miR-338 cluster products yields a single amplicon in both human and rodent samples, except for 3065-5p which was undetectable in the human samples used at this time. Note that miR-1250 and miR-657 are only predicted to be expressed by humans, thus, only the human samples are shown. (C) Amplification of miR-17-92 cluster products yields a single amplicon in both human and rodent samples. (D) Representative melting point analysis for each primer pair. The derivative of dissociations confirms that a single major amplicon is generated during quantitative real-time RT-PCR. The representative curves are average of four replicates.

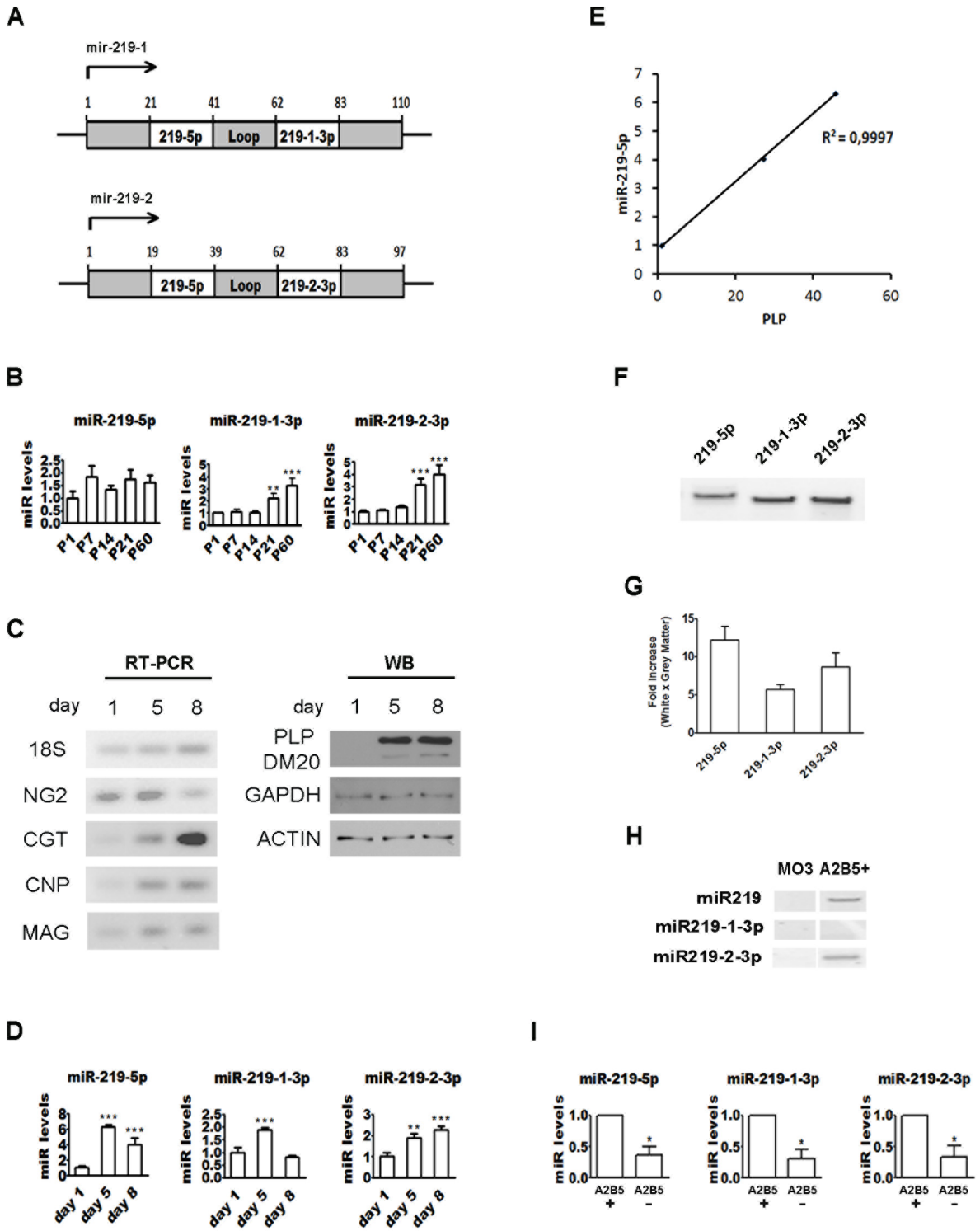
A
mir-219-1
1
21
41
62
83
110
219-5p
Loop
219-1-3p
mir-219-2
1
19
39
62
83
97
219-5p
Loop
219-2-3p
E
miR-219-5p
PLP
R² = 0,9997
B
miR-219-5p
miR-219-1-3p
miR-219-2-3p
miR levels
P1
P7
P14
P21
P60
F
219-5p
219-1-3p
219-2-3p
G
Fold Increase (White x Grey Matter)
219-5p
219-1-3p
219-2-3p
C
RT-PCR
WB
day 1 5 8
18S
NG2
CGT
CNP
MAG
PLP
DM20
GAPDH
ACTIN
H
MO3
A2B5+
miR219
miR219-1-3p
miR219-2-3p
D
miR-219-5p
miR-219-1-3p
miR-219-2-3p
miR levels
day 1
day 5
day 8
I
miR-219-5p
miR-219-1-3p
miR-219-2-3p
miR levels
A2B5 +
A2B5 -

Figure 2.2: Regulation of miR-219 expression during OPC differentiation - (A) Schematic showing human miR-219-1 and miR-219-2 genomic structures. Processing of the precursor transcripts generates the same miR-219-5p and two unique miRNAs, 219-1-3p and 219-2-3p. (B) Quantitative real-time RT-PCR showing elevation in all three mature products during postnatal mouse brain development. ΔΔCt method was used to calculate miRNA levels normalized to 18S RNA expression. Each time point represents at least three pooled animals analyzed in triplicates. P values are derived from one-way ANOVA analysis followed by the Tukey's post-test. **- P<0.01; ***- P<0.001. (C) Left panel: endpoint RT-PCR followed by agarose gel electrophoresis showing that early OPC genes are downregulated and myelin genes are upregulated when rat OPCs are cultured *in vitro* in the absence of mitogens. Right panel: western blot showing that PLP is upregulated during OPC differentiation. (D) Quantitative real-time RT-PCR showing upregulation of all three mature miR-219 products during rat OPC differentiation *in vitro*. ΔΔCt method was used to calculate miRNA levels normalized to 18S RNA expression. The graphs are representative of one of the three experiments performed in triplicates. P values are derived from one-way ANOVA analysis followed the Tukey's post-test.**-P<0.01; ***- p<0.001. (E) Pearson correlation between miR-219-5p and PLP levels during rat OPC differentiation *in vitro*. MiRNA levels were calculated as described in Figure (D). P values are derived from two-tailed unpaired student's t test. P<0.05. (F) Endpoint RT-PCR followed by polyacrylamide gel electrophoresis showing that all three mature miR-219 products are expressed in human brain. (G) Quantitative real-time RT-PCR showing that miR-219 mature products are enriched in human brain white matter. ΔΔCt method was used to calculate miRNA levels normalized to 18S RNA expression. Fold-change was calculated by dividing miRNA levels in white matter by levels in grey matter.

The graphs are obtained from analysis of two brains done in triplicates. P values are derived from two-tailed unpaired student's t-test. (H) Endpoint RT-PCR followed by polyacrylamide gel electrophoresis showing that miR-219 mature products are expressed by human $A2B5^{+}$ OLs. (I) Quantitative real-time RT-PCR showing that miR-219 levels are higher in adult human $A2B5^{+}$ cells when compared to $A2B5^{-}$ OLs. ΔΔCt method was used to calculate miRNA levels normalized to 18S RNA expression. Each bar represents the average of 4 subjects analyzed by real-time PCR done in triplicates. P values are derived from two-tailed unpaired student's t-test. *-$P<0.05$

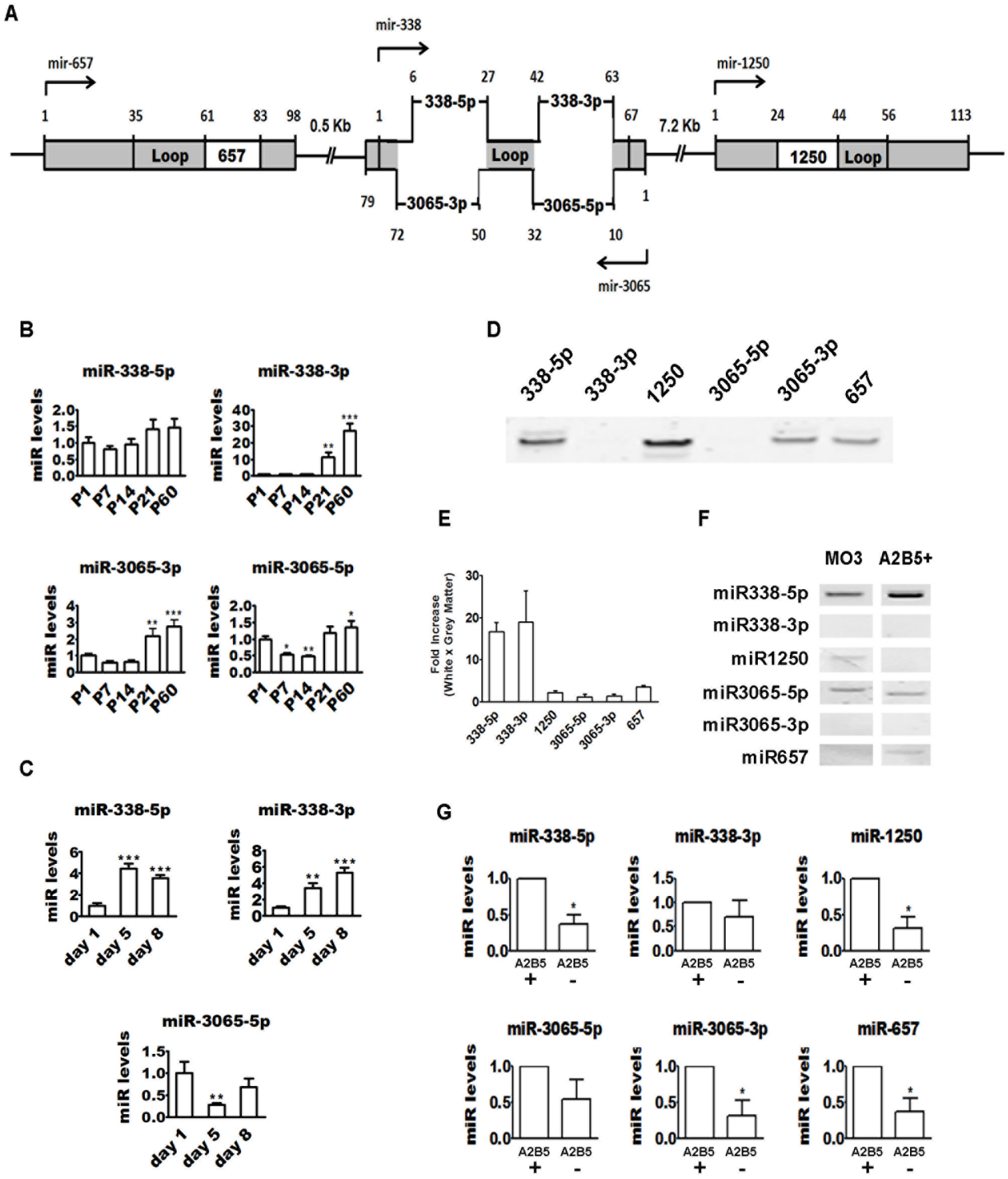
A
mir-338
mir-657
mir-1250
338-5p
338-3p
3065-3p
3065-5p
mir-3065
Loop
657
1250
0.5 Kb
7.2 Kb
B
miR-338-5p
miR-338-3p
miR-3065-3p
miR-3065-5p
miR levels
P1
P7
P14
P21
P60
C
day 1
day 5
day 8
D
E
Fold Increase
(White x Grey Matter)
F
MO3
A2B5+
miR338-5p
miR338-3p
miR1250
miR3065-5p
miR3065-3p
miR657
G
miR-1250
miR-657
A2B5

Figure 2.3: Regulation of miR-338 cluster expression during OPC differentiation - (A) Schematic showing human miR-338 cluster genomic structure. Note that miR-3065 is encoded by the complementary strand of miR-338. (B) Quantitative real-time PCR showing that overall expression of miR-338 cluster increases in the mouse brain during post-natal development. ΔΔCt method was used to calculate miRNA levels normalized to 18S RNA expression. Each time point represents at least three pooled animals analyzed in triplicates. P values are derived from one-way ANOVA analysis followed by the Tukey's post-test. *-P<0.05; **-P<0.01; ***-P<0.001. (C) Quantitative real-time PCR showing upregulation in miR-338-5p and -3p and downregulation of miR-3065-5p during rat OPC differentiation *in vitro*. ΔΔCt method was used to calculate miRNA levels normalized to 18S RNA expression. The graphs are representative of one of the three experiments performed in triplicates. P values are derived from one-way ANOVA analysis followed by the Tukey's post-test. **- P<0.01; ***- P<0.001. (D) Endpoint RT-PCR followed by polyacrylamide gel electrophoresis showing that the miR-338 cluster is expressed in the human brain. (E) Quantitative real-time PCR showing that all members of the miR-338 cluster except for miRNAs 3065-5p and -3p are enriched in human brain white matter. ΔΔCt method was used to calculate miRNA levels normalized to 18S RNA expression. Fold-change was calculated by dividing miRNA levels in white matter by levels in grey matter. The graphs are obtained from analysis of 2 different brains done in triplicates. P values are derived from two-tailed unpaired student's t-test. (F) Endpoint RT-PCR followed by polyacrylamide gel electrophoresis showing that miR-338 cluster is expressed by the human cell line MO3.13 and human $A2B5^{+}$ OLs. (G) Quantitative real-time PCR showing that levels of some miR-338 cluster members are higher in adult human $A2B5^{+}$ cells than $A2B5^{-}$ OLs. ΔΔCt method was

used to calculate miRNA levels normalized to 18S RNA expression. Each bar represents the average of 4 subjects analyzed by real-time PCR done in triplicates. P values are derived from two-tailed unpaired student's t-test. *- $P<0.05$

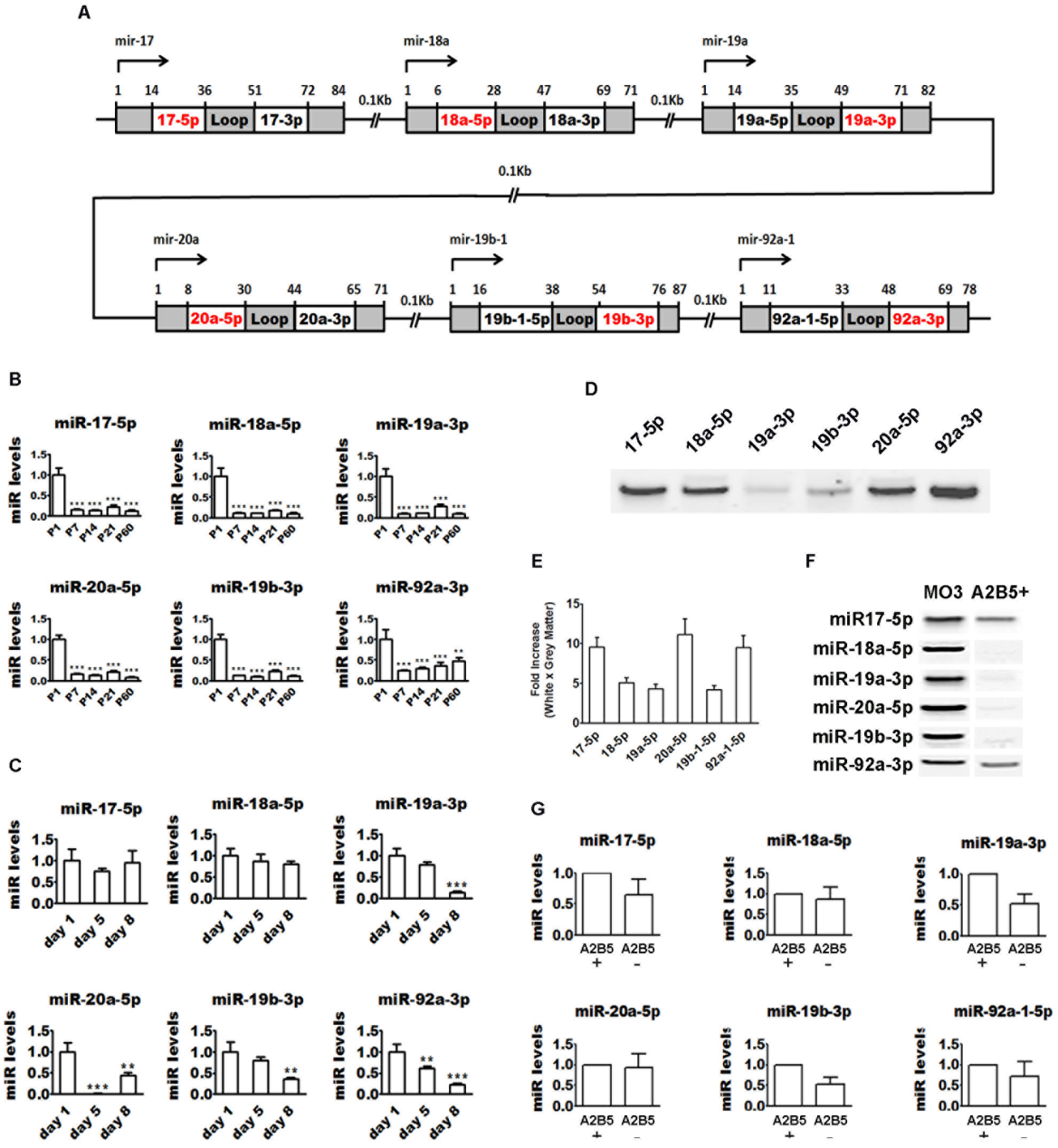

Figure 2.4: Regulation of miR-17-92 cluster expression during OPC differentiation - (A) Schematic showing the human miR-17-92 cluster genomic structure. (B) Quantitative real-time PCR showing that levels of members of the miR-17-92 cluster are dramatically downregulated

during post-natal mouse brain development. ΔΔCt method was used to calculate miRNA levels normalized to 18S RNA expression. Each time point represents at least three pooled animals analyzed in triplicates. P values are derived from one-way ANOVA analysis followed by the Tukey's post-test. **-P<0.01; ***-P<0.001. (C) Quantitative real-time PCR showing that levels of members of the miR-17-92 cluster are downregulated during rat OPC differentiation *in vitro*. ΔΔCt method was used to calculate miRNA levels normalized to 18S RNA expression. The graphs are representative of one of the three experiments performed in triplicates. P values are derived from one-way ANOVA analysis followed by the Tukey's post-test. **- P<0.01; ***-P<0.001(D) Endpoint RT-PCR followed by polyacrylamide gel electrophoresis showing that miR-17-92 members are expressed in the human brain. (E) Quantitative real-time PCR showing that miR-17-92 members are enriched in the human brain white matter. ΔΔCt method was used to calculate miRNA levels normalized to 18S RNA expression. Fold-change was calculated by dividing miRNA levels in white matter by levels in grey matter. The graphs are obtained from analysis of two brains done in triplicates. P values are derived from two-tailed unpaired student's t-test. (F) Endpoint RT-PCR followed by polyacrylamide gel electrophoresis showing that miR-17-92 members are expressed by MO3.13 cells and human $A2B5^{+}$ OLs. (G) Quantitative real-time PCR analysis of the miR-17-92 cluster members in human $A2B5^{+}$ and $A2B5^{-}$OLs shows no difference in expression between the two cell types. ΔΔCt method was used to calculate miRNA levels normalized to 18S RNA expression. Each bar represents the average of 4 subjects analyzed by real-time PCR done in triplicates. P values derive from unpaired student's t-test.

Table 1 – Relative expression analysis of miRs in rodent and human OLs [1]

Differentiating rat OPCs

Day 1		Day 5		Day 8	
miRNA	**Expression**	**miRNA**	**Expression**	**miRNA**	**Expression**
miR-92a-3p	118141.1	miR-92a-3p	161161.9	miR-17-5p	37940.8
miR-17-5p	60698.8	miR-17-5p	74128.1	miR-92a-3p	23362.8
miR-19a-3p	39190.5	miR-19a-3p	69644.3	miR-20a-5p	5811.3
miR-19b-3p	16972.9	miR-19b-3p	30598.8	miR-19b-3p	5270.2
miR-20a-5p	14889.0	miR-18a-5p	1907.5	miR-19a-3p	4518.0
miR-18a-5p	945.4	miR-219-5p	1549.6	miR-18a-5p	681.0
miR219-1-3p	108.5	miR219-1-3p	469.4	miR-219-5p	388.2
miR-219-5p	103.7	miR-20a-5p	395.7	miR-219-2-3p	141.2
miR-219-2-3p	83.1	miR-219-2-3p	303.6	miR-338-5p	82.2
miR-338-5p	25.6	miR-338-5p	265.2	miR219-1-3p	76.9
miR-3065-5p	1.0	miR-338-3p	7.9	miR-338-3p	4.8
miR-338-3p	1.0	miR-3065-5p	1.0	miR-3065-5p	1.0

Acutely isolated human OLs

A2B5 $^{+}$		A2B5 -	
miRNA	**Expression**	**miRNA**	**Expression**
miR-92a-3p	205465.6	miR-92a-3p	1598436.4
miR-219-2-3p	1748.6	miR-17-5p	14497.1
miR-17-5p	1141.9	miR-20a-5p	9793.6
miR-219-1-3p	815.7	miR-219-2-3p	5246.4
miR-20a-5p	802.2	miR-19b-3p	4078.7
miR-19a-3p	625.9	miR-19a-3p	4059.0
miR-19b-3p	559.8	miR-219-1-3p	1913.8
miR-18a-5p	147.6	miR-18a-5p	1609.6
miR-338-5p	73.9	miR-338-5p	122.7
miR-219-5p	64.0	miR-657	77.9
miR-657	18.3	miR-219-5p	55.9
miR-1250	14.7	miR-338-3p	43.2
miR-338-3p	10.7	miR-1250	15.3
miR-3065-5p	9.0	miR-3065-5p	15.0
miR-3065-3p	1.0	miR-3065-3p	1.0

[1] miR expression was normalized to 18S RNA. miR levels relative to the least expressed miR in precursor or mature OLs were calculated and are listed in the table.

Supplementary Table 2.1 – Percentage of miRNA targets conserved across vertebrates [2]

miRNA	Conserved targets	Total Targets	Conserved Targets (%)
17-5p	990	3635	27,2
18a-5p	189	1752	10,8
19a-3p	938	2616	35,9
19b-3p	938	2616	35,9
20a-5p	990	3635	27,2
92a-3p	692	2331	29,7
219-5p	273	1349	20,2
219-1-3p	70	1625	4,3
219-2-3p	95	1791	5,3
338-5p	608	3157	19,3
338-3p	198	2919	6,8
1250	6	450	1,3
657	140	2245	6,2

[2] Human, frog, chicken, rodent and non-human primate miRNA targets were predicted by Human TargetScan (www.targetscan.org) and the percentage of conserved and non-conserved targets for each miRNA was calculated.

Supplementary Table 2.2 – List of primers used on this study [3]

miRNA	Reverse Transcription Stem-loop Primer
miR-219-5p	5' CTCAACTGGTGTCGTGGAGTCGGCAATTCAGTTGAGAGAATTGC 3'
miR-219-1-3p	5' CTCAACTGGTGTCGTGGAGTCGGCAATTCAGTTGAGCGGGACGT 3'
miR-219-2-3p	5' CTCAACTGGTGTCGTGGAGTCGGCAATTCAGTTGAGACAGATGT 3'
miR-338-5p	5' CTCAACTGGTGTCGTGGAGTCGGCAATTCAGTTGAGCACTCAGC 3'
miR-338-3p	5' CTCAACTGGTGTCGTGGAGTCGGCAATTCAGTTGAGCAACAAAA 3'
miR-1250	5' CTCAACTGGTGTCGTGGAGTCGGCAATTCAGTTGAGAAAGGCCA 3'
miR-3065-5p	5' CTCAACTGGTGTCGTGGAGTCGGCAATTCAGTTGAGTCCAGCAT 3'
miR-3065-3p	5' CTCAACTGGTGTCGTGGAGTCGGCAATTCAGTTGAGCTCCAACA 3'
miR-657	5' CTCAACTGGTGTCGTGGAGTCGGCAATTCAGTTGAGCCTAGAGA 3'
miR-17	5' CTCAACTGGTGTCGTGGAGTCGGCAATTCAGTTGAGCTACCTGC 3'
miR-18a	5' CTCAACTGGTGTCGTGGAGTCGGCAATTCAGTTGAGCTATCTGC 3'
miR-19a	5' CTCAACTGGTGTCGTGGAGTCGGCAATTCAGTTGAGTCAGTTTT 3'
miR-20a	5' CTCAACTGGTGTCGTGGAGTCGGCAATTCAGTTGAGCTACCTGC 3'
miR-19b	5' CTCAACTGGTGTCGTGGAGTCGGCAATTCAGTTGAGTCAGTTTT 3'
miR-92a	5' CTCAACTGGTGTCGTGGAGTCGGCAATTCAGTTGAGCAGGCCGG 3'

miRNA	RT-PCR Forward Primer
miR-219-5p	5' ACACTCCAGCTGGGTGATTGTCCAAACGCA 3'
miR-219-1-3p	5' ACACTCCAGCTGGGAGAGTTGAGTCTGGAC 3'
miR-219-2-3p	5' ACACTCCAGCTGGGAGAATTGTGGCTGGAC 3'
miR-338-5p	5' ACACTCCAGCTGGGAACAATATCCTGGTGC 3'
miR-338-3p	5' ACACTCCAGCTGGGTCCAGCATCAGTGATT 3'
miR-1250	5' ACACTCCAGCTGGGACGGTGCTGGATGTGG 3'
miR-3065-5p	5' ACACTCCAGCTGGGTCAACAAAATCACTGA 3'
miR-3065-3p	5' ACACTCCAGCTGGGTCAGCACCAGGATATT 3'
miR-657	5' ACACTCCAGCTGGGGGCAGGTTCTCACCCT 3'
miR-17	5' ACACTCCAGCTGGGCAAAGTGCTTACAGTG 3'
miR-18a	5' ACACTCCAGCTGGGTAAGGTGCATCTAGTG 3'
miR-19a	5' ACACTCCAGCTGGGTGTGCAAATCTATGCAA 3'
miR-20a	5' ACACTCCAGCTGGGTAAAGTGCTTATAGTG 3'
miR-19b	5' ACACTCCAGCTGGGTGTGCAAATCCATGCA 3'
miR-92a	5' ACACTCCAGCTGGGTATTGCACTTGTCCCG 3'

	RT-PCR Universal Reverse Primer
All miRNAs	5'GTGTCGTGGAGTCGGCAATTCAGTTGAG 3'

[5] The nucleotide sequence of primers used for pre-PCR and mature miRNA amplification are listed. All primers were designed according to previously published criteria (Chen et al., 2005; Schmittgen et al., 2008; Tang et al., 2006).

Preface to Chapter 3

Transmembrane protein 10 (TMEM10) is a CNS myelin-specific glycoprotein with unknown function. Because TMEM10 expression is highly upregulated during early stages of OPC differentiation, we hypothesized that TMEM10 may be required for OPCs to differentiate.

We have tested this hypothesis *in vitro* by manipulating the levels of TMEM10 expression in differentiating OPCs. The results obtained in this study are described in the manuscript bellow.

CHAPTER 3

TMEM10 induces oligodendrocyte differentiation *in vitro*

Omar de Faria Jr, Ajit S. Dhaunchak, Alejandro D Roth, David R Colman and Timothy Kennedy

1 Abstract

Myelin is a multi-layered membrane that insulates axons allowing for fast conduction of the action potential. During postnatal development, oligodendrocyte precursor cells (OPCs) differentiate into myelin-forming oligodendrocytes in a process distinguished by substantial changes in morphology and the onset of myelin gene expression. A CNS-specific myelin gene, *tmem10*, codes for a type 1 transmembrane protein that is highly upregulated in relatively early stages of OPC differentiation *in vitro*. Here, we show that TMEM10 is first expressed in the mouse brain at P10 and that protein levels continue to increase as oligodendrocytes differentiate and myelinate axons *in vivo*. Constitutive TMEM10 overexpression in the oligodendroglia cell line, oli-neu, evokes an increase in process extension, branching, and transcriptional levels of myelin-associated genes (CNP, CGT and MAG). Conversely, oli-neu growth rate appears reduced, suggesting that TMEM10 overexpression slows down proliferation. During oli-neu cell differentiation, initiated by neuron-conditioned medium, TMEM10 knock down reduced levels of myelin-associated gene expression. Importantly, knock down experiments in primary oligodendrocyte cultures showed that OPCs differentiate to a lesser extent in the absence of TMEM10. Together, our data suggest a function for TMEM10 in the developing CNS and

indicate that *in vitro* differentiation of oligodendrocytes requires this mammalian-specific glycoprotein.

2 Introduction

Myelin is a multi-layered, lipid-rich membrane that insulates axons. In myelinated fibers, axonal depolarization is confined to the node of Ranvier and, as a result, action potentials rapidly propagate along the axon in a "saltatory" manner. Oligodendrocytes are the glial cells responsible for the generation of myelin in the central nervous system (CNS). During their differentiation, oligodendrocyte precursor cells (OPCs) undergo marked changes in morphology and gene expression. Initially bipolar, OPCs elaborate an extensive network of cellular processes, whose dynamic leading edges contact and ensheath axons. As process extension continues, nascent myelin segments grow both radially and longitudinally along the axon. During this time, well-defined stages of oligodendrocyte maturation are distinguishable by the sequential expression of cell surface galactolipids. These include the sulfatides recognized by A2B5 and O4 antibodies and the galactocerebroside GalC. In addition, differentiating oligodendrocytes activate the myelin program of gene expression and begin to express myelin genes such as 2', 3'-Cyclic-Nucleotide 3'-Phosphodiesterase (CNP), Myelin Associated Glycoprotein (MAG), Proteolipid Protein 1 (PLP) and Myelin Basic Protein (MBP).

Multiple regulatory mechanisms, both external and internally initiated, cooperate to control oligodendrocyte differentiation (Mitew et al., 2014). Part of this regulation is in place to ensure that oligodendrocyte differentiation and axon maturation are temporally coordinated. In this

context, premature uncoordinated OPC differentiation is prevented by the activation of inhibitory transcription factors Sox5, Sox6, Hes5, Id2 and Id4 (Liu et al., 2006; Stolt et al., 2006; Wang et al., 2001). These inhibitory transcription factors are regulated downstream of ligands that are expressed on the axon surface, such as Lingo-1 and Jagged-1, or soluble molecules that are secreted by neurons, like adenosine (Wang et al., 1998; Mi et al., 2005; Stevens et al., 2002; Trajkovic, Dhaunchak et al., 2006). On the glial side, the expression of several transcription factors and other regulatory molecules are necessary for OPCs to differentiate. These pro-differentiation factors include Olig2, Sox10, Myelin regulatory factor (Myrf) and miRNAs miR-219 and miR-338 (Cai et al., 2007; Stolt et al., 2002; Emery et al., 2009; Dugas et al., 2010; Zhao et al., 2010). Interestingly, miR-219 and miR-338 target the untranslated region of inhibitory transcription factor mRNAs as well as down regulate levels of Platelet-derived Growth Factor Alpha Receptor (PDGFαR). Therefore, these miRNAs provide a regulatory link between OPC differentiation and cell cycle exit (Dugas et al., 2010; Zhao et al., 2010). Although considerable progress has been made in this field, our current understanding of mechanisms regulating oligodendrocyte differentiation remains incomplete.

Transmembrane Protein 10, or TMEM10 (also known as Opalin, in primates), is a mammalian-specific type-1 transmembrane glycoprotein expressed by oligodendrocytes, but not Schwann cells. The first intron of the TMEM10 gene contains a conserved transcriptional enhancer that directs TMEM10 expression to white matter in the CNS (Aruga et al., 2007). Consistently, TMEM10 transcripts were 23-fold down regulated in the CNS following genetic ablation of oligodendrocytes in transgenic mice (Golan et al., 2008). *In situ* hybridization and immunohistochemical analyses confirmed that, *in vivo*, TMEM10 is expressed in the white

matter by oligodendrocytes and that expression is enriched in the cell soma, processes and non-compact myelin (Yoshikawa et al., 2008; Golan et al., 2008). In the mouse brain, TMEM10 mRNA is first detected at P9, coincident with oligodendrocyte differentiation and the beginning of axon myelination in the CNS (Golan et al., 2008; Yoshikawa et al., 2008). Immunolabelling of purified OPC cultures showed that TMEM10 is detected as soon as 2 DIV, in O4 positive cells, where it localizes in close association with F-actin filaments (Kippert et al., 2008). Strikingly, TMEM10 was the most upregulated transcript during differentiation of the OPC-like oli-neu cell line, an *in vitro* model of early oligodendrocyte differentiation (Kippert et al., 2008). Overall, these observations suggest that TMEM10 may contribute to oligodendrocyte differentiation and myelination (Aruga et al., 2007; Golan et al., 2008; Kippert et al., 2008).

Here, we generate a novel antibody and demonstrate that it is specific for TMEM10. We detect TMEM10 protein in lysates of P10 mouse brain and show that expression increases as OPCs differentiate *in vivo*. Overexpressing TMEM10 in oli-neu cells induced substantial changes in morphology and expression of myelin-associated genes, whereas the growth rate was reduced. Conversely, knock down experiments in oli-neu cells and primary OPCs revealed that TMEM10 expression promotes oligodendrocyte differentiation. Together, our data indicate that TMEM10 is necessary for OPC differentiation *in vitro*.

3 Material and methods

Animals

Sprague Dawley rats were obtained from Charles River laboratories (Quebec, CA). All procedures were performed in accordance with the Canadian Council on Animal Care guidelines for use in animal research.

Antibodies

The following antibodies were used in this study: mouse monoclonal anti-α-actin (Sigma); mouse monoclonal antiβ-tubulin III (Cell Signaling); rabbit polyclonal GAPDH (Santa Cruz Biotechnology). Mouse polyclonal anti-PLP was provided by Dr. Marjorie Lees, University of Massachusetts Medical School, Massachusetts, USA. Rabbit polyclonal anti-MAG (Salzer et al., 1987) and rabbit polyclonal anti-MBP (Colman et al., 1982) were made in lab and have been previously published. TMEM10 polyclonal antibody was generated by immunizing rabbits with a peptide antigen corresponding to amino acids 65-142 of rat TMEM10. The specificity of the antiserum was validated by western blot analysis of OPC cultures transfected with control and TMEM10 siRNAs.

Cell culture

The oli-neu cell line (provided by Dr. Jacqueline Trotter, University of Mainz, Mainz, Germany) was maintained in DMEM supplemented with N1 (Sigma-Aldrich,) and 3% horse serum (proliferation medium) on PLL-coated tissue culture dishes. Oli-neu differentiation was induced by culturing these cells in serum-free DMEM-N1 medium supplemented with 10% neuron-conditioned medium or 1-2 mM 8Br-cAMP (Sigma-Aldrich) for 48 hrs. Neuron-conditioned medium was collected from E15-17 cortical neurons cultures that were maintained *in vitro* for two weeks. TMEM10-expressing oli-neu cells were generated by transfecting oli-neu cells with a

GFP-TMEM10 construct. Hygromicin B was used to select cells that stably expressed the construct. After clone isolation, TMEM10 oli-neu cells were maintained in proliferation medium. Rat primary OPC cultures were prepared as previously described. Briefly, mixed glial cultures were generated from P2 rat cortices and maintained for 17 days prior to OPC isolation in DMEM, 10% fetal bovine serum (FBS) and antibiotics. OPCs were isolated using the shake-off method (Armstrong, 1998) and plated in Sato medium (DMEM, 5 µg/ml insulin, 100 µg/ml transferrin, 30 nM sodium selenite, 30 nM triiodothyronine, 100 µg/ml penicillin-streptomycin, 2mM glutamax). For electroporation experiments, OPCs were allowed to recover for 24 hrs after isolation and 12 hrs after electroporation in DMEM, 10% FBS, before medium was changed to Sato medium.

Growth rate assay

Wild type (WT) and TMEM10 oli-neu cells were plated at low cell density (1300 cells/cm^2) and cultured under normal conditions for 2, 24, 48 and 72 hrs. At each time point, cells were fixed with 4% paraformaldehyde (PFA) and stained with the nuclear marker, DAPi (4',6-diamidino-2-phenylindole). Images were taken with an ImageXpress microscope (Molecular Devices) and the number of DAPi-positive nuclei counted using MetaXpress software.

Immunohistochemistry

Mice were deeply anesthetized with 4X avertin and perfused intracardiaclly with phosphate buffered saline, pH 7.4 (PBS) followed by 4% PFA, PBS. Brains were dissected and postfixed with 4% PFA, overnight, at 4°C with gentle shaking and subsequently equilibrated in 30% sucrose for 1 week at 4°C. After embedding in optimal cutting temperature (OCT) compound

(Sakura Finetek), tissue was cut in 20 μm-thick sections using a Leica cryostat. Slides were allowed to dry for 15 min before being stored at -80°C. For immunohistochemistry, slides were allowed to equilibrate to room temperature (RT) then were washed with PBS 3 times for 5 minutes per wash. Sections were blocked with 5% BSA, 0.3% Triton-X, PBS for 1 hr, at RT, and incubated overnight, at 4°C, with primary antibodies diluted in 3% BSA, 0.3% Triton-X, PBS. Sections were then washed with PBS 3 times for 10 minutes per wash, and incubated overnight, at 4°C, with the appropriate secondary antibodies diluted in 3% BSA, PBS. PBS wash steps were repeated followed by a brief wash with water. Sections were immediately mounted in mounting media. Images were taken using an Olympus Fluoview confocal microscope.

Morphology analysis

WT and TMEM10 oli-neu cells were cultured under proliferation conditions for 48 hrs. Cells were then fixed with 4% PFA and stained with Cell Tracker dye (ThermoFisher). Images were taken with an ImageXpress microscope (Molecular Devices) and analyzed using MetaXpress software. Measurements taken included process outgrowth; number of branches per cell; number of processes per cell; and percentage of cells exhibiting process outgrowth. For morphological analysis of primary OPCs, cell cultures were fixed in 4% PFA and labeled for MBP. Images were taken using an Axiovert 100 microscope (Carl Zeiss) with a MagnaFire CCD camera (Optronics). 50-100 cells were randomly selected and individually outlined using the selection tool in ImageJ (Schneider et al., 2012). Multiple parameters, including mean fluorescence intensity, area, circularity and solidity were measured.

Real-time RT-PCR

Reverse transcription was performed as previously described (de Faria et al., 2012). For real-time RT-PCR, 20 ng of cDNA were added to 5 uM primers and 2X SYBR Green PCR master mix (Invitrogen). An Applied Biosystems 7000 thermocycler was used to perform all PCR reactions. Data analysis was done using the $2^{-[delta][delta]Ct}$ method (Schmittgen et al., 2000; Winer et al., 1999) and final expression values were normalized to 18S RNA.

Transfections

Plasmid and siRNA transfections on cell lines were performed using Lipofectamine 2000 and Lipofectamine RNAiMAX (Invitrogen) transfection reagents. Primary OPC electroporation was performed in an Amaxa nucleofactor using the Basic Nucleofactor kit for Primary Mammalian Glial Cells (Lonza).

TMEM10 truncations

Different pairs of primers were designed to amplify C-terminally truncated fragments of TMEM10. PCR products were cloned into pEGFP-N1 using BglII/AgeI sites and transformed into *Escherichia coli*.

Western Blot

Protein lysates were prepared from freshly dissected rodent hippocampus and cerebellum. Isolated tissues were homogenized on ice with Ripa buffer containing protease and phosphatase inhibitors. Equal amounts of protein were resolved by SDS-PAGE and transferred to PVDF membrane (BioRad). Membranes were blocked with 5% milk or 5% BSA, accordingly to the primary antibody manufactures instructions, in TBS containing 0.1% Tween (TBST) for 1 hr at

RT and incubated with primary antibodies diluted in 1% milk, TBST, overnight at 4°C. Membranes were washed three times with TBST and incubated with horseradish peroxidase-conjugated secondary antibodies for 1 hr at RT. Membranes were washed and developed with an Enhanced Chemoluminescence Detection kit (Pierce).

Statistical Analysis

Data was analyzed using the GraphPad Prism software. Results were considered significant when *p*-values were $*p < 0.05$. $**p < 0.01$ and $***p < 0.001$. Statistical tests used are indicated in the figure legends.

4 Results

TMEM10 is expressed during oligodendrocyte differentiation and myelination *in vivo*

In vitro, TMEM10 is expressed during relatively early stages of OPC differentiation, whereas *in vivo*, TMEM10 is first detected in brain sections of P7-P12 mice, depending on the brain region (Kippert et al., 2008; Golan et al., 2008). To better understand TMEM10 expression during development, we generated a new TMEM10 antibody. Western blot analysis using this antibody showed one major band at the expected size of ~36 KDa in lysates derived from rat OPC cultures transfected with a control siRNA, but not in lysates from cells transfected with two different TMEM10 siRNAs (Figure 3.1A). In addition, lysates from OPCs electroporated with a GFP-TMEM10 expression construct show an additional TMEM10 band with the expected shift in molecular weight (Figure 3.1A). Thus, our TMEM10 antibody recognizes TMEM10 specifically and is a valid tool to study TMEM10 expression.

Using our new TMEM10 antibody, we performed immunohistochemical analysis of brain sections of P35 mouse and observed strong TMEM10 expression in the corpus callosum and striatum, in a distribution similar to the major myelin protein PLP (Figure 3.1B). Strong TMEM10 immunoreactivity was also detected in cerebellar white matter where it was associated with cell bodies and processes (Figure 3.1C, arrowhead and arrows, respectively). These observations are in agreement with the findings of previous studies that have examined TMEM10 expression in the mouse brain (Yoshikawa et al., 2008; Golan et al., 2008, Sato et al., 2014). Next, we investigated the temporal pattern of TMEM10 expression. Western blot analysis of lysates from mouse hippocampus (Figure 3.1D) and cerebellum (data not shown) revealed that TMEM10 is first expressed at P10 and that expression levels continue to increase up to P60. We conclude that TMEM10 expression is upregulated in the mouse brain during oligodendrocyte differentiation and myelination *in vivo*.

To gain further insight into TMEM10 expression and function, we investigated TMEM10 expression at the cellular level. In HEK293 cells transfected with a GFP-TMEM10 expression construct, TMEM10 was found to localize at the membrane and accumulate in leading edges of extending processes (Figure 3.2A, arrowheads). In addition, immunolabelling experiments in differentiating OPC cultures revealed that TMEM10 localizes to oligodendrocyte cell bodies, primary processes and process tips, but not to MBP positive compact myelin-like membranes (Figure 3.2B). Consistent with the absence of TMEM10 from compact myelin membranes, protein extraction experiments using increasingly stringent detergents showed that TMEM10 is completely solubilized with mild, non-ionic detergent extraction (Figure 3.2C). This pattern of cellular distribution is consistent with TMEM10 potentially contributing to process extension

and branching; it also implies that TMEM10 function at the oligodendrocyte membrane likely requires association with cytoplasmic elements. Interestingly, TMEM10 appears to co-localize with actin filaments in cell processes (Kippert et al., 2008) and its intracellular domain contains several putative phosphorylation sites (Yoshikawa et al., 2008).

Mutational studies have shown that glycosylation within the N-terminal extracellular domain is necessary for the correct localization of TMEM10 to the plasma membrane (Yoshikawa et al., 2008). We examined if there is additional regulation of TMEM10 expression at the cell surface by deleting intracellular fragments of TMEM10 sequence (Figure 2D-E). We found that one region, composed of amino acids 79-95, which was deleted in deltaC4-TMEM10, is necessary for TMEM10 expression at the plasma membrane (Figure 3.2F). Interestingly, this fragment contains three putative phosphorylation sites, implying that TMEM10 localization at the cell surface may be regulated by phosphorylation. Our data in combination with data from Yoshikawa et al. (2008), suggest that TMEM10 expression at the plasma membrane is tightly regulated and that mechanisms controlling TMEM10 localization require an intact intracellular domain.

TMEM10 expression induces oli-neu cell line differentiation

The observation that TMEM10 expression is upregulated during postnatal development led us to investigate whether TMEM10 is involved in OPC differentiation. Because TMEM10 is the most upregulated transcript during differentiation of the OPC cell line oli-neu (Kippert et al., 2008), we examined if TMEM10 expression per se could induce oli-neu cells to differentiate. However, we first verified that this cell line is a valid model to study OPC differentiation. Oli-neu cells

cultured in 3% horse serum exhibited bipolar morphology and weak O4 staining. In contrast, cells that were maintained for 48 hr in serum-free medium supplemented with either 10% neuron-conditioned medium (NCM) or 1 mM cAMP extended long and branched processes (Figure 3.3A); in some cases, differentiated oli-neu cells clearly resembled immature pre-myelinating oligodendrocytes (Figure 3.3A, left panel). In addition, we performed western blot analyses of oli-neu cell lysates and found that differentiated oli-neu cells, but not cells cultured in the presence of serum, expressed the oligodendrocyte marker PLP (Figure 3.3B). We therefore conclude that oli-neu cells are able to differentiate under specific culture conditions and that this cell line is a suitable model for the study of early OPC differentiation.

To investigate the involvement of TMEM10 in oli-neu differentiation, we generated an oli-neu cell sub-line that constitutively overexpressed GFP-TMEM10 (Figure 3C). Analysis of oli-neu growth parameters showed that "TMEM10 oli-neu" has a significantly reduced growth rate in comparison to wild-type (WT) cells, suggesting that oli-neu proliferation may be impaired following TMEM10 overexpression (Figure 3.3D; daily growth was 193.4±34.5% for WT oli-neu and 95.4± 11.4% for TMEM10 oli-neu). Because oli-neu cells extend long and branched processes during induced differentiation, we determined if TMEM10 overexpression alone could induce a similar change in oli-neu morphology. WT oli-neu cultured in the presence of serum extended few and short processes, as expected. In contrast, TMEM10-oli-neu cells cultured in the same conditions extended many processes that were longer and more branched (Figure 3.3E). On average, TMEM10 oli-neu processes were nine times longer and more than thirty times more branched compared to WT oli-neu, indicating that TMEM10 expression triggers substantial morphological differentiation, even in the presence of serum (Figure 3.3F).

During OPC differentiation, changes in morphology are accompanied by expression of myelin genes. We therefore determined if TMEM10 expression could induce myelin gene transcription in oli-neu cells. Real-time RT-PCR analysis of myelin gene transcripts showed that CNP, MAG and CGT (Figure 3.3G), but not MBP and PLP (data not shown) were upregulated in TMEM10 oli-neu in comparison to WT cells. In addition, non-oligodendroglial genes such as GFAP and OPC markers such as NG2 were markedly downregulated in TMEM10 oli-neu cells (Figure 3.3G). Thus, we conclude that TMEM10 overexpression is sufficient to induce the expression of some, but not all, markers of OPC differentiation, even when oli-neu cells are cultured in serum. Together, our data indicate that overexpression of TMEM10 induces oli-neu cell differentiation.

OPC differentiation is limited in the absence of TMEM10

Our overexpression data suggested that TMEM10 may be required for oli-neu differentiation. To test this, we conducted knock down experiments in which oli-neu cells were transfected with control or TMEM10 siRNAs and induced to differentiate in serum-free media supplemented with 10% NCM. Two TMEM10 siRNAs successfully downregulated TMEM10 transcript levels in oli-neu cells that were cultured in differentiating conditions (Figure 3.4A, left panel). To further demonstrate TMEM10 knock down, we transfected TMEM10 oli-neu with TMEM10 siRNAs and conducted western blot analysis on lysates derived from transfected cells. We found that both TMEM10 siRNAs were able to knock down GFP-TMEM10 protein levels in comparison to control siRNA (Supplemental Figure 3.1).

When cultured in serum-free 10% NCM medium, oli-neu cells differentiated and upregulated the expression of myelin genes (Figure 3.3A-B). We therefore performed real-time RT-PCR analysis

of myelin gene expression on differentiating oli-neu cells that were transfected with control and TMEM10 siRNAs. CNP and CGT transcript levels were significantly reduced in differentiating oli-neu cells transfected with TMEM10 siRNAs in comparison to control levels (Figure 3.4A). We also performed western blot analysis on lysates derived from siRNA-transfected cells. Differentiating oli-neu cells transfected with TMEM10 siRNAs expressed significantly lower levels of MAG protein in comparison to control lysates (Figure 3.4B). We therefore conclude that TMEM10 is required for normal expression of myelin genes during NCM-induced oli-neu differentiation.

As TMEM10 overexpression and knock down experiments in oli-neu cells provided evidence that TMEM10 might contribute to OPC differentiation, we next investigated if TMEM10 knock down in primary cells could impair the differentiation of OPCs. Primary OPCs were isolated from the neonatal rat brain and electroporated with control and TMEM10 siRNA followed by 5 days of growth in Sato medium. To determine if TMEM10 siRNA was effective in down regulating TMEM10 expression in primary OPCs, western blot analyses were conducted on lysates derived from electroporated cells. Figure 3.5A shows that the endogenous levels of TMEM10 were drastically down regulated in TMEM10 siRNA transfected cells compared to controls (Figure 3.5A).

When cultured in Sato medium for 5 days *in vitro*, OPCs differentiate and express the mature oligodendrocyte marker MBP. Therefore, we stained MBP in OPC cultures transfected with control and TMEM10 siRNAs and determined the percentage of total cells that were MBP positive after 5 DIV. In TMEM10 siRNA-transfected OPC cultures, the percentage of MBP positive cells was reduced ~20% compared to control siRNA (Figure 3.5B; 54.4±5.3% in control

siRNA and 42.7±6.1% in TMEM10 siRNA). In addition, the average MBP fluorescence intensity of individual cells was significantly reduced in TMEM10 siRNA-transfected cultures in comparison to cultures transfected with control siRNA (Figure 3.5C, top left graph and pictures). Since TMEM10 overexpression induced substantial morphological differentiation of oli-neu cells (Figure 3.3F) we also performed shape descriptor measurements of MBP positive membranes extended by OPCs after 5 DIV. Although total area and solidity were not significantly altered, circularity was reduced in OPCs transfected with the TMEM10 siRNA, suggesting a deficit of membrane extension following TMEM10 downregulation (Figure 5C; 0.18±0.013 in control siRNA and 0.13±0.012 in TMEM10 siRNA-transfected cultures). Taken together, these data support our conclusion that TMEM10 functionally contributes to OPC differentiation.

5 Discussion

Despite the substantial advances that have been made in the study of oligodendrocyte differentiation, many aspects of this complex process have yet to be elucidated. Here, we show that the myelin glycoprotein TMEM10 regulates OPC differentiation. During postnatal brain development, TMEM10 protein is first detected at P10, but expression levels continue to increase thereafter. Constitutive TMEM10 expression by undifferentiated oli-neu cells induced morphological differentiation and increased levels of myelin gene transcripts. Conversely, knocking down TMEM10 expression in differentiating oli-neu cells decreased myelin gene expression and, in the absence of TMEM10, primary OPCs differentiated to a limited extent. Our results support the conclusion that TMEM10 promotes OPC differentiation *in vitro*.

TMEM10 was the most up regulated transcript detected during NCM-induced differentiation of oli-neu cells (Kippert et al., 2008). Because oli-neu differentiation is a cell line model for initial OPC differentiation, this suggested that the onset of TMEM10 expression might similarly occur at early stages of primary OPC development *in vitro*. Consistently, in primary OPC cultures, TMEM10 expression was detected as early as 2 DIV by cells double positive for the oligodendrocyte markers NG2 and O4. In these cultures, expression persisted thereafter and TMEM10 immunoreactivity strongly labeled differentiating and mature oligodendrocytes that expressed the mature marker MBP (Kippert et al., 2008). This temporal pattern of expression was recapitulated in the mouse brain, where we and others have shown that TMEM10 is first detected at ~P7-P10 and continues to be expressed at high levels at older ages (Figure 3.1D; Golan et al., 2008; Yoshikawa et al., 2008). This implies that in addition to contributing to OPC differentiation, TMEM10 expression may be required for maintenance of the mature oligodendrocyte phenotype, as has been demonstrated for other pro-differentiation factors. Conditional deletion of Myrf in adult oligodendrocytes resulted in demyelination and loss of myelin gene expression, indicating that this transcription factor is necessary for both OPC differentiation and maintenance of oligodendrocyte identity in the adult brain (Koenning et al., 2012). Similar results were obtained in the PNS following late-onset ablation of Krox-20 and Sox10. Together, these findings demonstrate that persistent expression of differentiation factors may be important for myelin maintenance in the mature nervous system (Bremer et al., 2011; Decker et al., 2006).

An aspect of TMEM10 function that has emerged from our findings and is consistent with other studies is a putative role in regulating cytoskeletal remodeling and morphology. TMEM10

accumulates at the leading edges of membrane extensions and tips of processes (Figure 2A-B), where it colocalizes with filaments of actin (Kippert et al., 2008). Following latrunculin A-induced destabilization of F-actin, a fraction of TMEM10 was found to accumulate in the cytoplasm, indicating that localization at the plasma membrane requires intact F-actin (Kippert et al., 2008). This phenotype is similar to the distribution we observed when the truncated form of TMEM10 that lacks amino acids 79-95 was expressed in oli-neu cells, suggesting that this intracellular region may interact directly or indirectly with F-actin (deltaC4-TMEM10, Figure 3.2F). TMEM10 overexpression also induced a striking increase in oli-neu process length and branching, that was reminiscent of morphological changes associated with oli-neu differentiation (Figure 3.3E-F). Consistent with this phenotype, differentiating primary OPCs in which TMEM10 had been knocked down extended abnormally shaped MBP-positive membranes (Figure 3.5C). Taken together, these results provide evidence that TMEM10 functions to regulate OPC morphology and suggest that this regulation involves interaction with the F-actin cytoskeleton.

During postnatal CNS development, the onset of oligodendrocyte differentiation and myelination must be temporally coordinated with axonal maturation. Signals mediating this neuron-glia interaction include protein ligands presented by the axonal plasma membrane (Mi et al., 2005; Park et al., 2001; Wang et al., 1998), as well as soluble molecules secreted by neurons (Stevens et al., 2002; Trajkovic et al., 2006). We report that TMEM10 knock down decreased myelin gene expression induced by a combination of NCM treatment and serum removal (Figure 3.4). In addition, TMEM10 overexpression was sufficient to replicate NCM-induced differentiation in serum-free conditions (Figure 3.2). These findings imply that TMEM10 is involved in regulatory

mechanisms that are initiated by serum withdrawal or, alternatively, that TMEM10 functions downstream of a neuron-secreted signal to facilitate oli-neu differentiation. We favour the latter possibility because TMEM10 expression itself is rapidly and strongly upregulated by NCM treatment (Kippert et al., 2007); however, further investigation will be required to determine the significance of this mechanism *in vivo*.

The signaling underlying NCM-induced TMEM10 expression is not known; however, it may involve the second messenger cAMP and its effector molecule CREB1. The oligodendrocyte enhancer located within the first intron of the TMEM10 gene contains a CREB1 binding site and elevation of cAMP intracellular levels induces TMEM10 expression (Aruga et al., 2007). Interestingly, both cAMP and TMEM10 contribute for *in vitro* oli-neu/OPC differentiation, suggesting that TMEM10 may function downstream of cAMP in a common signaling cascade (Figure 3.3 and (Raible and McMorris, 1989; Sato-Bigbee and DeVries, 1996)). Interestingly, inhibition of phosphodiesterase, a cAMP degrading enzyme, increases cAMP levels *in vitro* and enhances remyelination *in vivo*, suggesting that TMEM10 might be upregulated in the brain following myelin degeneration and may contribute downstream of cAMP during remyelination (Syed et al., 2013). Regulatory mechanisms downstream of TMEM10 might depend on the phosphorylation of its intracellular domain, as several putative sites for phosphorylation are present in this region. These include motifs for phosphorylation by MAPK and Calmodulin-dependent protein kinase II (Yoshikawa et al., 2002). Interestingly, an unbiased proteomic search for calmodulin partners revealed that TMEM10 binds calmodulin (Shen et al., 2005b). Although an interesting possibility, it remains to be determined if TMEM10 is in fact phosphorylated by any kinase.

Elucidation of mechanisms that regulate oligodendrocyte differentiation and myelin formation is critically important because myelin integrity is compromised during aging and in many neurological diseases. Recent findings indicate that adult onset myelination is an ongoing process with functional significance for adult behavior, further emphasizing the relevance of myelination and remyelination in the mature CNS (Gibson et al., 2014; McKenzie et al., 2014). Here, we have provided evidence that TMEM10 promotes oligodendrocyte differentiation *in vitro*. Further investigation of TMEM10 function will contribute to a better understanding of the mechanisms that control oligodendrocyte development and myelin formation in the CNS.

6 Figures and figure legends

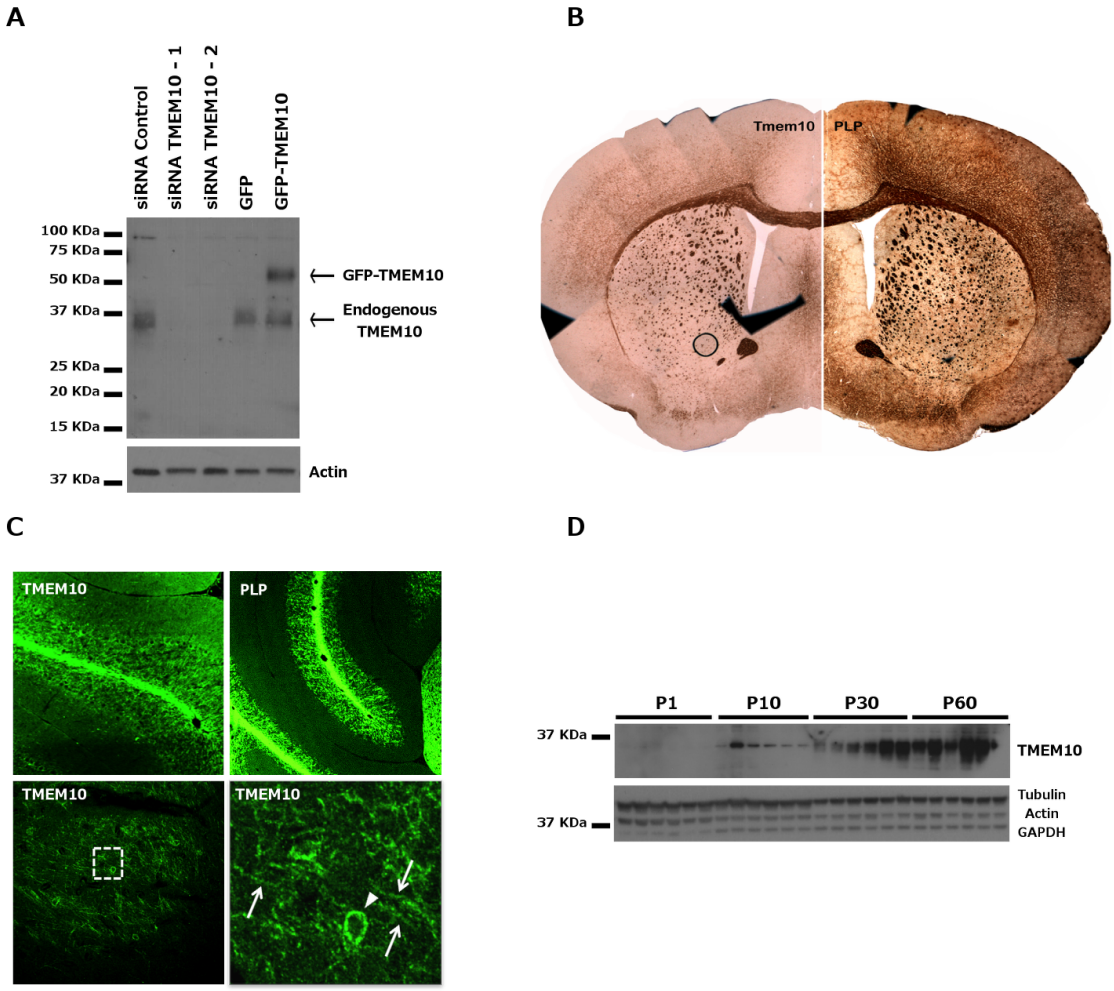

Figure 3.1: TMEM10 expression profile – (A) validation of a new TMEM10 antibody. One major band corresponding to endogenous TMEM10 is detected around 36 KDa. A second band, around 60KDa is detected in OPCs transfected with a GFP-TMEM10 expression construct. **(B)** Immunohistochemistry for TMEM10 and PLP on coronal sections of P35 mouse brain. **(C)**

Immunohistochemistry for TMEM10 and PLP on horizontal sections of P35 mouse brain. The area demarcated on the bottom left image is enlarged on the right. Arrowheads indicate TMEM10 expression in the cell body whereas arrows indicate expression in cell processes. **(D)** Western blot analysis of temporal pattern of expression in the mouse hippocampus. TMEM10 protein was first detected at P10.

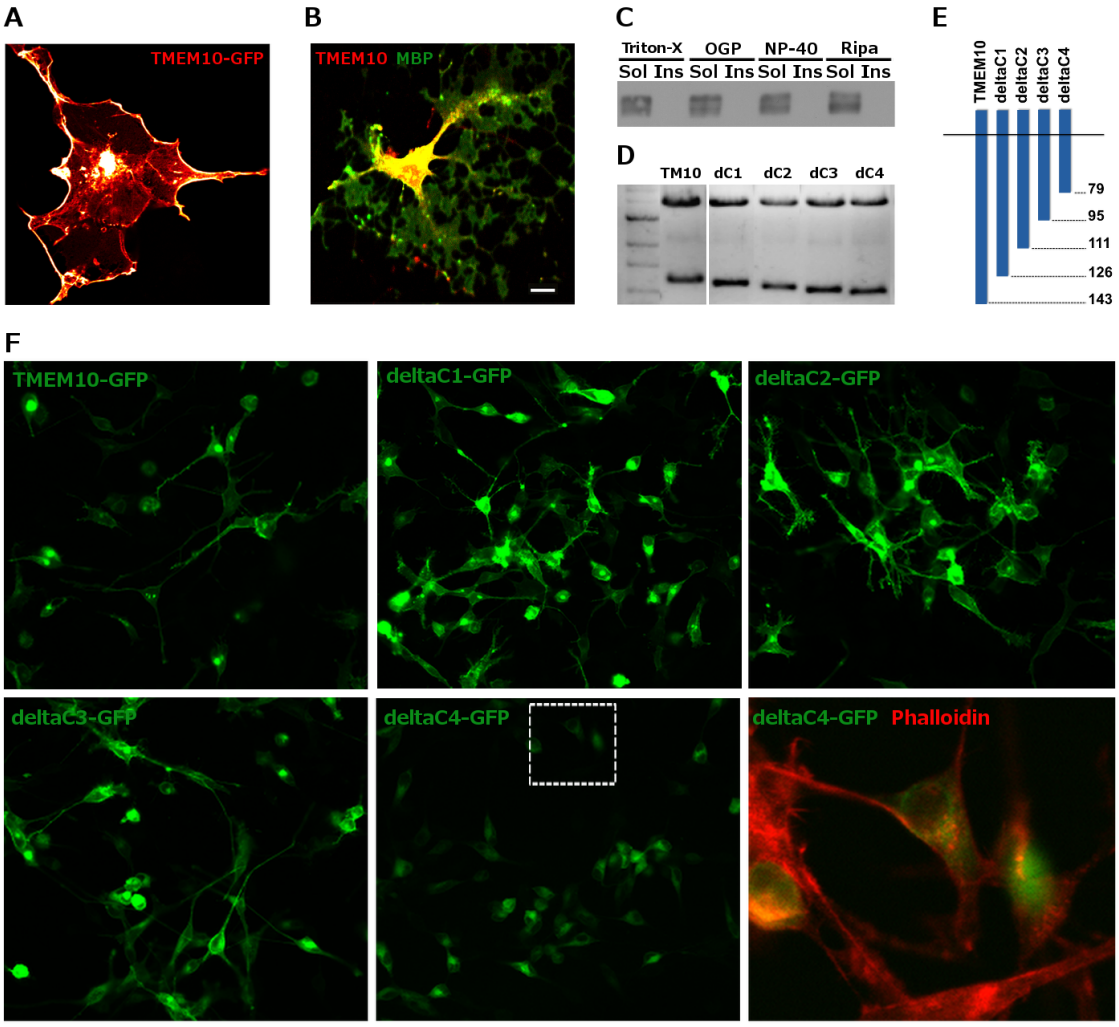

Figure 3.2: TMEM10 distribution at the cellular level – (A) Oli-neu cells were transfected with a GFP-TMEM10 expression construct. GFP signal was detected on the plasma membrane and accumulated on leading edges of extending processes. **(B)** Primary OPCs were cultured for 3 days and stained for TMEM10 and MBP. TMEM10 distributed along the cell body, primary processes and tips of processes, but not in MBP positive membranes. Scale bar: 10um **(C)** Western blot analysis of TMEM10 Oli-neu soluble and insoluble fractions following extraction with different detergents. **(D)** Agarose gel electrophoresis showing C-terminal truncated

TMEM10 fragments used to transfect oli-neu cells. **(E)** Schematic representation of truncated TMEM10 fragments. Numbers on the right indicate the position of the last amino acid encoded by the truncated TMEM10 fragment relative to the full-length protein. **(F)** Oli-neu cells were transfected with GFP-TMEM10 or different C-terminally truncated GFP-TMEM10 fragments. The area demarcated in the bottom middle image is enlarged on the right. Note that GFP-deltaC4TMEM10 does not distribute in the processes, but instead accumulates in the cytoplasm.

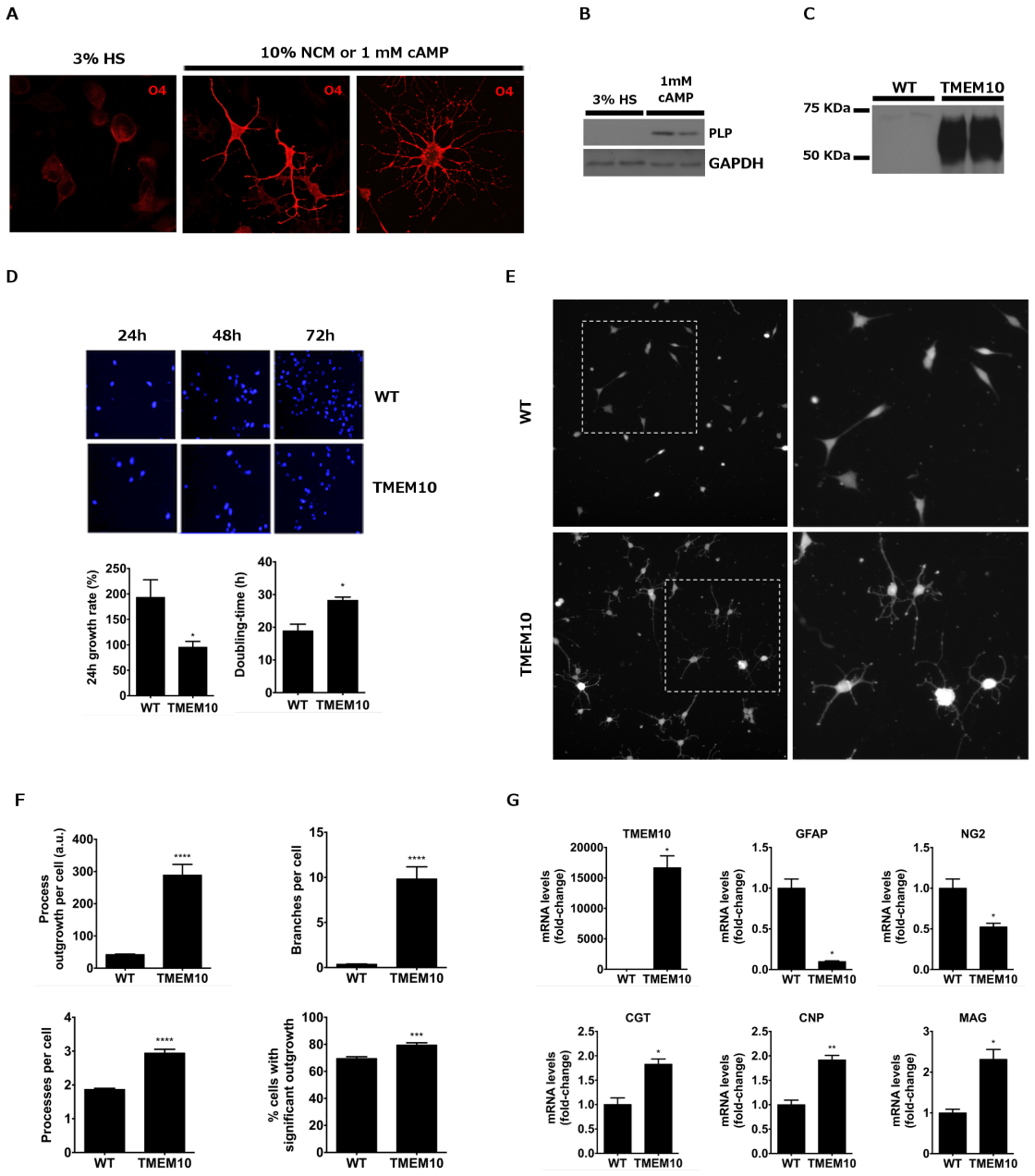

Figure 3.3: TMEM10 overexpression induces oli-neu differentiation – (A) O4 staining of oli-neu cells cultured in the presence of 3% horse serum or 10% NCM/1mM cAMP in serum-free medium. **(B)** Western blot analysis cell lysates from oli-neu cells cultured in 3% horse serum or 1mM cAMP in serum-free medium. **(C)** Western blot analysis of lysates derived from WT and

TMEM10 oli-neu. Image shows TMEM10 expression. **(D)** WT and TMEM10 oli-neu were monitored for their growth rate over 3 days. Cells were plated at the same density on day 0. Graphs show mean ±SEM of three independent experiments. * $p< 0.05$ (student t-test). **(E)** WT and TMEM10 oli-neu cells were cultured for 2 days and stained with a membrane labeling dye. Regions demarcated on the left are enlarged on the right. **(F)** Process length, number of branches, number of processes and percentage of cells with significant outgrowth were measured. Graphs show mean ±SEM. 90 fields from two independent experiments performed in triplicates were analyzed. *** $p< 0.001$; **** $p < 0.0001$ (student t-test). **(G)** Real-time RT-PCR analysis of lysates derived from WT and TMEM10 oli-neu cells. Graphs show mean ±SEM. * $p < 0.05$; ** $p < 0.01$ (student t-test).

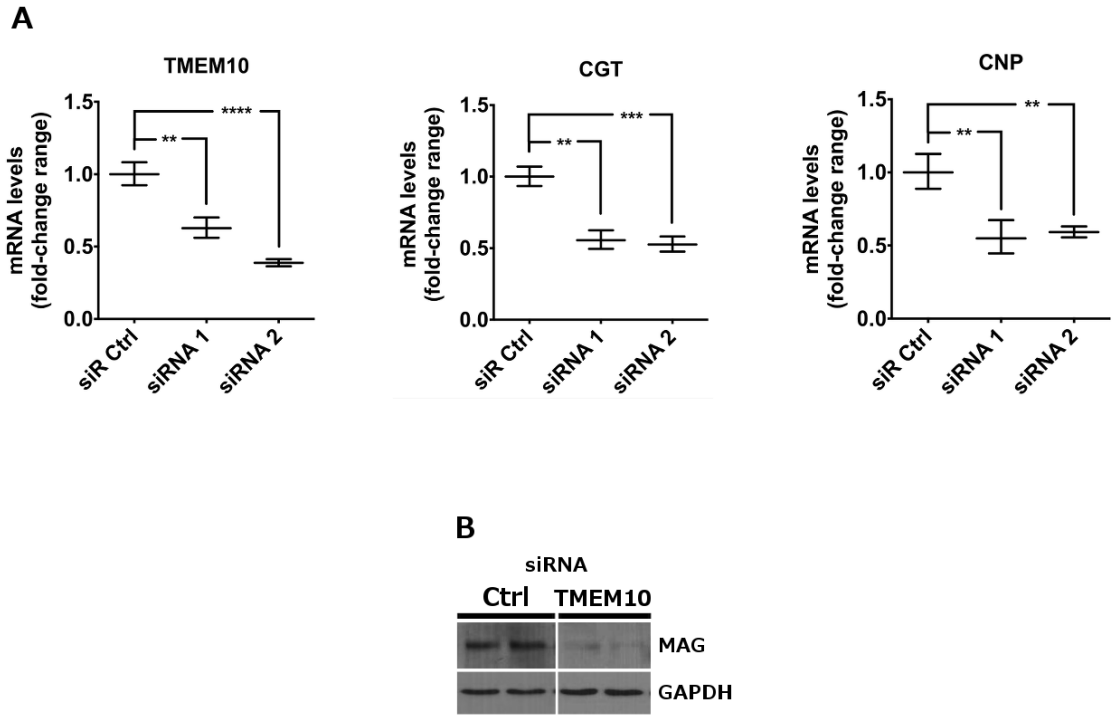

Figure 3.4: TMEM10 knock down decreases myelin gene expression in oli-neu cells – (A) Oli-neu cells were transfected with control and TMEM10 siRNA and induced to differentiate. RT-PCR analysis showed reduced CNP and CGT transcripts levels following TMEM10 knock down. Two experiments, performed in duplicate and analyzed by semi-quantitative RT-PCR, were confirmed by a third independent experiment analyzed by real-time RT-PCR (shown here). Graphs show mean ±SEM. * $p < 0.05$ (student t-test). **(B)** Western blot analysis of cell lysates derived from cells transfected with control and TMEM10 siRNA. The image is an example of two independent experiments, performed in duplicate.

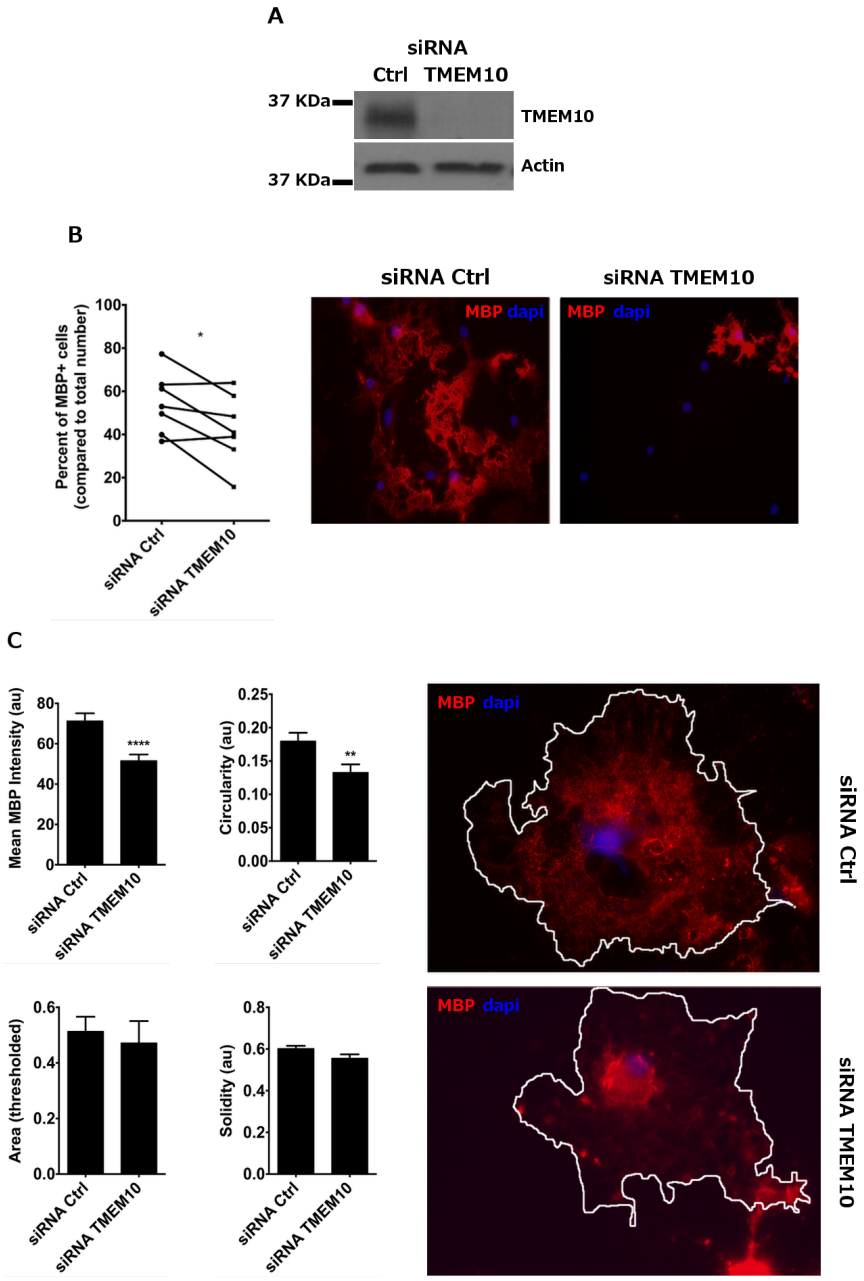

Figure 3.5: OPC differentiation is limited in the absence of TMEM10 – (A) Western blot analysis of TMEM10 levels on lysates derived from primary OPCs electroporated with control and TMEM10 siRNA. **(B)** Percentage of MBP positive cells relative to the total number of

DAPI-positive nuclei. Seven independent experiments, performed in triplicate, were analyzed. Graph shows mean ±SEM. * $p < 0.05$ (paired student t-test). **(C)** 50-100 cells from two independent experiments were randomly selected and individually outlined using the free selection tool of ImageJ software. Graphs show mean±SEM. ** $p < 0.01$; **** $p < 0.0001$ (student t-test).

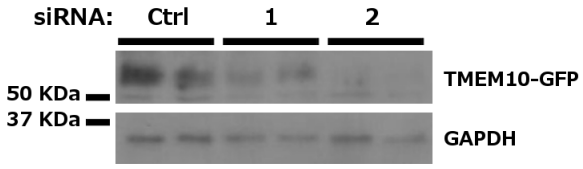

Supplemental Figure 3.1: TMEM10 knock down in Oli-neu cells – Western blot analysis of lysates derived from TMEM oli-neu cells transfected with control and TMEM10 siRNA. TMEM10-GFP was down regulated following TMEM10 siRNA transfection.

Preface to Chapter 4

Maintenance of myelin paranode organization in the mature CNS requires the guidance cue Netrin-1. Because UNC5B is the major Netrin-1 receptor in the white matter of adult spinal cord, we hypothesized that UNC5B mediates the Netrin-1 signaling required for paranode maintenance.

We used a conditional UNC5B knockout strategy to investigate the potential UNC5B function at the paranodes. The results obtained in this study are described in the manuscript bellow.

CHAPTER 4

Organization of paranode axoglial domain requires the netrin-1 receptor UNC5B

Omar de Faria Jr., Jenea M. Bin, Abbas Sadikot, Timothy E. Kennedy

1 Abstract

Netrin-1 and its receptors direct cell migration and axon extension in the developing CNS. After development, netrin-1 continues to be expressed in the mature CNS and is involved in multiple aspects of adult brain function, including the organization of oligodendroglia paranodal junctions. Here, we show that expression of the netrin-1 receptor UNC5B is upregulated in the adult mouse brain and is enriched at the paranodes of myelinated axons. Our findings indicate that oligodendrocyte-specific deletion of UNC5B does not alter compact myelin thickness or abundance *in vivo*. In contrast, in 9 month-old UNC5B knockouts, compact myelin periodicity is decreased and axoglial paranodes become severely disorganized, with glial loops detaching from the axon. As a result, Caspr-1 and Kv1.1 disperse along the axon, consistent with a loss of segregation between specialized myelin domains. Paranodal disruption is less severe in younger, 3 month-old cKOs, indicating that the myelin disruption progressively worsens with age. At all ages animals were tested, no deficit in motor behavior in knockout mice was observed. Taken together, our data reveal a novel contribution of UNC5B to the maintenance of the axoglial apparatus that is required for normal paranode organization.

2 Introduction

Netrins are a family of secreted proteins that guide cell migration and axon extension in the embryonic CNS (Kennedy et al., 1994; Serafini et al., 1994). Netrin-1 binding to receptors DCC/Neogenin and the UNC5 homologues initiates a complex signaling cascade that results in cytoskeleton rearrangement and chemotropic attraction or repulsion. Although netrin function may be best understood in the developing CNS, netrin-1 and its receptors continue to be expressed in the adult brain and spinal cord after embryonic development is complete (Manitt et al., 2001; Manitt et al., 2004). Consistent with this pattern of expression, netrin-1 has been demonstrated to contribute to several aspects of postnatal development and adult CNS function, including synaptogenesis, synaptic plasticity/memory, and maintenance of specialized axoglial domains (Goldman et al., 2013; Horn et al., 2013; Bull and Bin et al., 2014).

Distinct axoglial domains - the node, paranode, juxtaparanode, and internode - are assembled along myelinated axons to enable saltatory conduction of the action potential. Flanking the node of Ranvier, the oligodendroglial paranode consists of cytoplasm-filled glial loops that are firmly attached to each other and the axonal membrane. Electron-dense transverse bands, resembling invertebrate septate junctions, support adhesion across the axoglial interface. Components of this adhesive complex include Neurofascin-155 on the glial side and Contactin and Caspr on the axonal membrane (Einheber et al., 1997; Tait et al., 2000; Boyle et al., 2001; Charles et al., 2002). Tight junctions and adherens junctions provide adhesion on the interface between adjacent glial loops (Fannon et al., 1995). In addition to representing a crucial site of adhesion between myelin and the axonal membrane, the paranode functions as a molecular barrier, segregating potassium channels to the juxtaparanode and sodium channels to the node of Ranvier

(Pedraza et al., 2001). Mutants for Neurofascin, Contactin and Caspr, in addition to UDP:galactose Ceramide Galactosyl-Transferase (CGT) and Myelin and Lymphocyte protein (MAL), fail to form or maintain axoglial junctions. As a result, paranodes become disorganized, ion channels do not segregate and saltatory conduction is compromised (Dupree et al., 1998; Boyle et al., 2001; Schaeren-Wiemers et al., 2004; Sherman et al., 2005; Marcus et al., 2006).

Netrin-1 and DCC are also required for the organization of axoglial paranodes (Jarjour et al., 2008; Bull, Bin et al., 2014). White-matter fractionation has shown that netrin-1 is associated with axoglial membranes in the adult rat spinal cord and immunofluorescence confocal analysis has indicated that netrin-1 and DCC co-localizes with Caspr to the paranodes of myelinated axons (Manitt et al., 2001; Jarjour et al., 2008). In long-term cerebellar slice cultures derived from newborn netrin-1 or DCC KO mice, paranodal transverse bands were lost or diffuse, glial loops detached and everted away from the axon and Caspr immunoreactivity dispersed along the fiber. Strikingly, paranodes appeared normal in short-term cultures, providing evidence that netrin-1 and DCC are required for paranode maintenance, rather than formation (Jarjour et al., 2008). Bull et al. (2014) investigated if DCC is required for paranode maintenance *in vivo* by conditionally deleting DCC from mature oligodendrocytes at a time point when myelination was largely complete. In the absence of DCC, paranodes that had formed properly during development become disorganized and exhibited the same defects as had been previously found *in vitro* in long-term organotypic cerebellar slice cultures (Bull et al., 2014; Jarjour et al., 2008). These studies indicate that netrin-1 and DCC are required for the maintenance of the organization of paranodal junctions in the mature CNS.

UNC5 homologues are upregulated in the mature CNS and constitute the major family of netrin receptors in the adult spinal cord, although the contribution of UNC5A-D to netrin-1 function in the adult CNS remains to be revealed (Manitt et al., 2004). In adult spinal cord white matter, UNC5B (also called UNC5H2) is the predominant netrin receptor expressed, suggesting that it might participate in the netrin-1 signaling required for paranode organization (Manitt et al., 2004). Here, we show that UNC5B expression is upregulated in the adult mouse brain and that UNC5B protein is enriched at the paranodal junctions of myelinated axons. We report that in the absence of UNC5B expression by oligodendrocytes paranodal ultrastructure is disrupted and axonal domain segregation is compromised *in vivo*. Importantly, paranodal disruption is less severe in young animals, providing evidence that the defect progresses with age. Our data indicates that, in addition to DCC, UNC5B mediates the netrin-1 signaling that is necessary for the organization of axoglial paranode domain.

3 Material and Methods

Animals

UNC5B flox mouse line was provided by Dr. Susan Ackerman (The Jackson laboratories) and carries an UNC5B allele in which exon 5 is floxed. Olig2-Cre mice (Schuller et al., 2008) was provided by the Jackson Laboratory. ROSA^{26}-LacZ reporter mice (Soriano et al., 1998) were provided by Dr. Jean-François Cloutier (McGill University). All procedures were performed in accordance with the Canadian Council on Animal Care guidelines for use of animals in research.

Antibodies

The following antibodies were used in this study: mouse monoclonal anti-α-actin (Sigma), mouse monoclonal anti-caspr for immunohistochemistry (UCDavis/NIH NeuroMab Facility), rabbit anti-Kv1.1 (Abcam), mouse anti-pan sodium channel (Sigma), mouse monoclonal anti β-tubulin III (Abcam), goat polyclonal anti-UNC5B for immunostaining (R&D Research), and rabbit monoclonal anti-UNC5B for western blot (Cell Signaling). Rabbit polyclonal anti-Caspr (for western blot and immunostaining), rabbit polyclonal anti-CNP, rabbit polyclonal anti-MAG, rabbit polyclonal anti-MBP and mouse monoclonal anti-PLP were gifts from Dr. David Colman (McGill University).

Immunohistochemistry

Mice were deeply anesthetized with 4X Avertin and transcardially perfused with phosphate buffered saline, pH 7.4 (PBS) followed by 4% paraformaldehyde (PFA) diluted in PBS. The mouse brain was dissected and post fixed in 4% PFA for 1 hr at 4°C with gentle shaking. Fixed tissue was equilibrated in 30% sucrose, PBS for 1 week at 4°C. After embedding in optimal cutting temperature compound (Sakura Finetek), tissue was cut in 20 μm-thick sections in a Leica cryostat. Slides were air dried for 15 min before being stored at -80°C. For immunohistochemical analysis, slides were allowed to equilibrate to rt and washed 3 times with PBS for 5 min each wash. Sections were blocked at rt with 5% bovine serum albumin (BSA), 0.3% Triton-X, in PBS for 1 h followed by an overnight incubation with primary antibodies at 4°C. Primary antibodies were diluted in 3% BSA, 0.3% Triton-X, in PBS. Sections were then washed with PBS three times, 10 min per wash, and incubated overnight at 4°C with the appropriate secondary antibodies diluted in 3% BSA in PBS. Sections were washed three times with PBS (10 minutes per wash) and briefly dipped into water before mounting. Images were

taken using an Olympus Fluoview confocal microscope, 60X lens and 4X zoom. Measures of length and width of immunoreactive domains were carried out using ImageJ software (Rasband, 1997-2014).

Electron Microscopy

Mice were deeply anesthetized with 4X Avertin and transcardially perfused with cold 100 mM phosphate buffer, pH 7.4 followed by cold 2.5% glutaraldehyde, 2% PFA, phosphate buffer. Optic nerves were dissected and post-fixed in the same solution for 72 hours before being processed for electron microscopy, as previously described (Bull et al., 2014). Images were taken on an FEI Tecnai 12 transmission electron microscope at 120 Kv.

Behavioral analysis

Open field test – mice were allowed to freely explore a 50 x 50 cm arena for 1 h. Locomotor activity was video recorded and tracked using an infrared detector (ViewPoint Life Sciences). VideoTrack software (ViewPoint Life Sciences) was used to analyze motor activity.

Balance Beam test – mice were trained for four consecutive days, with four sessions per day, to cross a 100 cm-long, 2 cm-wide round beam, elevated 50 cm above the support base. By day four of training, all animals had learned the task. Because mice can wander for variable amounts of time before beginning the task, we determined the 25 cm mark as the task starting point. On the test day, the 2 cm-wide beam used during the training period was replaced by a 1 cm-wide beam. Time to cross the 75 cm distance and the number of paw slips and stops over the trajectory were measured over four sessions. The task was video recorded and viewed to count the number of slips and stops per animal.

Hanging Wire Grip test – mice were placed on the top of a 50 cm x 30 cm metal grid. The grid was turned upside down and latency for the mice to fall recorded.

Accelerating Rotarod test – mice were trained for three consecutive days, with 2-3 sessions per day, to equilibrate on a rotational rod accelerating at 1 rpm/10 seconds (Rotamex, 3 cm diameter rod). By day three, all mice had learned the task. On the test day, acceleration was increased to 1 rpm/8 seconds and latency to fall and maximum speed were recorded over six sessions.

Real-time RT-PCR

First-strand cDNA synthesis was performed as previously described (de Faria et al., 2012). Briefly, 50 ng of total RNA were added to 300 ng of random hexamer primers and incubated at 65°C for 10 min. Next, a master mix containing 1X reverse-transcription buffer, 2 U/µl ribonuclease inhibitor (Invitrogen), 1 mM dNTP, and 10 U/µl reverse transcriptase (Invitrogen) was added. RT reaction parameters were as follows: 25°C for 5 min, 50°C for 30 min, 55°C for 30 min, 70°C for 15 min. For real-time RT-PCR, 20 ng of cDNA was incubated with 5 µM forward and reverse primers and 2X SYBR Green PCR master mix (Invitrogen, catalogue #4364344). Reactions were performed in the Applied Biosystems 7000 thermocycler. Data were analyzed using the $2^{-[delta][delta]Ct}$ method (Schmittgen et al., 2000; Winer et al., 1999) and final expression values were normalized to 18S RNA levels.

Western Blot

Protein lysates were prepared from freshly isolated mouse optic nerve, brain stem, cerebellum and spinal cord. Isolated tissues were homogenized on ice with RIPA buffer containing protease and phosphatase inhibitors. Equal amounts of protein were resolved by SDS-PAGE and

transferred to PVDF membrane (BioRad). Membranes were blocked with 5% milk or 5% BSA, in accordance with primary antibody manufacture instructions, in TBS containing 0.1% Tween (TBST) for 1h at RT and incubated overnight with primary antibodies diluted in 1% milk, TBST, at 4°C. Membranes were washed three times with TBST and incubated with horseradish peroxidase-conjugated secondary antibodies for 1h at RT. Membranes were washed and developed with an Enhanced Chemoluminescence Detection kit (Pierce).

X-Gal staining

Olig2-Cre/ROSA26 mice were perfused transcardially as described above and 20 μm-thick sections stained for β-galactosidase activity as described (Mombaerts et al., 1996).

Statistical Analysis

Data were analyzed using GraphPad Prism software. Results were considered significant when *p*-values were $*p<0.05$, $**p<0.01$ and $***p<0.001$. Statistical tests used are indicated in the figure legends.

4 Results

UNC5B is enriched at the paranodes of myelinated axons

After embryonic development, netrin-1 continues to be expressed in the adult rat brain and spinal cord, whereas expression of the netrin-1 receptors DCC and Neogenin is downregulated (Manitt et al., 2001; Manitt et al., 2004). In contrast, the expression of UNC5 homologues A-D is upregulated during maturation and these are the predominant netrin receptors expressed in the CNS in adulthood (Manitt et al., 2004). Analysis of mRNA expression revealed that the *unc5b*

gene is highly expressed in adult spinal cord white matter, suggesting that UNC5B protein might contribute to netrin-1 signaling at paranodal junctions of myelinated axons in the mature CNS.

To extend these findings, we have characterized the distribution of UNC5B expression in the mouse brain. Real-time PCR analysis of mouse brain cDNA demonstrated that *unc5b* mRNA increases in expression during the first post-natal month and peaks by ~P30. After P30, the relative level of *unc5b* expression in whole brain RNA slowly decreases; however, high mRNA levels were still detected at 12 months of age (Figure 4.1A). To investigate levels of UNC5B protein, we conducted western blot analysis on lysates of cerebellum from newborn and 60 day-old mice. UNC5B protein was not detected at P1 but was abundantly expressed at P60, consistent with upregulation of *unc5b* expression in the mature brain (Figure 4.1B). We consulted the Allen Brain Atlas to visualize the distribution of *unc5b* expressing cells in the white matter tracts of the adult mouse brain. As depicted in Figure 4.1C, *unc5b* mRNA was detected in the white matter of the corpus callosum and cerebellum in a pattern similar to the expression of PLP, a major myelin protein. Next, we cultured oligodendrocyte precursor cells (OPC) isolated from the brains of newborn rat pups and immunolabeled these cultures for UNC5B protein and the oligodendrocyte marker MBP. UNC5B immunoreactivity was readily detected in MBP^{+} mature oligodendrocytes that have differentiated for 8 days *in vitro* (Figure 4.1D). Western blot analysis of UNC5B in differentiating OPC cultures indicated increased levels of UNC5B as OPCs differentiate, with expression peaking in mature oligodendrocytes (Figure 4.1E). To characterize the distribution of UNC5B expressing cells in the adult mouse brain, frozen sections were immunolabeled for UNC5B, revealing overlap between UNC5B and Caspr at paranodal junctions (Figure 4.1G). In summary, our findings indicate that *unc5b* is

expressed by oligodendrocytes and that UNC5B protein is enriched at paranodes of myelinated axons in the mature mouse brain.

Oligodendrocyte-specific deletion of UNC5B

Our finding that UNC5B is enriched at paranodal junctions suggests that UNC5B participates in the netrin-1 signaling necessary for paranode organization and maintenance. Therefore, we utilized a well-validated transgenic mouse line with a floxed UNC5B gene to study UNC5B function *in vivo* (Figure 4.2A and B). To conditionally delete UNC5B in oligodendrocytes, mice carrying the floxed UNC5B allele were crossed with Olig2-Cre expressing mice, in which Cre expression is regulated by the Olig2 promoter (Schuller et al., 2008). Crossing Olig2-Cre mice with the reporter line ROSA26 (Soriano et al., 1998) allowed identification of the brain regions and cell types in which Cre is expressed. β-galactosidase activity assays performed on brain sections of these mice revealed Cre expression by cells in the corpus callosum and cerebellum white matter, consistent with activation of Cre in oligodendrocytes (Figure 4.2C). Importantly, in this Olig2-Cre line, motor neurons in the ventral spinal cord also express Olig2; however, these cells do not express *unc5b,* but rather *unc5a* and *unc5c* (Burgess et al., 2006; Dillon et al., 2007; Leonardo et al., 1997).

To confirm that *unc5b* expression is deleted in oligodendrocytes in Olig2-Cre/UNC5Bflox mice (subsequently referred to as UNC5B cKO), we conducted real-time RT-PCR analysis of lysates derived from the brain stem of 3 month-old UNC5B cKOs and wild-type littermates. mRNA encoding *unc5b* was completely depleted from UNC5B cKO at this age, but not age matched wild-type brain stem (Figure 4.2D). Western blot analysis was performed on lysates from three

white matter-rich regions to confirm that UNC5B protein levels are downregulated in oligodendrocytes. At 3 and 12 months of age, levels of UNC5B were strongly reduced in the three CNS regions analyzed. Importantly, netrin-1 levels in the white matter of UNC5B cKOs are comparable to wild-type levels, indicating that *unc5b* was successfully deleted from oligodendrocytes without interfering with UNC5B-independent netrin-1 signaling in the paranode (Figure 4.2F).

Myelin abundance is normal while myelin periodicity is diminished in UNC5B cKO mice

Following validation of UNC5B deletion in cKOs, we investigated if UNC5B is necessary for the formation of normal amounts of myelin. Western blot analysis of lysates from white matter-rich regions of 9 month-old UNC5B cKO and wild-type littermates indicated no differences in the levels of major myelin proteins MBP, PLP, MAG and CNP (Figure 4.3A). Electron microscopic (EM) analysis of 9 month-old UNC5B cKO and wild-type optic nerves also showed no difference in the percentage of myelinated axons (91.12±2.03 for WT and 93.99±1.45 for UNC5B cKO, Figure 4.3B). G-ratio analysis of myelinated fibers further revealed that myelin thickness is unchanged in adult UNC5B cKO animals (0.605±0.012 for WT and 0.599±0.013 for UNC5B cKO, Figure 4.3C). These results demonstrate that normal amounts of myelin are formed in the absence of UNC5B.

We next examined if UNC5B is required for proper organization of compact myelin. EM micrographs of adult UNC5B cKO optic nerve identified no apparent defect in compact myelin ultrastructure: major dense lines and intraperiod lines appeared normal, mean number of wraps did not differ from wild-type fibers (data not shown) and no signs of degeneration were observed

(Figure 4A). However, myelin periodicity was significantly, albeit slightly, decreased in UNC5B cKO fibers (Figure 4B). Interestingly, a small, but significant increase in periodicity of compact myelin was previously detected in cerebellar slices of DCC KO mice (Jarjour et al., 2008).

Paranode ultrastructure and axonal domain segregation are disrupted in UNC5B cKOs

The lack of a major defect in compact-myelin ultrastructure is consistent with UNC5B being enriched and having a primary function at the paranodes. We therefore investigated if myelin paranode ultrastructure was disrupted in 9 month-old UNC5B cKOs. Wild-type paranodes exhibited properly aligned glial loops that appeared firmly attached to the axolemma with no signs of degeneration. In contrast, UNC5B cKO paranodes appeared severely disorganized, with glial loops improperly aligned and pulling away from the axon (Figure 4.5). Quantification of this phenotype revealed that the mean number of detached loops per paranode was significantly increased in adult UNC5B cKO animals compared to wild-type littermates (0.32±0.117 for WT and 0.91±0.215 for UNC5B cKO). The majority of wild-type paranodes (77%) were scored as normal (no detached loops), while only 39% scored normal in UNC5B cKOs (Figure 4.5). In addition, large vacuolar structures and a segmented interface between glial loops were detected in UNC5B cKO but not wild-type paranodes (Figure 4.5, zoom). These analyses reveal disruption of paranodal ultrastructure in UNC5B cKO mice.

Oligodendroglia paranodal junctions are proposed to function as a molecular "fence", segregating potassium channels to the juxtaparanode and sodium channels to the node of Ranvier (Pedraza et al., 2001; Poliak and Peles, 2003). Transgenic models in which paranodal organization is compromised often exhibit disruption of axonal domains (Dupree et al., 1998;

Bhat et al., 2001; Boyle et al., 2001; Schaeren-Wiemers et al., 2004; Sherman et al., 2005; Marcus et al., 2006, Bull, Bin et al., 2014). Thus, we investigated if axonal domain segregation was disrupted in 9 month-old UNC5B cKO mice by immunostaining sections of optic nerve and cerebellum for Caspr, Kv.1.1 and Na^+Ch. In order to quantify potential defects in segregation, we measured the length of the Caspr and Kv1.1 domains, the length of the distance between Caspr domains flanking the same node, and the extent of the overlap between Caspr with Na^+Ch and Caspr with Kv1.1 (Figure 4.6B). In both CNS regions analyzed, Caspr and Kv1.1 domains were lengthened in UNC5B cKOs compared to wild-type littermates (Figure 4.6C, E and F). This phenotype was more apparent in the optic nerve, where we observed increased overlap between Caspr and Na^+Ch domains and reduced space between Caspr domains flanking the same node of Ranvier (Figure 4.6E-J). In some cases, Caspr domains completely invaded the node of Ranvier and no gap between paranodes could be seen (Figure 4.6D, arrowheads). Western blot analysis of optic nerve lysates indicated that the loss of domain segregation cannot be explained by altered levels of Caspr expression, which were unchanged in the different genotypes (Figure 4.6A). These data indicate that axonal proteins are dispersed along the axon and that domain segregation is compromised in 9 month-old UNC5B cKO animals.

Paranode disruption is less severe in younger UNC5B cKOs

Paranodes are disorganized in long-term but not short-term organotypic cultures derived from netrin-1 and DCC KO mice, suggesting that netrin-1 and its receptors are important for paranode maintenance, rather than formation (Jarjour et al., 2008). Consistently, mice in which DCC is deleted from mature oligodendrocytes in the adult CNS develop a similar phenotype, confirming that DCC is required for paranode maintenance (Bull et al., 2014). In the UNC5B cKO that we

used in this study, it is possible that paranode disruption results from lack of UNC5B function in paranode formation, maintenance or both. To address this issue, EM and immunofluorescence confocal analyses were performed in animals of 3 months of age, a stage at which myelination has recently been completed. At this age, UNC5B cKOs exhibited paranodes that were slightly more disorganized than wild-types. Quantification of EM micrographs revealed that the mean number of detached loops per paranode was only marginally increased from 0.8±0.21 in wild-type littermates to 0.93±0.15 in UNC5B cKOs while the fraction of paranodes scored as normal decreased from 68% in wild-types to 41% in UNC5B cKOs (Figure 4.7A). This rather small increase in disorganization did not translate into axonal domain disruption, as immunofluorescence analysis of frozen brain sections showed that the Caspr domain length is not increased in paranodes of 3 month-old UNC5B cKOs (Figure 4.7B). Our findings demonstrate that paranode disruption is less severe in 3-month-old UNC5B cKO mice and that the phenotype progressively worsens as the animal ages. While these results do not rule out a role for UNC5B in paranode formation, they indicate that UNC5B, like DCC, plays an essential role in the maintenance of myelin paranodes.

Lack of a motor defect in UNC5B cKO mice at 3 or 9 months of age

Mouse mutants in which paranodal junctions are severely disrupted have delayed action potential conduction and exhibit defects in motor behavior (Dupree et al., 1998; Boyle et al., 2001; Schaeren-Wiemers et al., 2004; Sherman et al., 2005; Marcus et al., 2006, Bull et al., 2014). We therefore conducted a series of behavioral tests that evaluate different aspects of motor behavior in mice. Mice were examined at 3 months of age, when paranodal disruption is relatively minor, and at 9 months of age, when disruption is significantly more severe.

The open field test assesses levels of spontaneous locomotor activity. Mice were allowed to freely move in a 50 x 50 cm box for 1 h while their movement was tracked. Comparison between 3 and 9 months old mice showed a general decrease in locomotor activity in older mice, as expected. However, no differences in total time spent moving, total distance travelled, average speed, or fraction of time dedicated to slow/fast movements were found between UNC5B cKOs and wild-type littermates at either age (Figure 4.8A). The hanging wire grip test examines mouse motor strength. In this test, the total time that the mouse is able hang from a wire grid is measured. Again, older mice performed more poorly, but no difference between genotypes was detected in UNC5B cKO in comparison to wild-type littermates (Figure 4.8B). An accelerating Rotarod test was then conducted to evaluate balance and speed. For this test, mice were trained to run on a rotating rod and the maximum time and speed until falling are recorded. Once again, no significant difference was detected in 3-month-old UNC5B cKO mice in comparison to wild-type littermates. A trend towards better performance in 9-month-old UNC5B cKOs was observed but was not statistically significant (Figure 4.8C). Lastly, we conducted a balance beam test, which examines mouse balance and coordination. In this test, mice are taught to cross a 100 cm long, 1 cm wide, round beam. The time to cross the beam and the number of paw slips and stops along the trajectory are measured. No difference, in any measurement, was detected between UNC5B cKO and wild-type controls (Figure 4.8D). Our data indicate that, despite disruption of paranodal organization, no defects in motor behavior develop up to 9 months of age in UNC5B cKO mice. However, since the phenotype we describe here appears to progressively worsen with age, it remains possible that older animals lacking *unc5b* expression may develop behavioral defects.

5 Discussion

Netrin-1 and its receptors are well known for their function in axon guidance in the embryonic CNS. Here, we show that the netrin-1 receptor UNC5B has a function beyond embryonic development in the organization of myelin paranodes in the adult brain. We found that UNC5B is expressed at high levels after P30 and co-localizes with Caspr at the paranodes of myelinated axons. Oligodendrocyte-specific deletion of UNC5B does not change myelin abundance; however, paranode ultrastructure was disrupted following UNC5B deletion. Consequently, axonal domain segregation was compromised and proteins Caspr and Kv1.1 moderately dispersed along the axon. Interestingly, this phenotype is less severe in younger UNC5B cKOs, suggesting that the paranode defect is progressive and worsens as the animal ages. Our data demonstrate that the organization of oligodendroglial paranodes requires the netrin-1 receptor UNC5B.

Previously, we reported that in the absence of netrin-1 or DCC, paranodes in organotypic cerebellar cultures are formed properly but, in the long-term, become disorganized (Jarjour et al., 2008). Subsequently, using a mouse model in which DCC is selectively deleted from PLP-expressing oligodendrocytes in the adult brain, we showed that properly formed paranodes become progressively disorganized (Bull et al., 2014). These studies suggest that netrin-1 and DCC are necessary for paranode organization and that at least part of their function *in vivo* contributes to paranode maintenance, rather than formation. In the UNC5B cKO mouse used in the current study, Cre expression is activated early in postnatal development and as a result Cre recombination occurs in oligodendrocytes before myelination is complete (Schuller et al., 2008). Therefore, disruption of paranode organization in the 9 month-old UNC5B cKO could result

from a lack of UNC5B function in paranode formation, maintenance or both. To address this, we examined paranode organization in mice of 3 months of age, a time-point at which a substantial amount of myelination has recently been completed. We anticipated two distinct opposing scenarios: (1) UNC5B cKO paranodes are completely normal at 3 months of age and thus UNC5B has no essential function in paranode formation or (2) UNC5B cKO paranodes exhibit the same level of disorganization at 3 and 9 months and therefore UNC5B does not contribute to paranode maintenance. We found that 3 month-old UNC5B cKOs have slightly disorganized paranodes, suggesting a progressive worsening over time until paranodes are as disorganized as found in older mice. Therefore, we conclude that UNC5B makes an essential functional contribution to paranode maintenance. Consistent with this, UNC5B transcript levels are maintained at a high level in the brain of 12 months-old mice (Figure 4.1A). While the presence of some level of paranodal disorganization at 3 months suggests a role for UNC5B in normal paranode formation, this may reflect a failure in the maintenance of paranodes that were formed shortly earlier. Thus, at this time, we conclude that UNC5B is required for paranode maintenance, but do not rule out a contribution to paranode formation.

Selective deletion of UNC5B expression from oligodendrocytes was sufficient to disrupt paranodal organization, but not to the extent where motor defects were detected in our behavioral analyses. UNC5B cKO animals were challenged with four different tests that, as a whole, account for several aspects of motor behavior: spontaneous locomotion, balance, coordination, speed, strength and motor learning. In all the tests and at all ages tested, UNC5B cKOs did not perform differently from wild-type littermates (Figure 4.8). This is in opposition to transgenic lines where paranodes fail to form and some degree of neurological defects develop. Caspr,

Contactin, Neurofascin and CGT-null mice develop tremor and ataxia by the end of the first post-natal week, although, in these examples, a causal relationship between paranode disruption and neurological defects is not straightforward because these proteins are involved in multiple aspects of brain development and have been deleted irrespective of brain region, cell type or developmental time (Baht et al., 2001; Boyle et al., 2001; Sherman et al., 2005; Dupree et al., 1998). For instance, during development, Contactin and Caspr participate in axon growth and guidance, and part of the neurological defects observed in the Contactin-null mice has been attributed to malformations in cerebellum circuitry (Berglund et al., 1999). Because the phenotype that we describe here is progressive, it could be the case that behavioral defects appear only in older (> 9 month-old) UNC5B cKO mice. This would be consistent with motor defects that were observed in the inducible-PLP-Cre DCC flox animals 6 months after induction, but not after 1 month (Bull et al., 2014). Interestingly, motor impairments were also not reported in the Myelin and Lymphocyte (MAL) knockout mice. Like UNC5B, MAL is expressed late in myelinogenesis and deletion of this gene produces a disruption in PNS paranode organization that is relatively minor in young animals but worsens as the animal ages (Schaeren-Wiemers et al., 2004). Alternatively, netrin-1 levels are unchanged in UNC5B cKO mice (Figure 4.2F) and DCC-mediated netrin-1 signaling is presumed to be intact in the paranodes of UNC5B cKO mice. Therefore it is conceivable that, in the presence of DCC, the UNC5B phenotype is less severe and paranodes are not disrupted to the point where a detectable motor impairment is manifested.

UNC5B and DCC are both expressed by mature oligodendrocytes, enriched at the paranode and required for proper organization of axoglial paranodal junctions. Nonetheless, the possibility of a

functional interaction between the two receptors at paranodes remains to be tested (Jarjour et al., 2008; Bull et al., 2014). During development, examples exist of an UNC5-homologue acting either in concert with or independently of DCC to mediate netrin-induced chemorepulsion. In the axons of developing *Xenopus* spinal neurons, UNC5B mediates netrin-1 chemorepulsion in a DCC-dependent fashion. Importantly, this UNC5B-DCC association was confirmed at the molecular level, as netrin-1 promotes the physical interaction between the cytoplasmic domains of the two receptors (Hong et al., 1999; Colavita and Culotti, 1998). In the developing spinal cord, oligodendrocyte precursor cells (OPC) that normally migrate away from the source of netrin at the midline were aberrantly distributed in DCC knockout mice, suggesting that Unc5a-mediated chemorepulsion requires DCC in migratory OPCs (Jarjour et al., 2003). On the other hand, studies have indicated that DCC-independent Unc5-mediated chemorepulsion can also occur, even when DCC is co-expressed with UNC5 in the same cell type (Guijarro et al., 2006; Keleman and Dickson, 2001; Merz et al., 2001). UNC5 function independent of DCC also occurs outside of the nervous system, for instance, in the formation of *Drosophila* dorsal blood vessels. Here, mechanisms promoting cell adhesion and repulsion are required to be spatially-segregated within the same cell. Specifically, UNC5 is located to the middle-lateral domain of the cardioblast plasma membrane, where it mediates repulsion between the interfaces of contacting cells, while DCC is located at the basal and apical contact sites, where adhesion between adjacent cells is required (Albrecht et al., 2011; Macabenta et al., 2013). Of relevance to UNC5B and DCC function at the paranode, is the suggestion that short-range chemorepulsion is normally mediated by UNC5 alone (Hong et al., 1999; Keleman and Dickson, 2001). Regardless of the case, the UNC5B cytoplasmic region contains structural elements that may participate in

adhesive/repulsive mechanisms that function at the paranode. For example, the intracellular domain of UNC5B includes a domain homologous to ZU-5, which functions by cross-linking the cytoskeleton to transmembrane proteins of adhesive complexes, and is shared by the tight junction adaptor Zona Occludens-1 and the septate-like junction adaptor Ankyrin B (Schultz et al., 1998). It will be also important to define in future studies whether UNC5B participates in adhesive junctions at the axon-glia interface or between glial loops. We have observed a striking fragmentation of the loop-loop interface in UNC5B cKO paranodes, and speculate that UNC5B contributes to adhesive junctions that hold glial loops together. Interestingly, protein complexes mediating adhesion at the loop-loop interface (adherens junctions and tight junctions) are also important regulators of adhesion between endothelial cells that make up the blood-brain barrier (Abbott, 2005). Netrin-1 has recently been shown to regulate blood-brain barrier permeability by modulating the levels of the proteins that participate in these adhesive junctions, suggesting that netrin-1/UNC5B may possibly regulate tight/adherens junctions at the paranode (Podjaski et al., 2015).

The elucidation of mechanisms promoting myelin maintenance in the adult CNS is of distinct relevance because myelin integrity is compromised during aging and in neurological disorders. The volume of human white matter is reduced with age whereas in aged animals, myelin sheaths are less compact and redundant myelin profiles are often detected (Peters et al., 2000; Peters et al., 2001). In the brains of aged monkeys, paranodal loops are detached from axons and potassium channels invade the paranodal region from the juxtaparanode (Hinman et al., 2006). Transverse bands are also partially depleted at paranodes in the aged CNS (Shepherd et al., 2012). As expected, conduction velocity of myelinated axons decreases with age and many

aspects of age-related cognitive decline correlate with the loss of myelin integrity in the aged brain (Luebke et al., 2010; Morales et al., 1987). On the other hand, diverse neurological disorders such as Multiple Sclerosis (MS), Leukodystrophies, Autism, and Schizophrenia have been associated with myelin degeneration. Particularly in MS cases, evidence suggests that an early disorganization of paranodes is a relevant aspect of disease pathology. Immunofluorescence confocal analysis of brains sections derived from MS patients showed that Caspr and Kv1.2 localization was aberrant in myelinated axons located at the border of lesions. Importantly, these alterations seemed to precede disorganization of compact myelin (Howell et al., 2006; Wolswijk and Balesar, 2003). In agreement with this finding, mass spectrometry analysis of cerebrospinal fluid samples obtained from children during initial presentation of CNS inflammation revealed that proteins associated with the node of Ranvier and paranodal junctions, but not with compact myelin, are enriched in the CSF of children whose MS diagnostic was subsequently confirmed (Dhaunchak et al., 2012). Furthermore, a proteomic screen of human myelin has identified Neurofascin-155 as a target of humoral immune response in MS (Mathey et al., 2007). Together, these findings indicate that paranodal junctions may be selectively vulnerable to inflammatory attack and suggest that disruption of paranodal organization may be a key event at the onset of MS. Therefore, a better understanding of the principles governing paranode formation and maintenance will provide a clearer picture of age-related brain changes and disruption of function associated with neurological diseases such as MS.

In summary, UNC5B is enriched at the paranodes where it mediates netrin-1 signaling that regulate mechanisms promoting axoglial adhesion. This regulation is relevant because in the absence of UNC5B, paranodal loops detach from the axon and axonal domain segregation is

compromised. Our findings also suggest that UNC5B function significantly contributes to paranode maintenance, rather than formation. Together, our data reveal a novel contribution for UNC5B to the axoglial apparatus that is required for normal paranode organization.

.

6 Figures and figure legends

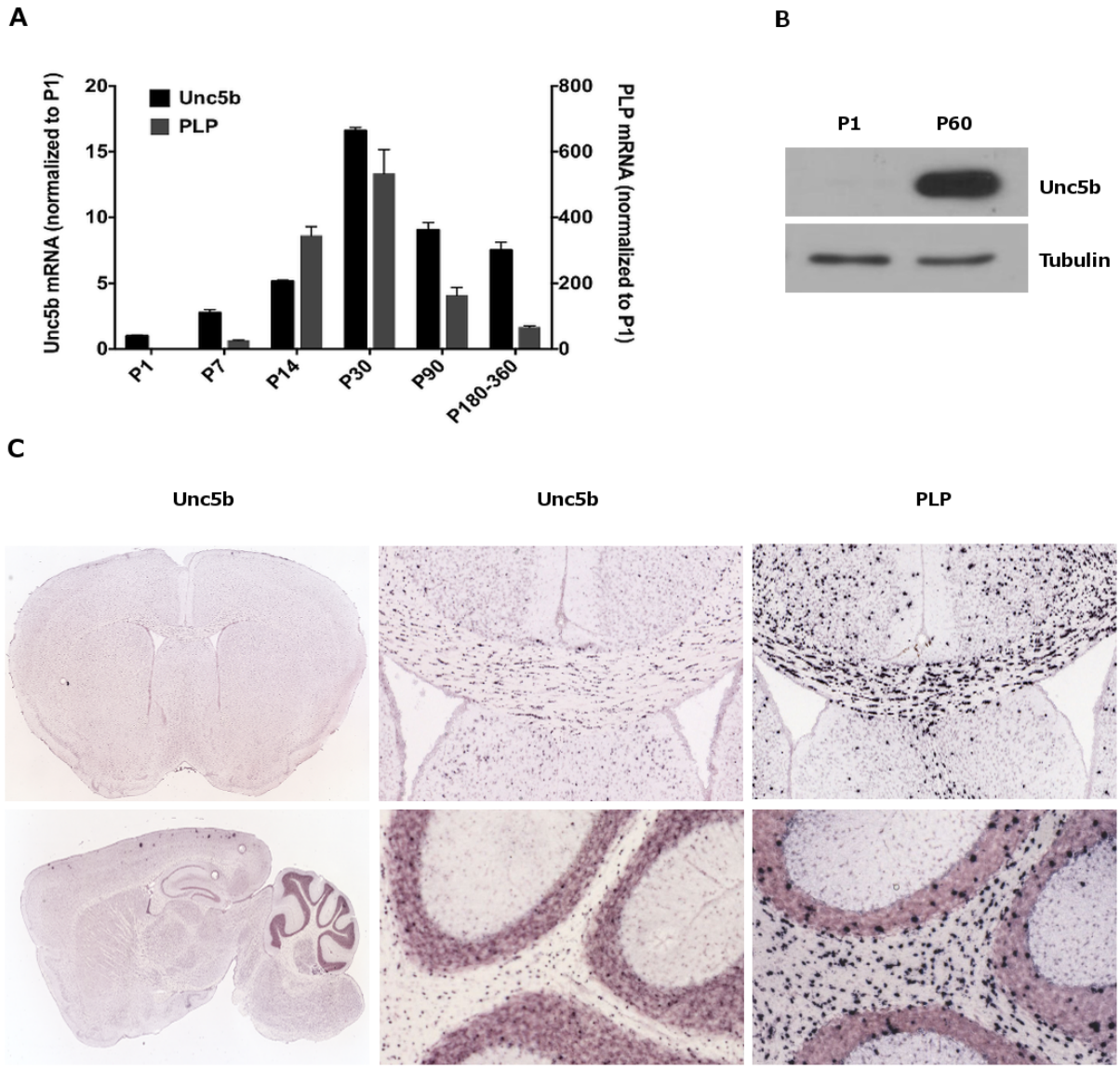

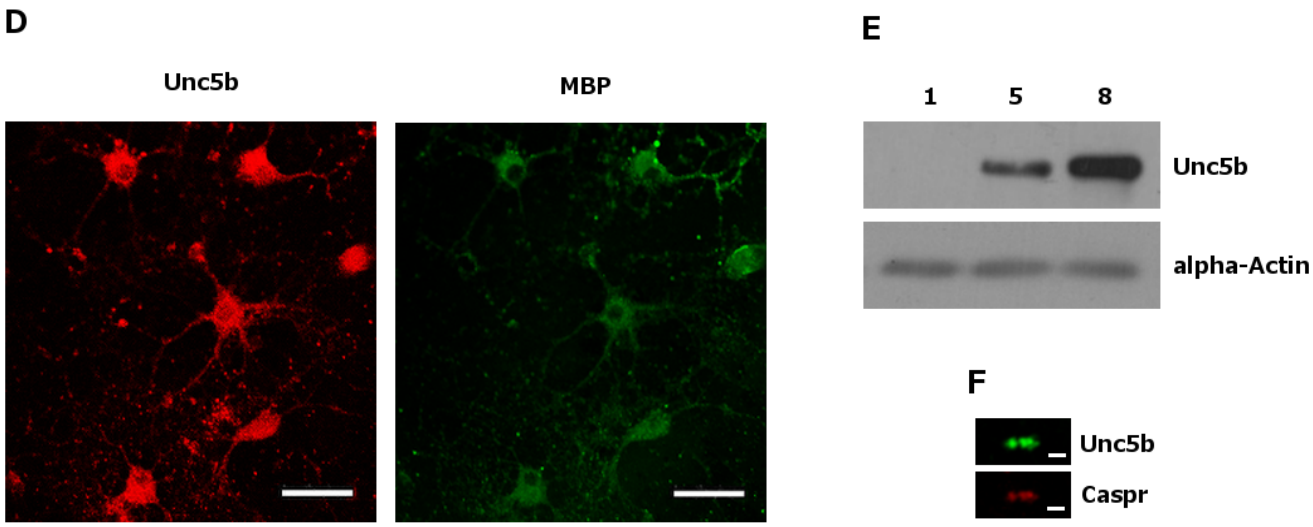

Figure 4.1: UNC5B is enriched at oligodendroglia paranodal junctions in adult mouse brain - (A) Real-time RT-PCR analysis of *unc5b* expression in the mouse brain. **(B)** Western blot of cerebellum lysates reveal readily detectable amounts of UNC5B protein in the adult CNS. **(C)** In situ hybridization of *unc5b* mRNA indicates expression in the white matter tracts of corpus callosum (top) and cerebellum (bottom). PLP expression is also shown for comparison (adapted from the Allen Brain Atlas). **(D)** UNC5B and MBP immunostaining of mature oligodendrocytes cultured *in vitro* for 8 days. Scale bar: 32.5 μm **(E)** Western blot analysis of UNC5B expression in cultures of purified oligodendrocytes at 1, 5 and 8 DIV. **(F)** Caspr and UNC5B immunostaining of adult mouse brain sections, showing UNC5B protein enriched with Caspr at the paranode. Scale bar: 3 μm.

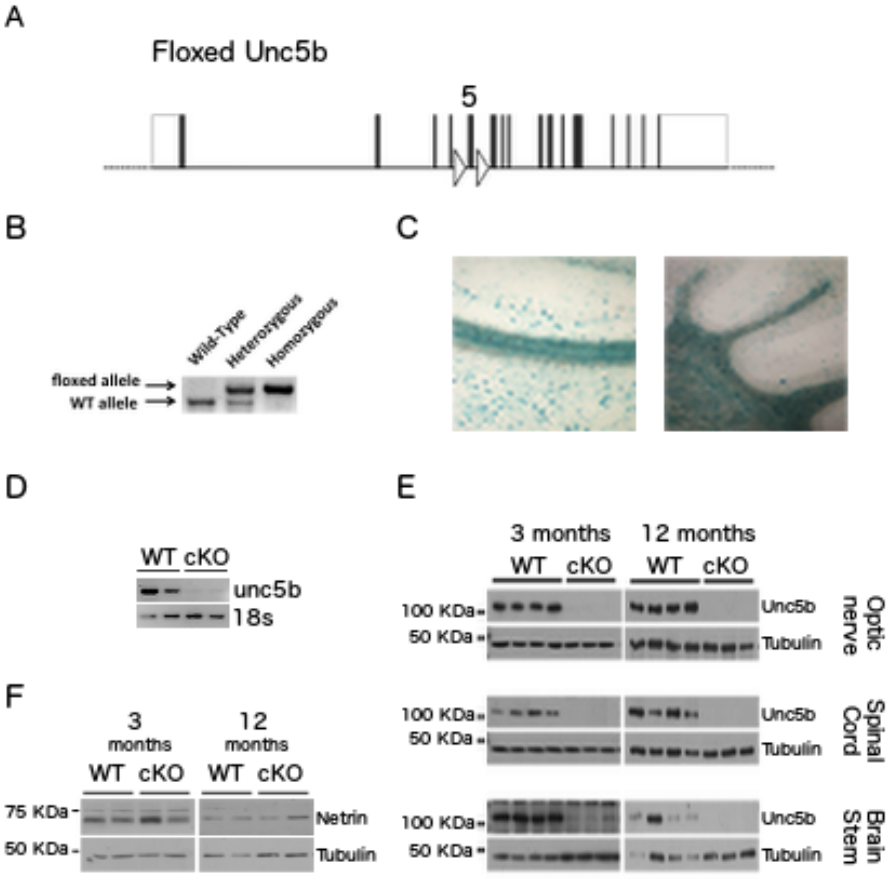

Figure 4.2: Deletion of UNC5B expression from oligodendrocytes in UNC5B cKO mice – **(A)** Schematic representation of the floxed *unc5b* allele and **(B)** representative image showing genotyping of *unc5bFlox* mouse line. **(C)** β-Gal staining on brain sections of adult Olig2-Cre/ROSA26 reporter mice shows Olig2-driven Cre expression in oligodendrocytes of corpus callosum (left) and cerebellum (right). **(D)** RT-PCR analysis of UNC5B expression in lysates of 3 month-old cKO mice and WT controls shows reduced *unc5b* mRNA expression. **(E)** Western blot analysis of 3 and 12 months-old optic nerve, spinal cord and brain stem lysates confirms that *unc5b* is deleted from oligodendrocytes. **(F)** Western blot analysis of brains stem lysates shows that netrin-1 levels are unchanged in UNC5B cKOs.

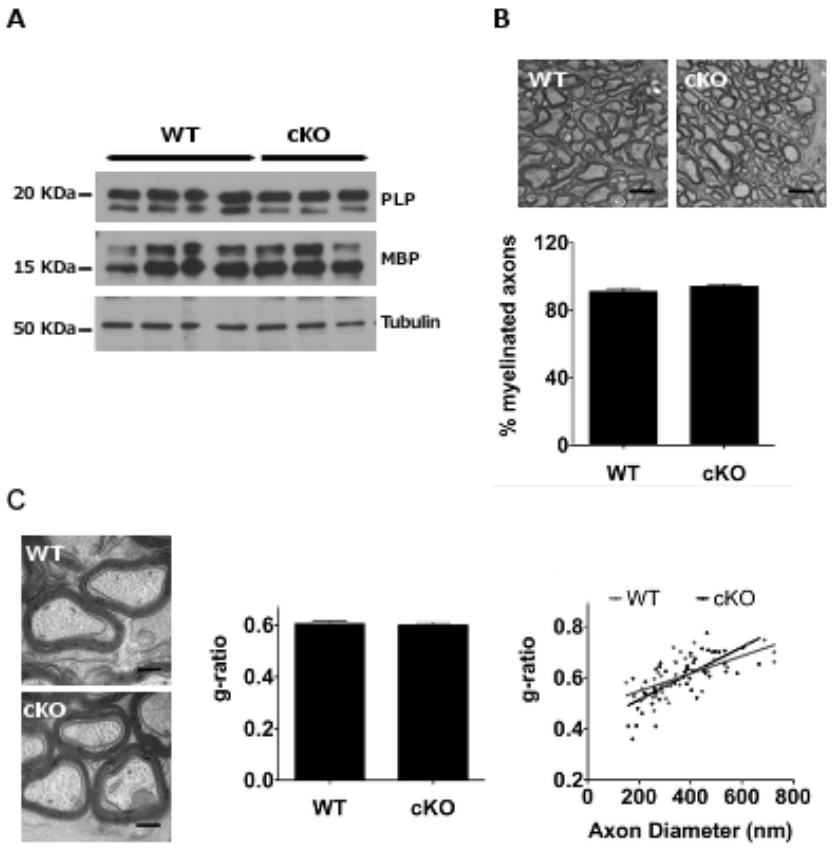

Figure 4.3: Myelin protein abundance appear unchanged following deletion of UNC5B – (A) Western blot analysis of major myelin proteins PLP and MBP in optic nerve lysates of adult cKO and wild-type littermates. **(B)** Percent of myelinated axons and **(C)** g-ratios were measured in electron micrographs of coronal sections of cKO and wild-type control optic nerves. Bar graphs represent the mean and error bars indicate ±SEM. $p > 0.05$ (unpaired student-t test). 450-650 axons from 2-3 animals were analyzed for percent of myelinated axons measurement; 40-50 axons from 2-3 animals were analyzed for g-ratio quantification. Scale bar (B): 1.5 um, (C): 300 nm

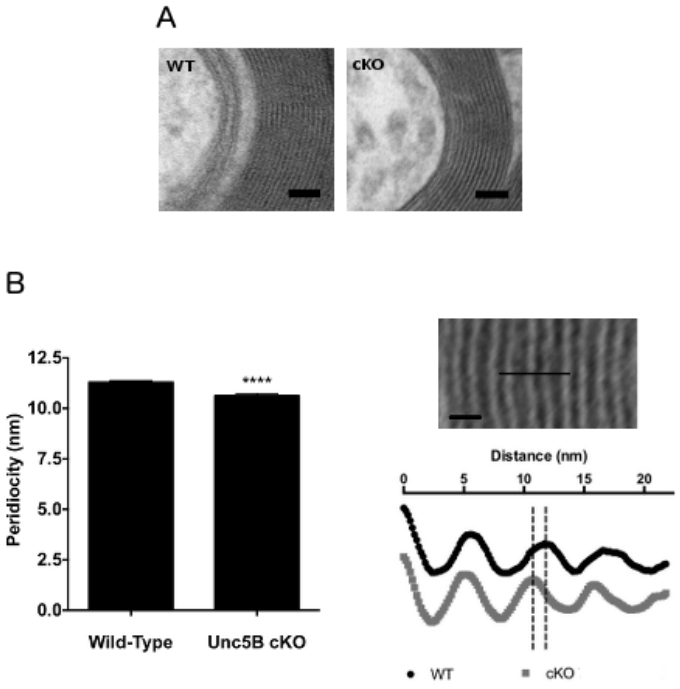

Figure 4.4: Compact myelin periodicity is decreased in UNC5B cKO mice – (A) Representative micrographs of wild-type and cKO optic nerve sections showing general features of compact myelin. Scale bar: 40 nm. **(B)** Mean periodicity is affected by *unc5b* deletion (left). Intensity profiles across the line at the center of the micrograph were taken for 20-25 micrographs from 2-3 animals and averaged. The vertical dotted lines represent the edge of one myelin period (right). Myelin periodicity is about 1 nm shorter in UNC5B cKOs. Bar graph represent the mean and error bars indicate ±SEM. ****$p < 0.0001$ (unpaired student-t test). Scale bar: 10 nm.

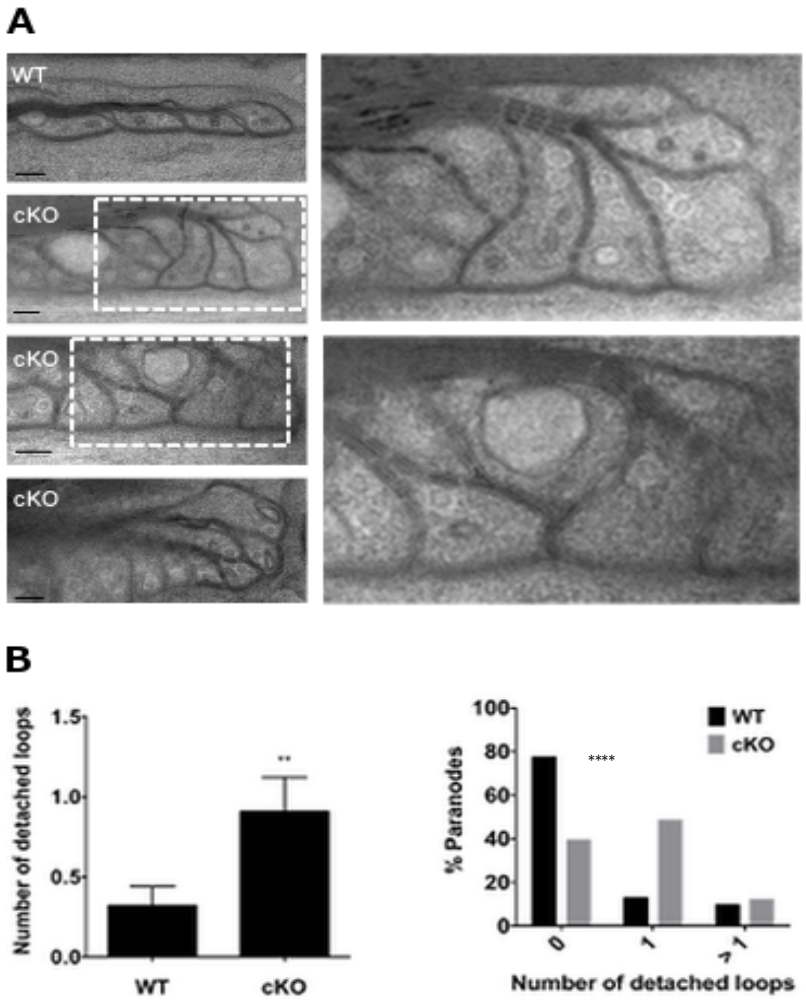

Figure 4.5: Paranode ultrastructure is disrupted following UNC5B deletion in oligodendrocytes – (A) Electron micrographs of longitudinal sections of wild-type and UNC5B cKO optic nerves. Panel shows one micrograph of a wild-type paranode (top) and three examples of highly disorganized UNC5B cKO paranodes (bottom three). The boxed areas in the left panels are magnified on the right. Note the segmented loop-loop interface and large vesicles inside glial loops. Scale bar: 100 nm. **(B)** Mean number of detached loops per paranode (left) and paranode distribution across different levels of disorganization (right). ** $p < 0.01$ (Mann-Whitney test); **** $p < 0.0001$ (Chi-square test). Error bars indicate ±SEM.

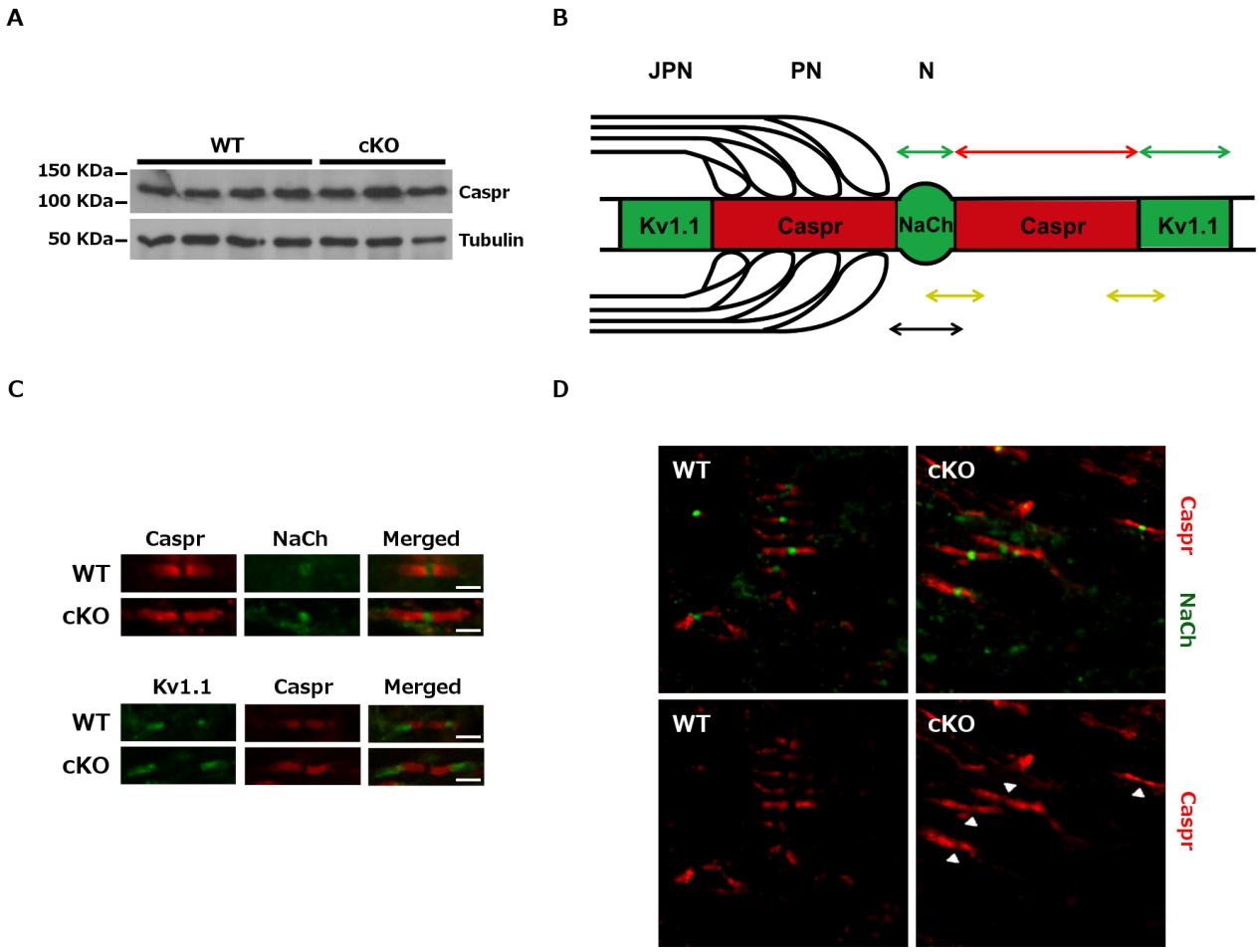
A
WT
cKO
150 KDa
100 KDa
50 KDa
Caspr
Tubulin
B
JPN
PN
N
Kv1.1
Caspr
NaCh
Caspr
Kv1.1
C
Caspr
NaCh
Merged
WT
cKO
Kv1.1
Caspr
Merged
WT
cKO
D
WT
cKO
Caspr
NaCh
WT
cKO
Caspr
E
Optic Nerve
Caspr length (normal. by width)
****
WT
cKO
Cerebellum
Caspr length (normal. by width)
****
WT
cKO
F
Optic Nerve
Kv1.1 length (normal. by width)
***
WT
cKO
Cerebellum
Kv1.1 length (um)
*
WT
cKO
G
Optic Nerve
Na+Ch length (normal. by width)
WT
cKO
Cerebellum
Na+Ch length (normal. by width)
*
WT
cKO
H
Optic Nerve
Distance btw Caspr (normal. by width)
**
WT
cKO
Cerebellum
Distance btw Caspr (normal. by axon width)
*
WT
cKO
I
Optic Nerve
Na+Ch-Caspr Overlap (um)
**
WT
cKO
Cerebellum
Na+Ch-Caspr Overlap (um)
WT
cKO
J
Optic Nerve
Kv1.1-Caspr overlap (um)
WT
cKO
Cerebellum
Kv1.1-Caspr overlap (um)
WT
cKO

Figure 4.6: **Axonal domain segregation is compromised following UNC5B deletion –**Optic nerve and cerebellum sections of adult UNC5B cKO and wild-type control mice were immunostained for Caspr, Kv1.1, and Na^+ channel and the length of the immunoreactive domains and extent of overlapping were measured. **(A)** Western blot analysis of optic nerve lysates from UNC5B cKOs and wild-type littermates. **(B)** Schematic representation of measurements presented in this figure. **(C)** Representative images of Caspr, Kv1.1 and Na^+ channel staining in the optic nerve of UNC5B cKO and wild-type mice. Scale bar: 10 um. **(D)** Caspr/Na^+ channel staining of optic nerve sections showing highly disorganized paranodes in UNC5B cKOs. Arrowheads indicate nodes of Ranvier that have been invaded by Caspr. **(E-J)** Length measurements of immunoreactive domains and extent of overlapping. Lengths were normalized by domain width. * $p < 0.05$; ** $p < 0.01$; *** $p < 0.001$; **** $p < 0.0001$ (unpaired student-t test). 150-200 measurements from 6 animals were taken for each immunoreactive domain and genotype. Error bars indicate ±SEM.

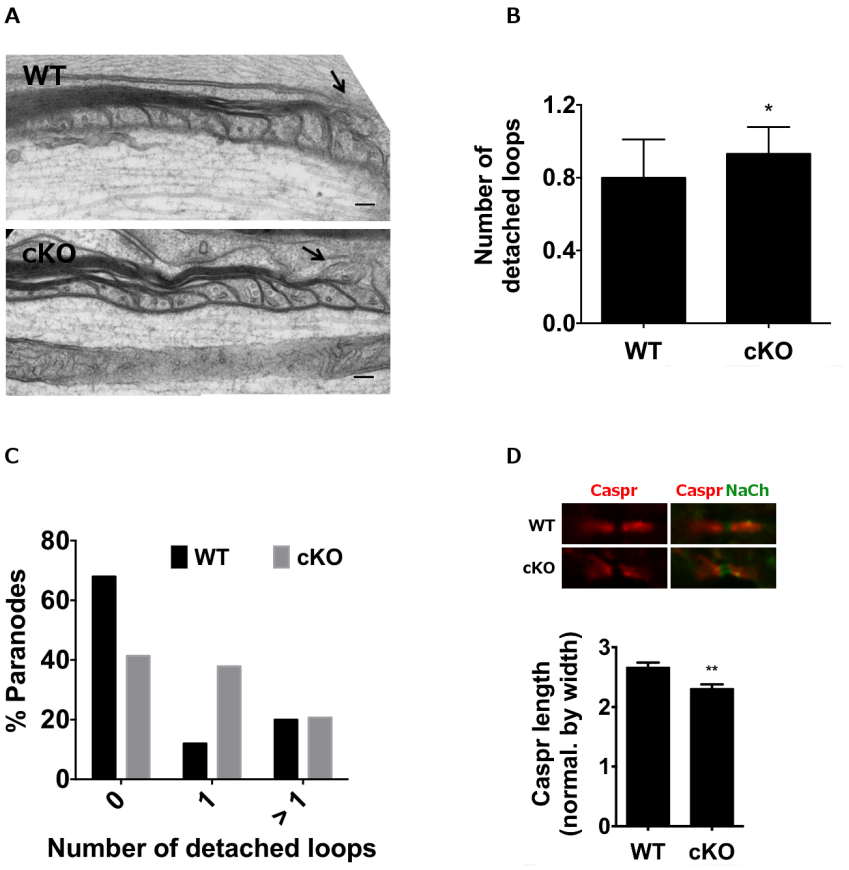

Figure 4.7: Paranode disruption is less severe in 3 months-old UNC5B cKO – (A) Representative EM micrographs of 3 months-old UNC5B cKO and wild-type littermates (top). Arrows indicate a detached loop. Scale bar: 100 nm. Graphs show **(B)** mean number of detached loops per paranode and **(C)** paranode distribution across different levels of organization. * $p <$ 0.05 (Mann-Whitney test); *** $p < 0.001$ (Chi-square test). 50-58 paranodes from 3 animals were analyzed per genotype. **(D)** Cerebellum sections of 3 months-old UNC5B cKO and wild-type controls were immunostained for Caspr and Na^+ channel (top). Caspr immunoreactive domain length was measured (bottom). ** $p < 0.01$ (unpaired student-t test). 150-200 measurements from 5 animals were taken for each genotype. Error bars indicate ±SEM.

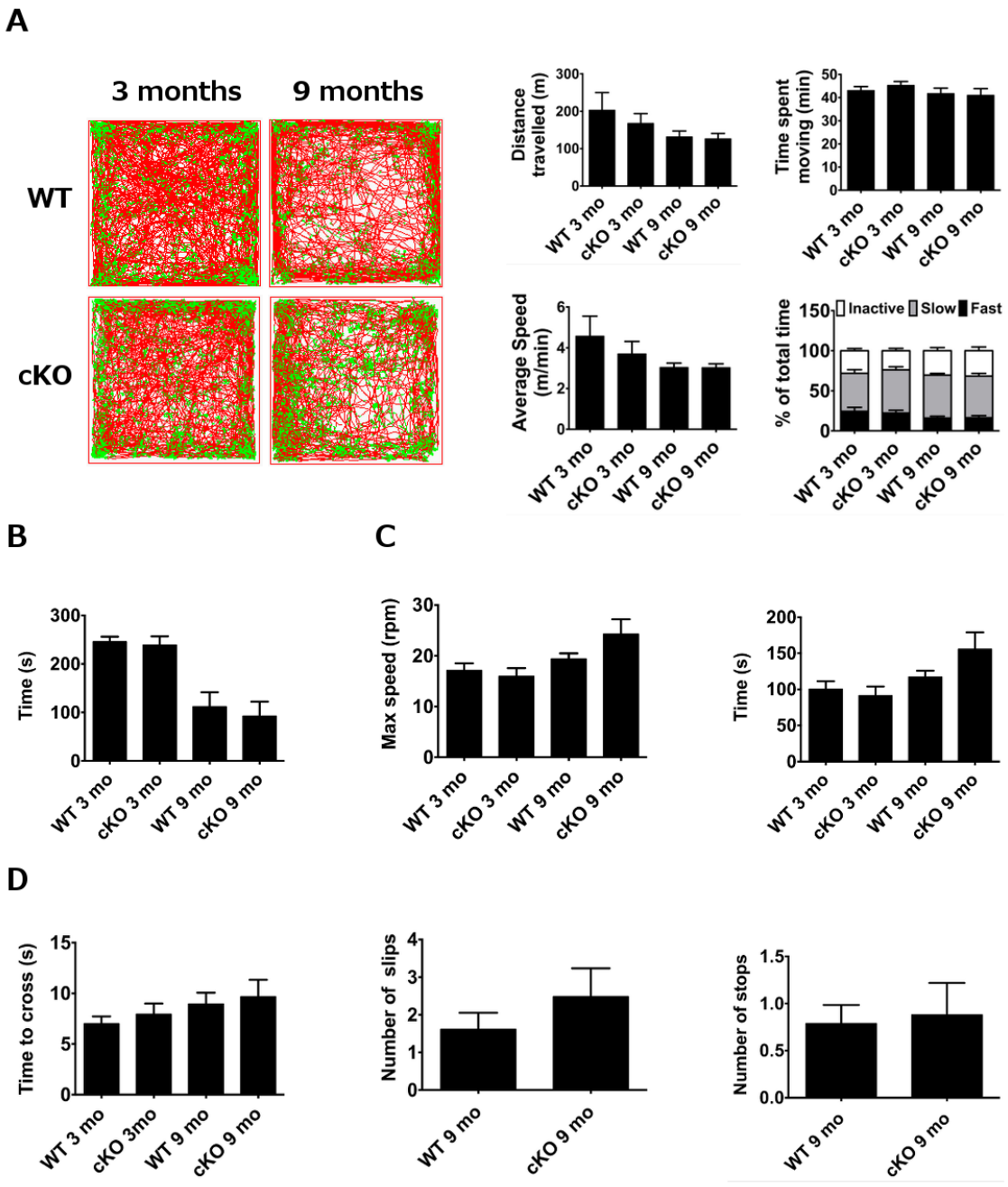

Figure 4.8: 3- and 9-month-old UNC5B cKOs exhibit normal motor behavior – (A) Open field analysis of UNC5B cKO and wild-type littermates spontaneous locomotor activity. Left: representative profiles of motor activity. Right: mean active time, distance, speed and percent of time dedicated to fast/slow movements. No significant differences were found between UNC5B

cKO and wild-type littermates. **(B)** Hanging wire grip test. Graph shows mean latency to fall. No significant differences between genotypes were detected. **(C)** Accelerating Rotarod test. Graphs show maximum speed and the mean latency to fall. No significant differences were found between UNC5B cKOs and wild-type littermates. **(D)** Balance beam test. Graph (left) shows the mean time in which UNC5B cKO and wild-type controls cross the beam. Graphs on the right show mean number of paw slips and stops along the crossing. No significant differences were detected. Error bars indicate ±SEM.

CHAPTER 5

GENERAL DISCUSSION

OPCs are generated in germinative foci along the neural tube and disperse throughout the developing CNS to populate areas of future white matter. In these regions, post-migratory cells proliferate and differentiate into myelinating oligodendrocytes that contact and ensheath mature axons. As myelination proceeds, distinct axoglial domains are assembled along the fiber, allowing for efficient and rapid conduction of the action potential. Multiple mechanisms, that individually control these various developmental steps, cooperate to globally regulate OPC development and CNS myelin organization.

In this thesis, we have used *in vitro* and *in vivo* experimental approaches to investigate different aspects of this regulation. In chapter II, we studied the expression of developmentally regulated miRNAs in oligodendroglia lineage cells isolated from the adult human brain. In chapter III, we have gathered evidence suggesting that a new CNS myelin-specific glycoprotein – TMEM10 – contributes to OPC differentiation *in vitro*. Finally, in chapter IV, we provide evidence that the netrin-1 receptor UNC5B is required for oligodendroglial paranode organization. In this final chapter of the thesis, we will discuss relevant topics and questions that were raised by the results presented in the previous chapters and that were not fully addressed in the individual discussion sections of these chapters.

1 MiRNAs and regulation of human OPC development

OPC development is regulated by several overlapping mechanisms. This complex regulation presumes that regulatory factors are expressed at precise levels, locations and developmental times over the course of OPC maturation. Part of this control is provided by miRNAs, well established regulators that fine-tune gene expression. In rodent models of OPC development, miRNAs are critical for OPC migration, proliferation, survival and differentiation. In the second chapter, we provided evidence that rodent-relevant miRNAs are also expressed in OPC/oligodendrocytes isolated from the adult human brain. We conclude that miRNA regulation of OPC proliferation and differentiation is likely conserved between rodents and humans.

MiRNA function is not always conserved because predicted miRNA binding sites in 3' untranslated regions of target mRNAs are poorly conserved. MiR-219-5p, which controls OPC differentiation in rodents, has only 20% of its targets conserved across vertebrates. MiR-338-3p, a miRNA that is key for OPC differentiation in mice has only 7% of its targets conserved from humans to frog (Supplementary Table 2.1). Consistently, miR-219-5p was shown to regulate OPC differentiation in rodents but not in chicken, whereas miR-338-3p controls differentiation in mice, but not in rats or zebrafish (Dugas et al., 2010; Zhao et al., 2010). This suggests the possibility that different sets of miRNAs control OPC development in different species. Our expression data showing that miRNAs 219-5p, 338-3p and 338-5p are regulated in differentiating oligodendrocytes of the adult human brain suggest that the same miRNAs control OPC differentiation in rodents and humans. Preliminary data indicating that PLP is upregulated following miR-219-5p overexpression in the human OPC cell line MO3.13 further supports this hypothesis (de Faria et al., unpublished results).

During development, OPCs maintain progenitor properties and do not differentiate until the appropriate time, when axons are mature for myelination. A number of OPCs do not differentiate during development and remain in their proliferative state in the adulthood. Late onset OPC differentiation and adult myelin plasticity play an important role in adaptive CNS function and animal behavior, as blocking oligodendrocyte generation in the adult brain impaired motor learning (McKenzie et al., 2014). In addition, stimulation of neuronal activity in the adult brain promoted OPC proliferation, differentiation and myelin remodeling and these changes were correlated with improved motor performance (Gibson et al., 2014). Adult OPC differentiation and myelination is also observed following demyelination in human white-matter diseases. In Multiple Sclerosis (MS), functional recovery from relapses is associated with the recruitment of adult OPCs to the sites of lesions followed by remyelination of demyelinated axons (Prineas et al., 1989; Raine and Wu, 1993). In our miRNA expression study, oligodendrocyte lineage cells were isolated from the adult human brain and fractionated into A2B5 positive and negative cells. Previous characterization of fetal and adult A2B5 positive fractions indicated that the adult counterpart is further committed to the oligodendroglial lineage, as it expresses mature markers MAG, MOG, PLP and MBP. These cells can be differentiated from adult A2B5 negative oligodendrocytes by their ability to incorporate BrdU (although only 10-15% of these cells incorporate the uridine analog) and by expressing the immature marker NG2 (Ruffini et al., 2004). These findings indicate that adult A2B5 positive oligodendroglial cells are more differentiated than fetal OPCs but less mature in comparison to adult A2B5 negative oligodendrocytes, consistent with this fraction representing an immature/differentiating oligodendrocyte stage. This is in agreement with increased levels of miR-219-5p and miR-338-

5p that we detected in adult A2B5 positive oligodendroglial cells (Figures 2.2 and 2.3). Such differences are also an indicator that caution should be adopted when translating mechanisms that operate in OPC differentiation during development to differentiation that occurs in the adult CNS.

2 TMEM10 and oligodendrocyte differentiation

OPC differentiation is characterized by dramatic changes in cell morphology and gene expression. During differentiation, bipolar progenitors give rise to mature cells that exhibit an elaborate network of cellular processes. *In vitro*, continued extension of these processes generates myelin-like membranes that express MBP and are compacted. Differentiating oligodendrocytes sequentially express distinct myelin galactolipids and mature markers of the oligodendroglia cell lineage, such as MAG, CNP, PLP and MBP. In the third chapter, we showed that TMEM10 is expressed in the brain by the time oligodendrocytes differentiate *in vivo* and that TMEM10 overexpression induces oli-neu process extension and myelin gene expression. In addition, TMEM10 knockdown in oli-neu and primary cells suggested that differentiation is limited in the absence of TMEM10. Overall, we provide evidence that TMEM10 contributes to OPC differentiation *in vitro*.

Oli-neu oligodendroglia cell line was used in a relevant part of this *in vitro* approach. Oli-neu cells were originally derived from dividing primary mouse OPCs immortalized by the ectopic expression of the t-neu oncogene. They reflect an early stage of oligodendrocyte development and can undergo differentiation *in vitro* and engage axons *in vivo* when transplanted into demyelinated regions of the CNS (Jung et al., 1995). Oli-neu cells have been used in the field to

study different aspects of oligodendrocyte development, from OPC migration to differentiation (Fok-Seang et al., 1995; Gohla et al., 2008; Schuster et al., 2002). Several groups have taken advantage of synchronously initiated differentiation of pure oligodendroglial cell cultures to investigate changes in global gene expression that follow differentiation and to identify compounds that induce OPCs to differentiate (Gobert et al., 2009; Joubert et al., 2010; Kippert et al., 2008). In addition, oli-neu cells have been used to study specific aspects of oligodendrocyte differentiation such as regulation of process extension (Klein et al., 2002; Kramer et al., 1999), incorporation of newly synthesized membranes into the plasma membrane (Kippert et al., 2007) and control of myelin protein trafficking by neuron-glia communication (Trajkovic et al., 2006). Of note, there have been several gene products, including TMEM10, which were initially identified and characterized in oli-neu cells and subsequently studied in primary OPCs (Archelos et al., 1998; Aruga et al., 2007; Grzenkowski et al., 1999; Kippert et al., 2008). In our study, we found that neuron-conditioned medium and cAMP treatment could induce oli-neu morphological differentiation and myelin gene expression (Figure 3.3). We concluded that oli-neu is a suitable cellular model to study early OPC differentiation and investigate potential regulators of OPC development. To circumvent limitations that are generally intrinsic to cell line models, we also investigated TMEM10 function in primary OPCs isolated form the neonatal rat brain (Figure 5). Comparable results in primary OPCs and oli-neu cells further validate the use of this cell line as an *in vitro* model for the study of OPC differentiation.

Neuron-glial communication regulates OPC development and is key to temporally coordinate CNS myelinating capacity and axonal demand for myelination. Most of the axon-derived signals described thus far are inhibitors of oligodendrocyte differentiation and myelination. These

include Jagged-1/Delta-1, Lingo-1 and Wnt, which bind to their respective receptors Notch-1, Lingo-1 and Frizzled at the OPC plasma membrane (Wang et al., 1998; Mi et al., 2005; Shimizu et al., 2005). A pro-differentiation factor, Adenosine, is released by neurons in response to action potentials and blocks OPC proliferation while promoting OPC differentiation (Stevens et al., 2002). In addition, a pro-differentiation signal, contained in neuron-conditioned medium (NCM), was found to regulate PLP trafficking from late endosomes to the plasma membrane in oli-neu and OPCs (Trajkovic et al., 2006). Kippert and colleagues (2007) reported that short-term (16h) treatment of oli-neu cells with NCM induces a strong upregulation of TMEM10 expression. In our study, we found that long-term (48h) NCM treatment and TMEM10 overexpression induce similar morphological differentiation and myelin gene expression in oli-neu cells (Figure 3). In addition, TMEM10 knockdown reduced the levels of myelin gene expression following NCM-induced oli-neu differentiation (Figure 4). These findings support the possibility that an axon-derived signal, enriched in NCM, requires TMEM10 expression to induce oli-neu differentiation. Adenosine is a potential candidate to possess this pro-differentiation activity. Future experiments investigating if TMEM10 expression is regulated by adenosine and if TMEM10 is necessary for adenosine-induced OPC differentiation will confirm or disprove this hypothesis. It will also be of interest to investigate if other aspects of OPC differentiation that are controlled by neuron-glia communication are additionally dependent on TMEM10 expression. PLP trafficking to the plasma membrane is one such aspect (Trajkovic et al., 2006).

Oligodendrocyte differentiation has been considered a derepression event (Li et al., 2009). Indeed, pro-differentiation signaling is reinforced by feed-forward mechanisms that inhibit inhibitors of differentiation, such as transcription factors ID2, ID4, Hes1, Hes5, Tcf4 and Sox6.

It will be interesting to investigate if TMEM10 expression can block the function/expression of some of these inhibitory factors. Additionally, TMEM10 may be directly involved in mechanisms promoting morphological differentiation, as TMEM10 overexpression induced massive oli-neu cell process extension and branching. In this context, it may be possible that TMEM10 contributes to RhoA GTPase inhibition, which is required for OPC process extension and myelin membrane formation (Liang et al., 2004; Mi et al., 2005; Rajasekharan et al., 2010). Preliminary evidence suggesting that TMEM10 co-immunoprecipitates with FAK, a tyrosine kinase involved in RhoA GTPase inactivation supports this possibility (de Faria, unpublished). Further investigation is necessary to uncover the mechanism through which TMEM10 promotes OPC differentiation *in vitro*. Likewise, it remains to be addressed if TMEM10 additionally regulates OPC differentiation *in vivo.*

3 UNC5B and paranode organization

Myelinating oligodendrocytes extend numerous processes that contact and ensheath axons. As a new myelin segment grows longitudinally and the thickening lamella becomes compacted, distinct domains - the node, paranode, juxtaparanode, and internode - assemble along the axonal plasma membrane. Initially diffusely expressed, voltage-dependent Na^+ and K^+ channels cluster into the node and juxtaparanode, a distribution pattern that requires a diffusion barrier activity provided by the paranode. At the same time, multiple layers of compacted oligodendrocyte plasma membrane electrically insulate the axolemma along the internode. Organization of myelinated axons into distinct axoglial domains allows for spatially restricted depolarization of the axonal membrane and is therefore critical for saltatory conduction of the action potential. In

chapter IV of this thesis, we provided evidence that the netrin-1 receptor UNC5B concentrates in the paranode of myelinated axons and that, in absence of UNC5B, paranode ultrastructure becomes disorganized and segregation of axoglial domains is compromised *in vivo*. This phenotype is less severe in younger animals, indicating that UNC5B makes a functional contribution to paranode maintenance. We conclude that UNC5B mediates netrin-1 signaling that is necessary for paranode organization in the adult mouse CNS.

Several other proteins, including netrin-1 and its receptor DCC, were previously reported to be required for paranode organization (Jarjour et al 2008; Bull et al., 2014). Mice deficient for the paranode axoglial junction components Caspr, Contactin or NF155 do not form transverse bands and glial loops do not attach to the axolemma. As a consequence, axonal domains do not segregate properly and K+ channels invade the paranode and partially overlap Na+ channels at the node. Compromised ion channel segregation results in defective saltatory conduction of action potential and axon signals propagate at a lower velocity. As expected, these paranode mutants develop a range of neurological defects, including tremors, seizures and hindlimb paralysis (Bhat et al., 2001; Boyle et al., 2001; Sherman et al., 2005; Pillai et al., 2009).

CGT, CST, MAL and CNP deficient mice also develop disorganized paranodes, although the onset and severity of the phenotypes vary considerably between these lines (Dupree et al., 1998; Marcus et al., 2006; Rasband et al., 2005; Schaeren-Wiemers et al., 2004). In common, these four proteins contribute to the formation and/or regulation of lipid raft composition in glial cells. CGT is a key enzyme in the synthesis of galactocerebroside (GalC) and sulfatide, while CST is necessary for sulfatide synthesis specifically; both GalC and sulfatide are important lipid raft components in oligodendrocytes (Kramer et al., 1997; Taylor et al., 2002). MAL is a lipid-raft

associated protein that is involved in the sorting of proteins to lipid raft domains and CNP is another component of oligodendrocyte lipid rafts (Schaeren-Wiemers et al., 1995; Taylor et al., 2002). NF155 localizes to lipid rafts at the glial loop membrane and in CGT and MAL-null mice NF155 distribution is disrupted (Menon et al., 2003; Schaeren-Wiemers et al., 2004; Schafer et al., 2004). Because NF155 act as an instructive signal for Caspr/Contactin recruitment, the paranode disruption observed in CGT, CST, MAL and CNP deficient mice might result from exclusion of NF155 from lipid rafts at the paranode. Interestingly, paranode defects observed in CST, MAL and CNP arise only after development, suggesting that these proteins are important for paranode maintenance, rather than formation (Marcus et al., 2006; Schaeren-Wiemers et al., 2004; Rasband et al., 2005).

Netrin-1 and its receptor DCC are also necessary for paranode maintenance. In organotypic cultures of cerebellar slices derived from netrin-1 and DCC-deficient mice, paranodes form normally but become disorganized with time (Jarjour et al., 2008). *In vivo*, DCC deletion in PLP positive oligodendrocytes results in loss of transverse bands, glial loop detachment and lengthening of paranodal Caspr domains that had formed properly during development. In addition, conduction velocity becomes reduced and mice develop motor behavior defects (Bull et al., 2014).

Similar to DCC and other proteins discussed above, we show that UNC5B functions in paranode maintenance, although we have not excluded an additional impact on paranode formation (Figure 4.7). In absence of UNC5B, levels of paranode disorganization are comparable - in terms of number of detached loops – to the disorganization that follows DCC ablation in mature oligodendrocytes (Figure 4.5; Bull et al., 2014) and both models show a considerably less severe

phenotype in comparison to Caspr, Contactin or NF155 deficient animals (Bhat et al., 2001; Boyle et al., 2001; Sherman et al., 2005; Pillai et al., 2009). An unexpected defect that was characteristic of UNC5B cKO animals is the apparent fragmentation of the glial loop-loop interface (Figure 4.5, zoom). Because we did not observe transverse band loss as a result of UNC5B deletion (data not shown), it may be the case that UNC5B functions primarily at the loop-loop interface and that axon-loop detachment in UNC5B cKO follows destabilization of loop-loop interactions. This is in opposition to the phenotype described in the DCC deficient mice where transverse bands are lost while the loop-loop interface appears normal (Bull et al., 2014). Together these findings suggests a model for netrin-1 regulation of paranode organization in which DCC is required for maintenance of axoglial junctions and UNC5B is necessary for maintenance of the loop-loop interface. Consistent with this model, paranodes develop both axoglial and loop-loop defects following netrin-1 loss *in vitro* (Jarjour et al., 2008). Also consistent, short-range netrin-1 function is often mediated by independent activation of UNC5 and DCC, even in the case where both receptors are co-expressed in the same cell (Keleman and Dickson, 2001; Merz et al., 2001; Macabenta et al., 2013).

The glial loop interface contains junctional specializations, originally described in epithelial cells, that includes tight and adherens junctions. These junctions prevent the diffusion of small molecules through the paracellular space and underlie the polarization of epithelial membranes into distinct molecular domains. In the PNS, glial loop tight junctions contain Claudins-1 and 9, whereas Claudin-11 is detected in tight junctions of CNS paranodes (Gow et al., 1999; Miyamoto et al., 2005; Poliak et al., 2002). E-cadherin forms adherens junctions in glial loops of PNS, whereas adherens junctions have not been found on CNS paranodes thus far (Fannon et al.,

1995). Adaptor proteins, such as Zona Occludens-1, 2 and 3 (ZO-1, 2, 3), link the transmembrane junction proteins to the underlying cytoskeleton (Stevenson and Keon, 1998). Interestingly, netrin-1 regulates the expression of tight junction proteins that control brain-blood barrier permeability, suggesting that tight junctions at the paranode may be modulated by netrin-1 signaling (Podjaski et al., 2015). In addition, knockdown of netrin-1 receptor Neogenin disrupts the organization of E-cadherin and results in the loss of cell-cell adhesion in Caco-2 human colon epithelial cells, indicating that netrin-1 signaling might also regulate adherens junctions (H. Cooper, personal communication). Moreover, the intracellular region of UNC5B contains a ZU-5 domain, which is shared by ZO-1 and is involved in the linkage of tight and adherens junctions to the cytoskeleton. This suggests that UNC5B may be recruited to an adhesive complex at the loop-loop interface, where it may be required for regulation of junctional specializations. It will be of interest to investigate in the future if the expression and distribution of tight and adherens junction proteins are affected in UNC5B cKO paranode loops.

Axoglial paranode junctions form a diffusion barrier at the axon surface that is required for proper segregation of Na+ channels in the node and K+ channels in the juxtaparanode (Pedraza et al., 2009). In the absence of this barrier function, following axoglial junction disruption in Caspr and Contactin deficient mice, K+ channels mislocalize to the paranode and partially overlap with Na+ channel distribution in the node (Boyle et al., 2001; Bhat et al., 2001). In cerebellar slice cultures derived from netrin-1 and DCC knockout mice, the mean distance between K+ and Na+ channel domains was decreased and Caspr distribution was lengthened along the axon (Jarjour et al., 2008). A comparable increase in Caspr domain length was observed in myelinated axons in the adult brains of DCC conditional knockout animals (Bull et

al., 2014). Following UNC5B deletion in oligodendrocytes, we found that the Caspr domain was consistently lengthened in multiple CNS regions, and that the overlap between Caspr and Na+ domains was consistently increased in the axons of 9 months-old animals, consistent with Caspr invading the node of Ranvier (Figure 4.6, optic nerve and cerebellum; data not shown, corpus callosum). This phenotype was most evident in the optic nerve, where the distance between adjacent Caspr domains was reduced and the nodal gap completely absent in some axons (Figure 4.6D and H). We also observed that the K+ channel domain increased in length, while the overlap between K+ and Caspr domains was not changed (Figure 4.6F and J). These alterations suggest that K+ channels diffuse toward the internode following UNC5B downregulation in the paranodes. Remarkably, the absence of a change in the distance between adjacent K+ channel domains and lack of overlap between Caspr and K+ immunoreactivities indicates that K+ channels do not invade the paranode nor diffuse towards the Na+ channel domain in the node. This suggests that the paranodal diffusion barrier is preserved following UNC5B deletion and appears consistent with normal density of transverse bands and UNC5B having a primary function at the loop-loop interface. It also suggests that the normal motor behavior observed in 9 months-old UNC5B cKO mice might reflect the persistence of appropriately segregated K+ and Na+ channels in myelinated axons that lack UNC5B.

Further investigation is necessary to fully uncover UNC5B and netrin-1 function during oligodendrocyte development and myelination. Formation of normal amounts of myelin following UNC5B deletion (Figure 4.3) suggests that OPC development does not require UNC5B. However, multiple regulatory mechanism act in parallel during OPC development and compensation between different mechanisms allows for the formation of seemingly normal

myelin in absence of important regulators. Indeed, during spinal cord development, migrating OPCs are repelled by floor plate-derived netrin-1 and UNC5B may have a function in mediating netrin signaling in this context (Jarjour et al., 2003; Tsai et al., 2003). Additionally, in 3 months-old UNC5B cKOs, we noticed that Caspr domain length was significantly decreased following UNC5B deletion, suggesting that UNC5B may have a function in myelin segment extension during development. In addition, we cannot exclude that UNC5B is relevant for paranode formation since we detected some level of paranode disruption in UNC5B cKOs at 3 months of age.

4 miRNAs, TMEM10 and netrins

Regulation of oligodendrocyte development and myelin formation exhibits a remarkable degree of cooperation between multiple regulatory mechanisms. Often, one mechanism regulates more than one step in development and, conversely, the same step is normally regulated by several compensatory mechanisms that act in parallel. In fact, thus far, no single molecule has been shown to be absolutely essential for oligodendrocyte differentiation in the CNS. miRNAs, TMEM10 and netrin/UNC5B regulate oligodendrocyte development in the postnatal and adult CNS. Here, we speculate how these novel regulators may interact with each other and how such integration may function during oligodendrocyte maturation and myelin organization during development.

MiRNAs regulate gene expression by targeting 3'UTR in mRNAs. Analysis of putative miRNA binding sites in netrin-1 mRNA revealed the presence of conserved biding motifs for miRNAs miR-17 and miR-20a (www.targetscan.org; Agarwal et al., 2015). These miRNAs are part of

miR-17-92 cluster, which is involved in OPC survival/proliferation and is downregulated in rodent and human OPCs as they differentiate into mature oligodendrocytes (Figure 2.4; Budde et al., 2010). Interestingly, Netrin-1 is expressed by myelinating oligodendrocytes, but not by immature OPCs (Manitt et al., 2001; Rajasekharan et al., 2009), suggesting that netrin-1 expression in the oligodendrocyte lineage may be developmentally regulated by miRNAs miR-17 and miR-20a. Lack of netrin-1 expression at early stages of development may be critical for OPCs to properly migrate in response to netrin gradients established along the neural tube. At later stages, autocrine netrin-1 signaling in post-migratory differentiating oligodendrocytes is then required for process extension and myelin membrane elaboration (Jarjour et al., 2003; Rajasekharan et al., 2009). Further experimentation will be necessary to validate if predicted binding sites in the netrin-1 mRNA 3'UTR are actual targets of miRNAs miR-17 and miR-20a and to investigate if these miRNAs are essential for normal OPC migration during embryonic development. Interestingly, spinal cords of miR-17-92 cKOs display a small decrease in the number of Olig2-positive cells, which could result from impaired OPC migration in absence of miR-17 and miR-20a (Budde et al., 2010).

While dissecting the molecular mechanisms underlying miRNA regulation of OPC differentiation, Dugas and colleagues discovered that two miR-219 targets – ZFP238 and FoxJ3 - are previously unappreciated inhibitors of OPC differentiation (Dugas et al., 2010). It is thus possible that other genes, expressed by oligodendrocytes and regulated by oligodendrocyte relevant miRNAs, may also have an uncharacterized function during oligodendrocyte development. Surprisingly, 6 out of the 10 most downregulated miRNAs during OPC differentiation have predicted binding sites in the 3'UTR of rat, mouse or human TMEM10

mRNA (data not shown; Lau et al., 2008). Although the majority of these motifs are not conserved among mammals, the only conserved miRNA binding site predicted to exist in the 3'UTR of TMEM10 (miR-125b) is among the top downregulated miRNAs (Lau et al., 2008). TMEM10 is the most upregulated transcript during Oli-neu differentiation and also ranks among the top upregulated transcripts during differentiation of primary OPCs (Kippert et al., 2008; Dugas et al., 2006), suggesting that TMEM10 expression may be developmentally regulated by miRNAs expressed at early stages of the oligodendrocyte lineage. It remains to be tested if miR-125b (and others) directly targets TMEM10 and if it negatively regulates OPC differentiation by repressing TMEM10 expression.

TMEM10 induces process extension and, in the absence of TMEM10, MBP-positive membranes generated by primary oligodendrocytes are abnormally shaped, indicating that TMEM10 regulates OPC morphological differentiation (Figures 3.3 and 3.5). *In vitro* and *in vivo*, netrin-1 promotes process branching and formation of myelin-like membrane sheets, suggesting that netrin-1 also regulates oligodendrocyte morphology (Rajasekharan et al., 2009). In differentiating oligodendrocytes, netrin-1 inhibits RhoA and RhoA Kinase (ROCK) and downregulation of RhoA signaling is necessary for netrin-1-induced process elaboration (Rajasekharan et al., 2009). Interestingly, treatment of Oli-neu cells with a ROCK inhibitor induces high levels of TMEM10 expression (Kippert et al., 2008), suggesting that TMEM10 may activate signaling similar to netrin-1, or function downstream of netrin-1 signaling, to promote membrane extension during oligodendrocyte differentiation. In this context, it will be of interest to investigate if TMEM10 expression is required for netrin-1 regulation of membrane formation

and if TMEM10 acts downstream of netrins in other aspects of oligodendrocyte development that are regulated by netrin-1, such as myelin domain maintenance.

During development, netrin-1, in the form of a secreted protein gradient, acts at a distance, as a long-range cue for migrating cells and extending axons. Conversely, in the adult CNS, the distribution of netrin-1 protein is highly localized, restricted to the vicinity of secreting cells - for example, at the paranodes. This localized pattern of expression suggests that a mechanism may exist to restrict netrin-1 distribution to specific domains of the CNS. This mechanism may rely on the ability of the positively charged C domain of netrins to interact with negatively charged molecules expressed at plasma membrane of secreting cells. TMEM10 is heavily glycosylated and a part of TMEM10 carbohydrates contains negatively charged sialic acids (Yoshikawa et al., 2008). In addition, TMEM10 is enriched at the paranodes, suggesting that TMEM10 may contribute to localize netrin-1 at this domain. If this is the case, TMEM10 knock-down would disrupt netrin-1 enrichment in the paranodes of myelinating co-cultures. Additionally, a TMEM10 knockout mouse should recapitulate the paranodal defects we demonstrate to exist in UNC5B cKOs.

We have shown in this thesis that miRNAs, TMEM10 and netrin/UNC5B are regulators of OPC development and myelin organization. Future experiments addressing the possibilities discussed in this section may reveal an unanticipated level of interplay between these mechanisms taking place during development.

5 Figures

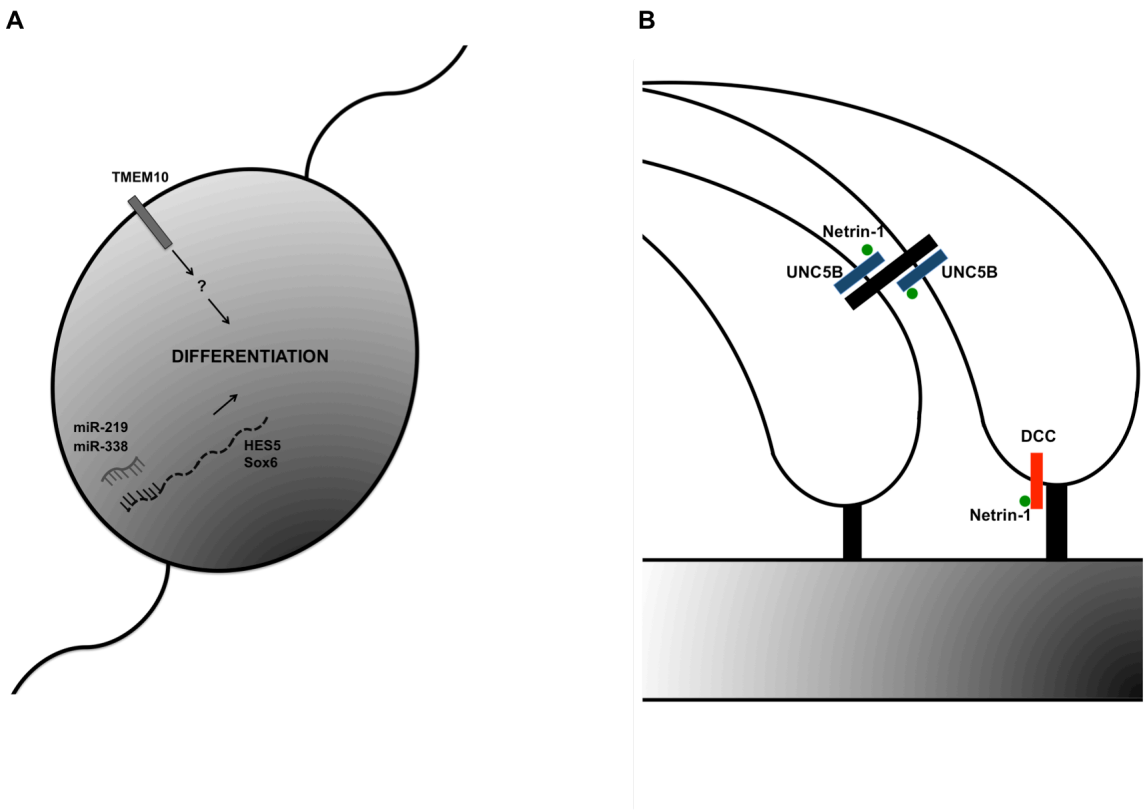

Figure 5: miRNAs, TMEM10 and UNC5B are new regulators of oligodendrocyte development and myelin organization – (A) MiR-219 and miR-338 promote OPC differentiation by repressing the expression of differentiation inhibitors, such as HES5 and Sox6. TMEM10 induces OPC differentiation through an unknown mechanism. **(B)** Our findings provide evidence that the netrin-1 receptor UNC5B is recruited to an adhesive complex at the glial loop interface, where it regulates adhesion between loops. DCC, on the other hand, is recruited to the axoglial interface and it is necessary for the maintenance of axoglial junctions.

CONCLUSIONS AND PERPECTIVES

The study of myelin and myelinating glia is as critical for the comprehension of the nervous system function as fast and efficient conduction of the action potential is critical for neural activity in vertebrates. Its significance reaches beyond normal function of the nervous system, as myelin dysfunction is a component of several neurological disorders. This thesis contributes to our understanding of myelin and myelinating cells, as it provides new insights on the regulation of oligodendrocyte development and myelin organization in the CNS.

miRNAs regulate different aspects of rodent OPC development. We have now shown that rodent-relevant miRNAs are expressed in OPC/oligodendrocytes isolated from the human adult brain, suggesting that miRNA regulation of OPC development is conserved in humans and rodents. However, direct evidence for conserved function remains to be provided. Preliminary results obtained with a human OPC cell line are promising (de Faria, unpublished results) but further experimentation using primary cells derived from the adult human brain is necessary to confirm the relevance of these initial findings. Continuing characterization of oligodendrocyte lineage cells that are resident to the adult human brain and investigation of mechanisms that regulate differentiation of adult OPCs will provide insights on the reasons why remyelination is limited in demyelinating disorders and point to new strategies to overcome such limitations.

Thus far, most regulators of OPC differentiation have been identified in the context of CNS development. We have also provided initial evidence suggesting that *in vitro* differentiation of an OPC cell line and primary OPCs isolated from the developing rat brain require TMEM10. The relevance of this regulation needs to be demonstrated *in vivo* and, for that, generation of a

TMEM10 null mouse line is paramount. In addition, investigation of the biochemical events that follow TMEM10 expression will provide mechanistic insights on TMEM10 regulation of OPC differentiation.

Identification of regulatory mechanisms that contribute to myelin stability and maintenance is key to understand the onset of myelin dysfunction in demyelinating disorders. We have demonstrated that the netrin-1 receptor UNC5B is required for maintenance of the paranode myelin domain. It remains to be elucidated exactly how netrin-1 signaling regulates axoglial domain organization and to which extent DCC and UNC5B function independently. To address this issue, we are using super resolution microscopy to define, at the ultrastructure level, the localization of these two netrin receptors in the paranodes. In addition, generation of a DCC-UNC5B double-knockout mouse line will help to elucidate the interplay between DCC and UNC5B in netrin-1 regulation of paranode organization.

The results described in this thesis identify new regulators of oligodendrocyte development and myelin organization. Further progress in myelin research will advance our understanding of nervous system function and pave the way to the cure of demyelinating neurological disorders.

BIBLIOGRAPHY

Abbott, N.J. (2005). Dynamics of CNS barriers: evolution, differentiation, and modulation. Cell Mol Neurobiol *25*, 5-23.

Ackerman, S.L., Kozak, L.P., Przyborski, S.A., Rund, L.A., Boyer, B.B., and Knowles, B.B. (1997). The mouse rostral cerebellar malformation gene encodes an UNC-5-like protein. Nature *386*, 838-842.

Aggarwal, S., Snaidero, N., Pahler, G., Frey, S., Sanchez, P., Zweckstetter, M., Janshoff, A., Schneider, A., Weil, M.T., Schaap, I.A.*, et al.* (2013). Myelin membrane assembly is driven by a phase transition of myelin basic proteins into a cohesive protein meshwork. PLoS Biol *11*, e1001577.

Albrecht, S., Altenhein, B., and Paululat, A. (2011). The transmembrane receptor Uncoordinated5 (Unc5) is essential for heart lumen formation in Drosophila melanogaster. Dev Biol *350*, 89-100.

Alcantara, S., Ruiz, M., De Castro, F., Soriano, E., and Sotelo, C. (2000). Netrin 1 acts as an attractive or as a repulsive cue for distinct migrating neurons during the development of the cerebellar system. Development *127*, 1359-1372.

Altman, J., and Bayer, S.A. (1984). The development of the rat spinal cord. Adv Anat Embryol Cell Biol *85*, 1-164.

Ambros, V., and Horvitz, H.R. (1987). The lin-14 locus of Caenorhabditis elegans controls the time of expression of specific postembryonic developmental events. Genes Dev *1*, 398-414.

Andrews, G.L., Tanglao, S., Farmer, W.T., Morin, S., Brotman, S., Berberoglu, M.A., Price, H., Fernandez, G.C., Mastick, G.S., Charron, F.*, et al.* (2008). Dscam guides embryonic axons by Netrin-dependent and -independent functions. Development *135*, 3839-3848.

Archelos, J.J., Trotter, J., Previtali, S., Weissbrich, B., Toyka, K.V., and Hartung, H.P. (1998). Isolation and characterization of an oligodendrocyte precursor-derived B-cell epitope in multiple sclerosis. Ann Neurol *43*, 15-24.

Agarwal V, Bell GW, Nam J, Bartel DP. (2015) Predicting effective microRNA target sites in mammalian mRNAs. *eLife, 4:e05005*

Armstrong, R.C. (1998). Isolation and characterization of immature oligodendrocyte lineage cells. Methods *16*, 282-292.

Armstrong, R.C., Harvath, L., and Dubois-Dalcq, M.E. (1990). Type 1 astrocytes and oligodendrocyte-type 2 astrocyte glial progenitors migrate toward distinct molecules. J Neurosci Res *27*, 400-407.

Aruga, J., Yoshikawa, F., Nozaki, Y., Sakaki, Y., Toyoda, A., and Furuichi, T. (2007). An oligodendrocyte enhancer in a phylogenetically conserved intron region of the mammalian myelin gene Opalin. J Neurochem *102*, 1533-1547.

Ashkenazi, A., and Dixit, V.M. (1998). Death receptors: signaling and modulation. Science *281*, 1305-1308.

Astic, L., Pellier-Monnin, V., Saucier, D., Charrier, C., and Mehlen, P. (2002). Expression of netrin-1 and netrin-1 receptor, DCC, in the rat olfactory nerve pathway during development and axonal regeneration. Neuroscience *109*, 643-656.

Baek, D., Villen, J., Shin, C., Camargo, F.D., Gygi, S.P., and Bartel, D.P. (2008). The impact of microRNAs on protein output. Nature *455*, 64-71.

Bangsow, T., Schepelmann, S., Martin, C., May, M., Oberthur, A., Perl, S., Knupfer, E., Zinke, H., and Gassen, H.G. (1998). Identification of a gene selectively expressed in the brain, which encodes a putative transmembrane protein and a soluble cytoplasmic isoform. Eur J Biochem *256*, 24-35.

Barad, O., Meiri, E., Avniel, A., Aharonov, R., Barzilai, A., Bentwich, I., Einav, U., Gilad, S., Hurban, P., Karov, Y.*, et al.* (2004). MicroRNA expression detected by oligonucleotide

microarrays: system establishment and expression profiling in human tissues. Genome Res *14*, 2486-2494.

Baron, W., Shattil, S.J., and ffrench-Constant, C. (2002). The oligodendrocyte precursor mitogen PDGF stimulates proliferation by activation of alpha(v)beta3 integrins. EMBO J *21*, 1957-1966.

Barres, B.A., Hart, I.K., Coles, H.S., Burne, J.F., Voyvodic, J.T., Richardson, W.D., and Raff, M.C. (1992). Cell death and control of cell survival in the oligodendrocyte lineage. Cell *70*, 31-46.

Barres, B.A., and Raff, M.C. (1994). Control of oligodendrocyte number in the developing rat optic nerve. Neuron *12*, 935-942.

Barres, B.A., and Raff, M.C. (1999). Axonal control of oligodendrocyte development. J Cell Biol *147*, 1123-1128.

Bartoe, J.L., McKenna, W.L., Quan, T.K., Stafford, B.K., Moore, J.A., Xia, J., Takamiya, K., Huganir, R.L., and Hinck, L. (2006). Protein interacting with C-kinase 1/protein kinase Calpha-mediated endocytosis converts netrin-1-mediated repulsion to attraction. J Neurosci *26*, 3192-3205.

Bauer, N.G., Richter-Landsberg, C., and Ffrench-Constant, C. (2009). Role of the oligodendroglial cytoskeleton in differentiation and myelination. Glia *57*, 1691-1705.

Berglund, E.O., Murai, K.K., Fredette, B., Sekerkova, G., Marturano, B., Weber, L., Mugnaini, E., and Ranscht, B. (1999). Ataxia and abnormal cerebellar microorganization in mice with ablated contactin gene expression. Neuron *24*, 739-750.

Bernstein, E., Caudy, A.A., Hammond, S.M., and Hannon, G.J. (2001). Role for a bidentate ribonuclease in the initiation step of RNA interference. Nature *409*, 363-366.

Bernstein, E., Kim, S.Y., Carmell, M.A., Murchison, E.P., Alcorn, H., Li, M.Z., Mills, A.A., Elledge, S.J., Anderson, K.V., and Hannon, G.J. (2003). Dicer is essential for mouse development. Nat Genet *35*, 215-217.

Bhat, M.A., Rios, J.C., Lu, Y., Garcia-Fresco, G.P., Ching, W., St Martin, M., Li, J., Einheber, S., Chesler, M., Rosenbluth, J.*, et al.* (2001). Axon-glia interactions and the domain organization of myelinated axons requires neurexin IV/Caspr/Paranodin. Neuron *30*, 369-383.

Bin, J.M., Rajasekharan, S., Kuhlmann, T., Hanes, I., Marcal, N., Han, D., Rodrigues, S.P., Leong, S.Y., Newcombe, J., Antel, J.P.*, et al.* (2013). Full-length and fragmented netrin-1 in multiple sclerosis plaques are inhibitors of oligodendrocyte precursor cell migration. Am J Pathol *183*, 673-680.

Blaschuk, K.L., Frost, E.E., and ffrench-Constant, C. (2000). The regulation of proliferation and differentiation in oligodendrocyte progenitor cells by alphaV integrins. Development *127*, 1961-1969.

Boggs, J.M. (2006). Myelin basic protein: a multifunctional protein. Cell Mol Life Sci *63*, 1945-1961.

Boiko, T., Rasband, M.N., Levinson, S.R., Caldwell, J.H., Mandel, G., Trimmer, J.S., and Matthews, G. (2001). Compact myelin dictates the differential targeting of two sodium channel isoforms in the same axon. Neuron *30*, 91-104.

Bouchard, J.F., Moore, S.W., Tritsch, N.X., Roux, P.P., Shekarabi, M., Barker, P.A., and Kennedy, T.E. (2004). Protein kinase A activation promotes plasma membrane insertion of DCC from an intracellular pool: A novel mechanism regulating commissural axon extension. J Neurosci *24*, 3040-3050.

Boyle, M.E., Berglund, E.O., Murai, K.K., Weber, L., Peles, E., and Ranscht, B. (2001). Contactin orchestrates assembly of the septate-like junctions at the paranode in myelinated peripheral nerve. Neuron *30*, 385-397.

Bredesen, D.E., Ye, X., Tasinato, A., Sperandio, S., Wang, J.J., Assa-Munt, N., and Rabizadeh, S. (1998). p75NTR and the concept of cellular dependence: seeing how the other half die. Cell Death Differ *5*, 365-371.

Bremer, M., Frob, F., Kichko, T., Reeh, P., Tamm, E.R., Suter, U., and Wegner, M. (2011). Sox10 is required for Schwann-cell homeostasis and myelin maintenance in the adult peripheral nerve. Glia *59*, 1022-1032.

Bribian, A., Barallobre, M.J., Soussi-Yanicostas, N., and de Castro, F. (2006). Anosmin-1 modulates the FGF-2-dependent migration of oligodendrocyte precursors in the developing optic nerve. Mol Cell Neurosci *33*, 2-14.

Budde, H., Schmitt, S., Fitzner, D., Opitz, L., Salinas-Riester, G., and Simons, M. (2010). Control of oligodendroglial cell number by the miR-17-92 cluster. Development *137*, 2127-2132.

Bull, S.J., Bin, J.M., Beaumont, E., Boutet, A., Krimpenfort, P., Sadikot, A.F., and Kennedy, T.E. (2014). Progressive disorganization of paranodal junctions and compact myelin due to loss of DCC expression by oligodendrocytes. J Neurosci *34*, 9768-9778.

Bunge, R.P., Bunge, M.B., and Bates, M. (1989). Movements of the Schwann cell nucleus implicate progression of the inner (axon-related) Schwann cell process during myelination. J Cell Biol *109*, 273-284.

Cai, J., Qi, Y., Hu, X., Tan, M., Liu, Z., Zhang, J., Li, Q., Sander, M., and Qiu, M. (2005). Generation of oligodendrocyte precursor cells from mouse dorsal spinal cord independent of Nkx6 regulation and Shh signaling. Neuron *45*, 41-53.

Cajal, S.R.Y. (1909). Histologie du système nerveux de l'homme & des vertébrés. Consejo Superior de Investigaciones Cientificas, Madrid.

Cajal, S.R.Y. (1913). Contribucion al conocimiento de la neuroglia deI cerebro

humano. Travaux du Laboratoire de recherches biologiques de l'Université de Madrid *11*, 255-315.

Calver, A.R., Hall, A.C., Yu, W.P., Walsh, F.S., Heath, J.K., Betsholtz, C., and Richardson, W.D. (1998). Oligodendrocyte population dynamics and the role of PDGF in vivo. Neuron *20*, 869-882.

Canoll, P.D., Kraemer, R., Teng, K.K., Marchionni, M.A., and Salzer, J.L. (1999). GGF/neuregulin induces a phenotypic reversion of oligodendrocytes. Mol Cell Neurosci *13*, 79-94.

Carson, M.J., Behringer, R.R., Brinster, R.L., and McMorris, F.A. (1993). Insulin-like growth factor I increases brain growth and central nervous system myelination in transgenic mice. Neuron *10*, 729-740.

Chan, S.S., Zheng, H., Su, M.W., Wilk, R., Killeen, M.T., Hedgecock, E.M., and Culotti, J.G. (1996). UNC-40, a C. elegans homolog of DCC (Deleted in Colorectal Cancer), is required in motile cells responding to UNC-6 netrin cues. Cell *87*, 187-195.

Charles, P., Hernandez, M.P., Stankoff, B., Aigrot, M.S., Colin, C., Rougon, G., Zalc, B., and Lubetzki, C. (2000). Negative regulation of central nervous system myelination by polysialylated-neural cell adhesion molecule. Proc Natl Acad Sci U S A *97*, 7585-7590.

Chen, C., Ridzon, D.A., Broomer, A.J., Zhou, Z., Lee, D.H., Nguyen, J.T., Barbisin, M., Xu, N.L., Mahuvakar, V.R., Andersen, M.R.*, et al.* (2005). Real-time quantification of microRNAs by stem-loop RT-PCR. Nucleic Acids Res *33*, e179.

Chen, Y., Wu, H., Wang, S., Koito, H., Li, J., Ye, F., Hoang, J., Escobar, S.S., Gow, A., Arnett, H.A.*, et al.* (2009). The oligodendrocyte-specific G protein-coupled receptor GPR17 is a cell-intrinsic timer of myelination. Nat Neurosci *12*, 1398-1406.

Ching, W., Zanazzi, G., Levinson, S.R., and Salzer, J.L. (1999). Clustering of neuronal sodium channels requires contact with myelinating Schwann cells. J Neurocytol *28*, 295-301.

Chun, S.J., Rasband, M.N., Sidman, R.L., Habib, A.A., and Vartanian, T. (2003). Integrin-linked kinase is required for laminin-2-induced oligodendrocyte cell spreading and CNS myelination. J Cell Biol *163*, 397-408.

Colamarino, S.A., and Tessier-Lavigne, M. (1995). The axonal chemoattractant netrin-1 is also a chemorepellent for trochlear motor axons. Cell *81*, 621-629.

Colavita, A., and Culotti, J.G. (1998). Suppressors of ectopic UNC-5 growth cone steering identify eight genes involved in axon guidance in Caenorhabditis elegans. Dev Biol *194*, 72-85.

Colman, D.R., Kreibich, G., Frey, A.B., and Sabatini, D.D. (1982). Synthesis and incorporation of myelin polypeptides into CNS myelin. J Cell Biol *95*, 598-608.

Colognato, H., Ramachandrappa, S., Olsen, I.M., and ffrench-Constant, C. (2004). Integrins direct Src family kinases to regulate distinct phases of oligodendrocyte development. J Cell Biol *167*, 365-375.

Colon-Ramos, D.A., Margeta, M.A., and Shen, K. (2007). Glia promote local synaptogenesis through UNC-6 (netrin) signaling in C. elegans. Science *318*, 103-106.

Cotrufo, T., Andres, R.M., Ros, O., Perez-Branguli, F., Muhaisen, A., Fuschini, G., Martinez, R., Pascual, M., Comella, J.X., and Soriano, E. (2012). Syntaxin 1 is required for DCC/Netrin-1-dependent chemoattraction of migrating neurons from the lower rhombic lip. Eur J Neurosci *36*, 3152-3164.

Cotrufo, T., Perez-Branguli, F., Muhaisen, A., Ros, O., Andres, R., Baeriswyl, T., Fuschini, G., Tarrago, T., Pascual, M., Urena, J.*, et al.* (2011). A signaling mechanism coupling netrin-1/deleted in colorectal cancer chemoattraction to SNARE-mediated exocytosis in axonal growth cones. J Neurosci *31*, 14463-14480.

Crocker, P.R. (2002). Siglecs: sialic-acid-binding immunoglobulin-like lectins in cell-cell interactions and signalling. Curr Opin Struct Biol *12*, 609-615.

Cui, Q.L., Fragoso, G., Miron, V.E., Darlington, P.J., Mushynski, W.E., Antel, J., and Almazan, G. (2010). Response of human oligodendrocyte progenitors to growth factors and axon signals. J Neuropathol Exp Neurol *69*, 930-944.

Davis, T.H., Cuellar, T.L., Koch, S.M., Barker, A.J., Harfe, B.D., McManus, M.T., and Ullian, E.M. (2008). Conditional loss of Dicer disrupts cellular and tissue morphogenesis in the cortex and hippocampus. J Neurosci *28*, 4322-4330.

de Faria, O., Jr., Cui, Q.L., Bin, J.M., Bull, S.J., Kennedy, T.E., Bar-Or, A., Antel, J.P., Colman, D.R., and Dhaunchak, A.S. (2012). Regulation of miRNA 219 and miRNA Clusters 338 and 17-92 in Oligodendrocytes. Front Genet *3*, 46.

Decker, L., Desmarquet-Trin-Dinh, C., Taillebourg, E., Ghislain, J., Vallat, J.M., and Charnay, P. (2006). Peripheral myelin maintenance is a dynamic process requiring constant Krox20 expression. J Neurosci *26*, 9771-9779.

Deiner, M.S., Kennedy, T.E., Fazeli, A., Serafini, T., Tessier-Lavigne, M., and Sretavan, D.W. (1997). Netrin-1 and DCC mediate axon guidance locally at the optic disc: loss of function leads to optic nerve hypoplasia. Neuron *19*, 575-589.

Dhaunchak, A.S., Becker, C., Schulman, H., De Faria, O., Jr., Rajasekharan, S., Banwell, B., Colman, D.R., Bar-Or, A., and Canadian Pediatric Demyelinating Disease, G. (2012). Implication of perturbed axoglial apparatus in early pediatric multiple sclerosis. Ann Neurol *71*, 601-613.

Dhaunchak, A.S., Colman, D.R., and Nave, K.A. (2011). Misalignment of PLP/DM20 Transmembrane Domains Determines Protein Misfolding in Pelizaeus-Merzbacher Disease. J Neurosci *31*, 14961-14971.

Dhaunchak, A.S., Huang, J.K., De Faria Junior, O., Roth, A.D., Pedraza, L., Antel, J.P., Bar-Or, A., and Colman, D.R. (2010). A proteome map of axoglial specializations isolated and purified from human central nervous system. Glia *58*, 1949-1960.

Dhaunchak, A.S., and Nave, K.A. (2007). A common mechanism of PLP/DM20 misfolding causes cysteine-mediated endoplasmic reticulum retention in oligodendrocytes and Pelizaeus-Merzbacher disease. Proc Natl Acad Sci U S A *104*, 17813-17818.

Dickson, B.J., and Keleman, K. (2002). Netrins. Curr Biol *12*, R154-155.

Dugandzija-Novakovic, S., Koszowski, A.G., Levinson, S.R., and Shrager, P. (1995). Clustering of Na+ channels and node of Ranvier formation in remyelinating axons. J Neurosci *15*, 492-503.

Dugas, J.C., Cuellar, T.L., Scholze, A., Ason, B., Ibrahim, A., Emery, B., Zamanian, J.L., Foo, L.C., McManus, M.T., and Barres, B.A. (2010). Dicer1 and miR-219 Are required for normal oligodendrocyte differentiation and myelination. Neuron *65*, 597-611.

Dugas, J.C., Tai, Y.C., Speed, T.P., Ngai, J., and Barres, B.A. (2006). Functional genomic analysis of oligodendrocyte differentiation. J Neurosci *26*, 10967-10983.

Dupouey, P., Jacque, C., Bourre, J.M., Cesselin, F., Privat, A., and Baumann, N. (1979). Immunochemical studies of myelin basic protein in shiverer mouse devoid of major dense line of myelin. Neurosci Lett *12*, 113-118.

Dupree, J.L., Coetzee, T., Blight, A., Suzuki, K., and Popko, B. (1998). Myelin galactolipids are essential for proper node of Ranvier formation in the CNS. J Neurosci *18*, 1642-1649.

Dziembowska, M., Tham, T.N., Lau, P., Vitry, S., Lazarini, F., and Dubois-Dalcq, M. (2005). A role for CXCR4 signaling in survival and migration of neural and oligodendrocyte precursors. Glia *50*, 258-269.

Einheber, S., Zanazzi, G., Ching, W., Scherer, S., Milner, T.A., Peles, E., and Salzer, J.L. (1997). The axonal membrane protein Caspr, a homologue of neurexin IV, is a component of the septate-like paranodal junctions that assemble during myelination. J Cell Biol *139*, 1495-1506.

Elbashir, S.M., Harborth, J., Lendeckel, W., Yalcin, A., Weber, K., and Tuschl, T. (2001a). Duplexes of 21-nucleotide RNAs mediate RNA interference in cultured mammalian cells. Nature *411*, 494-498.

Elbashir, S.M., Lendeckel, W., and Tuschl, T. (2001b). RNA interference is mediated by 21- and 22-nucleotide RNAs. Genes Dev *15*, 188-200.

Emery, B. (2010). Regulation of oligodendrocyte differentiation and myelination. Science *330*, 779-782.

Engelkamp, D. (2002). Cloning of three mouse Unc5 genes and their expression patterns at mid-gestation. Mech Dev *118*, 191-197.

Ernfors, P., Lonnerberg, P., Ayer-LeLievre, C., and Persson, H. (1990). Developmental and regional expression of basic fibroblast growth factor mRNA in the rat central nervous system. J Neurosci Res *27*, 10-15.

Eshed, Y., Feinberg, K., Poliak, S., Sabanay, H., Sarig-Nadir, O., Spiegel, I., Bermingham, J.R., Jr., and Peles, E. (2005). Gliomedin mediates Schwann cell-axon interaction and the molecular assembly of the nodes of Ranvier. Neuron *47*, 215-229.

Esteller, M. (2011). Non-coding RNAs in human disease. Nat Rev Genet *12*, 861-874.

Faivre-Sarrailh, C., and Rougon, G. (1997). Axonal molecules of the immunoglobulin superfamily bearing a GPI anchor: their role in controlling neurite outgrowth. Mol Cell Neurosci *9*, 109-115.

Fannon, A.M., Sherman, D.L., Ilyina-Gragerova, G., Brophy, P.J., Friedrich, V.L., Jr., and Colman, D.R. (1995). Novel E-cadherin-mediated adhesion in peripheral nerve: Schwann cell architecture is stabilized by autotypic adherens junctions. J Cell Biol *129*, 189-202.

Fazeli, A., Dickinson, S.L., Hermiston, M.L., Tighe, R.V., Steen, R.G., Small, C.G., Stoeckli, E.T., Keino-Masu, K., Masu, M., Rayburn, H.*, et al.* (1997). Phenotype of mice lacking functional Deleted in colorectal cancer (Dcc) gene. Nature *386*, 796-804.

Fearon, E.R., Cho, K.R., Nigro, J.M., Kern, S.E., Simons, J.W., Ruppert, J.M., Hamilton, S.R., Preisinger, A.C., Thomas, G., Kinzler, K.W.*, et al.* (1990). Identification of a chromosome 18q gene that is altered in colorectal cancers. Science *247*, 49-56.

Feinberg, K., Eshed-Eisenbach, Y., Frechter, S., Amor, V., Salomon, D., Sabanay, H., Dupree, J.L., Grumet, M., Brophy, P.J., Shrager, P.*, et al.* (2010). A glial signal consisting of gliomedin

and NrCAM clusters axonal Na+ channels during the formation of nodes of Ranvier. Neuron *65*, 490-502.

Fernandez, P.A., Tang, D.G., Cheng, L., Prochiantz, A., Mudge, A.W., and Raff, M.C. (2000). Evidence that axon-derived neuregulin promotes oligodendrocyte survival in the developing rat optic nerve. Neuron *28*, 81-90.

Fire, A., Xu, S., Montgomery, M.K., Kostas, S.A., Driver, S.E., and Mello, C.C. (1998). Potent and specific genetic interference by double-stranded RNA in Caenorhabditis elegans. Nature *391*, 806-811.

Fitzner, D., Schneider, A., Kippert, A., Mobius, W., Willig, K.I., Hell, S.W., Bunt, G., Gaus, K., and Simons, M. (2006). Myelin basic protein-dependent plasma membrane reorganization in the formation of myelin. EMBO J *25*, 5037-5048.

Flores, A.I., Mallon, B.S., Matsui, T., Ogawa, W., Rosenzweig, A., Okamoto, T., and Macklin, W.B. (2000). Akt-mediated survival of oligodendrocytes induced by neuregulins. J Neurosci *20*, 7622-7630.

Fok-Seang, J., Mathews, G.A., ffrench-Constant, C., Trotter, J., and Fawcett, J.W. (1995). Migration of oligodendrocyte precursors on astrocytes and meningeal cells. Dev Biol *171*, 1-15.

Fok-Seang, J., and Miller, R.H. (1994). Distribution and differentiation of A2B5+ glial precursors in the developing rat spinal cord. J Neurosci Res *37*, 219-235.

Frank, M. (2000). MAL, a proteolipid in glycosphingolipid enriched domains: functional implications in myelin and beyond. Prog Neurobiol *60*, 531-544.

Frederick, T.J., Min, J., Altieri, S.C., Mitchell, N.E., and Wood, T.L. (2007). Synergistic induction of cyclin D1 in oligodendrocyte progenitor cells by IGF-I and FGF-2 requires differential stimulation of multiple signaling pathways. Glia *55*, 1011-1022.

Frederick, T.J., and Wood, T.L. (2004). IGF-I and FGF-2 coordinately enhance cyclin D1 and cyclin E-cdk2 association and activity to promote G1 progression in oligodendrocyte progenitor cells. Mol Cell Neurosci *25*, 480-492.

Frezzetti, D., Reale, C., Cali, G., Nitsch, L., Fagman, H., Nilsson, O., Scarfo, M., De Vita, G., and Di Lauro, R. The microRNA-processing enzyme Dicer is essential for thyroid function. PLoS One *6*, e27648.

Friedman, R.C., Farh, K.K., Burge, C.B., and Bartel, D.P. (2009). Most mammalian mRNAs are conserved targets of microRNAs. Genome Res *19*, 92-105.

Frost, E., Kiernan, B.W., Faissner, A., and ffrench-Constant, C. (1996). Regulation of oligodendrocyte precursor migration by extracellular matrix: evidence for substrate-specific inhibition of migration by tenascin-C. Dev Neurosci *18*, 266-273.

Frost, E.E., Buttery, P.C., Milner, R., and ffrench-Constant, C. (1999). Integrins mediate a neuronal survival signal for oligodendrocytes. Curr Biol *9*, 1251-1254.

Fruttiger, M., Calver, A.R., and Richardson, W.D. (2000). Platelet-derived growth factor is constitutively secreted from neuronal cell bodies but not from axons. Curr Biol *10*, 1283-1286.

Fruttiger, M., Karlsson, L., Hall, A.C., Abramsson, A., Calver, A.R., Bostrom, H., Willetts, K., Bertold, C.H., Heath, J.K., Betsholtz, C.*, et al.* (1999). Defective oligodendrocyte development and severe hypomyelination in PDGF-A knockout mice. Development *126*, 457-467.

Fu, H., Qi, Y., Tan, M., Cai, J., Takebayashi, H., Nakafuku, M., Richardson, W., and Qiu, M. (2002). Dual origin of spinal oligodendrocyte progenitors and evidence for the cooperative role of Olig2 and Nkx2.2 in the control of oligodendrocyte differentiation. Development *129*, 681-693.

Gao, F.B., Durand, B., and Raff, M. (1997). Oligodendrocyte precursor cells count time but not cell divisions before differentiation. Curr Biol *7*, 152-155.

Garcion, E., Faissner, A., and ffrench-Constant, C. (2001). Knockout mice reveal a contribution of the extracellular matrix molecule tenascin-C to neural precursor proliferation and migration. Development *128*, 2485-2496.

Gard, A.L., and Pfeiffer, S.E. (1993). Glial cell mitogens bFGF and PDGF differentially regulate development of O4+GalC- oligodendrocyte progenitors. Dev Biol *159*, 618-630.

Geisbrecht, B.V., Dowd, K.A., Barfield, R.W., Longo, P.A., and Leahy, D.J. (2003). Netrin binds discrete subdomains of DCC and UNC5 and mediates interactions between DCC and heparin. J Biol Chem *278*, 32561-32568.

Geren, B.B. (1954). The formation from the Schwann cell surface of myelin in the peripheral nerves of chick embryos. Exp Cell Res *7*.

Gibson, E.M., Purger, D., Mount, C.W., Goldstein, A.K., Lin, G.L., Wood, L.S., Inema, I., Miller, S.E., Bieri, G., Zuchero, J.B.*, et al.* (2014). Neuronal activity promotes oligodendrogenesis and adaptive myelination in the mammalian brain. Science *344*, 1252304.

Gobert, R.P., Joubert, L., Curchod, M.L., Salvat, C., Foucault, I., Jorand-Lebrun, C., Lamarine, M., Peixoto, H., Vignaud, C., Fremaux, C.*, et al.* (2009). Convergent functional genomics of oligodendrocyte differentiation identifies multiple autoinhibitory signaling circuits. Mol Cell Biol *29*, 1538-1553.

Goebbels, S., Oltrogge, J.H., Kemper, R., Heilmann, I., Bormuth, I., Wolfer, S., Wichert, S.P., Mobius, W., Liu, X., Lappe-Siefke, C.*, et al.* (2010). Elevated phosphatidylinositol 3,4,5-trisphosphate in glia triggers cell-autonomous membrane wrapping and myelination. J Neurosci *30*, 8953-8964.

Gohla, G., Krieglstein, K., and Spittau, B. (2008). Tieg3/Klf11 induces apoptosis in OLI-neu cells and enhances the TGF-beta signaling pathway by transcriptional repression of Smad7. J Cell Biochem *104*, 850-861.

Golan, N., Adamsky, K., Kartvelishvily, E., Brockschnieder, D., Mobius, W., Spiegel, I., Roth, A.D., Thomson, C.E., Rechavi, G., and Peles, E. (2008). Identification of Tmem10/Opalin as

an oligodendrocyte enriched gene using expression profiling combined with genetic cell ablation. Glia *56*, 1176-1186.

Goldman, J.S., Ashour, M.A., Magdesian, M.H., Tritsch, N.X., Harris, S.N., Christofi, N., Chemali, R., Stern, Y.E., Thompson-Steckel, G., Gris, P.*, et al.* (2013). Netrin-1 promotes excitatory synaptogenesis between cortical neurons by initiating synapse assembly. J Neurosci *33*, 17278-17289.

Goto, J., Tezuka, T., Nakazawa, T., Sagara, H., and Yamamoto, T. (2008). Loss of Fyn tyrosine kinase on the C57BL/6 genetic background causes hydrocephalus with defects in oligodendrocyte development. Mol Cell Neurosci *38*, 203-212.

Gow, A., Southwood, C.M., Li, J.S., Pariali, M., Riordan, G.P., Brodie, S.E., Danias, J., Bronstein, J.M., Kachar, B., and Lazzarini, R.A. (1999). CNS myelin and sertoli cell tight junction strands are absent in Osp/claudin-11 null mice. Cell *99*, 649-659.

Griffiths, I., Klugmann, M., Anderson, T., Yool, D., Thomson, C., Schwab, M.H., Schneider, A., Zimmermann, F., McCulloch, M., Nadon, N.*, et al.* (1998). Axonal swellings and degeneration in mice lacking the major proteolipid of myelin. Science *280*, 1610-1613.

Grzenkowski, M., Niehaus, A., and Trotter, J. (1999). Monoclonal antibody detects oligodendroglial cell surface protein exhibiting temporal regulation during development. Glia *28*, 128-137.

Guijarro, P., Simo, S., Pascual, M., Abasolo, I., Del Rio, J.A., and Soriano, E. (2006). Netrin1 exerts a chemorepulsive effect on migrating cerebellar interneurons in a Dcc-independent way. Mol Cell Neurosci *33*, 389-400.

Gupta, R.K., Bhatia, V., Poptani, H., and Gujral, R.B. (1995). Brain metabolite changes on in vivo proton magnetic resonance spectroscopy in children with congenital hypothyroidism. J Pediatr *126*, 389-392.

Hamilton, A.J., and Baulcombe, D.C. (1999). A species of small antisense RNA in posttranscriptional gene silencing in plants. Science *286*, 950-952.

Hammond, S.M., Bernstein, E., Beach, D., and Hannon, G.J. (2000). An RNA-directed nuclease mediates post-transcriptional gene silencing in Drosophila cells. Nature *404*, 293-296.

Harris, K.S., Zhang, Z., McManus, M.T., Harfe, B.D., and Sun, X. (2006). Dicer function is essential for lung epithelium morphogenesis. Proc Natl Acad Sci U S A *103*, 2208-2213.

Harris, R., Sabatelli, L.M., and Seeger, M.A. (1996). Guidance cues at the Drosophila CNS midline: identification and characterization of two Drosophila Netrin/UNC-6 homologs. Neuron *17*, 217-228.

Hayashita, Y., Osada, H., Tatematsu, Y., Yamada, H., Yanagisawa, K., Tomida, S., Yatabe, Y., Kawahara, K., Sekido, Y., and Takahashi, T. (2005). A polycistronic microRNA cluster, miR-17-92, is overexpressed in human lung cancers and enhances cell proliferation. Cancer Res *65*, 9628-9632.

He, L., Thomson, J.M., Hemann, M.T., Hernando-Monge, E., Mu, D., Goodson, S., Powers, S., Cordon-Cardo, C., Lowe, S.W., Hannon, G.J.*, et al.* (2005). A microRNA polycistron as a potential human oncogene. Nature *435*, 828-833.

Hedgecock, E.M., Culotti, J.G., and Hall, D.H. (1990). The unc-5, unc-6, and unc-40 genes guide circumferential migrations of pioneer axons and mesodermal cells on the epidermis in C. elegans. Neuron *4*, 61-85.

Hellemans, J., Mortier, G., De Paepe, A., Speleman, F., and Vandesompele, J. (2007). qBase relative quantification framework and software for management and automated analysis of real-time quantitative PCR data. Genome Biol *8*, R19.

Hinman, J.D., Peters, A., Cabral, H., Rosene, D.L., Hollander, W., Rasband, M.N., and Abraham, C.R. (2006). Age-related molecular reorganization at the node of Ranvier. J Comp Neurol *495*, 351-362.

Hofmann, K., and Tschopp, J. (1995). The death domain motif found in Fas (Apo-1) and TNF receptor is present in proteins involved in apoptosis and axonal guidance. FEBS Lett *371*, 321-323.

Hong, K., Hinck, L., Nishiyama, M., Poo, M.M., Tessier-Lavigne, M., and Stein, E. (1999). A ligand-gated association between cytoplasmic domains of UNC5 and DCC family receptors converts netrin-induced growth cone attraction to repulsion. Cell *97*, 927-941.

Horn, K.E., Glasgow, S.D., Gobert, D., Bull, S.J., Luk, T., Girgis, J., Tremblay, M.E., McEachern, D., Bouchard, J.F., Haber, M.*, et al.* (2013). DCC expression by neurons regulates synaptic plasticity in the adult brain. Cell Rep *3*, 173-185.

Howell, O.W., Palser, A., Polito, A., Melrose, S., Zonta, B., Scheiermann, C., Vora, A.J., Brophy, P.J., and Reynolds, R. (2006). Disruption of neurofascin localization reveals early changes preceding demyelination and remyelination in multiple sclerosis. Brain *129*, 3173-3185.

Huang, J.Y., Wang, Y.X., Gu, W.L., Fu, S.L., Li, Y., Huang, L.D., Zhao, Z., Hang, Q., Zhu, H.Q., and Lu, P.H. (2012). Expression and function of myelin-associated proteins and their common receptor NgR on oligodendrocyte progenitor cells. Brain Res *1437*, 1-15.

Huang, Z.P., Chen, J.F., Regan, J.N., Maguire, C.T., Tang, R.H., Dong, X.R., Majesky, M.W., and Wang, D.Z. Loss of microRNAs in neural crest leads to cardiovascular syndromes resembling human congenital heart defects. Arterioscler Thromb Vasc Biol *30*, 2575-2586.

Ishii, A., Furusho, M., and Bansal, R. (2013). Sustained activation of ERK1/2 MAPK in oligodendrocytes and schwann cells enhances myelin growth and stimulates oligodendrocyte progenitor expansion. J Neurosci *33*, 175-186.

Ishii, N., Wadsworth, W.G., Stern, B.D., Culotti, J.G., and Hedgecock, E.M. (1992). UNC-6, a laminin-related protein, guides cell and pioneer axon migrations in C. elegans. Neuron *9*, 873-881.

Jagannathan, N.R., Tandon, N., Raghunathan, P., and Kochupillai, N. (1998). Reversal of abnormalities of myelination by thyroxine therapy in congenital hypothyroidism: localized in vivo proton magnetic resonance spectroscopy (MRS) study. Brain Res Dev Brain Res *109*, 179-186.

Jarjour, A.A., Bull, S.J., Almasieh, M., Rajasekharan, S., Baker, K.A., Mui, J., Antel, J.P., Di Polo, A., and Kennedy, T.E. (2008). Maintenance of axo-oligodendroglial paranodal junctions requires DCC and netrin-1. J Neurosci *28*, 11003-11014.

Jarjour, A.A., Manitt, C., Moore, S.W., Thompson, K.M., Yuh, S.J., and Kennedy, T.E. (2003). Netrin-1 is a chemorepellent for oligodendrocyte precursor cells in the embryonic spinal cord. J Neurosci *23*, 3735-3744.

Jepson, S., Vought, B., Gross, C.H., Gan, L., Austen, D., Frantz, J.D., Zwahlen, J., Lowe, D., Markland, W., and Krauss, R. (2012). LINGO-1, a transmembrane signaling protein, inhibits oligodendrocyte differentiation and myelination through intercellular self-interactions. J Biol Chem *287*, 22184-22195.

Joe, E.H., and Angelides, K. (1992). Clustering of voltage-dependent sodium channels on axons depends on Schwann cell contact. Nature *356*, 333-335.

Joubert, L., Foucault, I., Sagot, Y., Bernasconi, L., Duval, F., Alliod, C., Frossard, M.J., Pescini Gobert, R., Curchod, M.L., Salvat, C.*, et al.* (2010). Chemical inducers and transcriptional markers of oligodendrocyte differentiation. J Neurosci Res *88*, 2546-2557.

Jung, M., Kramer, E., Grzenkowski, M., Tang, K., Blakemore, W., Aguzzi, A., Khazaie, K., Chlichlia, K., von Blankenfeld, G., Kettenmann, H.*, et al.* (1995). Lines of murine oligodendroglial precursor cells immortalized by an activated neu tyrosine kinase show distinct degrees of interaction with axons in vitro and in vivo. Eur J Neurosci *7*, 1245-1265.

Junker, A., Krumbholz, M., Eisele, S., Mohan, H., Augstein, F., Bittner, R., Lassmann, H., Wekerle, H., Hohlfeld, R., and Meinl, E. (2009). MicroRNA profiling of multiple sclerosis lesions identifies modulators of the regulatory protein CD47. Brain *132*, 3342-3352.

Kaplan, M.R., Meyer-Franke, A., Lambert, S., Bennett, V., Duncan, I.D., Levinson, S.R., and Barres, B.A. (1997). Induction of sodium channel clustering by oligodendrocytes. Nature *386*, 724-728.

Kappler, J., Franken, S., Junghans, U., Hoffmann, R., Linke, T., Muller, H.W., and Koch, K.W. (2000). Glycosaminoglycan-binding properties and secondary structure of the C-terminus of netrin-1. Biochem Biophys Res Commun *271*, 287-291.

Keino-Masu, K., Masu, M., Hinck, L., Leonardo, E.D., Chan, S.S., Culotti, J.G., and Tessier-Lavigne, M. (1996). Deleted in Colorectal Cancer (DCC) encodes a netrin receptor. Cell *87*, 175-185.

Keleman, K., and Dickson, B.J. (2001). Short- and long-range repulsion by the Drosophila Unc5 netrin receptor. Neuron *32*, 605-617.

Kennedy, T.E., Serafini, T., de la Torre, J.R., and Tessier-Lavigne, M. (1994). Netrins are diffusible chemotropic factors for commissural axons in the embryonic spinal cord. Cell *78*, 425-435.

Kennedy, T.E., Wang, H., Marshall, W., and Tessier-Lavigne, M. (2006). Axon guidance by diffusible chemoattractants: a gradient of netrin protein in the developing spinal cord. J Neurosci *26*, 8866-8874.

Kessaris, N., Fogarty, M., Iannarelli, P., Grist, M., Wegner, M., and Richardson, W.D. (2006). Competing waves of oligodendrocytes in the forebrain and postnatal elimination of an embryonic lineage. Nat Neurosci *9*, 173-179.

Kiernan, B.W., Gotz, B., Faissner, A., and ffrench-Constant, C. (1996). Tenascin-C inhibits oligodendrocyte precursor cell migration by both adhesion-dependent and adhesion-independent mechanisms. Mol Cell Neurosci *7*, 322-335.

Kim, S., Burette, A., Chung, H.S., Kwon, S.K., Woo, J., Lee, H.W., Kim, K., Kim, H., Weinberg, R.J., and Kim, E. (2006). NGL family PSD-95-interacting adhesion molecules regulate excitatory synapse formation. Nat Neurosci *9*, 1294-1301.

Kippert, A., Trajkovic, K., Fitzner, D., Opitz, L., and Simons, M. (2008). Identification of Tmem10/Opalin as a novel marker for oligodendrocytes using gene expression profiling. BMC Neurosci *9*, 40.

Klugmann, M., Schwab, M.H., Puhlhofer, A., Schneider, A., Zimmermann, F., Griffiths, I.R., and Nave, K.A. (1997). Assembly of CNS myelin in the absence of proteolipid protein. Neuron *18*, 59-70.

Knobler, R.L., Stempak, J.G., and Laurencin, M. (1976). Nonuniformity of the oligodendroglial ensheathment of axons during myelination in the developing rat central nervous system. A serial section electron microscopical study. J Ultrastruct Res *55*, 417-432.

Kobayashi, T., Lu, J., Cobb, B.S., Rodda, S.J., McMahon, A.P., Schipani, E., Merkenschlager, M., and Kronenberg, H.M. (2008). Dicer-dependent pathways regulate chondrocyte proliferation and differentiation. Proc Natl Acad Sci U S A *105*, 1949-1954.

Koch, M., Murrell, J.R., Hunter, D.D., Olson, P.F., Jin, W., Keene, D.R., Brunken, W.J., and Burgeson, R.E. (2000). A novel member of the netrin family, beta-netrin, shares homology with the beta chain of laminin: identification, expression, and functional characterization. J Cell Biol *151*, 221-234.

Koenning, M., Jackson, S., Hay, C.M., Faux, C., Kilpatrick, T.J., Willingham, M., and Emery, B. (2012). Myelin gene regulatory factor is required for maintenance of myelin and mature oligodendrocyte identity in the adult CNS. J Neurosci *32*, 12528-12542.

Kolodziej, P.A., Timpe, L.C., Mitchell, K.J., Fried, S.R., Goodman, C.S., Jan, L.Y., and Jan, Y.N. (1996). frazzled encodes a Drosophila member of the DCC immunoglobulin subfamily and is required for CNS and motor axon guidance. Cell *87*, 197-204.

Koralov, S.B., Muljo, S.A., Galler, G.R., Krek, A., Chakraborty, T., Kanellopoulou, C., Jensen, K., Cobb, B.S., Merkenschlager, M., Rajewsky, N.*, et al.* (2008). Dicer ablation affects antibody diversity and cell survival in the B lymphocyte lineage. Cell *132*, 860-874.

Kramer, E.M., Koch, T., Niehaus, A., and Trotter, J. (1997). Oligodendrocytes direct glycosyl phosphatidylinositol-anchored proteins to the myelin sheath in glycosphingolipid-rich complexes. J Biol Chem *272*, 8937-8945.

Lagos-Quintana, M., Rauhut, R., Lendeckel, W., and Tuschl, T. (2001). Identification of novel genes coding for small expressed RNAs. Science *294*, 853-858.

Lai, E.C. (2002). Micro RNAs are complementary to 3' UTR sequence motifs that mediate negative post-transcriptional regulation. Nat Genet *30*, 363-364.

Lau, N.C., Lim, L.P., Weinstein, E.G., and Bartel, D.P. (2001). An abundant class of tiny RNAs with probable regulatory roles in Caenorhabditis elegans. Science *294*, 858-862.

Lau, P., Verrier, J.D., Nielsen, J.A., Johnson, K.R., Notterpek, L., and Hudson, L.D. (2008). Identification of dynamically regulated microRNA and mRNA networks in developing oligodendrocytes. J Neurosci *28*, 11720-11730.

Laursen, L.S., Chan, C.W., and ffrench-Constant, C. (2009). An integrin-contactin complex regulates CNS myelination by differential Fyn phosphorylation. J Neurosci *29*, 9174-9185.

Lebrand, C., Dent, E.W., Strasser, G.A., Lanier, L.M., Krause, M., Svitkina, T.M., Borisy, G.G., and Gertler, F.B. (2004). Critical role of Ena/VASP proteins for filopodia formation in neurons and in function downstream of netrin-1. Neuron *42*, 37-49.

Lee, R.C., and Ambros, V. (2001). An extensive class of small RNAs in Caenorhabditis elegans. Science *294*, 862-864.

Lee, R.C., Feinbaum, R.L., and Ambros, V. (1993). The C. elegans heterochronic gene lin-4 encodes small RNAs with antisense complementarity to lin-14. Cell *75*, 843-854.

Lee, S., Leach, M.K., Redmond, S.A., Chong, S.Y., Mellon, S.H., Tuck, S.J., Feng, Z.Q., Corey, J.M., and Chan, J.R. (2012). A culture system to study oligodendrocyte myelination processes using engineered nanofibers. Nat Methods *9*, 917-922.

Lee, Y., Ahn, C., Han, J., Choi, H., Kim, J., Yim, J., Lee, J., Provost, P., Radmark, O., Kim, S.*, et al.* (2003). The nuclear RNase III Drosha initiates microRNA processing. Nature *425*, 415-419.

Lee, Y., Jeon, K., Lee, J.T., Kim, S., and Kim, V.N. (2002). MicroRNA maturation: stepwise processing and subcellular localization. EMBO J *21*, 4663-4670.

Leonardo, E.D., Hinck, L., Masu, M., Keino-Masu, K., Ackerman, S.L., and Tessier-Lavigne, M. (1997). Vertebrate homologues of C. elegans UNC-5 are candidate netrin receptors. Nature *386*, 833-838.

Letzen, B.S., Liu, C., Thakor, N.V., Gearhart, J.D., All, A.H., and Kerr, C.L. (2010). MicroRNA expression profiling of oligodendrocyte differentiation from human embryonic stem cells. PLoS One *5*, e10480.

Leung-Hagesteijn, C., Spence, A.M., Stern, B.D., Zhou, Y., Su, M.W., Hedgecock, E.M., and Culotti, J.G. (1992). UNC-5, a transmembrane protein with immunoglobulin and thrombospondin type 1 domains, guides cell and pioneer axon migrations in C. elegans. Cell *71*, 289-299.

Li, H., de Faria, J.P., Andrew, P., Nitarska, J., and Richardson, W.D. (2011). Phosphorylation regulates OLIG2 cofactor choice and the motor neuron-oligodendrocyte fate switch. Neuron *69*, 918-929.

Li, H., He, Y., Richardson, W.D., and Casaccia, P. (2009). Two-tier transcriptional control of oligodendrocyte differentiation. Curr Opin Neurobiol *19*, 479-485.

Li, W., Lee, J., Vikis, H.G., Lee, S.H., Liu, G., Aurandt, J., Shen, T.L., Fearon, E.R., Guan, J.L., Han, M.*, et al.* (2004). Activation of FAK and Src are receptor-proximal events required for netrin signaling. Nat Neurosci *7*, 1213-1221.

Li, X., Gao, X., Liu, G., Xiong, W., Wu, J., and Rao, Y. (2008). Netrin signal transduction and the guanine nucleotide exchange factor DOCK180 in attractive signaling. Nat Neurosci *11*, 28-35.

Li, X., Saint-Cyr-Proulx, E., Aktories, K., and Lamarche-Vane, N. (2002). Rac1 and Cdc42 but not RhoA or Rho kinase activities are required for neurite outgrowth induced by the Netrin-1 receptor DCC (deleted in colorectal cancer) in N1E-115 neuroblastoma cells. J Biol Chem *277*, 15207-15214.

Li, Y., and Piatigorsky, J. (2009). Targeted deletion of Dicer disrupts lens morphogenesis, corneal epithelium stratification, and whole eye development. Dev Dyn *238*, 2388-2400.

Liang, X., Draghi, N.A., and Resh, M.D. (2004). Signaling from integrins to Fyn to Rho family GTPases regulates morphologic differentiation of oligodendrocytes. J Neurosci *24*, 7140-7149.

Lim, L.P., Lau, N.C., Garrett-Engele, P., Grimson, A., Schelter, J.M., Castle, J., Bartel, D.P., Linsley, P.S., and Johnson, J.M. (2005). Microarray analysis shows that some microRNAs downregulate large numbers of target mRNAs. Nature *433*, 769-773.

Lim, Y.S., and Wadsworth, W.G. (2002). Identification of domains of netrin UNC-6 that mediate attractive and repulsive guidance and responses from cells and growth cones. J Neurosci *22*, 7080-7087.

Lin, J.C., Ho, W.H., Gurney, A., and Rosenthal, A. (2003). The netrin-G1 ligand NGL-1 promotes the outgrowth of thalamocortical axons. Nat Neurosci *6*, 1270-1276.

Lin, S.T., and Fu, Y.H. (2009). miR-23 regulation of lamin B1 is crucial for oligodendrocyte development and myelination. Dis Model Mech *2*, 178-188.

Liu, A., Li, J., Marin-Husstege, M., Kageyama, R., Fan, Y., Gelinas, C., and Casaccia-Bonnefil, P. (2006). A molecular insight of Hes5-dependent inhibition of myelin gene expression: old partners and new players. EMBO J *25*, 4833-4842.

Liu, G., Li, W., Wang, L., Kar, A., Guan, K.L., Rao, Y., and Wu, J.Y. (2009). DSCAM functions as a netrin receptor in commissural axon pathfinding. Proc Natl Acad Sci U S A *106*, 2951-2956.

Liu, Y., Stein, E., Oliver, T., Li, Y., Brunken, W.J., Koch, M., Tessier-Lavigne, M., and Hogan, B.L. (2004). Novel role for Netrins in regulating epithelial behavior during lung branching morphogenesis. Curr Biol *14*, 897-905.

Liu, Z., Hu, X., Cai, J., Liu, B., Peng, X., Wegner, M., and Qiu, M. (2007). Induction of oligodendrocyte differentiation by Olig2 and Sox10: evidence for reciprocal interactions and dosage-dependent mechanisms. Dev Biol *302*, 683-693.

Livesey, F.J., and Hunt, S.P. (1997). Netrin and netrin receptor expression in the embryonic mammalian nervous system suggests roles in retinal, striatal, nigral, and cerebellar development. Mol Cell Neurosci *8*, 417-429.

Llambi, F., Causeret, F., Bloch-Gallego, E., and Mehlen, P. (2001). Netrin-1 acts as a survival factor via its receptors UNC5H and DCC. EMBO J *20*, 2715-2722.

Llambi, F., Lourenco, F.C., Gozuacik, D., Guix, C., Pays, L., Del Rio, G., Kimchi, A., and Mehlen, P. (2005). The dependence receptor UNC5H2 mediates apoptosis through DAP-kinase. EMBO J *24*, 1192-1201.

Lu, Q.R., Sun, T., Zhu, Z., Ma, N., Garcia, M., Stiles, C.D., and Rowitch, D.H. (2002). Common developmental requirement for Olig function indicates a motor neuron/oligodendrocyte connection. Cell *109*, 75-86.

Lu, Q.R., Yuk, D., Alberta, J.A., Zhu, Z., Pawlitzky, I., Chan, J., McMahon, A.P., Stiles, C.D., and Rowitch, D.H. (2000). Sonic hedgehog--regulated oligodendrocyte lineage genes encoding bHLH proteins in the mammalian central nervous system. Neuron *25*, 317-329.

Lu, X., Le Noble, F., Yuan, L., Jiang, Q., De Lafarge, B., Sugiyama, D., Breant, C., Claes, F., De Smet, F., Thomas, J.L.*, et al.* (2004). The netrin receptor UNC5B mediates guidance events controlling morphogenesis of the vascular system. Nature *432*, 179-186.

Luebke, J., Barbas, H., and Peters, A. (2010). Effects of normal aging on prefrontal area 46 in the rhesus monkey. Brain Res Rev *62*, 212-232.

Lund, E., Guttinger, S., Calado, A., Dahlberg, J.E., and Kutay, U. (2004). Nuclear export of microRNA precursors. Science *303*, 95-98.

Ly, A., Nikolaev, A., Suresh, G., Zheng, Y., Tessier-Lavigne, M., and Stein, E. (2008). DSCAM is a netrin receptor that collaborates with DCC in mediating turning responses to netrin-1. Cell *133*, 1241-1254.

Lynn, F.C., Skewes-Cox, P., Kosaka, Y., McManus, M.T., Harfe, B.D., and German, M.S. (2007). MicroRNA expression is required for pancreatic islet cell genesis in the mouse. Diabetes *56*, 2938-2945.

Macabenta, F.D., Jensen, A.G., Cheng, Y.S., Kramer, J.J., and Kramer, S.G. (2013). Frazzled/DCC facilitates cardiac cell outgrowth and attachment during Drosophila dorsal vessel formation. Dev Biol *380*, 233-242.

Makinodan, M., Rosen, K.M., Ito, S., and Corfas, G. (2012). A critical period for social experience-dependent oligodendrocyte maturation and myelination. Science *337*, 1357-1360.

Manitt, C., Colicos, M.A., Thompson, K.M., Rousselle, E., Peterson, A.C., and Kennedy, T.E. (2001). Widespread expression of netrin-1 by neurons and oligodendrocytes in the adult mammalian spinal cord. J Neurosci *21*, 3911-3922.

Manitt, C., Nikolakopoulou, A.M., Almario, D.R., Nguyen, S.A., and Cohen-Cory, S. (2009). Netrin participates in the development of retinotectal synaptic connectivity by modulating axon arborization and synapse formation in the developing brain. J Neurosci *29*, 11065-11077.

Manitt, C., Thompson, K.M., and Kennedy, T.E. (2004). Developmental shift in expression of netrin receptors in the rat spinal cord: predominance of UNC-5 homologues in adulthood. J Neurosci Res *77*, 690-700.

Marcus, J., Honigbaum, S., Shroff, S., Honke, K., Rosenbluth, J., and Dupree, J.L. (2006). Sulfatide is essential for the maintenance of CNS myelin and axon structure. Glia *53*, 372-381.

Marta, C.B., Adamo, A.M., Soto, E.F., and Pasquini, J.M. (1998). Sustained neonatal hyperthyroidism in the rat affects myelination in the central nervous system. J Neurosci Res *53*, 251-259.

Mathey, E.K., Derfuss, T., Storch, M.K., Williams, K.R., Hales, K., Woolley, D.R., Al-Hayani, A., Davies, S.N., Rasband, M.N., Olsson, T.*, et al.* (2007). Neurofascin as a novel target for autoantibody-mediated axonal injury. J Exp Med *204*, 2363-2372.

Matsubara, H., Takeuchi, T., Nishikawa, E., Yanagisawa, K., Hayashita, Y., Ebi, H., Yamada, H., Suzuki, M., Nagino, M., Nimura, Y.*, et al.* (2007). Apoptosis induction by antisense oligonucleotides against miR-17-5p and miR-20a in lung cancers overexpressing miR-17-92. Oncogene *26*, 6099-6105.

McIntire, S.L., Garriga, G., White, J., Jacobson, D., and Horvitz, H.R. (1992). Genes necessary for directed axonal elongation or fasciculation in C. elegans. Neuron *8*, 307-322.

McKenzie, I.A., Ohayon, D., Li, H., de Faria, J.P., Emery, B., Tohyama, K., and Richardson, W.D. (2014). Motor skill learning requires active central myelination. Science *346*, 318-322.

McKinnon, R.D., Matsui, T., Dubois-Dalcq, M., and Aaronson, S.A. (1990). FGF modulates the PDGF-driven pathway of oligodendrocyte development. Neuron *5*, 603-614.

McLaurin, J., Trudel, G.C., Shaw, I.T., Antel, J.P., and Cashman, N.R. (1995). A human glial hybrid cell line differentially expressing genes subserving oligodendrocyte and astrocyte phenotype. J Neurobiol *26*, 283-293.

Mehlen, P., Rabizadeh, S., Snipas, S.J., Assa-Munt, N., Salvesen, G.S., and Bredesen, D.E. (1998). The DCC gene product induces apoptosis by a mechanism requiring receptor proteolysis. Nature *395*, 801-804.

Menon, K., Rasband, M.N., Taylor, C.M., Brophy, P., Bansal, R., and Pfeiffer, S.E. (2003). The myelin-axolemmal complex: biochemical dissection and the role of galactosphingolipids. J Neurochem *87*, 995-1009.

Merz, D.C., Zheng, H., Killeen, M.T., Krizus, A., and Culotti, J.G. (2001). Multiple signaling mechanisms of the UNC-6/netrin receptors UNC-5 and UNC-40/DCC in vivo. Genetics *158*, 1071-1080.

Mi, S., Lee, X., Shao, Z., Thill, G., Ji, B., Relton, J., Levesque, M., Allaire, N., Perrin, S., Sands, B., *et al.* (2004). LINGO-1 is a component of the Nogo-66 receptor/p75 signaling complex. Nat Neurosci *7*, 221-228.

Mi, S., Miller, R.H., Lee, X., Scott, M.L., Shulag-Morskaya, S., Shao, Z., Chang, J., Thill, G., Levesque, M., Zhang, M., *et al.* (2005). LINGO-1 negatively regulates myelination by oligodendrocytes. Nat Neurosci *8*, 745-751.

Miller, R.H., Payne, J., Milner, L., Zhang, H., and Orentas, D.M. (1997). Spinal cord oligodendrocytes develop from a limited number of migratory highly proliferative precursors. J Neurosci Res *50*, 157-168.

Milner, R., Edwards, G., Streuli, C., and Ffrench-Constant, C. (1996). A role in migration for the alpha V beta 1 integrin expressed on oligodendrocyte precursors. J Neurosci *16*, 7240-7252.

Ming, G., Song, H., Berninger, B., Inagaki, N., Tessier-Lavigne, M., and Poo, M. (1999). Phospholipase C-gamma and phosphoinositide 3-kinase mediate cytoplasmic signaling in nerve growth cone guidance. Neuron *23*, 139-148.

Ming, G.L., Song, H.J., Berninger, B., Holt, C.E., Tessier-Lavigne, M., and Poo, M.M. (1997). cAMP-dependent growth cone guidance by netrin-1. Neuron *19*, 1225-1235.

Mitchell, K.J., Doyle, J.L., Serafini, T., Kennedy, T.E., Tessier-Lavigne, M., Goodman, C.S., and Dickson, B.J. (1996). Genetic analysis of Netrin genes in Drosophila: Netrins guide CNS commissural axons and peripheral motor axons. Neuron *17*, 203-215.

Mitew, S., Hay, C.M., Peckham, H., Xiao, J., Koenning, M., and Emery, B. (2014). Mechanisms regulating the development of oligodendrocytes and central nervous system myelin. Neuroscience *276*, 29-47.

Miyamoto, T., Morita, K., Takemoto, D., Takeuchi, K., Kitano, Y., Miyakawa, T., Nakayama, K., Okamura, Y., Sasaki, H., Miyachi, Y.*, et al.* (2005). Tight junctions in Schwann cells of peripheral myelinated axons: a lesson from claudin-19-deficient mice. J Cell Biol *169*, 527-538.

Mizuguchi, R., Sugimori, M., Takebayashi, H., Kosako, H., Nagao, M., Yoshida, S., Nabeshima, Y., Shimamura, K., and Nakafuku, M. (2001). Combinatorial roles of olig2 and neurogenin2 in the coordinated induction of pan-neuronal and subtype-specific properties of motoneurons. Neuron *31*, 757-771.

Moore, S.W., Correia, J.P., Lai Wing Sun, K., Pool, M., Fournier, A.E., and Kennedy, T.E. (2008). Rho inhibition recruits DCC to the neuronal plasma membrane and enhances axon chemoattraction to netrin 1. Development *135*, 2855-2864.

Morales, F.R., Boxer, P.A., Fung, S.J., and Chase, M.H. (1987). Basic electrophysiological properties of spinal cord motoneurons during old age in the cat. J Neurophysiol *58*, 180-194.

Mudhasani, R., Puri, V., Hoover, K., Czech, M.P., Imbalzano, A.N., and Jones, S.N. Dicer is required for the formation of white but not brown adipose tissue. J Cell Physiol *226*, 1399-1406.

Muljo, S.A., Ansel, K.M., Kanellopoulou, C., Livingston, D.M., Rao, A., and Rajewsky, K. (2005). Aberrant T cell differentiation in the absence of Dicer. J Exp Med *202*, 261-269.

Murtie, J.C., Zhou, Y.X., Le, T.Q., and Armstrong, R.C. (2005). In vivo analysis of oligodendrocyte lineage development in postnatal FGF2 null mice. Glia *49*, 542-554.

Nagalakshmi, V.K., Ren, Q., Pugh, M.M., Valerius, M.T., McMahon, A.P., and Yu, J. Dicer regulates the development of nephrogenic and ureteric compartments in the mammalian kidney. Kidney Int *79*, 317-330.

Nakashiba, T., Ikeda, T., Nishimura, S., Tashiro, K., Honjo, T., Culotti, J.G., and Itohara, S. (2000). Netrin-G1: a novel glycosyl phosphatidylinositol-linked mammalian netrin that is functionally divergent from classical netrins. J Neurosci *20*, 6540-6550.

Nakashiba, T., Nishimura, S., Ikeda, T., and Itohara, S. (2002). Complementary expression and neurite outgrowth activity of netrin-G subfamily members. Mech Dev *111*, 47-60.

Nave, K.A. (2010). Oligodendrocytes and the "micro brake" of progenitor cell proliferation. Neuron *65*, 577-579.

Nobile, C., Hinzmann, B., Scannapieco, P., Siebert, R., Zimbello, R., Perez-Tur, J., Sarafidou, T., Moschonas, N.K., French, L., Deloukas, P.*, et al.* (2002). Identification and characterization of a novel human brain-specific gene, homologous to S. scrofa tmp83.5, in the chromosome 10q24 critical region for temporal lobe epilepsy and spastic paraplegia. Gene *282*, 87-94.

Noble, M., Murray, K., Stroobant, P., Waterfield, M.D., and Riddle, P. (1988). Platelet-derived growth factor promotes division and motility and inhibits premature differentiation of the oligodendrocyte/type-2 astrocyte progenitor cell. Nature *333*, 560-562.

Novitch, B.G., Chen, A.I., and Jessell, T.M. (2001). Coordinate regulation of motor neuron subtype identity and pan-neuronal properties by the bHLH repressor Olig2. Neuron *31*, 773-789.

O'Meara, R.W., Michalski, J.P., Anderson, C., Bhanot, K., Rippstein, P., and Kothary, R. (2013). Integrin-linked kinase regulates process extension in oligodendrocytes via control of actin cytoskeletal dynamics. J Neurosci *33*, 9781-9793.

Ono, K., Bansal, R., Payne, J., Rutishauser, U., and Miller, R.H. (1995). Early development and dispersal of oligodendrocyte precursors in the embryonic chick spinal cord. Development *121*, 1743-1754.

Ono, K., Yasui, Y., Rutishauser, U., and Miller, R.H. (1997). Focal ventricular origin and migration of oligodendrocyte precursors into the chick optic nerve. Neuron *19*, 283-292.

Orentas, D.M., Hayes, J.E., Dyer, K.L., and Miller, R.H. (1999). Sonic hedgehog signaling is required during the appearance of spinal cord oligodendrocyte precursors. Development *126*, 2419-2429.

Ota, A., Tagawa, H., Karnan, S., Tsuzuki, S., Karpas, A., Kira, S., Yoshida, Y., and Seto, M. (2004). Identification and characterization of a novel gene, C13orf25, as a target for 13q31-q32 amplification in malignant lymphoma. Cancer Res *64*, 3087-3095.

Pan, Y., Balazs, L., Tigyi, G., and Yue, J. Conditional deletion of Dicer in vascular smooth muscle cells leads to the developmental delay and embryonic mortality. Biochem Biophys Res Commun *408*, 369-374.

Pang, Y., Zheng, B., Fan, L.W., Rhodes, P.G., and Cai, Z. (2007). IGF-1 protects oligodendrocyte progenitors against TNFalpha-induced damage by activation of PI3K/Akt and interruption of the mitochondrial apoptotic pathway. Glia *55*, 1099-1107.

Park, J., Knezevich, P.L., Wung, W., O'Hanlon, S.N., Goyal, A., Benedetti, K.L., Barsi-Rhyne, B.J., Raman, M., Mock, N., Bremer, M.*, et al.* (2011). A conserved juxtacrine signal regulates synaptic partner recognition in Caenorhabditis elegans. Neural Dev *6*, 28.

Parras, C.M., Hunt, C., Sugimori, M., Nakafuku, M., Rowitch, D., and Guillemot, F. (2007). The proneural gene Mash1 specifies an early population of telencephalic oligodendrocytes. J Neurosci *27*, 4233-4242.

Pedraza, L., Huang, J.K., and Colman, D. (2009). Disposition of axonal caspr with respect to glial cell membranes: Implications for the process of myelination. J Neurosci Res *87*, 3480-3491.

Pedraza, L., Huang, J.K., and Colman, D.R. (2001). Organizing principles of the axoglial apparatus. Neuron *30*, 335-344.

Peles, E., and Salzer, J.L. (2000). Molecular domains of myelinated axons. Curr Opin Neurobiol *10*, 558-565.

Penfield, W. (1924). Oligodendroglia and its relation to classical neuroglia. Brain *47*, 430-452.

Peters, A., Moss, M.B., and Sethares, C. (2000). Effects of aging on myelinated nerve fibers in monkey primary visual cortex. J Comp Neurol *419*, 364-376.

Peters, A., Sethares, C., and Killiany, R.J. (2001). Effects of age on the thickness of myelin sheaths in monkey primary visual cortex. J Comp Neurol *435*, 241-248.

Pillai, A.M., Thaxton, C., Pribisko, A.L., Cheng, J.G., Dupree, J.L., and Bhat, M.A. (2009). Spatiotemporal ablation of myelinating glia-specific neurofascin (Nfasc NF155) in mice reveals gradual loss of paranodal axoglial junctions and concomitant disorganization of axonal domains. J Neurosci Res *87*, 1773-1793.

Podjaski, C., Alvarez, J.I., Bourbonniere, L., Larouche, S., Terouz, S., Bin, J.M., Lecuyer, M.A., Saint-Laurent, O., Larochelle, C., Darlington, P.J.*, et al.* (2015). Netrin 1 regulates blood-brain barrier function and neuroinflammation. Brain *138*, 1598-1612.

Poliak, S., Matlis, S., Ullmer, C., Scherer, S.S., and Peles, E. (2002). Distinct claudins and associated PDZ proteins form different autotypic tight junctions in myelinating Schwann cells. J Cell Biol *159*, 361-372.

Poliak, S., Salomon, D., Elhanany, H., Sabanay, H., Kiernan, B., Pevny, L., Stewart, C.L., Xu, X., Chiu, S.Y., Shrager, P.*, et al.* (2003). Juxtaparanodal clustering of Shaker-like K+ channels in myelinated axons depends on Caspr2 and TAG-1. J Cell Biol *162*, 1149-1160.

Prineas, J.W., Kwon, E.E., Goldenberg, P.Z., Ilyas, A.A., Quarles, R.H., Benjamins, J.A., and Sprinkle, T.J. (1989). Multiple sclerosis. Oligodendrocyte proliferation and differentiation in fresh lesions. Lab Invest *61*, 489-503.

Pringle, N.P., and Richardson, W.D. (1993). A singularity of PDGF alpha-receptor expression in the dorsoventral axis of the neural tube may define the origin of the oligodendrocyte lineage. Development *117*, 525-533.

Raff, M.C., Williams, B.P., and Miller, R.H. (1984). The in vitro differentiation of a bipotential glial progenitor cell. EMBO J *3*, 1857-1864.

Raible, D.W., and McMorris, F.A. (1989). Cyclic AMP regulates the rate of differentiation of oligodendrocytes without changing the lineage commitment of their progenitors. Dev Biol *133*, 437-446.

Raine, C.S., and Wu, E. (1993). Multiple sclerosis: remyelination in acute lesions. J Neuropathol Exp Neurol *52*, 199-204.

Rajasekharan, S., Baker, K.A., Horn, K.E., Jarjour, A.A., Antel, J.P., and Kennedy, T.E. (2009). Netrin 1 and Dcc regulate oligodendrocyte process branching and membrane extension via Fyn and RhoA. Development *136*, 415-426.

Rajasekharan, S., Bin, J.M., Antel, J.P., and Kennedy, T.E. (2010). A central role for RhoA during oligodendroglial maturation in the switch from netrin-1-mediated chemorepulsion to process elaboration. J Neurochem *113*, 1589-1597.

Rajewsky, N. (2006). microRNA target predictions in animals. Nat Genet *38 Suppl*, S8-13.

Ranscht, B. (1988). Sequence of contactin, a 130-kD glycoprotein concentrated in areas of interneuronal contact, defines a new member of the immunoglobulin supergene family in the nervous system. J Cell Biol *107*, 1561-1573.

Rasband, M.N., Tayler, J., Kaga, Y., Yang, Y., Lappe-Siefke, C., Nave, K.A., and Bansal, R. (2005). CNP is required for maintenance of axon-glia interactions at nodes of Ranvier in the CNS. Glia *50*, 86-90.

Readhead, C., Popko, B., Takahashi, N., Shine, H.D., Saavedra, R.A., Sidman, R.L., and Hood, L. (1987). Expression of a myelin basic protein gene in transgenic shiverer mice: correction of the dysmyelinating phenotype. Cell *48*, 703-712.

Reinhart, B.J., Slack, F.J., Basson, M., Pasquinelli, A.E., Bettinger, J.C., Rougvie, A.E., Horvitz, H.R., and Ruvkun, G. (2000). The 21-nucleotide let-7 RNA regulates developmental timing in Caenorhabditis elegans. Nature *403*, 901-906.

Ren, X.R., Ming, G.L., Xie, Y., Hong, Y., Sun, D.M., Zhao, Z.Q., Feng, Z., Wang, Q., Shim, S., Chen, Z.F.*, et al.* (2004). Focal adhesion kinase in netrin-1 signaling. Nat Neurosci *7*, 1204-1212.

Río-Hortega, P.d. (1922). Son homologables la glia de escasas radiaciones y la celula de

Schwann? Boletin de la Real Sociedad Espafiola de Historia Natural Seccion biologica *10*.

Rios, J.C., Melendez-Vasquez, C.V., Einheber, S., Lustig, M., Grumet, M., Hemperly, J., Peles, E., and Salzer, J.L. (2000). Contactin-associated protein (Caspr) and contactin form a complex that is targeted to the paranodal junctions during myelination. J Neurosci *20*, 8354-8364.

Roach, A., Takahashi, N., Pravtcheva, D., Ruddle, F., and Hood, L. (1985). Chromosomal mapping of mouse myelin basic protein gene and structure and transcription of the partially deleted gene in shiverer mutant mice. Cell *42*, 149-155.

Robinson, S., Tani, M., Strieter, R.M., Ransohoff, R.M., and Miller, R.H. (1998). The chemokine growth-regulated oncogene-alpha promotes spinal cord oligodendrocyte precursor proliferation. J Neurosci *18*, 10457-10463.

Rodriguez, A., Vigorito, E., Clare, S., Warren, M.V., Couttet, P., Soond, D.R., van Dongen, S., Grocock, R.J., Das, P.P., Miska, E.A.*, et al.* (2007). Requirement of bic/microRNA-155 for normal immune function. Science *316*, 608-611.

Rodriguez-Pena, A., Ibarrola, N., Iniguez, M.A., Munoz, A., and Bernal, J. (1993). Neonatal hypothyroidism affects the timely expression of myelin-associated glycoprotein in the rat brain. J Clin Invest *91*, 812-818.

Rosenberg, S.S., Kelland, E.E., Tokar, E., De la Torre, A.R., and Chan, J.R. (2008). The geometric and spatial constraints of the microenvironment induce oligodendrocyte differentiation. Proc Natl Acad Sci U S A *105*, 14662-14667.

Rosenbluth, J., Liang, W.L., Liu, Z., Guo, D., and Schiff, R. (1995). Paranodal structural abnormalities in rat CNS myelin developing in vivo in the presence of implanted O1 hybridoma cells. J Neurocytol *24*, 818-824.

Ruffini, F., Arbour, N., Blain, M., Olivier, A., and Antel, J.P. (2004). Distinctive properties of human adult brain-derived myelin progenitor cells. Am J Pathol *165*, 2167-2175.

Rutishauser, U., and Landmesser, L. (1996). Polysialic acid in the vertebrate nervous system: a promoter of plasticity in cell-cell interactions. Trends Neurosci *19*, 422-427.

Sato-Bigbee, C., and DeVries, G.H. (1996). Treatment of oligodendrocytes with antisense deoxyoligonucleotide directed against CREB mRNA: effect on the cyclic AMP-dependent induction of myelin basic protein expression. J Neurosci Res *46*, 98-107.

Schaeren-Wiemers, N., Bonnet, A., Erb, M., Erne, B., Bartsch, U., Kern, F., Mantei, N., Sherman, D., and Suter, U. (2004). The raft-associated protein MAL is required for maintenance of proper axon--glia interactions in the central nervous system. J Cell Biol *166*, 731-742.

Schaeren-Wiemers, N., Schaefer, C., Valenzuela, D.M., Yancopoulos, G.D., and Schwab, M.E. (1995). Identification of new oligodendrocyte- and myelin-specific genes by a differential screening approach. J Neurochem *65*, 10-22.

Schafer, D.P., Bansal, R., Hedstrom, K.L., Pfeiffer, S.E., and Rasband, M.N. (2004). Does paranode formation and maintenance require partitioning of neurofascin 155 into lipid rafts? J Neurosci *24*, 3176-3185.

Schafer, D.P., Custer, A.W., Shrager, P., and Rasband, M.N. (2006). Early events in node of Ranvier formation during myelination and remyelination in the PNS. Neuron Glia Biol *2*, 69-79.

Schmittgen, T.D., Lee, E.J., Jiang, J., Sarkar, A., Yang, L., Elton, T.S., and Chen, C. (2008). Real-time PCR quantification of precursor and mature microRNA. Methods *44*, 31-38.

Schmittgen, T.D., Zakrajsek, B.A., Mills, A.G., Gorn, V., Singer, M.J., and Reed, M.W. (2000). Quantitative reverse transcription-polymerase chain reaction to study mRNA decay: comparison of endpoint and real-time methods. Anal Biochem *285*, 194-204.

Schneider, C.A., Rasband, W.S., and Eliceiri, K.W. (2012). NIH Image to ImageJ: 25 years of image analysis. Nat Methods *9*, 671-675.

Schuller, U., Heine, V.M., Mao, J., Kho, A.T., Dillon, A.K., Han, Y.G., Huillard, E., Sun, T., Ligon, A.H., Qian, Y.*, et al.* (2008). Acquisition of granule neuron precursor identity is a critical determinant of progenitor cell competence to form Shh-induced medulloblastoma. Cancer Cell *14*, 123-134.

Schultz, J., Milpetz, F., Bork, P., and Ponting, C.P. (1998). SMART, a simple modular architecture research tool: identification of signaling domains. Proc Natl Acad Sci U S A *95*, 5857-5864.

Schuster, N., Bender, H., Philippi, A., Subramaniam, S., Strelau, J., Wang, Z., and Krieglstein, K. (2002). TGF-beta induces cell death in the oligodendroglial cell line OLI-neu. Glia *40*, 95-108.

Sekine, S., Ogawa, R., McManus, M.T., Kanai, Y., and Hebrok, M. (2009). Dicer is required for proper liver zonation. J Pathol *219*, 365-372.

Selbach, M., Schwanhausser, B., Thierfelder, N., Fang, Z., Khanin, R., and Rajewsky, N. (2008). Widespread changes in protein synthesis induced by microRNAs. Nature *455*, 58-63.

Sempere, L.F., Freemantle, S., Pitha-Rowe, I., Moss, E., Dmitrovsky, E., and Ambros, V. (2004). Expression profiling of mammalian microRNAs uncovers a subset of brain-expressed microRNAs with possible roles in murine and human neuronal differentiation. Genome Biol *5*, R13.

Serafini, T., Colamarino, S.A., Leonardo, E.D., Wang, H., Beddington, R., Skarnes, W.C., and Tessier-Lavigne, M. (1996). Netrin-1 is required for commissural axon guidance in the developing vertebrate nervous system. Cell *87*, 1001-1014.

Serafini, T., Kennedy, T.E., Galko, M.J., Mirzayan, C., Jessell, T.M., and Tessier-Lavigne, M. (1994). The netrins define a family of axon outgrowth-promoting proteins homologous to C. elegans UNC-6. Cell *78*, 409-424.

Shatzmiller, R.A., Goldman, J.S., Simard-Emond, L., Rymar, V., Manitt, C., Sadikot, A.F., and Kennedy, T.E. (2008). Graded expression of netrin-1 by specific neuronal subtypes in the adult mammalian striatum. Neuroscience *157*, 621-636.

Shekarabi, M., and Kennedy, T.E. (2002). The netrin-1 receptor DCC promotes filopodia formation and cell spreading by activating Cdc42 and Rac1. Mol Cell Neurosci *19*, 1-17.

Shekarabi, M., Moore, S.W., Tritsch, N.X., Morris, S.J., Bouchard, J.F., and Kennedy, T.E. (2005). Deleted in colorectal cancer binding netrin-1 mediates cell substrate adhesion and recruits Cdc42, Rac1, Pak1, and N-WASP into an intracellular signaling complex that promotes growth cone expansion. J Neurosci *25*, 3132-3141.

Shen, S., Li, J., and Casaccia-Bonnefil, P. (2005a). Histone modifications affect timing of oligodendrocyte progenitor differentiation in the developing rat brain. J Cell Biol *169*, 577-589.

Shen, S., Sandoval, J., Swiss, V.A., Li, J., Dupree, J., Franklin, R.J., and Casaccia-Bonnefil, P. (2008). Age-dependent epigenetic control of differentiation inhibitors is critical for remyelination efficiency. Nat Neurosci *11*, 1024-1034.

Shen, X., Valencia, C.A., Szostak, J.W., Dong, B., and Liu, R. (2005b). Scanning the human proteome for calmodulin-binding proteins. Proc Natl Acad Sci U S A *102*, 5969-5974.

Shepherd, M.N., Pomicter, A.D., Velazco, C.S., Henderson, S.C., and Dupree, J.L. (2012). Paranodal reorganization results in the depletion of transverse bands in the aged central nervous system. Neurobiol Aging *33*, 203 e213-224.

Sherman, D.L., and Brophy, P.J. (2005). Mechanisms of axon ensheathment and myelin growth. Nat Rev Neurosci *6*, 683-690.

Sherman, D.L., Tait, S., Melrose, S., Johnson, R., Zonta, B., Court, F.A., Macklin, W.B., Meek, S., Smith, A.J., Cottrell, D.F.*, et al.* (2005). Neurofascins are required to establish axonal domains for saltatory conduction. Neuron *48*, 737-742.

Shimizu, T., Kagawa, T., Wada, T., Muroyama, Y., Takada, S., and Ikenaka, K. (2005). Wnt signaling controls the timing of oligodendrocyte development in the spinal cord. Dev Biol *282*, 397-410.

Shin, D., Shin, J.Y., McManus, M.T., Ptacek, L.J., and Fu, Y.H. (2009). Dicer ablation in oligodendrocytes provokes neuronal impairment in mice. Ann Neurol *66*, 843-857.

Shin, S.K., Nagasaka, T., Jung, B.H., Matsubara, N., Kim, W.H., Carethers, J.M., Boland, C.R., and Goel, A. (2007). Epigenetic and genetic alterations in Netrin-1 receptors UNC5C and DCC in human colon cancer. Gastroenterology *133*, 1849-1857.

Simpson, P.B., and Armstrong, R.C. (1999). Intracellular signals and cytoskeletal elements involved in oligodendrocyte progenitor migration. Glia *26*, 22-35.

Small, R.K., Riddle, P., and Noble, M. (1987). Evidence for migration of oligodendrocyte--type-2 astrocyte progenitor cells into the developing rat optic nerve. Nature *328*, 155-157.

Snaidero, N., Mobius, W., Czopka, T., Hekking, L.H., Mathisen, C., Verkleij, D., Goebbels, S., Edgar, J., Merkler, D., Lyons, D.A.*, et al.* (2014). Myelin membrane wrapping of CNS axons by PI(3,4,5)P3-dependent polarized growth at the inner tongue. Cell *156*, 277-290.

Sobottka, B., Ziegler, U., Kaech, A., Becher, B., and Goebels, N. (2011). CNS live imaging reveals a new mechanism of myelination: the liquid croissant model. Glia *59*, 1841-1849.

Soula, C., Danesin, C., Kan, P., Grob, M., Poncet, C., and Cochard, P. (2001). Distinct sites of origin of oligodendrocytes and somatic motoneurons in the chick spinal cord:

oligodendrocytes arise from Nkx2.2-expressing progenitors by a Shh-dependent mechanism. Development *128*, 1369-1379.

Spassky, N., de Castro, F., Le Bras, B., Heydon, K., Queraud-LeSaux, F., Bloch-Gallego, E., Chedotal, A., Zalc, B., and Thomas, J.L. (2002). Directional guidance of oligodendroglial migration by class 3 semaphorins and netrin-1. J Neurosci *22*, 5992-6004.

Srinivasan, K., Strickland, P., Valdes, A., Shin, G.C., and Hinck, L. (2003). Netrin-1/neogenin interaction stabilizes multipotent progenitor cap cells during mammary gland morphogenesis. Dev Cell *4*, 371-382.

Stein, E., Zou, Y., Poo, M., and Tessier-Lavigne, M. (2001). Binding of DCC by netrin-1 to mediate axon guidance independent of adenosine A2B receptor activation. Science *291*, 1976-1982.

Stevens, B., Porta, S., Haak, L.L., Gallo, V., and Fields, R.D. (2002). Adenosine: a neuron-glial transmitter promoting myelination in the CNS in response to action potentials. Neuron *36*, 855-868.

Stevenson, B.R., and Keon, B.H. (1998). The tight junction: morphology to molecules. Annu Rev Cell Dev Biol *14*, 89-109.

Stolt, C.C., Lommes, P., Sock, E., Chaboissier, M.C., Schedl, A., and Wegner, M. (2003). The Sox9 transcription factor determines glial fate choice in the developing spinal cord. Genes Dev *17*, 1677-1689.

Stolt, C.C., Schlierf, A., Lommes, P., Hillgartner, S., Werner, T., Kosian, T., Sock, E., Kessaris, N., Richardson, W.D., Lefebvre, V.*, et al.* (2006). SoxD proteins influence multiple stages of oligodendrocyte development and modulate SoxE protein function. Dev Cell *11*, 697-709.

Sugatani, T., and Hruska, K.A. (2009). Impaired micro-RNA pathways diminish osteoclast differentiation and function. J Biol Chem *284*, 4667-4678.

Sugimori, M., Nagao, M., Parras, C.M., Nakatani, H., Lebel, M., Guillemot, F., and Nakafuku, M. (2008). Ascl1 is required for oligodendrocyte development in the spinal cord. Development *135*, 1271-1281.

Syed, Y.A., Baer, A., Hofer, M.P., Gonzalez, G.A., Rundle, J., Myrta, S., Huang, J.K., Zhao, C., Rossner, M.J., Trotter, M.W.*, et al.* (2013). Inhibition of phosphodiesterase-4 promotes oligodendrocyte precursor cell differentiation and enhances CNS remyelination. EMBO Mol Med *5*, 1918-1934.

Tait, S., Gunn-Moore, F., Collinson, J.M., Huang, J., Lubetzki, C., Pedraza, L., Sherman, D.L., Colman, D.R., and Brophy, P.J. (2000). An oligodendrocyte cell adhesion molecule at the site of assembly of the paranodal axo-glial junction. J Cell Biol *150*, 657-666.

Takebayashi, H., Nabeshima, Y., Yoshida, S., Chisaka, O., Ikenaka, K., and Nabeshima, Y. (2002). The basic helix-loop-helix factor olig2 is essential for the development of motoneuron and oligodendrocyte lineages. Curr Biol *12*, 1157-1163.

Tang, F., Hajkova, P., Barton, S.C., Lao, K., and Surani, M.A. (2006). MicroRNA expression profiling of single whole embryonic stem cells. Nucleic Acids Res *34*, e9.

Tang, X., Jang, S.W., Okada, M., Chan, C.B., Feng, Y., Liu, Y., Luo, S.W., Hong, Y., Rama, N., Xiong, W.C.*, et al.* (2008). Netrin-1 mediates neuronal survival through PIKE-L interaction with the dependence receptor UNC5B. Nat Cell Biol *10*, 698-706.

Tanikawa, C., Matsuda, K., Fukuda, S., Nakamura, Y., and Arakawa, H. (2003). p53RDL1 regulates p53-dependent apoptosis. Nat Cell Biol *5*, 216-223.

Taveggia, C., Zanazzi, G., Petrylak, A., Yano, H., Rosenbluth, J., Einheber, S., Xu, X., Esper, R.M., Loeb, J.A., Shrager, P.*, et al.* (2005). Neuregulin-1 type III determines the ensheathment fate of axons. Neuron *47*, 681-694.

Taylor, C.M., Coetzee, T., and Pfeiffer, S.E. (2002). Detergent-insoluble glycosphingolipid/cholesterol microdomains of the myelin membrane. J Neurochem *81*, 993-1004.

Tessier-Lavigne, M., Placzek, M., Lumsden, A.G., Dodd, J., and Jessell, T.M. (1988). Chemotropic guidance of developing axons in the mammalian central nervous system. Nature *336*, 775-778.

Thiebault, K., Mazelin, L., Pays, L., Llambi, F., Joly, M.O., Scoazec, J.Y., Saurin, J.C., Romeo, G., and Mehlen, P. (2003). The netrin-1 receptors UNC5H are putative tumor suppressors controlling cell death commitment. Proc Natl Acad Sci U S A *100*, 4173-4178.

Trajkovic, K., Dhaunchak, A.S., Goncalves, J.T., Wenzel, D., Schneider, A., Bunt, G., Nave, K.A., and Simons, M. (2006). Neuron to glia signaling triggers myelin membrane exocytosis from endosomal storage sites. J Cell Biol *172*, 937-948.

Traka, M., Dupree, J.L., Popko, B., and Karagogeos, D. (2002). The neuronal adhesion protein TAG-1 is expressed by Schwann cells and oligodendrocytes and is localized to the juxtaparanodal region of myelinated fibers. J Neurosci *22*, 3016-3024.

Tripathi, R.B., Clarke, L.E., Burzomato, V., Kessaris, N., Anderson, P.N., Attwell, D., and Richardson, W.D. (2011). Dorsally and ventrally derived oligodendrocytes have similar electrical properties but myelinate preferred tracts. J Neurosci *31*, 6809-6819.

Tsai, H.H., Frost, E., To, V., Robinson, S., Ffrench-Constant, C., Geertman, R., Ransohoff, R.M., and Miller, R.H. (2002). The chemokine receptor CXCR2 controls positioning of oligodendrocyte precursors in developing spinal cord by arresting their migration. Cell *110*, 373-383.

Tsai, H.H., Tessier-Lavigne, M., and Miller, R.H. (2003). Netrin 1 mediates spinal cord oligodendrocyte precursor dispersal. Development *130*, 2095-2105.

Ueda, H., Levine, J.M., Miller, R.H., and Trapp, B.D. (1999). Rat optic nerve oligodendrocytes develop in the absence of viable retinal ganglion cell axons. J Cell Biol *146*, 1365-1374.

Umemori, H., Sato, S., Yagi, T., Aizawa, S., and Yamamoto, T. (1994). Initial events of myelination involve Fyn tyrosine kinase signalling. Nature *367*, 572-576.

Vabnick, I., Novakovic, S.D., Levinson, S.R., Schachner, M., and Shrager, P. (1996). The clustering of axonal sodium channels during development of the peripheral nervous system. J Neurosci *16*, 4914-4922.

Vabnick, I., Trimmer, J.S., Schwarz, T.L., Levinson, S.R., Risal, D., and Shrager, P. (1999). Dynamic potassium channel distributions during axonal development prevent aberrant firing patterns. J Neurosci *19*, 747-758.

van Rooij, E., Sutherland, L.B., Qi, X., Richardson, J.A., Hill, J., and Olson, E.N. (2007). Control of stress-dependent cardiac growth and gene expression by a microRNA. Science *316*, 575-579.

Ventura, A., Young, A.G., Winslow, M.M., Lintault, L., Meissner, A., Erkeland, S.J., Newman, J., Bronson, R.T., Crowley, D., Stone, J.R.*, et al.* (2008). Targeted deletion reveals essential and overlapping functions of the miR-17 through 92 family of miRNA clusters. Cell *132*, 875-886.

Wang, H., Copeland, N.G., Gilbert, D.J., Jenkins, N.A., and Tessier-Lavigne, M. (1999). Netrin-3, a mouse homolog of human NTN2L, is highly expressed in sensory ganglia and shows differential binding to netrin receptors. J Neurosci *19*, 4938-4947.

Wang, S., Sdrulla, A., Johnson, J.E., Yokota, Y., and Barres, B.A. (2001). A role for the helix-loop-helix protein Id2 in the control of oligodendrocyte development. Neuron *29*, 603-614.

Wang, S., Sdrulla, A.D., diSibio, G., Bush, G., Nofziger, D., Hicks, C., Weinmaster, G., and Barres, B.A. (1998). Notch receptor activation inhibits oligodendrocyte differentiation. Neuron *21*, 63-75.

Warf, B.C., Fok-Seang, J., and Miller, R.H. (1991). Evidence for the ventral origin of oligodendrocyte precursors in the rat spinal cord. J Neurosci *11*, 2477-2488.

Watkins, T.A., Emery, B., Mulinyawe, S., and Barres, B.A. (2008). Distinct stages of myelination regulated by gamma-secretase and astrocytes in a rapidly myelinating CNS coculture system. Neuron *60*, 555-569.

Wienholds, E., Koudijs, M.J., van Eeden, F.J., Cuppen, E., and Plasterk, R.H. (2003). The microRNA-producing enzyme Dicer1 is essential for zebrafish development. Nat Genet *35*, 217-218.

Wight, P.A., and Dobretsova, A. (2004). Where, when and how much: regulation of myelin proteolipid protein gene expression. Cell Mol Life Sci *61*, 810-821.

Wightman, B., Ha, I., and Ruvkun, G. (1993). Posttranscriptional regulation of the heterochronic gene lin-14 by lin-4 mediates temporal pattern formation in C. elegans. Cell *75*, 855-862.

Williams, A.H., Valdez, G., Moresi, V., Qi, X., McAnally, J., Elliott, J.L., Bassel-Duby, R., Sanes, J.R., and Olson, E.N. (2009). MicroRNA-206 delays ALS progression and promotes regeneration of neuromuscular synapses in mice. Science *326*, 1549-1554.

Williams, M.E., Lu, X., McKenna, W.L., Washington, R., Boyette, A., Strickland, P., Dillon, A., Kaprielian, Z., Tessier-Lavigne, M., and Hinck, L. (2006). UNC5A promotes neuronal apoptosis during spinal cord development independent of netrin-1. Nat Neurosci *9*, 996-998.

Winberg, M.L., Mitchell, K.J., and Goodman, C.S. (1998). Genetic analysis of the mechanisms controlling target selection: complementary and combinatorial functions of netrins, semaphorins, and IgCAMs. Cell *93*, 581-591.

Windrem, M.S., Nunes, M.C., Rashbaum, W.K., Schwartz, T.H., Goodman, R.A., McKhann, G., 2nd, Roy, N.S., and Goldman, S.A. (2004). Fetal and adult human oligodendrocyte progenitor cell isolates myelinate the congenitally dysmyelinated brain. Nat Med *10*, 93-97.

Winer, J., Jung, C.K., Shackel, I., and Williams, P.M. (1999). Development and validation of real-time quantitative reverse transcriptase-polymerase chain reaction for monitoring gene expression in cardiac myocytes in vitro. Anal Biochem *270*, 41-49.

Wolswijk, G., and Balesar, R. (2003). Changes in the expression and localization of the paranodal protein Caspr on axons in chronic multiple sclerosis. Brain *126*, 1638-1649.

Woo, J., Kwon, S.K., Choi, S., Kim, S., Lee, J.R., Dunah, A.W., Sheng, M., and Kim, E. (2009). Trans-synaptic adhesion between NGL-3 and LAR regulates the formation of excitatory synapses. Nat Neurosci *12*, 428-437.

Xie, Y., Hong, Y., Ma, X.Y., Ren, X.R., Ackerman, S., Mei, L., and Xiong, W.C. (2006). DCC-dependent phospholipase C signaling in netrin-1-induced neurite elongation. J Biol Chem *281*, 2605-2611.

Yamakawa, K., Huot, Y.K., Haendelt, M.A., Hubert, R., Chen, X.N., Lyons, G.E., and Korenberg, J.R. (1998). DSCAM: a novel member of the immunoglobulin superfamily maps in a Down syndrome region and is involved in the development of the nervous system. Hum Mol Genet *7*, 227-237.

Ye, P., Carson, J., and D'Ercole, A.J. (1995). Insulin-like growth factor-I influences the initiation of myelination: studies of the anterior commissure of transgenic mice. Neurosci Lett *201*, 235-238.

Ye, P., Li, L., Richards, R.G., DiAugustine, R.P., and D'Ercole, A.J. (2002). Myelination is altered in insulin-like growth factor-I null mutant mice. J Neurosci *22*, 6041-6051.

Yebra, M., Montgomery, A.M., Diaferia, G.R., Kaido, T., Silletti, S., Perez, B., Just, M.L., Hildbrand, S., Hurford, R., Florkiewicz, E.*, et al.* (2003). Recognition of the neural chemoattractant Netrin-1 by integrins alpha6beta4 and alpha3beta1 regulates epithelial cell adhesion and migration. Dev Cell *5*, 695-707.

Yeh, H.J., Ruit, K.G., Wang, Y.X., Parks, W.C., Snider, W.D., and Deuel, T.F. (1991). PDGF A-chain gene is expressed by mammalian neurons during development and in maturity. Cell *64*, 209-216.

Yin, Y., Sanes, J.R., and Miner, J.H. (2000). Identification and expression of mouse netrin-4. Mech Dev *96*, 115-119.

Yoshikawa, F., Sato, Y., Tohyama, K., Akagi, T., Hashikawa, T., Nagakura-Takagi, Y., Sekine, Y., Morita, N., Baba, H., Suzuki, Y.*, et al.* (2008). Opalin, a transmembrane sialylglycoprotein

located in the central nervous system myelin paranodal loop membrane. J Biol Chem *283*, 20830-20840.

Zamore, P.D., Tuschl, T., Sharp, P.A., and Bartel, D.P. (2000). RNAi: double-stranded RNA directs the ATP-dependent cleavage of mRNA at 21 to 23 nucleotide intervals. Cell *101*, 25-33.

Zeger, M., Popken, G., Zhang, J., Xuan, S., Lu, Q.R., Schwab, M.H., Nave, K.A., Rowitch, D., D'Ercole, A.J., and Ye, P. (2007). Insulin-like growth factor type 1 receptor signaling in the cells of oligodendrocyte lineage is required for normal in vivo oligodendrocyte development and myelination. Glia *55*, 400-411.

Zehir, A., Hua, L.L., Maska, E.L., Morikawa, Y., and Cserjesi, P. Dicer is required for survival of differentiating neural crest cells. Dev Biol *340*, 459-467.

Zhang, J., and Cai, H. (2010). Netrin-1 prevents ischemia/reperfusion-induced myocardial infarction via a DCC/ERK1/2/eNOS s1177/NO/DCC feed-forward mechanism. J Mol Cell Cardiol *48*, 1060-1070.

Zhao, X., He, X., Han, X., Yu, Y., Ye, F., Chen, Y., Hoang, T., Xu, X., Mi, Q.S., Xin, M.*, et al.* (2010). MicroRNA-mediated control of oligodendrocyte differentiation. Neuron *65*, 612-626.

Zhou, Q., Choi, G., and Anderson, D.J. (2001). The bHLH transcription factor Olig2 promotes oligodendrocyte differentiation in collaboration with Nkx2.2. Neuron *31*, 791-807.

Zonta, B., Tait, S., Melrose, S., Anderson, H., Harroch, S., Higginson, J., Sherman, D.L., and Brophy, P.J. (2008). Glial and neuronal isoforms of Neurofascin have distinct roles in the assembly of nodes of Ranvier in the central nervous system. J Cell Biol *181*, 1169-1177.